UNIVERSITY OF CALIFORNIA, SAN DIEGO

Characterization of the *esa1* suppressor *LYS20* and discovery of its novel nuclear functions

A dissertation submitted in partial satisfaction of the requirements for the degree Doctor of Philosophy

in

Biology

by

Erin M. Scott

Committee in charge:

Professor Lorraine Pillus, Chair
Professor Beverly Emerson
Professor Randolph Hampton
Professor Trey Ideker
Professor James Kadonaga

2010

The Dissertation of Erin M. Scott is approved, and it is acceptable in quality and form for publication on microfilm and electronically:

_____

_____

_____

_____

_____

Chair

University of California, San Diego

2010

DEDICATION

This thesis is dedicated to my grandparents, Arletha Raymond and Rayford Scott, who would have been proud to see its completion.

EPIGRAPH

...y aquí estoy en la cumbre de toda la buena fortuna.

-Lazarillo de Tormes

TABLE OF CONTENTS

LIST OF ABBREVIATIONS

Ade	Adenine
AEC	Aminoethylcysteine
Arg	Arginine
Amp	Ampicillin
BSA	Bovine serum albumin
Cam	Chloramphenicol
Can	Canavanine
CPT	Camptothecin
CTH	Calf thymus histones
HAT	Histone acetyltransferase
HCS	Homocitrate synthase
HDAC	Histone deacetylase
HU	Hydroxyurea
IP	Immunoprecipitation
LB	Luria broth
Leu	Leucine
Lys	Lysine
PMSF	Phenylmethylsulfonyl fluoride
rDNA	Ribosomal DNA

TPCK	Tosylphenylalanyl chloromethylketone
Ura	Uracil
Vec	Vector
YPD	Yeast extract, peptone, dextrose
YH	Yeast histones

LIST OF FIGURES

LIST OF TABLES

ACKNOWLEDGEMENTS

I thank Lorraine for welcoming me into the lab seven years ago. Since then she has spent much time training me. I particularly enjoy discussing random bits of interesting science with her.

I thank Astrid Clarke, Erik Spedale and Viet Le for starting this project and for their contributions to the project's early stages.

I thank my committee for communicating to me their unstinting enthusiasm about this project, and appreciation of its novelty.

Ray Trievel and Stacie Bulfer have been excellent collaborators. They have shared both reagents and ideas. Our combined efforts have produced two manuscripts and opened a new line of inquiry, focused around characterization of homocitrate synthases in multiple species.

John Aris very generously provided monoclonal antibodies to Lys20, Lys21, and other homocitrate synthases. Joon Huh and Bob Dutnall provided recombinant histones and much advice about protein purification and protein activity assays. Many others have contributed strains, plasmids, reagents and advice, and are acknowledged in the forthcoming chapters.

Members of the Pillus lab, past and present, deserve my thanks for creating a working environment with a sense of humor. I also want to acknowledge lab members who have done support work. They have provided a valuable service that saved me lots of time.

I thank Melissa Koch and Christie Chang, both of whom I have known for over six years, and who have become friends as well as colleagues. Discussions with them, on a wide variety of subjects have been invaluable. They have resulted, respectively, in a large collection of Chinese food recipes and a lemon tree. I will miss seeing both of them every day as we each move on.

I will also miss other denizens of the second floor of Pacific Hall, who have occasionally provided reagents, access to fancy equipment, and interesting conversation. Administrative assistants Sharon Young and Libby Weber are included in this category, especially in recognition of their exceptional happy hour planning skills.

I thank members of my family, especially my grandparents, Leroy and Arletha Raymond and Rayford and Mary Scott, and my un-inlaws Heather, Keith and James Ridgeway for a sense of perspective. I thank my uncles, Mark, Ray, Jeff and Jack for not being scientists. I thank my parents Linda and Bryan Scott and my brother Trevor for providing support, sarcasm and food. Finally, I acknowledge my significant other and my cat for obvious reasons.

Material in Chapter 2 is currently under review for publication in Genes and Development, and may appear as Scott EM and Pillus L. 2010. Homocitrate synthase connects amino acid metabolism to chromatin functions through Esa1 and DNA damage. The dissertation author was the primary author of this material. Material in Chapter 5 has been published as Bulfer SL, Scott EM, Couture JF, Pillus L, Trievel RC. 2009. Crystal structure and functional analysis of homocitrate synthase, an

essential enzyme in lysine biosynthesis. *J Biol Chem*. **51**: 35769-80. and Bulfer SL, Scott EM, Couture JF, Pillus L, Trievel RC. 2009. Crystal structure and functional analysis of homocitrate synthase, an essential enzyme in lysine biosynthesis. *J Biol Chem*. **51**: 35769-80. The dissertation author was a contributing author to this material. This material has been formatted to conform to thesis guidelines. All experiments in Appendix B were done in collaboration with Christie Chang. Renee Garza, Christie Chang, Melissa Koch and Moriah Eustice kindly read chapters of this thesis and offered their comments and suggestions.

VITA

2003	Bachelor of Arts, University of California, Berkeley
	Major: Molecular and Cell Biology
	Minor: Spanish and Portuguese
2005-2007	Teaching Assistant, University of California, San Diego
2010	Doctor of Philosophy University of California, San Diego
	Field of Study: Biology

PUBLICATIONS

Scott EM and Pillus L. 2010. Homocitrate synthase connects amino acid metabolism to chromatin functions through Esa1 and DNA damage. *In review*

Bulfer SL, Scott EM, Pillus L, Trievel RC. 2010. Structural basis for L-lysine feedback inhibition of homocitrate synthase. *J Biol Chem.* **14**: 10446-53.

Bulfer SL, Scott EM, Couture JF, Pillus L, Trievel RC. 2009. Crystal structure and functional analysis of homocitrate synthase, an essential enzyme in lysine biosynthesis. *J Biol Chem*. **51**: 35769-80.

Lafon A, Chang CS, Scott EM, Jacobson SJ, Pillus L. 2007. MYST opportunities for growth control: yeast genes illuminate human cancer gene functions. *Oncogene*. **37**: 5373-84.

ABSTRACT OF THE DISSERTATION

Characterization of the *esa1* suppressor *LYS20* and
discovery of its novel nuclear functions

by

Erin M. Scott

Doctor of Philosophy in Biology

University of California, San Diego, 2010

Professor Lorraine Pillus, Chair

Histone acetyltransferases (HATs) are one class of enzymes that contribute to chromatin structure and function in eukaryotic cells. The MYST family HAT Esa1 is an essential HAT known to be involved in transcriptional silencing, cell cycle progression and DNA repair, along with its role in transcriptional activation. *LYS20* was identified as a high copy suppressor of *esa1* mutant phenotypes. This marked the discovery of a previously unsuspected role for Lys20, an enzyme that was only known

to function in lysine biosynthesis, yet was localized to the nucleus for purposes that remained unclear. Lys20 is a homocitrate synthase (HCS) that catalyzes the first and rate-limiting step in the alpha-amino adipate pathway used by fungi to make lysine. Reported here is a role for Lys20 in DNA damage repair that is mediated through the H2A variant H2A.Z, thereby defining its nuclear roles. Lys20's HCS catalytic activity is not required for its DNA damage functions, but nuclear localization is important for these roles. Collaborative analysis focused around the well-conserved family of HCSs, in particular the *S. pombe* HCS Lys4. Structural, kinetic and mechanistic insights are provided for Lys4. Further characterization of *ESA1* has also been undertaken, bringing to light new genetic interactions focused around H2A its H2A.Z variant. New factors that influence the biochemical activity of Esa1 are also identified. Results reported here contribute to defining connections between metabolism and chromatin functions by demonstrating nuclear roles for a HCS. Further characterization of both the chromatin association factors and the HCS in this interaction is performed to set the stage for the future of similar analyses.

Chapter 1 Introduction to chromatin, histones and lysine biosynthesis

Histone acetyltransferases and transcription

In the nucleus of a eukaryotic cell, DNA is organized by being wound around a protein core. This core consists of an octamer of histone proteins. The histone proteins have lysine rich N-terminal tails that protrude from the core of the nuclosome. Cells may regulate transcription of the DNA by adding or removing acetyl groups from the lysine residues in the N-terminal tails of the histones. Histones may also be methylated, phosphorylated, ubiquitinated (reviewed in Berger 2002), SUMOylated (Nathan et al. 2006), ADP-ribosylated (Boulikas et al. 1990), proteolyzed (Duncan et al. 2008) and propionylated/ butrylated (Zhang et al. 2009) To add to this list, new modifications of histones are still being discovered, broadening the ranks of enzymes that modify chromatin.

Histones are extremely well characterized proteins, with well annotated structures (Luger et al. 1997; Suto et al. 2000). There are four main histones H2A, H2B, H3 and H4. They are widely conserved, with only minor sequence varations between unicellular life and humans. A database of histone sequences is described in

(Makalowska et al. 1999). The role of each histone residue is being studied in some widescale studies that will be discussed later. However, unsuspected roles for even these proteins are being discovered, especially in multicellular organisms.

In particular, evidence suggests that histones may have separate roles when extracellular. For example, histone H4 is secreted from human sebocytes and once outside the cell acts as an antimicrobial agent (Lee et al. 2009). Also, extracellular histones have a role in mediating sepsis (Xu et al. 2009). Some characteristics, such as histones' ability to bind DNA, may depend upon the fact that they are small, highly positively charged proteins.

Enzymes that add the acetyl groups to the histone tails are known as histone acetyl transferases. One of the essential histone acetyltransferases (HATs) in *S. cerevisiae* is Esa1p (Essential Sas related Acetyltransferase-1), a member of the MYST family of HATs (Clarke et al. 1999), which is also conserved into humans. Being a member of the MYST family means that Esa1 contains certain domains, including an acetyl CoA binding domain, in common with other MYST family members, such as MOZ, Ybf2/Sas3, Sas2, and Tip60 (reviewed in Lafon et al. 2007). All of the HATs discussed here may also be classified under the broader criterion of protein lysine acetyltransferases (KATs), and indeed some do acetylate non-histone protein substrates (Sterner and Berger 2000). However, they will be discussed more specifically as histone-specific protein acetyltransferases and so will be referred to as HATs.

Like other HATs, Esa1 regulates transcription by acetylating a specific subset of lysine residues spread across multiple core histones (Smith et al. 1998; Clarke et al. 1999) and histone variants (Babiarz et al. 2006; Keogh et al. 2006; Millar et al. 2006). The subset of lysine residues targeted for acetylation by a specific HAT helps define its role in different cellular processes (Suka et al. 2002). Some HATs, such as Sas3, another MYST family HAT, may have affinity for only one histone. This specificity may be partially determined by the complex in which the HAT resides. Sas3 is the catalytically active subunit of the NuA3 complex (John et al. 2000). Gcn5, which also acetylates primarily H3 *in vivo,* is part of several different complexes, including SAGA and SLIK/SALSA (Pray-Grant et al. 2002; Sterner et al. 2002). HAT activity can also be regulated based on the other proteins with which it forms a complex. For example, Esa1 is the catalytic subunit of both the NuA4 complex and the smaller piccolo complex (Fig1.1), yet the two complexes have different specificities and cellular functions (Allard et al. 1999; Boudreault et al. 2003). Piccolo is responsible for global histone acedtylation whereas NuA4 mediated acetylation tends to be directed to transcription start site at promoters of genes .

Chromatin modifying enzymes

Gcn5 was the first HAT discovered and has become the founding member of the GNAT family of HATs (Brownell and Allis 1995; Kuo et al. 1996). The GNAT family is a major family of HATs, which is conserved from yeast to humans (reviewed in Carrozza et al. 2003). The well characterized GNAT HATs share sequence

homology with MYST family HATs only in the acetyl CoA binding domain (Neuwald and Landsman 1997).

Some HATs are specific to multicellular eukaryotes, yet still share sequence similarity with the larger families. The mammalian HAT CBP/p300, for example, contains a bromodomain similar to that found in the yeast MYST family member Esa1, and the GNAT HAT Gcn5 and also a PHD domain, found in other HATs, including those from plants. CBP/p300 comprise their own family of HATs. The conserved PHD domain turns out to be dispensable for the HAT activity of p300 (Bordoli et al. 2001). HATs in different families have different domains that allow them to catalyze the same reaction using different mechanisms; there is no one single way to catalyze the HAT reaction. An acetyl CoA binding domain is the only necessarily conserved element identified to date (Neuwald and Landsman 1997).

HAT enzymes and HAT families are well conserved across species. It has also been observed that the complexes in which HATs operate are also well conserved (reviewed in Doyon and Côté 2004), for example, with each protein in the yeast NuA4 complex having an identifiable counterpart in the human TIP60 complex. Counterparts are identified on the basis of sequence homology. Tip60 is homologous to Esa1 (reviewed in Doyon and Côté 2004). Additionally, the largest subunit of each complex (Tra1 in yeast and TRAAP in humans) is conserved. Tra1 is also a component of SAGA, the Gcn5-containing HAT complex. No enzymatic activity is demonstrated for either Tra1 or TRAAP, instead it is reported to have a role

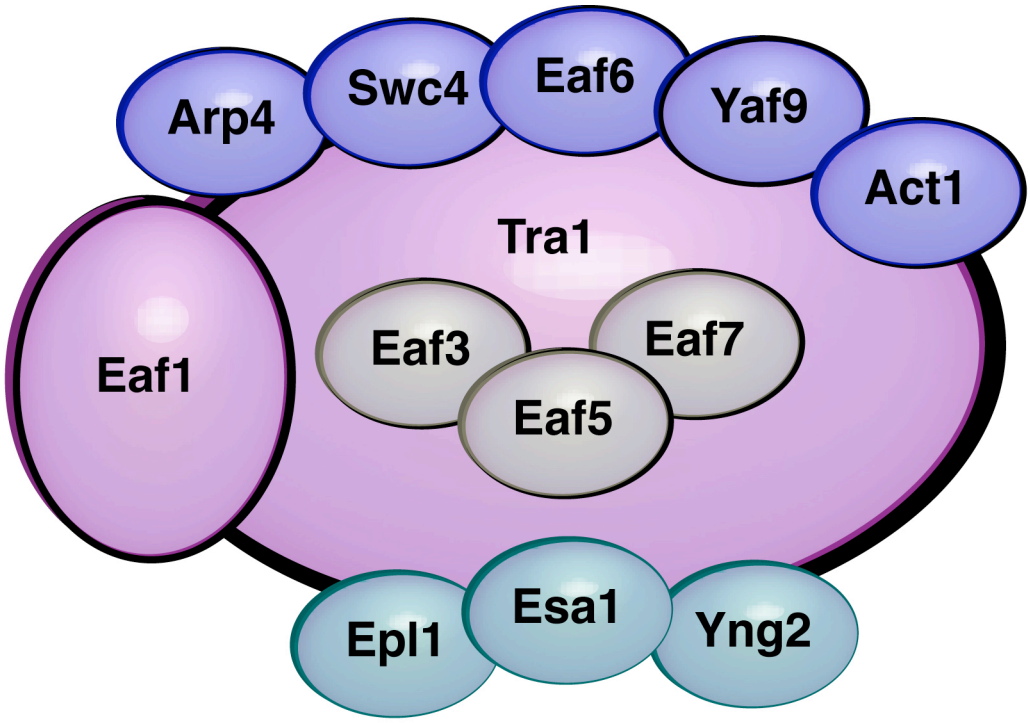

Figure 1.1 The NuA4 complex. Esa1 is the catalytic HAT subunit of the NuA4 complex. Tra1 and Eaf1 (purple) are thought to play structural and targeting roles. Epl1, Esa1 and Yng2 (green) constitute piccolo, an independent subcomplex. Esa1 is the catalytic subunit of both NuA4 and piccolo. Arp4, Swc4 Eaf6, Yaf9 and Act1 have specific functions in the complex, whereas Eaf3, Eaf5 and Eaf7 are less well characterized.

in recruitment of the complex to coding regions. This illustrates that the complex architecture is conserved in addition to enzymatic activity. Both Tip60 and NuA4 contain an ING (Inhibitor of Growth) family complex member. In humans, this is ING 3 protein and in yeast, Yng2 (Yeast ING) (reviewed in Doyon and Côté 2004). Yng2 is also one of the three members of NuA4 that make up the smaller HAT complex piccolo (Fig 1.1). Another conserved feature in both yeast and human complexes is the presence of a YEATS domain protein. Yaf9 is the YEATS protein in yeast, in humans GAS41 fulfills this role. The functions of these domains are not yet understood, but their presence is conserved in the complexes (reviewed in Lafon et al. 2007). When comparing complexes across species, a series of salient features emerges that defines the complex - this complex always has one HAT, one ING homolog, one YEATS domain, etc. This set of features is conserved even if multiple features are blended into one protein in some instances. It is the pattern that remains constant (reviewed in Doyon and Côté 2004; Lu et al. 2009).

Many HATs were originally identified as transcriptional activators (such as Gcn5 (Lucchini et al. 1984)) before it was known that they had HAT activity (reviewed in Struhl 1998). TAF (II) 250, also called TAFI, is its own family of HATs. TAF II 250 was originally defined for its role in transcription initiation, when its HAT activity was discovered (Mizzen et al. 1996). It is also part of the complex that associates with RNA Pol II prior to initiation of transcription. However, the *in vivo* relevance of the HAT activity of TAF (II) 250 has been called into question (Durant and Pugh 2006).

Histone deacetylases (HDACs) reverse the HAT reaction, removing the acetyl groups deposited by histones. For example, the HDAC Rpd3 and the HAT Gcn5 coordinately regulate acetylation status of lysines on histone H3 (Suka et al. 2001). HATs and HDACs whose activities oppose each other may also interact genetically, as in the case of Rpd3 and Esa1which cooperate to regulate acetylation at H4K12 (Chang and Pillus 2009).

Chromatin modifying enzymes and transcriptional silencing

Certain loci within the genome are transcriptionally regulated by HATs and HDACs such that they are not transcribed or only transcribed in very controlled circumstances, at tightly regulated levels. These loci are said to be transcriptionally silenced (reviewed in Koch and Pillus 2009). In the yeast genome, there are three loci that are subject to transcriptional silencing. These are the silent mating type loci, the telomeres and the ribosomal DNA repeats (reviewed in Rusche et al. 2003). Chromatin modifying enzymes such as HATs and HDACs directly affect transcription from these silenced loci, often in a dosage dependent manner. Acetylation levels of the histones at these loci may keep them in a repressed state (reviewed in Koch and Pillus 2009). When genes encoding histone modifying enzymes are deleted, there are often aberrations in the silencing of these loci (reviewed in Koch and Pillus 2009). Significantly, *esa1* mutants are defective in silencing at both the telomeres and the rDNA (Clarke et al. 2006).

Histones and chromatin modifying enzymes together contribute to correct regulation of silencing at the rDNA. Mutations in histones, particularly H4 can result

in defective rDNA silencing (reviewed in Shahbazian and Grunstein 2007). Point mutations in histone residues that are known targets of HATs and HDACs confer specific phenotypes as in mutation of H4K16. The HAT Sas2 and the HDAC Sir2 oppositely modify H4K16 ; disruption of either gene affects rDNA silencing (reviewed in Lafon et al. 2007).

Additional roles for HATs

HATs and HDACs may regulate the acetylation status of a variety of proteins in the cell other than histones. The Sir2 HDAC, to take just one example, is also a recognized protein deacetylase in bacteria, regulating acetylation levels of acetyl-CoA synthetase (Starai et al. 2002). These two substrates (histones and acetyl-CoA) combine in one protein a means for both metabolic control and transcriptional regulation. The HAT p300/CBP has been well characterized for its role in acetylating non-histone protein substrates such as viral E1A and HIV Tat, transcription factors including p53 (reviewed in Grossman 2001; Sterner and Berger 2000), and chromatin associated HMG proteins. Esa1 also acetylates itself (Yan et al. 2002), and acetylates the metabolic enzyme Pck1 (Lin et al. 2009). The human homolog of Esa1, Tip60, has many non-histone targets (reviewed in Sapountzi et al. 2006; Squatrito et al. 2006).

HAT enzymes have roles that are not necessarily connected to their may be independent of acetyltransferase activity. The catalytic mechanism of Esa1 is still controversial (Yan et al. 2002; Berndsen et al. 2007), but further discussion is stimulated by recent work (Decker et al. 2008) that questions the roles of catalytic residues of Esa1. Residues essential for acetyltransferase activity may not be essential

for cell viability. Esa1 is involved in multiple cellular processes, but it remains unknown which of these require the HAT activity. For example, cell cycle defects are evident in *esa1* mutants (Clarke et al. 1999). In addition, Esa1 has been implicated in DNA damage sensing and repair, transcriptional silencing (reviewed in Doyon and Côté 2004; Lafon et al. 2007). Mutations in *ESA1* cause sensitivity to camptothecin, (Bird et al. 2002) a drug which causes DNA double strand breaks by inhibiting topoisomerase I (Hsiang et al. 1985). Mutation of the histone H4 lysine residues targeted by Esa1 for acetylation phenocopies this drug sensitivity, suggesting that it is the histone lysine acetylation function of Esa1 that is required for resistance to camptothecin. Much is still being discovered about Esa1 including additional targets of acetylation, and its acetylation metabolic enzymes such as Pck1 (Lin et al. 2009) and the histone variant H2A.Z is one area where research efforts have focused.

DNA damage and H2A

Most well-characterized HATs primarily target histones H3 and H4, however histone H2A is known to be acetylated by the HATs Esa1 and Nat4 (Smith et al. 1998; Clarke et al. 1999; Song et al. 2003). H2A is also phosphorylated in response to DNA damage (Downs et al. 2000). Histone H2A is sensitive to DNA damaging agents of various classes. Mutational analysis of the C-terminus of H2A uncovered residues that conferred sensitivity to specific classes of genotoxins (Moore et al. 2007). Like *esa1* mutants, mutants in *HTA1* have a G2/M cell cycle delay (Pinto and Winston 2000). Some roles for Esa1 and H2A overlap.

DNA damage results from exposure to many challenges. Genotoxins cause different types of damage to the DNA, including single base lesions, single strand and double strand breaks. Different types of damage require different repair machinery (reviewed in Lisby and Rothstein 2009; Falk et al. 2010).

When damage occurs, a concerted response must be orchestrated by the cell to sense and then repair the damage (reviewed in Wahl and Carr 2001). Many of the repair pathways are highly conserved. In yeast, many checkpoint proteins alert cells to DNA damage (reviewed in Putnam et al. 2009; Willis and Rhind 2009). The main pathway for DNA damage sensing in *S. cerevisiae* begins with the two kinases Mec1 and Tel1, homologs of human ATR and ATM, respectively. When these checkpoint kinases are alerted to the presence of DNA damage, they activate downstream effector kinases, particularly Chk1 and Rad53. Rad53 subsequently autophosphorlyates; detection of Rad53 hyperphosphorylation is frequently used as an experimental measure of the response to DNA damage.

In addition to Rad53, many other proteins are activated upon DNA damage. Each protein has a distinct yet necessary role: some stall the cell cycle until the damage can be repaired, others activate repair machinery (reviewed in Segurado and Tercero 2009; Huertas 2010; Humpal et al. 2009). Many complexes are involved in the process, including NuA4, which is recruited to double strand breaks via the Arp4 subunit (Fig. 1.1) (Tamburini and Tyler 2005). Other chromatin-associated complexes are also recruited, including SWR (which deposits Htz1 into nucleosomes at sites of

DNA damage) and the chromatin remodeling complex Ino80 (reviewed in Putnam et al. 2009).

H2A.Z in chromatin and DNA damage

Variant sequences exist for each of the four core histones, with the exception of H4 (reviewed in (Talbert and Henikoff 2010). In yeast, there is only one variant of H2A, H2A.Z. Both NuA4 (Esa1 containing HAT complex) and SAGA (Gcn5 containing complex) acetylate H2A.Z. (Babiarz et al. 2006; Keogh et al. 2006; Millar et al. 2006). Both HATs participate in DNA damage repair as *gcn5*Δ is also CPT sensitive (Choy and Kron 2002). H2A.Z has been implicated in boundary formation in silent chromatin (Meneghini et al. 2003; Shia et al. 2006). Like *esa1* mutants, mutants in H2A.Z (encoded in yeast by the *HTZ1* gene) are sensitive to a variety of DNA damaging agents (Kobor et al. 2004; Krogan et al. 2004), implying a role for H2A.Z in resistance to genotoxins. This set of phenotypes establishes Htz1's role in DNA damage resistance and more closely links those enzymes that modify it to the process of DNA damage repair. However, Esa1 and H2A.Z have not been shown to act together in any one pathway, for example in response to DNA damage or to initiate repair.

H2A.Z is conserved from yeast to humans, and appears to retain the same functions across species, potentially making discoveries about the role of Htz1 in yeast broadly applicable (reviewed in Dryhurst et al. 2004; Thambirajah et al. 2009). Interestingly, H2A.Z is essential in other species, but not in *S. cerevisiae* (reviewed in Dryhurst et al. 2004). This allows mutational and deletion analysis to be done in yeast

that would be impossible in other species. Discoveries about specific residues in the histone that are critical for overall function or about the types of modifications to which H2A.Z is subjected may become particularly relevant to addressing H2A.Z functions in other species.

Lys20 in fungal lysine biosynthesis

A high copy suppressor screen done in this lab identified a genetic interaction between *LYS20* and *ESA1* (Clarke 2001) Lys20 and its isozyme Lys21 have been studied for their roles in lysine biosynthesis (reviewed in Bhattacharjee 1985). They are homocitrate synthases (HCS), and catalyze the first step in fungal lysine biosynthesis by combining an acetyl group from acetyl CoA and alpha-ketoglutarate, an intermediate in the Krebs cycle, to make homocitrate (Fig. 1.2).

Homocitrate, like acetyl CoA, is involved in a variety of different processes in the cell. Most of these have to do with cellular metabolism and amino acid biosynthesis, but homocitrate also has more exotic functions. For example, homocitrate is an essential cofactor for the biosynthesis of the Fe-Mo cluster of the nitrogenase enzyme (reviewed in Allen et al. 1994). Homocitrate's role in nitrogenase activity modulates a symbiosis between plants and bacteria (Hakoyama et al. 2009).

The two isozymes act very similarly. Both are localized to the nucleus (Chen et al. 1997; Huh et al. 2003). (Quezada et al. 2008) bring to light a difference in HCS function between Lys20 and Lys21; when grown on ethanol as the carbon source, Lys21 is the enzyme that predominates, synthesizing more homocitrate than Lys20 .

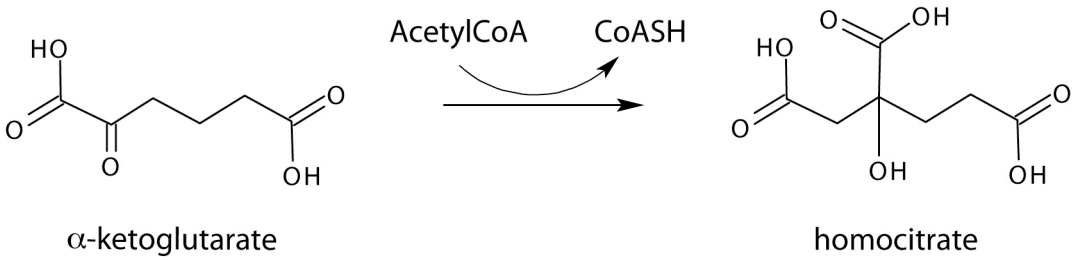

Figure 1.2 The homocitrate synthase reaction. Homocitrate synthase enzymes, such as Lys20 and Lys21 synthesize one molecule of α-ketoglutarate using one molecule of homocitrate and one acetyl group donated by Acetyl-CoA. The products of the reaction are homocitrate and reduced CoA.

As the first step of the lysine biosynthesis pathway, both isozymes are feedback inhibited by lysine, (Tucci and Ceci 1972; Feller et al. 1999; Andi et al. 2005; Quezada et al. 2008). They catalyze the same reaction, although with different kinetics (Feller et al. 1999; Andi et al. 2005). Using monoclonal antibodies to Lys20, Chen and colleagues reported that Lys20 is localized to the nucleus (Chen et al. 1997), and this has been confirmed for both isozymes by the yeast GFP database (Huh et al. 2003; Feller et al. 1999). Lys20 and Lys21 are unique in this, as most of the enzymes that catalyze lysine biosynthesis are located either in the cytoplasm or the mitochondria, including Lys4, an enzyme with homoaconitase activity (Fig 1.3) that is localized to the mitochondrion and catalyzes the step in the lysine biosynthesis pathway that immediately follows Lys20.

Individually, null mutations in *LYS20* and *LYS21* are insufficient to cause lysine auxotrophy, however the double null mutant requires lysine for growth. The fungal lysine biosynthetic pathway, also called the alpha-amino adipate (AAA) pathway, is well conserved across fungi and in some bacteria and archaea (Fig 1.3) (Kosuge and Hoshino 1998; Nishida et al. 1999); (reviewed in Zabriskie and Jackson 2000; Xu et al. 2006). This pathway is distinct from the diaminopimelate lysine biosynthetic pathway found in plants and many prokaryotes. These enzymes are specific to and well conserved in fungi. HCS is particularly well conserved across fungi (Fig 1.4). Some fungal species, such as *C. albicans*, have two HCS isozymes as does *S. cerevisiae*. Other fungi, such as *S. pombe*, have only one. HCS is the rate-limiting step of the pathway and as such, makes an attractive target for new antifungal

therapies. Extensive analysis if the *S. pombe* HCS, Lys4 is published as (Bulfer et al. 2009) and (Bulfer et al. 2010) and will be discussed in Chapter 5.

Evidence in this thesis provides grounds for Lys20 to join the growing list of enzymes known to have multiple functions. These so called "moonlighting" enzymes (reviewed in Jeffery 2003) are often metabolic enzymes and can have very different second functions which provide a link between cellular metabolism and other processes. Some known moonlighting enzymes have DNA repair functions. These enzymes embody the suspected connection between cellular metabolism and other processes. They provide a precedent by which a lysine biosynthesis enzyme may be involved in DNA repair and chromatin regulation.

In this study

This work defines a nuclear role for Lys20, an enzyme whose only previously known function was in lysine biosynthesis. Overexpression of this gene suppressed the DNA damage sensitivity of mutants in *ESA1*, whereas deletion of *LYS20* and *LYS21* suppressed the DNA damage sensitivity of *htz1*Δ. The interaction among Htz1, Lys20 and Esa1 is explored in this work. Suppression of *esa1* phenotypes requires nuclear localization of Lys20, but not its HCS catalytic activity, nor its ability to be feedback inhibited by lysine. Lys20 has HAT activity towards yeast histone substrates. It also interacts genetically with a subset of other chromatin modifying enzymes.

Lys20 interferes with transcriptional silencing at the rDNA. The interactions between Esa1 and H2A.Z is explored in greater detail and possible contributions of the

Figure 1.3 The lysine biosynthetic pathway in *S. cerevisiae.* Lys20 and Lys21 catalyze the first step in lysine biosynthesis. Figure is taken from www.yeastgenome.org.

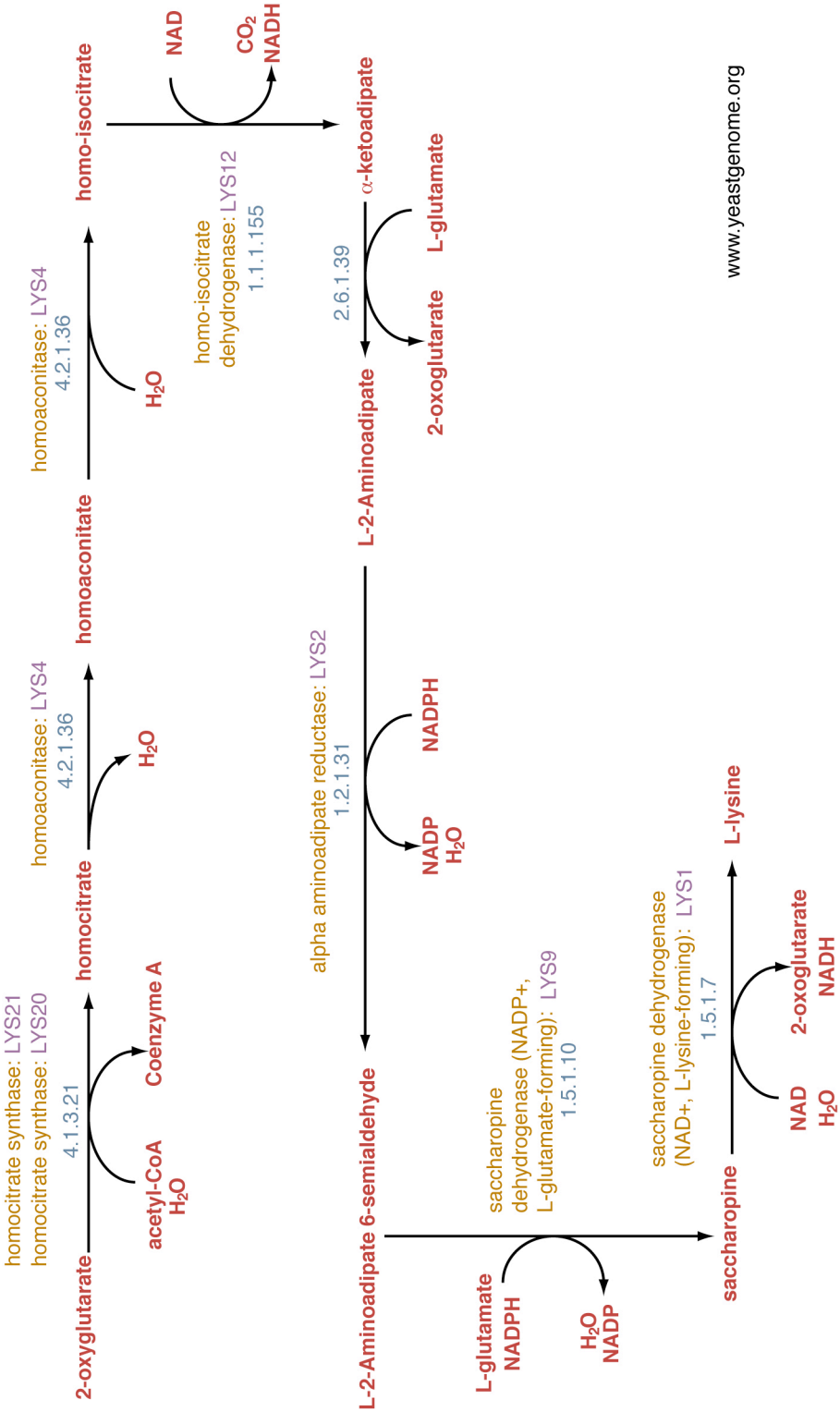
2-oxyglutarate
homocitrate synthase: LYS21
homocitrate synthase: LYS20
4.1.3.21
acetyl-CoA
H2O
Coenzyme A
homocitrate
homocitrate
homoaconitase: LYS4
4.2.1.36
H2O
homoaconitate
homoaconitate
homoaconitase: LYS4
4.2.1.36
H2O
homo-isocitrate
homo-isocitrate
dehydrogenase: LYS12
1.1.1.155
NAD
CO2
NADH
α-ketoadipate
2.6.1.39
L-glutamate
2-oxoglutarate
L-2-Aminoadipate
alpha aminoadipate reductase: LYS2
1.2.1.31
NADPH
NADP
H2O
L-2-Aminoadipate 6-semialdehyde
saccharopine
dehydrogenase (NADP+,
L-glutamate-forming): LYS9
1.5.1.10
L-glutamate
NADPH
H2O
NADP
saccharopine
saccharopine dehydrogenase
(NAD+, L-lysine-forming): LYS1
1.5.1.7
NAD
H2O
L-lysine
2-oxoglutarate
NADH
www.yeastgenome.org

histone chaperone Nap1 and the histone deacetylase Sir2 are considered. Other conditions that affect the catalytic activity of Esa1 are explored. Finally, a collaborative analysis of the *S. pombe* HCS, Lys4 is reported, resulting in structural insights and kinetic parameters for the activity of this enzyme, as well as mechanistic insight. Implications of the connection between chromatin and metabolism are considered and relevant examples of this phenomenon are discussed.

Figure 1.4 Sequence alignment of homocitrate synthases across fungal species.
Sequence alignment of representative HCSs. The secondary structure of the TIM barrel (red), C-terminal subdomain I (orange), and C-terminal subdomain II (yellow) of the *S. pombe* Lys4 2-OG closed lid complex are depicted above the alignment. Residues involved in metal coordination, 2-OG binding, and potential binding to the acetyl group of Acetyl CoA are denoted with red, yellow, and blue backgrounds, respectively, while residues implicated in acid-base catalysis are highlighted in a magenta background. The residues comprising the lid motif are illustrated with a cyan background. This figure and legend are taken from (Bulfer et al. 2009).

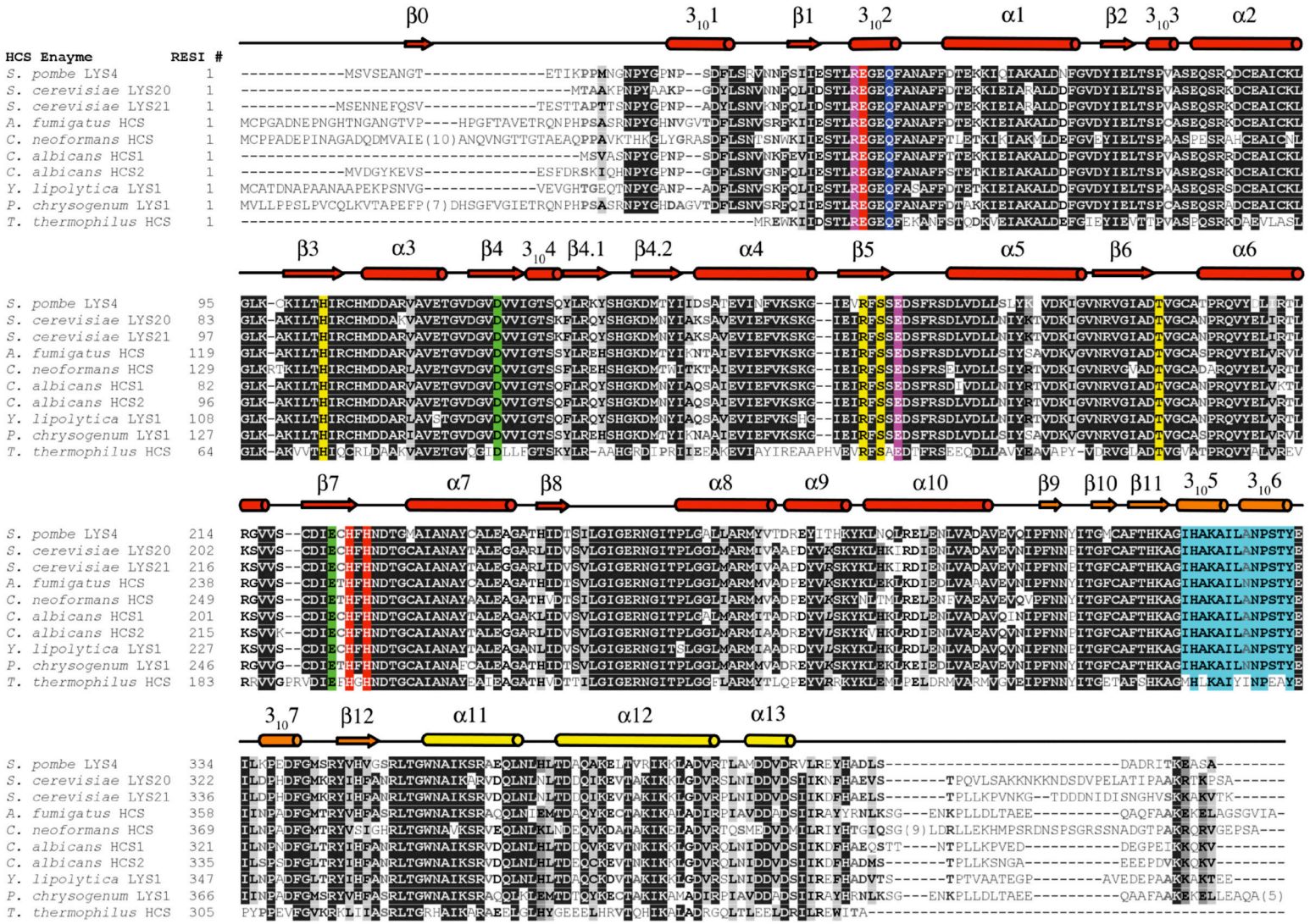
β0 3₁₀1 β1 3₁₀2 α1 β2 3₁₀3 α2
HCS Enayme RESI #
S. pombe LYS4 1
S. cerevisiae LYS20 1
S. cerevisiae LYS21 1
A. fumigatus HCS 1
C. neoformans HCS 1
C. albicans HCS1 1
C. albicans HCS2 1
Y. lipolytica LYS1 1
P. chrysogenum LYS1 1
T. thermophilus HCS 1
β3 α3 β4 3₁₀4 β4.1 β4.2 α4 β5 α5 β6 α6
S. pombe LYS4 95
S. cerevisiae LYS20 83
S. cerevisiae LYS21 97
A. fumigatus HCS 119
C. neoformans HCS 129
C. albicans HCS1 82
C. albicans HCS2 96
Y. lipolytica LYS1 108
P. chrysogenum LYS1 127
T. thermophilus HCS 64
β7 α7 β8 α8 α9 α10 β9 β10 β11 3₁₀5 3₁₀6
S. pombe LYS4 214
S. cerevisiae LYS20 202
S. cerevisiae LYS21 216
A. fumigatus HCS 238
C. neoformans HCS 249
C. albicans HCS1 201
C. albicans HCS2 215
Y. lipolytica LYS1 227
P. chrysogenum LYS1 246
T. thermophilus HCS 183
3₁₀7 β12 α11 α12 α13
S. pombe LYS4 334
S. cerevisiae LYS20 322
S. cerevisiae LYS21 336
A. fumigatus HCS 358
C. neoformans HCS 369
C. albicans HCS1 321
C. albicans HCS2 335
Y. lipolytica LYS1 347
P. chrysogenum LYS1 366
T. thermophilus HCS 305

Acknowledgements

Figure 1.3 is adapted from www.yeastgenome.org, with changes to the fonts. Figure 1.4 and Figure legend are published as Figure S1 in: Crystal structure and functional analysis of homocitrate synthase, an essential enzyme in lysine biosynthesis. Bulfer SL, Scott EM, Couture JF, Pillus L, Trievel RC. J Biol Chem. 2009 Dec 18;284(51):35769-80.

Chapter 2 Homocitrate Synthase Connects Amino Acid Metabolism to Chromatin Functions through Esa1 and DNA Damage

Introduction

Histone acetyltransferases (HATs) modulate chromatin functions by acetylating lysines on histones, transcription factors, and other substrates. Among HATs, the MYST family is highly conserved and notably includes multiple essential enzymes in organisms ranging from yeast to humans (reviewed in Lafon et al. 2007). One well-studied MYST enzyme in yeast, Esa1 (Smith et al. 1998; Clarke et al. 1999), acetylates a specific subset of lysine residues on the four core histones, along with the H2A.Z histone variant encoded by *HTZ1* (Babiarz et al. 2006; Keogh et al. 2006; Millar et al. 2006). Esa1 is the catalytic subunit of the yeast NuA4 and piccolo complexes, (Allard et al. 1999; Boudreault et al. 2003) and has functional interactions with many other genes that encode chromatin-modifying enzymes (Kobor et al. 2004; Krogan et al. 2004; Lin et al. 2008). In addition, Esa1 has been implicated in diverse chromatin-mediated processes, including DNA damage sensing and repair, transcriptional silencing and cell cycle control (reviewed in Doyon and Côté 2004;

Lafon et al. 2007), although not all of these functions may require its catalytic activity (Decker et al. 2008). Mutations in *ESA1* cause sensitivity to DNA double stranded breaks induced by the topoisomerase I inhibitor camptothecin (Bird et al. 2002). Mutation of the histone H4 lysine residues targeted by Esa1 likewise results in camptothecin sensitivity (CPT^{s}). These observations mean that lysine acetylation by Esa1 is required for resistance to camptothecin. Much remains to be learned about Esa1's role in DNA repair and other nuclear processes, and its acetylation of H2A.Z is one recent area of focus.

Both Esa1 (Babiarz et al. 2006; Keogh et al. 2006; Millar et al. 2006) and the key transcriptional HAT, Gcn5 (Babiarz et al. 2006) target H2A.Z as a substrate for acetylation. Mutations in either gene also lead to similar mutant phenotypes such as sensitivity to DNA damage (Choy and Kron 2002). H2A.Z has been implicated in boundary formation in silent chromatin, and is also found dispersed throughout the genome (Meneghini et al. 2003; Shia et al. 2006; Raisner and Madhani 2008). Like *esa1* conditional mutants, null mutants of *HTZ1* are sensitive to DNA damaging agents (Kobor et al. 2004; Krogan et al. 2004), revealing a role for H2A.Z in repair of induced DNA damage. A mechanism for this resistance is not yet established (Kalocsay et al. 2009).

A dosage suppressor screen initially identified *LYS20* as a weak suppressor of the *esa1* mutant temperature sensitivity (Clarke, 2001). Lys20 and the closely related Lys21 isozyme have been extensively studied for their roles in lysine biosynthesis (reviewed in Bhattacharjee 1985). Individually, null mutations in *LYS20* and *LYS21*

are prototrophic for lysine: only the double null mutant requires lysine for growth. The enzymes catalyze the first and rate-limiting step in lysine biosynthesis by combining an acetyl group from acetyl CoA with α-ketoglutarate, an intermediate in the Krebs cycle, to make homocitrate. Both enzymes are feedback inhibited by lysine, and catalyze the same reaction, although with different kinetics and sensitivity to cell metabolism (reviewed in Xu et al. 2006; Quezada et al. 2008).

Biochemical fractionation monitored by HCS-specific antibodies and immunofluorescence microscopy place both Lys20 and Lys21 predominantly within the nucleus in a chromatin bound, not freely diffusible form (Chen et al. 1997). This is an unusual localization as the other enzymes in the lysine biosynthetic pathway are located either in the cytoplasm or the mitochondria, as HCS itself had been reported in earlier studies (Jones and Fink 1982).

Results presented here define a role for Lys20 in chromatin function that provides a rationale for the nuclear location of HCS. Overexpression of *LYS20* suppressed the DNA damage sensitivity of *esa1* strains. The suppression is dependent on *HTZ1*. Further, deletion of *LYS20* and *LYS21* suppressed the DNA damage sensitivity of *htz1*Δ, but only if Esa1 was functional. These effects appear mediated through the DNA damage checkpoint, measured by levels of Rad53 phosphorylation upon DNA damage. *LYS20 LYS21* double deletions display increased levels of Rad53 phosphorylation upon DNA damage, and confer increased Rad53 phosphorylation upon *htz1*Δ mutants. *In vitro* assays revealed that Lys20 has weak HAT activity directed toward H4. Lys20 is associated in vivo with the HAT Gcn5. Importantly,

Lys20's contributions to DNA repair are dependent on its nuclear localization, yet independent of its catalytic activity. Thus, Lys20 has dual metabolic and nuclear roles that further connect Esa1 and H2A.Z through histone acetylation and DNA damage.

Results

LYS20 overexpression suppresses esa1 DNA damage phenotypes

LYS20 was identified as a dosage suppressor of the temperature sensitivity of a catalytically compromised *esa1-414* allele of the essential Esa1 HAT (Clarke, 2001). When evaluated for effects on the DNA damage sensitivity of the same strain, increased gene dosage of *LYS20* proved to be a strong suppressor, as indicated by restored growth on camptothecin (Fig 2.1). Suppression of *esa1* mutant phenotypes was also observed upon overexpression of *LYS21* (see Chapter 4) yet was not as robust as that observed with *LYS20.* We therefore focused analysis on *LYS20* as the stronger suppressor and the one more likely to provide unambiguous data.

Of note, simply overexpressing *LYS20* had no effect on either growth or camptothecin sensitivity (CPT^S) of wild-type cells. Furthermore, the effect on *ESA1* mutants was not allele specific as similar suppression was observed with two independent alleles, *esa1-K256Q,Y325N* and *esa-L327S* which are also CPT^S (Fig 2.1).

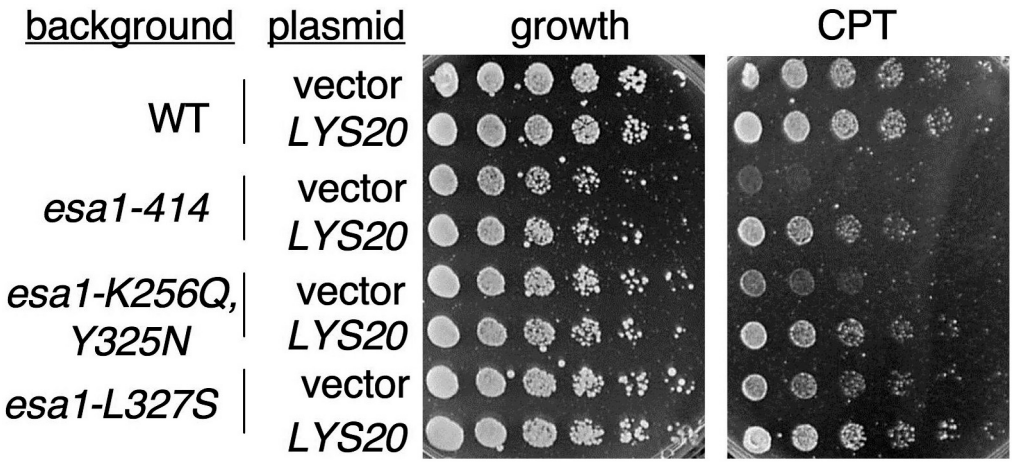

Figure 2.1 *LYS20* suppresses the camptothecin sensitivity of *esa1* mutants. *LYS20* suppresses the CPTs of multiple alleles of *esa1*. Wild type cells, *esa1-414* mutants *esa1-K256Q, Y325N* and *esa1-L327S* mutants were transformed with empty vector or the *LYS20* 2µm plasmid. *LYS20* is transcribed by its endogenous promoter, but is expressed at elevated levels due to increased copy number of the plasmid. The camptothecin plate contains 20µg/mL camptothecin in DMSO.

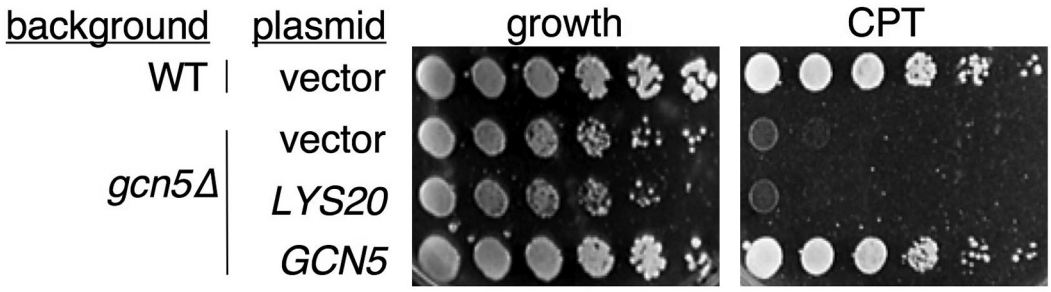

Figure 2.2 Overexpression of *LYS20* does not suppress the camptothecin sensitivity of a *gcn5*Δ mutant. Wild type cells (WT) were transformed with either empty vector or overexpression plasmid containing *LYS20*. The *gcn5*Δ cells were transformed with either empty vector, *LYS20* overexpression plasmid or *GCN5* overexpression plasmid. Plates were synthetic complete medium lacking uracil and were incubated at 30˚C. The camptothecin plate contains 20µg/mL camptothecin in DMSO. Assays were performed as in Fig 2.1.

Because multiple chromatin modifications contribute to DNA damage repair, and loss of the HAT encoded by *GCN5* also results in CPT^S (Choy and Kron 2002), specificity of *LYS20*-mediated suppression was evaluated. In *gcn5*Δ mutants, resistance to camptothecin was restored by transformation with *GCN5*, yet not upon *LYS20* overexpression (Fig 2.2). Thus, *LYS20*-mediated suppression of loss of HAT activity in response to DNA damage appeared specific for the essential Esa1 HAT and is not a general means of restoring defective repair functions.

A key role for the H2A.Z histone variant in esa1 mutants

Because Esa1 acetylates the H2A variant H2A.Z (Babiarz et al. 2006; Keogh et al. 2006; Millar et al. 2006) and both *esa1* and *htz1*Δ mutants are sensitive to camptothecin, the *esa1 htz1*Δ double mutant was evaluated. This strain was even more CPT^s than either individual mutant (Fig 2.3), suggesting that the two genes independently contribute to repair of DNA damage. Supporting this interpretation, CPT^s of the *esa1 htz1*Δ mutants could not be suppressed by *LYS20* overexpression (Fig 2.3). Thus, *LYS20* mediated suppression of *esa1* DNA repair defects depends on *HTZ1*.

In contrast to the protective effect conferred by *LYS20* overexpression in *esa1* mutants, it was possible that deletion of either HCS-encoding gene in otherwise wild type cells might result in sensitivity to CPT. However, no sensitivity was observed upon deletion of *LYS20* or *LYS21*, instead deletion of either gene provided resistance to damage induced by camptothecin (Fig 2.4). The *lys20*Δ *lys21*Δ mutant was

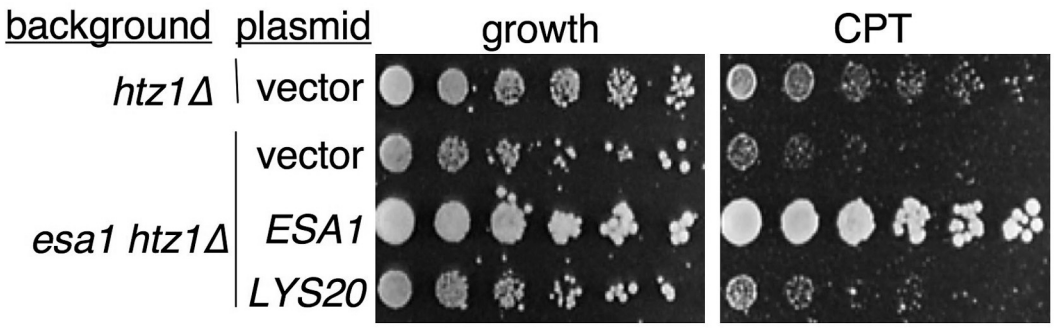

Figure 2.3 *LYS20* suppression of the camptothecin sensitivity of *esa1* mutants is dependent on *HTZ1*. The *esa1 htz1*Δ double mutant was transformed with either empty vector or *LYS20* overexpression plasmid. All plates are synthetic complete medium lacking uracil. The CPT plate contains 30μg/mL of camptothecin in DMSO.

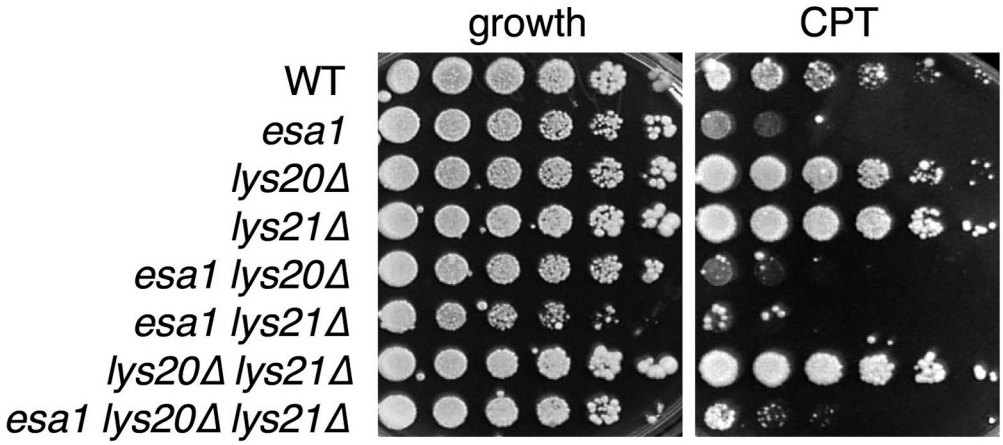

Figure 2.4 Mutants in *LYS20* and *LYS21* are resistant to camptothecin. Resistance to CPT is dependent upon *ESA1*. Strains were assayed as in Figure 2.1. YPD based CPT plate contains 40μg/mL of camptothecin in DMSO.

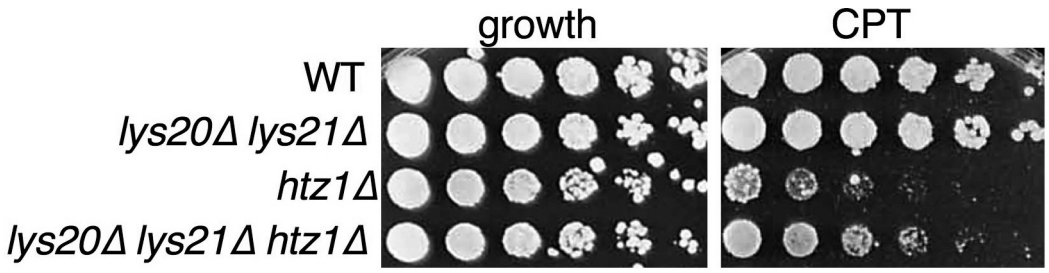

Figure 2.5 Deletion of *LYS20* and *LYS21* suppresses *htz1*Δ DNA damage sensitivity. All plates were incubated at 33˚C. All plates are YPD based. The CPT plates contain 20μg/mL camptothecin in DMSO and were incubated 5 days longer than growth control.

comparably resistant. The *esa1 lys20*Δ *lys21*Δ triple mutant was sensitive, demonstrating that *esa1*'s defect was epistatic to the resistance afforded by loss of HCS. Next, the *htz1*Δ *lys20*Δ *lys21*Δ mutant was evaluated. In this case, deletion of *LYS20* and *LYS21* suppressed the camptothecin sensitivity of *htz1*Δ (Fig 2.5), in contrast to the *esa1* result. These observations suggest that HCS might be involved in two pathways in response to DNA damage that are distinguished by functional interaction with the variant histone H2A.Z and the Esa1 HAT.

As shown in Figure 2.3, the suppression of *esa1* CPT^s by overexpression of *LYS20* is dependent on *HTZ1*. This raises the question of whether the suppression of *htz1*Δ CPT^s is reciprocally dependent upon *ESA1* function. To address this question, the quadruple *esa1 htz1*Δ *lys20*Δ *lys21*Δ mutant was generated and tested for DNA damage sensitivity (Fig 2.6). Because of the extreme hypersensitivity of *htz1*Δ *esa1* cells, lower concentrations of drug were used than in earlier assays. As seen in the bottom row, the quadruple mutant remained as sensitive as the *esa1 htz1*Δ double mutant, thus demonstrating that Esa1activity is required for the rescue of *htz1*Δ mutants by deletion of *LYS20* and *LYS21* upon DNA damage caused by inhibition of topoisomerase I.

DNA damage can be induced in many ways. In contrast to camptothecin, hydroxyurea (HU) inactivates ribonucleotide reductase, ultimately leading to accumulation of double stranded breaks near DNA replication forks (reviewed in Saban and Bujak 2009). To evaluate the specificity of damage sensitivity and resistance, analysis was performed with HU as the drug challenge (Fig 2.7).

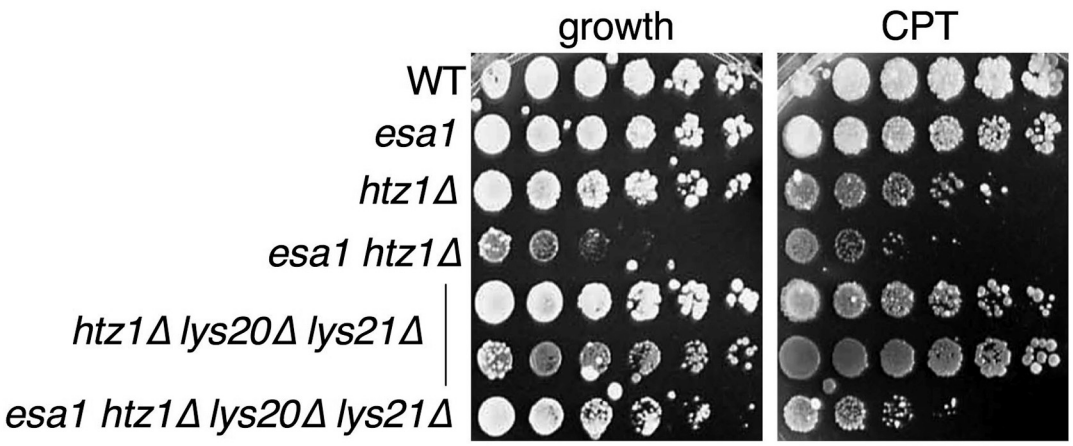

Figure 2.6 Suppression is dependent upon *ESA1*. Independent strain isolates were assayed as in Figure 2.1. Plates were incubated at 30˚C. All plates are YPD based. CPT plate contains 20μg/mL camptothecin in DMSO. Vertical bar indicates plating of two independent triple mutants.

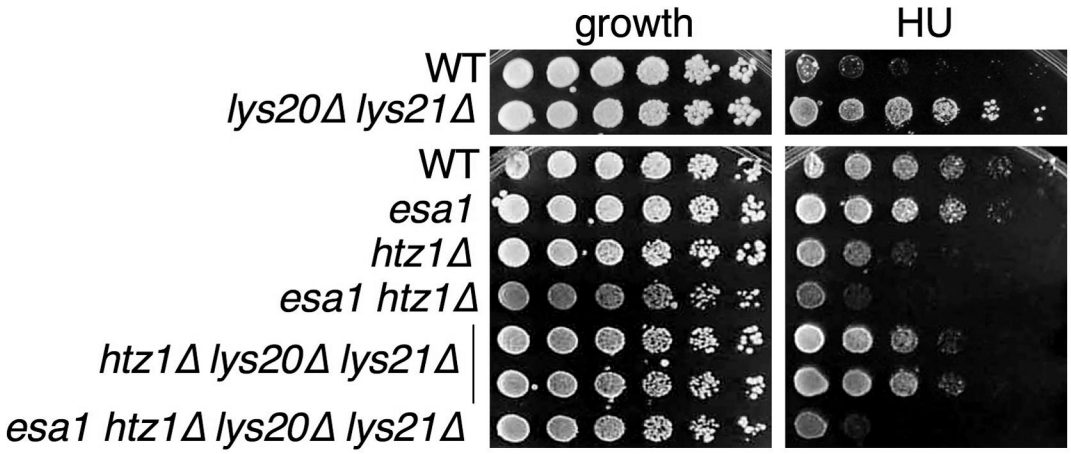

Figure 2.7 Suppression is evident with hydroxyurea induced damage. Strains assayed as before on YPD or SC as growth control or on 0.1M hydroxyurea (HU). HU plate incubated an additional 3 days in top panel, additional 5 days in bottom panel. Plates incubated at 30˚C. Vertical bar indicates plating of two independent triple mutants.

As for CPT, the *lys20*Δ *lys21*Δ double mutant was more resistant than wild type cells. Similar to our observations with CPT, and as previously reported, *htz1*Δ mutants are sensitive to HU (Kobor et al. 2004). This sensitivity is suppressed by elimination of *LYS20* and *LYS21*, and in parallel to Figure 2.6, the extreme sensitivity of the *esa1 htz1*Δ mutant cannot be suppressed by the elimination of *LYS20* and *LYS21.*

It remained a possibility that the suppressive effect of deleting *LYS20* and *LYS21*, thereby preventing all HCS activity, was due to lysine auxotrophy. To evaluate this possibility, a *lys2*Δ *htz1*Δ strain that requires lysine for growth due to loss of an independent step in the biosynthetic pathway was examined. In this case, suppression of DNA damage sensitivity was not observed (Fig 2.8). Thus, the restored growth in the presence of at least two DNA damaging agents imparted by deletion of *LYS20* or *LYS21* is independent of the known synthetic function of these genes.

A molecular link between LYS20 and the DNA damage checkpoint response

DNA damage repair can fail at multiple steps: sensing of damage, checkpoint activation, or by defects in the repair process itself. There are molecular hallmarks for many of these steps. For example, phosphorylation of Rad53 is a key indicator of DNA damage checkpoint activation. This is readily monitored by immunoblotting for Rad53, which is hyperphosphorylated upon checkpoint activation and thereby migrates with decreased electrophoretic mobility (Sanchez et al. 1996; Sun et al. 1996).

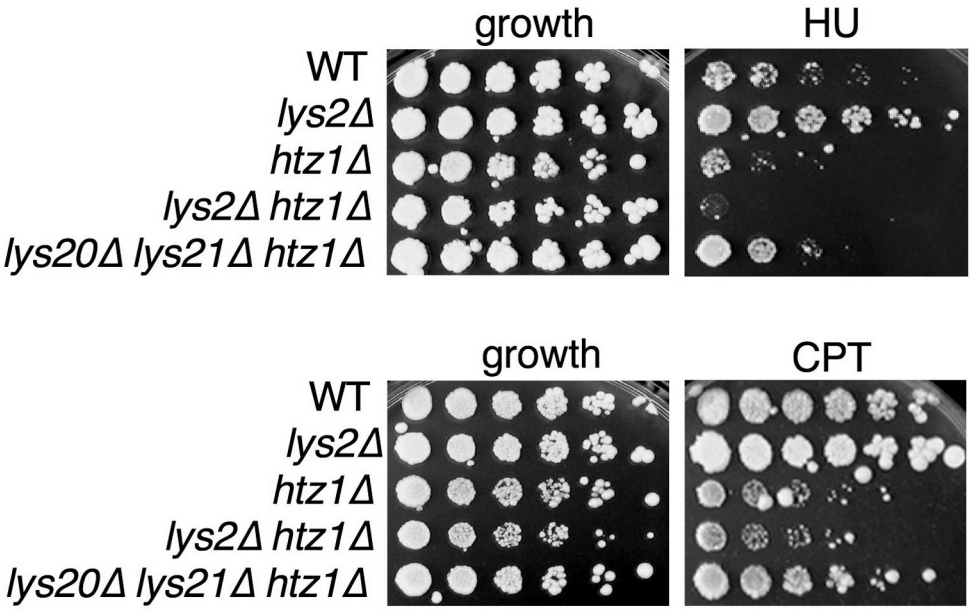

Figure 2.8 Suppression of *htz1*Δ 's DNA damage sensitivity by *lys20*Δ *lys21*Δ is not due to lysine auxotrophy. YPD-based plates were incubated at 30˚C. Camptothecin plate is 20μg/mL of CPT. HU plate contains 100mM HU. Growth control plates were incubated 4 fewer days than drug plates. Deletion of either *LYS20* or *LYS21* alone causes resistance, but does not cause auxotrophy, further evidence that DNA damage phenotypes are not due to lysine auxotrophy.

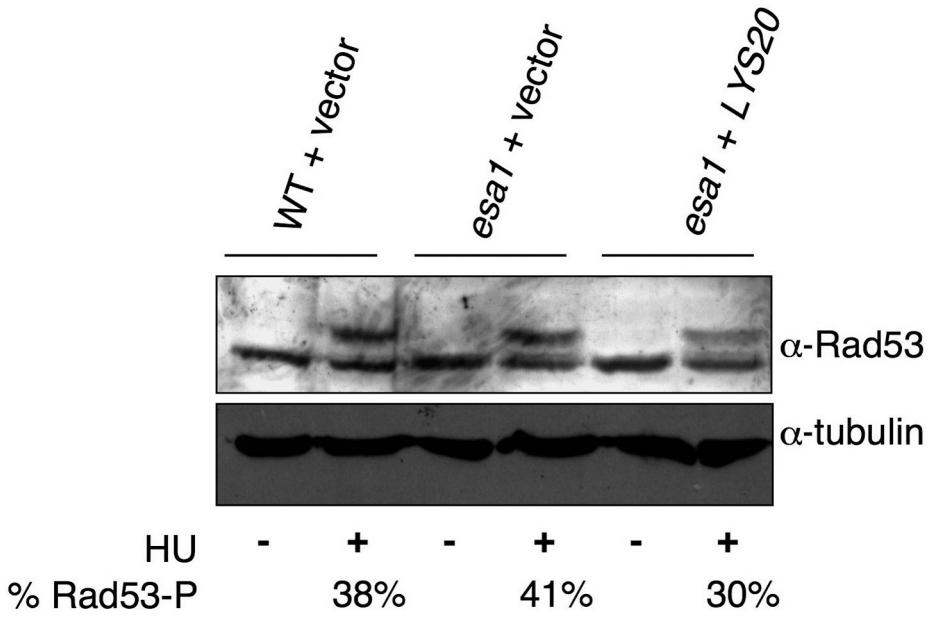

Figure 2.9 Rad53 phosphorylation status during DNA damage and suppression. The Rad53 phosphorylation shift upon HU–induced DNA damage is not significantly affected by overexpression of *LYS20*. Extracts were prepared for cells with indicated genotype. Immunoblots with anti-Rad53 antibody are shown. In samples treated with HU, the proportion of phosphorylated Rad53 was quantified and is indicated as a percentage of total Rad53.

A Rad53 phosphorylation shift is visible in wild type cells upon incubation with HU (Fig 2.9). Rad53 phosphorylation is also seen in *esa1* mutants and phosphorylation does not change significantly upon overexpression of *LYS20*. This indicates that *esa1* mutants activate the Rad53 checkpoint normally, so their CPT^S and rescue by *LYS20* must result from a different mechanism. By comparison, *lys20*Δ *lys21*Δ double mutants have increased Rad53 phosphorylation upon induction of damage by HU (Fig 2.10). If this indicates improved or hyperactivation of the checkpoint, it could explain the protective effects seen in *lys20*Δ *lys21*Δ mutants (Fig 2.4).

In contrast, *HTZ1* mutants were recently reported to be defective in Rad53 phosphorylation in response to DNA damage (Kalocsay et al. 2009). In Figure 2.10, this defect is observed, whereas in the *htz1*Δ *lys20*Δ *lys21*Δ triple mutant DNA damage-induced phosphorylation is restored, thereby correlating a molecular marker of DNA repair with suppression of DNA damage (Fig 2.11).

Since *esa1* mutants have no defect in Rad53 phosphorylation, it was noteworthy that *esa1 htz1*Δ mutants had reduced Rad53 phosphorylation when damage was induced (Fig 2.11). This defect was partially suppressed by deletion of *LYS20* and *LYS21*. In the quadruple mutant, deletion of *LYS20* and *LYS21* can still restore Rad53 phosphorylation to *htz1*Δ cells. Therefore, mutation of *esa1* must confer sensitivity to DNA damage by a Rad53-phosphorylation independent mechanism and suppression by overexpression of *LYS20* does not proceed via a Rad53-dependent

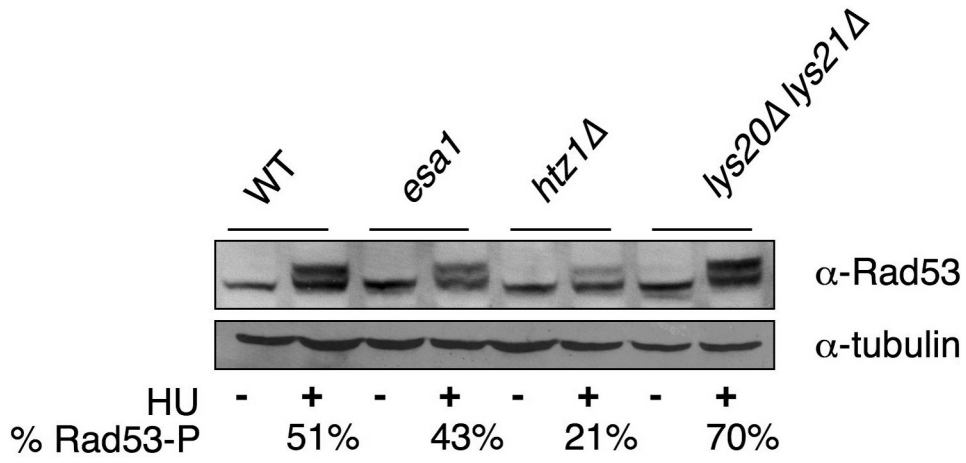

Figure 2.10 The *htz1*Δ mutants had reduced Rad53 phosphorylation upon hydroxyurea (HU) treatment. Methods are as described in Figure 2.9.

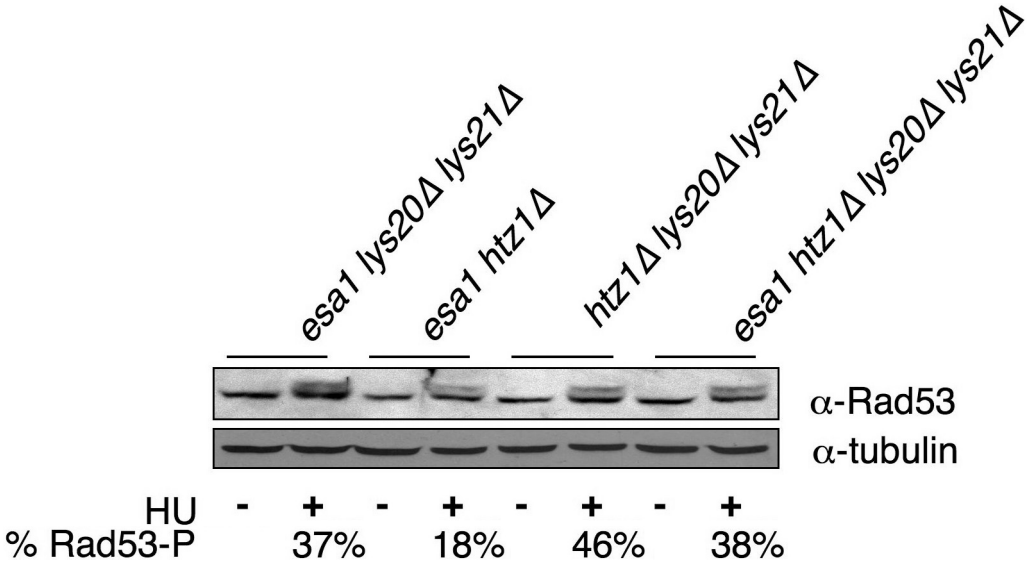

Figure 2.11 The *htz1*Δ mutants had reduced Rad53 phosphorylation upon DNA damage. This defect was suppressed by deletion of *LYS20* and *LYS21*.

mechanism. Since suppression of *htz1*Δ damage is correlated with Rad53 phosphorylation, yet suppression of *esa1* damage is not, it appears that HCS functions in DNA damage by more than one mechanism.

Defining catalytic and chromatin functions of Lys20

Given Lys20's nuclear localization (Chen et al. 1997), its newly discovered role in DNA damage reported here, and its acetyl CoA binding for catalysis as part of the HCS reaction, we considered the possibility that the enzyme might function as a non-canonical HAT. To test this hypothesis, *in vitro* HAT assays were performed with recombinant Lys20 protein, using Esa1 as the positive control. In these assays, enzymes were incubated with histone substrates and [^{3}H] acetyl CoA. Assays using recombinant core histones as substrate yielded activity for Esa1 but not for Lys20 (data not shown). Assays performed with commercially prepared calf thymus histones were also negative. However, when histones purified from yeast were used as substrate, HAT activity was observed for both Esa1 and Lys20. Lys20 activity was directed toward histone H4 and often visible only in the presence of lysine (Fig 2.12).

The observations that Lys20 has roles both in lysine biosynthesis and in DNA repair suggest it may act as a bifunctional protein. The requirement for yeast histones as substrate implies that Lys20 may require some pre-existing modification(s) on the histones to be active as a HAT. Esa1 HAT activity in these assays is robust, perhaps due to the fact that Esa1 is a global HAT, acetylating multiple lysine residues spread over core and variant histones. Lys20, in contrast, may have more restricted activity and target many fewer residues or only one residue. Activity in the assay appears

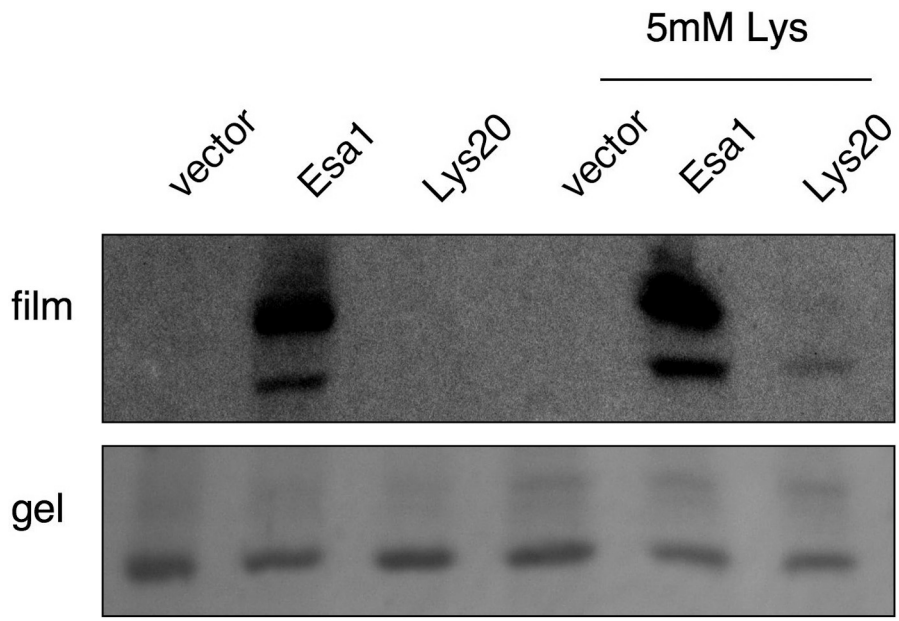

Figure 2.12 Lys20 has HAT activity in the presence of lysine. Lys20 has HAT activity *in vitro* in the presence of lysine. Recombinant Lys20, Esa1 or empty vector extract were added to purified yeast histones and incubated with [^{3}H]-acetyl-CoA. The reaction was analyzed by 18% SDS-PAGE, and by autoradiography. Vector indicates samples prepared from cells transformed with the empty vector. In lanes at right, lysine was added to 5mM.

primarily directed towards histone H4, but this may be in the context of H2A.Z containing nucleosomes, since suppression studies demonstrate that Lys20's activity in vivo is dependent on H2A.Z (Fig 2.3). The absolute requirement for histones purified from yeast as substrate has thus far prevented definition of substrate site specificity. We have, however, tested several Esa1 H4 target residues (including H4K5,8,12 and H3K14, see Fig 4.1 and 4.2) under suppressing conditions by immunoblotting with isoform specific antibodies, but no definitive target for Lys20 has yet been uncovered.

Because Lys20 had been previously reported to be chromatin bound (Chen et al. 1997), we considered that it might be associated with nuclear components that participate in processes under study here. To test this possibility, Lys20 was assayed for co-immunoprecipitation with known chromatin associated proteins. Under the conditions tested with epitope-tagged proteins or protein-specific antisera, there was no evidence for association with histones H3, H4, Htz1 or Esa1 (Fig 4.15-4.18). However, Lys20 and the HAT Gcn5 were observed to coprecipitate (Fig 2.13). The association is specific and not due to the epitope-tag on Gcn5 No signal was observed in the *lys20*Δ *lys21*Δ untagged strain.

These data reveal that not only is Lys20 in the nucleus, a fact that was known previously, but that it is also associated with the HAT Gcn5. Because we found that *LYS20* and *gcn5*Δ did not interact functionally as *LYS20* did with *esa1* (Fig 2.2), this

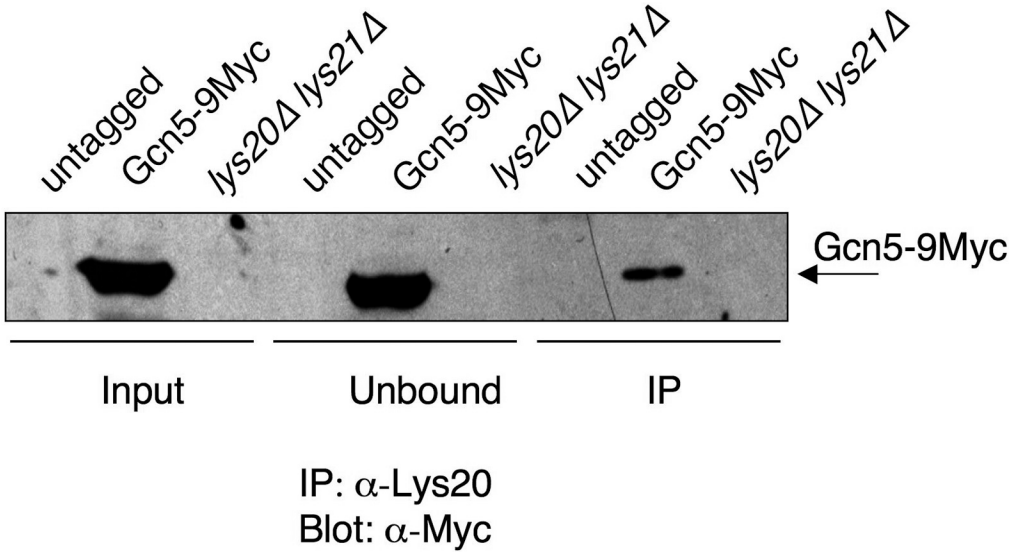

Figure 2.13 Lys20 interacts with Gcn5-9Myc. Immunoprecipitations of whole cells extracts from the indicated strain were performed with anti-HCS antibody. The precipitated material was blotted to detect Gcn5-9Myc.

physical interaction might be unexpected. However, it has been argued (Collins et al. 2007), that molecules interacting physically often do not do so genetically, thereby demonstrating that functional and physical interaction networks can be distinct.

In defining Lys20's nuclear role, it was important to determine if its role in lysine biosynthesis is separable from its functions in repair. To this end, point mutants were constructed to abolish the HCS activity of Lys20 that were based on the crystal structure of the *S. pombe* HCS (Bulfer et al. 2009). Two residues were selected, R31 and E155, both of which lie in the active site and which have been shown to be essential *in vitro* and *in vivo* for catalysis. The residues were mutated to encode alanine and assayed for HCS activity by testing for cell growth in the absence of lysine. In wild type cells, there was no interference with growth, indicating that the mutants are recessive. In *lys20*Δ *lys21*Δ strain, there was no growth, demonstrating that the mutants were unable to sustain HCS activity (Fig 2.14). The mutants were then tested to see whether they could still suppress the camptothecin sensitivity of *esa1*. The mutants could suppress (Fig 2.14). Therefore, the catalytically inactive alleles of *LYS20* demonstrate that it is possible to distinguish two functions for HCS and that its function in biosynthesis is not required for its role in the repair of DNA damage.

Nuclear localization of Lys20 is required for its DNA repair functions

Since Lys20's role in lysine synthesis can be distinguished from its role in DNA damage repair, is it possible to link one or both of these roles to the protein's localization to the nucleus? To answer this question, two approaches were taken.

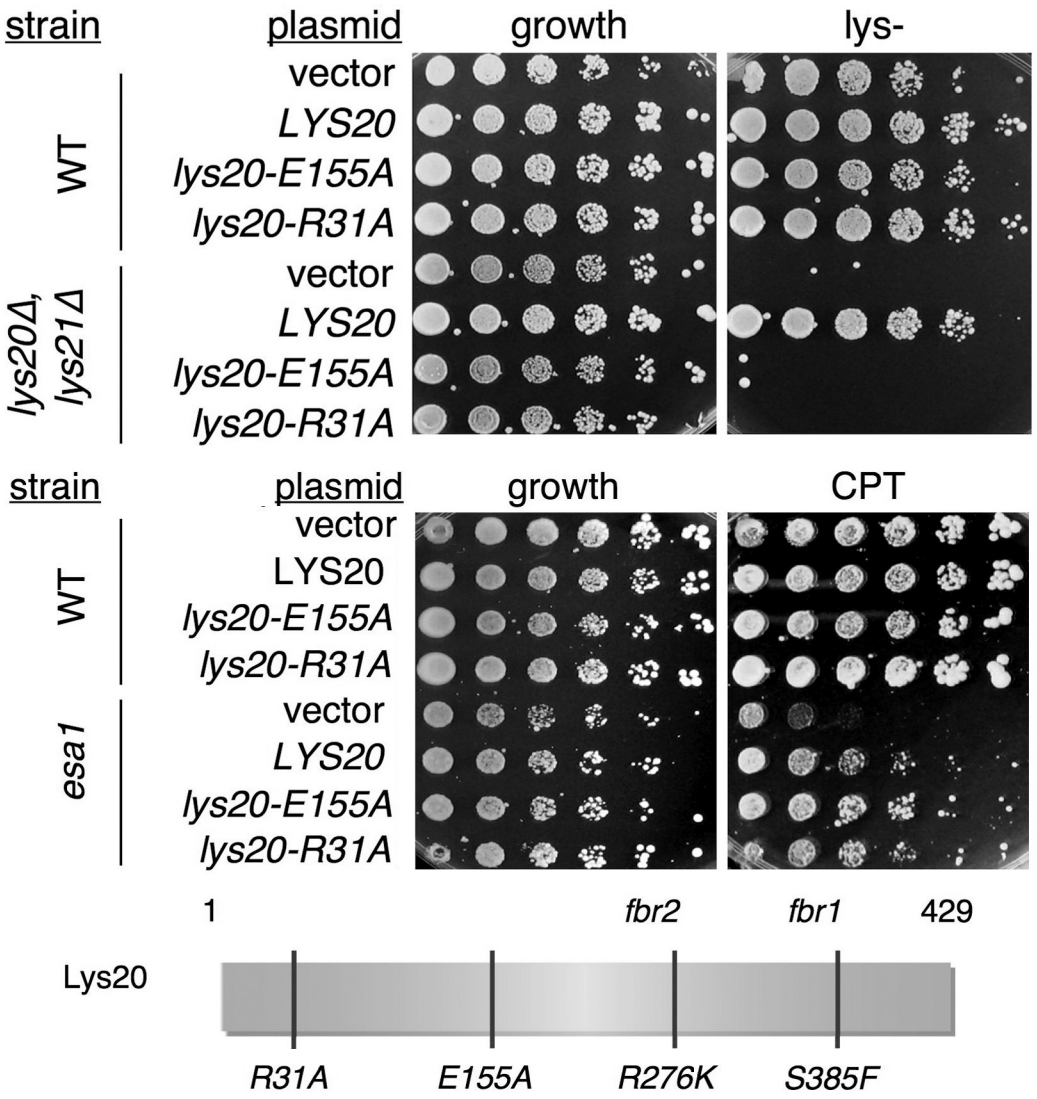

Figure 2.14 HCS catalytic activity is not required for nuclear functions of Lys20. Mutant alleles that are defective in lysine biosynthesis remain competent for suppression of DNA damage. CPT plate was incubated 3 days longer than control plate.

First, in an effort to understand how Lys20 is localized *in vivo*, we considered that at a predicted molecular mass of 47KDa, Lys 20 is above the limit defined for free diffusion through the nuclear pore and accumulation in the nucleus (reviewed in Terry et al. 2007). Uptake of proteins may be facilitated by other nuclear import molecules, or by integral nuclear localization sequences (NLSs) that serve to drive the import of proteins to the nucleus after their synthesis in the cytoplasm. Several distinct classes of NLSs have been characterized, some of which are short tags that are rich in charged lysine and arginine residues (Hicks and Raikhel 1995).The PSORT algorithm (Horton and Nakai 1997) was used to search for a nuclear localization sequence (NLS) in Lys20. A potential NLS of the Pat7 class was found beginning with the proline 10 residues from the C-terminus of the protein. To test the functional significance of this potential NLS, the lys20ΔC10 construct was created that truncated the protein to remove the PAAKRTK putative localization signal and the final 3 amino acids of the protein. In a second independent approach a nuclear export sequence (NES) was added to Lys20 (*lys20-NES*). By analogy with NLSs, NESs function to facilitate shuttling of proteins from the nucleus to the cytoplasm (Moroianu 1999). The NES selected was a variant of the robust signal defined in PKI that can drive export of heterologous proteins (Gadal et al. 2001; Zhang and Xiong 2001).

Both constructs Lys20ΔC10 and Lys20-NES were expressed in wild type (Fig 2.15), *lys20*Δ *lys21*Δ*,* and *esa1* cells. They were tested for localization by immunofluorescence microscopy, and for function in lysine biosynthesis and repair of DNA damage.

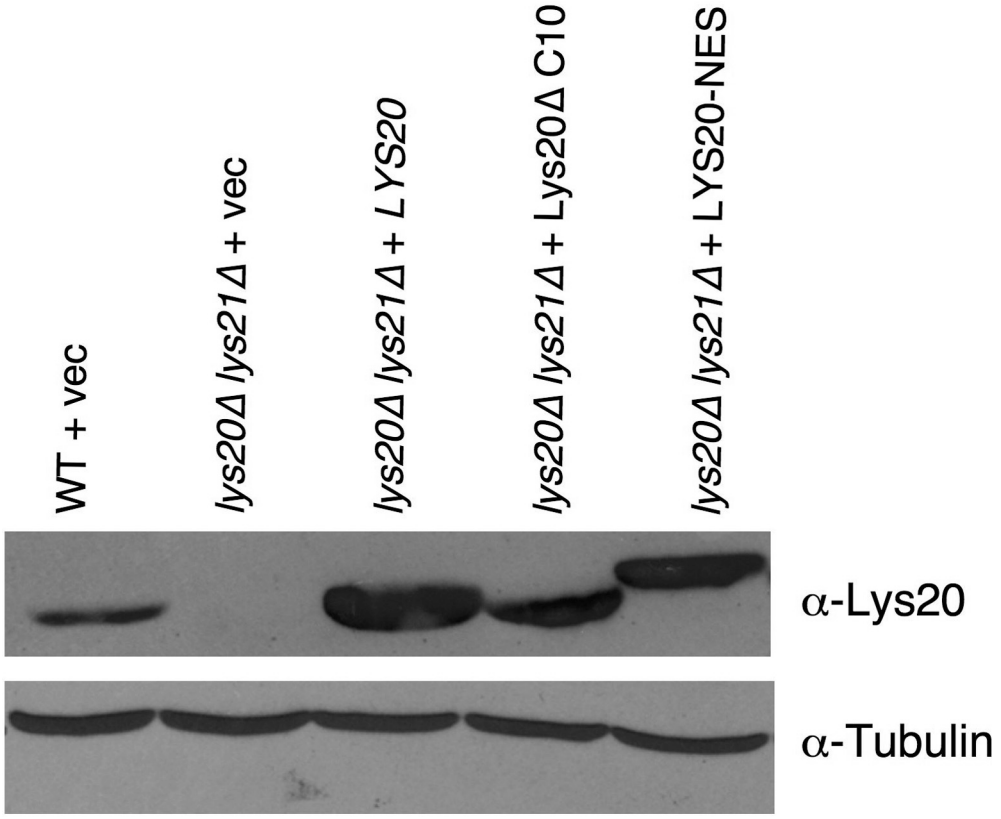

Figure 2.15 Both Lys20ΔC10 and Lys20-NES are expressed in *S. cerevisiae*. Plasmids containing empty vector, WT Lys20, lys20ΔC10 or lys20-NES are transformed into *lys20*Δ *lys21*Δ cells to assay protein expression. Wild type cells are shown at left. Protein extracts from cells were analyzed by immunoblot. Protein levels were assayed with anti-Lys20 antibody.

Figure 2.16 Nuclear functions of Lys20 depend upon nuclear localization. Mutants were constructed to remove a putative nuclear localization sequence (NLS) at the C-terminus of Lys20 (Lys20ΔC10) and to add a potent nuclear export sequence to the wild type Lys20 protein (Lys20-NES). Immunofluorescence microscopy demonstrated that the wild type protein was enriched in the nucleus, whereas the two mutant proteins are enriched in the cytoplasm. Cells are stained with DAPI for DNA and Lys20 is seen in red. Representative cells are shown for each strain. Scale bar represents 1μm.

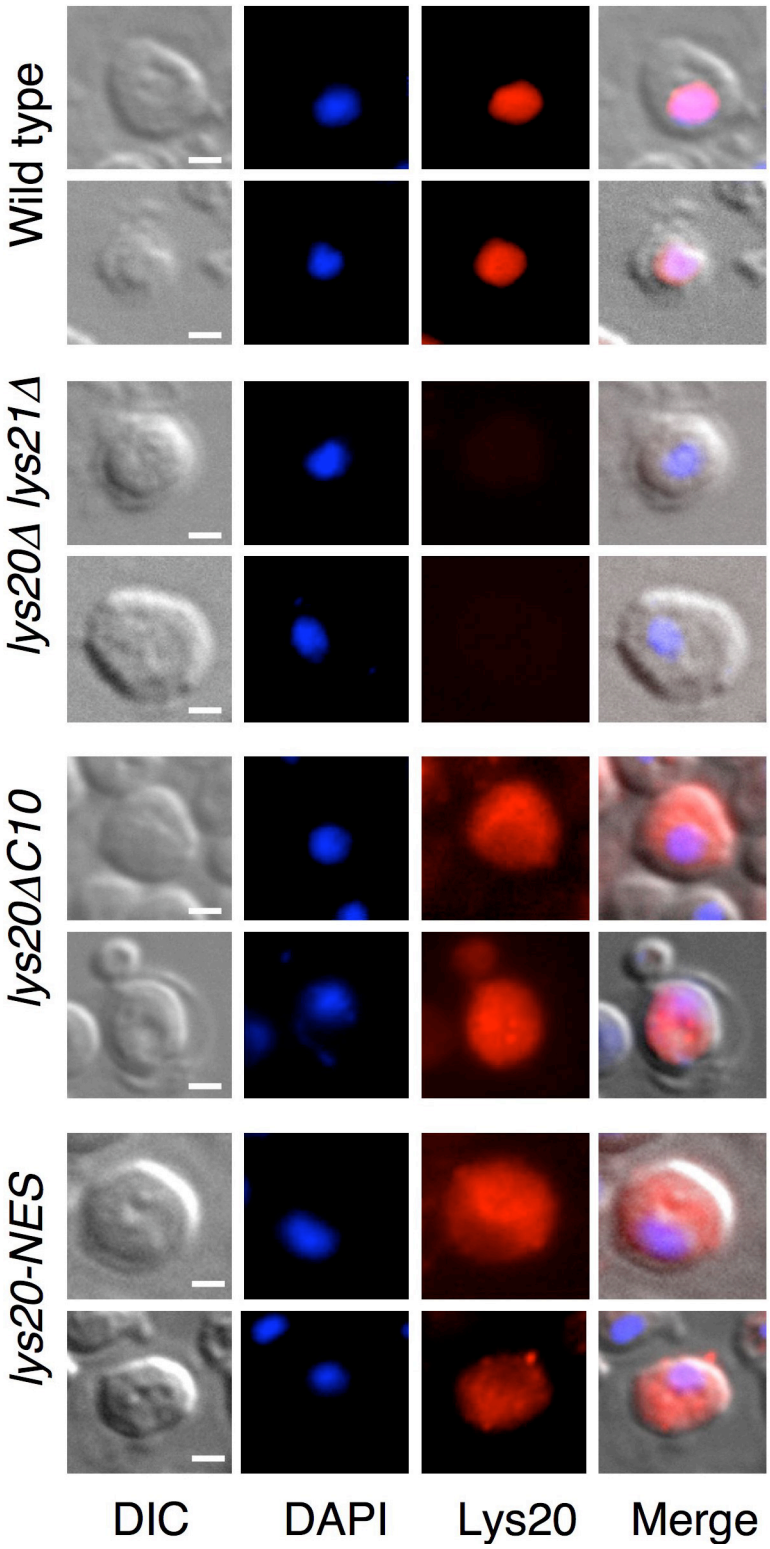
Wild type
lys20Δ lys21Δ
lys20ΔC10
lys20-NES
DIC
DAPI
Lys20
Merge

Using the antibody that first defined its nuclear localization (Chen et al. 1997), we found that wild type Lys20 was nuclear, as reported, with no signal in the *lys20*Δ *lys21*Δ cells. In contrast, neither Lys20-NES nor Lys20-ΔC10 was restricted to the nucleus (Fig 2.16).

When assayed for HCS activity, both Lys20ΔC10 and Lys20-NES were fully competent to support growth in the absence of lysine (Fig 2.17). When assayed on camptothecin, *esa1* 's sensitivity was not suppressed to wild type levels (Fig 2.18). Thus, Lys20 metabolic activity does not depend on its nuclear localization, but efficient DNA damage suppression does require intact localization.

Discussion

We demonstrate that *LYS20*, which encodes homocitrate synthase, functionally interacts with the essential HAT Esa1 in vivo. The *HTZ1* gene encoding the H2A variant H2A.Z mediates this interaction and also interacts with *LYS20* through a functionally distinct mechanism. All three genes are linked to the repair of DNA damage. These findings define a previously unappreciated role for Lys20 that explains the longstanding mystery of its nuclear localization (Chen et al. 1997). In suppressing *htz1*Δ CPT^S, the *LYS20, LYS21* deletion restores DNA damage-induced hyperphosphorylation of the Rad53 checkpoint protein (Fig 2.10). However, it appears that the step affected by *esa1* DNA damage sensitivity is downstream of Rad53 because Rad53 phosphorylation levels are not perturbed in *esa1* mutants and *esa1 lys20*Δ *lys21*Δ triple mutants are still sensitive to DNA damage (Fig 2.10 and 2.11).

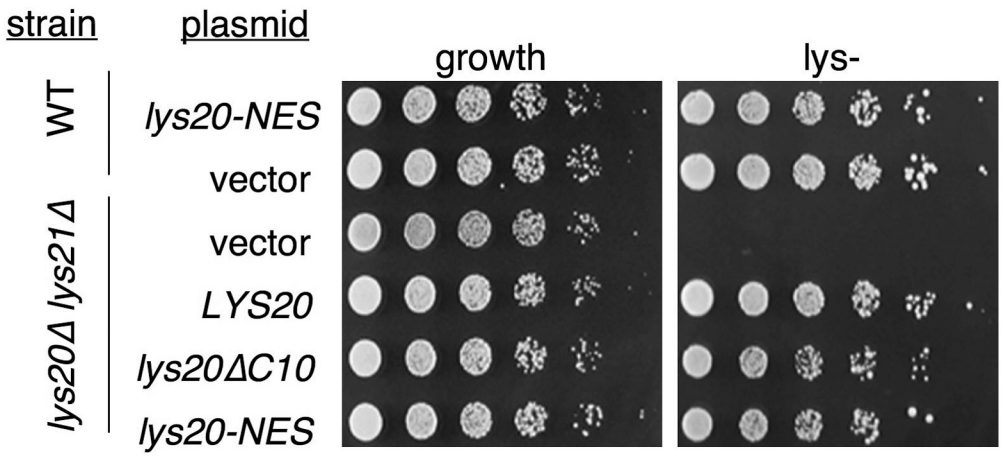

Figure 2.17 The Lys20ΔC10 and Lys20-NES, cytoplasmic proteins, are competent for HCS activity and not dominant when plated on lys- medium.

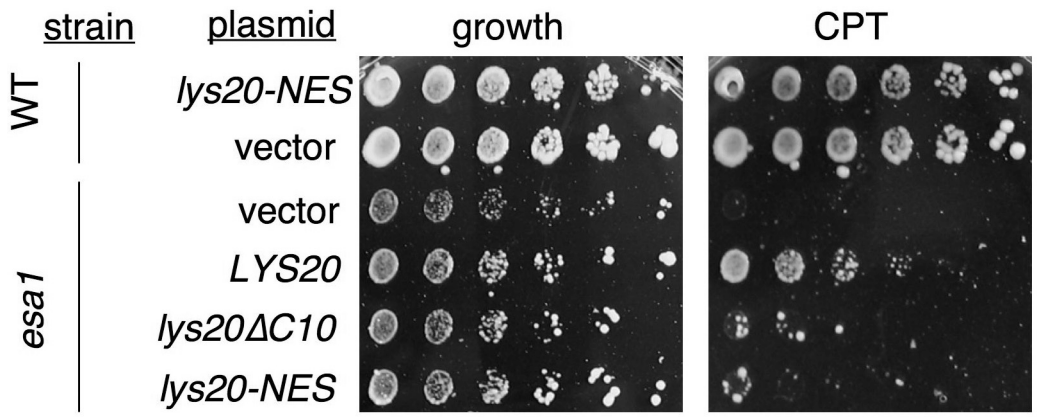

Figure 2.18 When tested for suppression of DNA damage, *lys20ΔC10* and *lys20-NES* do not strongly suppress the *esa1* CPTs to *LYS20* levels.

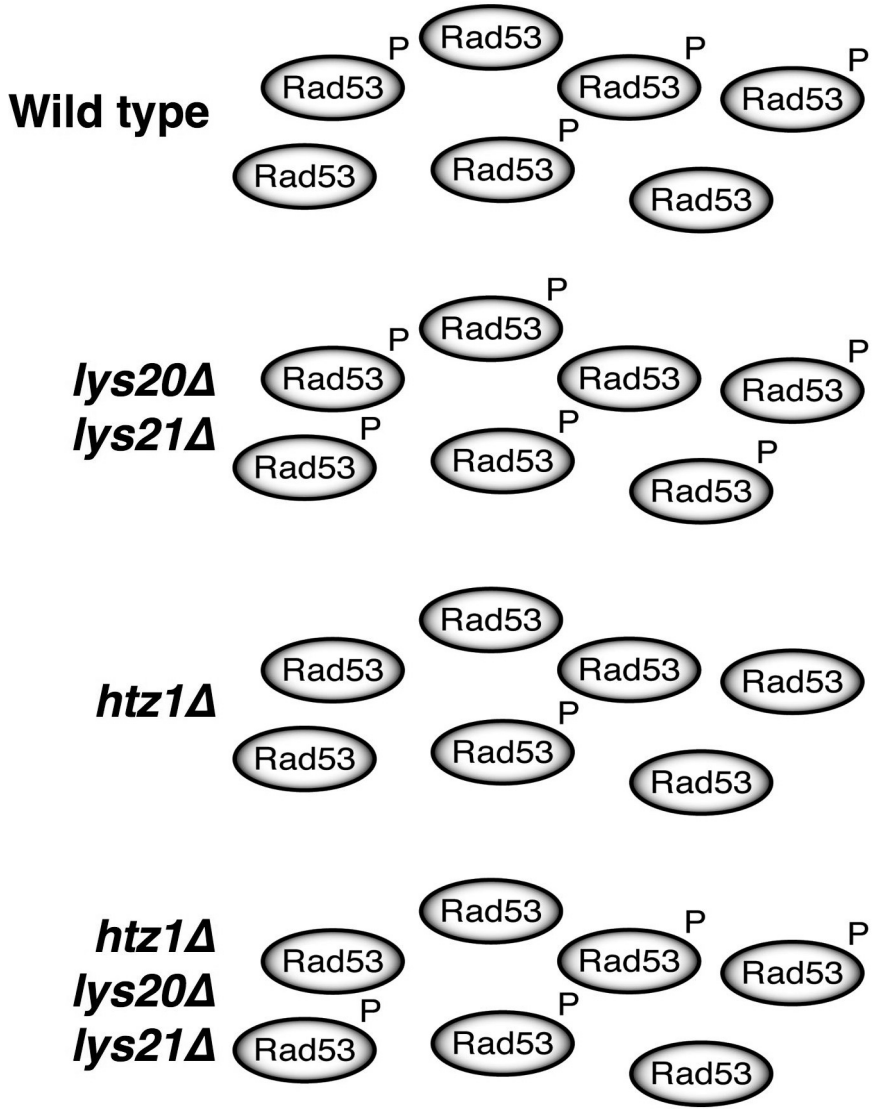

Figure 2.19 Roles for the bifunctional protein Lys20 in chromatin and DNA damage repair. Suppression of *htz1*Δ CPT^s by deletion of *LYS20* and *LYS21* may be mediated through Rad53 phosphorylation upon DNA damage. WT cells respond by phosphorylating Rad53, indicated by a pool of phosphorylated protein. The *lys20*Δ *lys21*Δ cells have increased Rad53 phosphorylation relative to wild type. In contrast, *htz1*Δ mutants are defective in Rad53 phosphorylation, whereas suppression of the *htz1*Δ mutants by *lys20*Δ *lys21*Δ is correlated with restoration of Rad53 phosphorylation.

A lysine-induced switch?

Lysine itself is a regulator of Lys20 and Lys21 through feedback inhibition (Tucci and Ceci 1972; Feller et al. 1999). It has recently been demonstrated (Bulfer et al. 2010) that the mechanism used for feedback inhibition by the functionally conserved *S. pombe* HCS is competitive inhibition, where lysine competes with α-ketoglutarate for access to the active site, effectively shutting down the homocitrate synthase reaction at high levels of lysine. It is possible that when lysine inhibits HCS activity, it may stimulate a switch to enhance HAT activity, as observed *in vitro* (Fig 2.12). We note that two point mutants that abolish Lys20's sensitivity to lysine, rendering it resistant to feedback inhibition (Feller et al. 1999), still suppress the CPT^S of *esa1* (Fig 2.20). In this case, although the switch for the HCS reaction is lost, it appears that the distinct nuclear function(s) for Lys20 remain active.

Non-canonical HATS and metabolic enzymes in the nucleus

Studies of the global repertoire of histone acetylation by mass spectrometry indicate that many lysine residues on histones are acetylated (reviewed in Mersfelder and Parthun 2006). For many of these, the enzymes responsible for acetylation have not yet been identified. Whereas most analysis has focused on N-terminal residues, residues in the globular domain and C-terminal tails are also acetylated (reviewed in Mersfelder and Parthun 2006).

For example, H3K56, a residue that lies at the protein:DNA interface of the nucleosome surface is acetylated and functions in cell cycle regulation and DNA

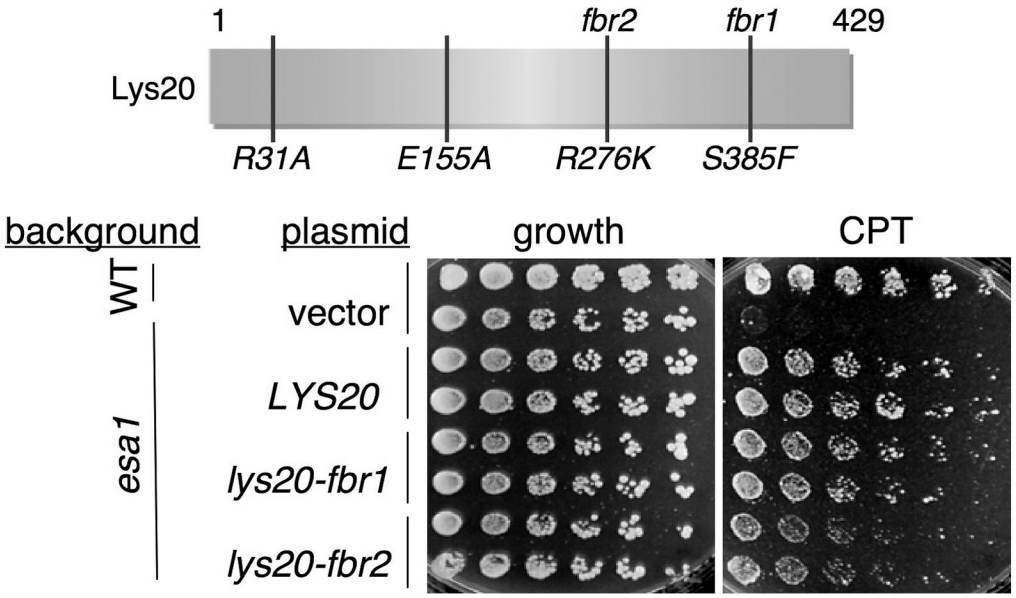

Figure 2.20 Lysine feedback inhibition resistant mutants of *LYS20* suppress *esa1* camptothecin sensitivity. Wild type cells were transformed with vector plasmid. *esa1* mutants were transformed with empty vector, *LYS20* plasmid, *lys20-fbr1* plasmid or *lys20-fbr2* plasmid. The allele *lys20-fbr1* is a substitution of Ser 385 for Phe; *lys20-fbr2* isa substitution of Arg 276 for Lys (Feller et al. 1999). Both plates are synthetic complete medium lacking uracil. The CPT plate contains 30µg/mL camptothecin in DMSO. Plates were incubated at 30˚C.

damage sensitivity (Masumoto et al. 2005; Xu et al. 2005; Celic et al. 2006). Rtt109, a non-canonical HAT, is responsible for this modification (Driscoll et al. 2007; Han et al. 2007). For other less well-defined modified residues, it remains an open question of whether they are additional targets of known global HATs, such as Esa1, or if they are targets of non-canonical HATs, Lys20 potentially among them.

Residues in the globular and C-terminal domains of histones are also likely to be important for cell viability. Recently, 18 non-N-terminal residues were shown to be essential for cell viability (Hyland et al. 2005; Matsubara et al. 2007; Nakanishi et al. 2008). Although none are lysine residues, six encode residues potentially subject to posttranslational modification and may contribute to additional 'cross'-talk and regulation by non-canonical histone modifying enzymes.

The mammalian enzyme NCOAT may serve as a paradigm for Lys20. NCOAT was first identified as an O-GlcNAc transferase that was subsequently shown to have HAT activity (Toleman et al. 2004). Discovery of its HAT activity made it one of a small but growing number of enzymes that have a role in chromatin in addition to distinct metabolic functions.

Cellular metabolism, in the form of glycolytic activity and acetyl CoA levels, also directly influences global levels of histone acetylation, providing additional links between metabolic enzymes and modification of chromatin (Takahashi et al. 2006). Of note is that the enzymes responsible for these effects in both yeast and humans have distinct nuclear pools (Friis et al. 2009; Wellen et al. 2009). Other connections

between transcription and metabolism relate specifically to Esa1. Already known to acetylate some nonhistone substrates, Esa1 was also reported to acetylate Pck1, a metabolic enzyme. This directly connects Esa1 to regulation of cellular metabolism (Lin et al. 2009). Whether Lys20 shares the ability to modify non-histone substrates remains to be determined.

Independent studies have begun to link metabolism to DNA damage. Mutants in the gluconeogenesis enzyme Fbp1 (fructose bisphosphatase), for example, are resistant to MMS-induced DNA damage, potentially through a mechanism tied to metabolic flux (Kitanovic and Wolfl 2006). Another parallel for Lys20, in terms of DNA repair, may be the Krebs cycle enzyme fumarase, which was recently discovered to have DNA repair functions dependent on its catalytic activity (Yogev et al. 2010). Checkpoint activation is impaired in fumarase mutants, and mutants are sensitive to DNA damage, in contrast to *lys20*Δ. Nevertheless, this report provides further evidence linking DNA damage to a metabolic enzyme.

Another example of an enzyme involved in both DNA damage and lysine biosynthesis is Lys7, now called Ccs1. Ccs1 is the copper chaperone for the major superoxide dismutase (SOD) enzyme in yeast that functions in detoxifying reactive oxygen species (Gamonet and Lauquin 1998). Mutants in *CCS1* are very sensitive to radical-induced DNA damage, as the function of SOD is compromised. For as yet undiscovered reasons, *ccs1*Δ mutants are lysine auxotrophs. Indeed, *sod1*Δ mutants are also auxotrophic for both lysine and methionine. One proposed mechanism for the *sod1*Δ lysine auxotrophy is that one of the enzymes in the biosynthetic pathway may

simply be very sensitive to the presence of reactive oxygen species (Slekar et al. 1996). However, our data argue for a tighter link between DNA damage and lysine biosynthesis: *lys20*Δ *lys21*Δ mutants are not only resistant to DNA damage, but the agents used to induce the damage are not radical generators. Instead, the resistance of *lys20* Δ*lys21*Δ mutants seems to be specific to DNA double-stand break inducing agents such as HU and CPT as resistance does not extend to UV induced damage (data not shown).

Implications for the evolution of bifunctional proteins and chromatin regulation

Linking two cellular processes to one enzyme, as shown here for Lys20, raises evolutionary implications. The ability to bind and utilize a molecule common to many processes, such as acetyl CoA, confers on an enzyme the possibility to contribute to multiple pathways and simultaneously links those pathways. Like the discovery of Arg5's transcriptional activation function, and NCOAT's HAT activity, bifunctionality expands the number of reactions that can be catalyzed by any genome. The appreciation of bifunctional or 'moonlighting' enzymes is growing in humans (reviewed in Jeffery 2003). Bifunctionality provides a mechanism for increasing the number of possible enzymatic reactions conserved between species, even if individual enzymes are not. Indeed in evolution it may be more effective to modify an existing protein to take on additional functions rather than to evolve an entirely separate molecule for each new challenge.

Bifunctional proteins may often be regulated by localization. In organisms with many cell types, one protein may have distinct functions when expressed in different cells or tissues. For example, in addition to its role in chromatin, histone H4 has a role in sepsis in humans (Xu et al. 2009), and acts as an antimicrobial agent when secreted from human sebocytes (Lee et al. 2009). Similarly, Lys20 can fully participate in chromatin functions only when its nuclear localization is intact.

Analysis of the essential Esa1 HAT led to the discovery that the Lys20 HCS, previously known only for its role in amino acid synthesis, has an additional role in chromatin and in modulating the effects of DNA damage. Lys20 also physically associates with a nucleosome assembly factor, Nap1 (Krogan et al. 2006), others of which are known to function in both chromatin assembly and HAT activation (Selth and Svejstrup 2007). Thus, it seems likely that the range of nuclear functions for HCS and other metabolic enzymes will continue to expand with further study.

Materials and methods

Yeast methods, media and strains

Strains used were generated for this study unless otherwise noted (Table 2.1). Plates containing camptothecin were buffered with 100mM potassium phosphate pH 7.5, and camptothecin stock, 5mg/mL dissolved in DMSO, was added after autoclaving (Nitiss and Wang 1988). Growth control plates were buffered and contained an equivalent amount of DMSO. Hydroxyurea plates were YPD based and 100mm in HU (Zhou and Elledge 1992). The concentration of camptothecin or

hydroxyurea was selected to optimize for the different dynamic ranges of growth for each mutant or mutant combination. Details for each experiment are in the Figure legends. For dilution assays, cells were grown in YPD or indicated selective medium at 30˚C to stationary phase, normalized to A_{600}1, and plated in five fold serial dilutions.

Plasmids

Plasmids are listed in Table 2.2. Bacterial expression constructs in the pRSET vector system (Invitrogen) are pLP820 (pRSETc), pLP831 (*ESA1)* and pLP1934 (*LYS20)*. Lys20E155A was created by direct mutagenesis of pLP1412 with oLP1305 and oLP1306. Lys20R31A was created by direct mutagenesis of pLP1412 with oLP1303 and oLP1304. Lys20ΔC10 (pLP2391) was created by PCR with oLP944 and oLP1363, digested with *Eco*RI and *Bam*HI and ligated into pRS202. pLP2392 (Lys20ΔC10 without a stop codon) was created by PCR with oLP 944 and oLP1364. The product was digested with *Eco*RI and *Bam*HI and ligated into pRS202. Lys20ΔC10-NES (pLP2402) was created by annealing oLP 1390 and 1391, which comprised a variant (ELALKLAGLDINLI) of the strong NES from PKI (Gadal et al. 2001) and a stop codon, digesting this fragment with *Bam*HI and *Xba*I and ligating into pLP2392, which contained Lys20ΔC10 from which the stop codon was removed. Lys20-NES (pLP2404) was created by PCR with oLP944 and oLP1399. This fragment, Lys20 without a stop codon, was digested with *Eco*RI and *Bam*HI and subcloned into pLP2402 to create pLP2404. pLP2295 (Lys20S385F, Lys20fbr1) was created by direct mutagenesis of pLP1412 with oLP1055 and oLP1056. Lys20R276K

(pLP2296, Lys20fbr2) was created by direct mutagenesis of pLP1412 with oLP1057 and oLP1058. Constructs were confirmed by sequencing.

Protein immunoblots

For Rad53 blots, cells were grown to mid log phase and exposed to 0.1M hydroxyurea for 90 min. Cells were harvested and TCA extracts made (Foiani et al. 1994) Whole cell extracts equivalent to A_{600}=0.5 were separated on 8% SDS PAGE gel, transferred to PVDF membrane and immunoblotted with anti-Rad53 antibody (Santa Cruz) and anti-goat secondary antibody (Xymed), followed by detection with ECL Plus (GE Healthcare Amersham).

For Lys20 blots, cell extracs were made as described above without DNA damage. Gels were transferred to nitrocellulose, blocked woith 2% milk and immunoblotted overnight with anti-Lys20 antibody (gift of J. Aris). Secondary antibody was anti-mouse (Promega) at 1:5000 in 2% milk. Blots were developed with Pierce developing reagent.

HAT assays

HAT assays were performed at room temperature for 30 min using standard methods (Clarke et al. 1999) with yeast histones as substrate (see below). Reaction was evaluated by 18% SDS PAGE. Gels were transferred to nitrocellulose for 1hr at 100V. Nitrocellulose was exposed to Kodak MS film at –80˚C with a Kodak LE transcreen to detect incorporation of radioactivity. Gels after transfer were stained according to standard Coomassie Brilliant Blue protocols. For recombinant protein,

bacterial extracts were prepared from *E. coli* B834 DE3 cells containing the pRARE plasmid (Novagen) and *ESA1*, *LYS20* or vector plasmids. Transcription was induced with 1mM IPTG at 30˚C for 3 hr.

Preparation of yeast histones

Yeast cells were grown to log phase and spheroplasted. Histones were extracted with 0.25N HCl, precipitated with 20%TCA and resuspended in 10% glycerol, 50mMTris pH8 (Lo et al. 2004; Vaquero et al. 2006).

Immunoprecipitations

For immunoprecipitations, cells, including Gcn5-9Myc strain (Robert et al. 2004) were grown to log phase, and lysed by bead beating. Immunoprecipitations were carried out overnight at 4˚C with anti-Lys20 antibodies (generous gifts of J. Aris) used at dilutions of 1:50. 70µL Protein A sepharose CL-4B beads (GE HealthCare) were added, and rocked 3-4 hrs at room temperature. Western blotting was carried out as above, blotting with anti-Myc 9E-10 antibody 1:5000, (hybridoma from ATCC (Manassas, VA)), (gift of R. Hampton) to detect Gcn5-Myc.Secondary antibody (anti-mouse IgG HRP, Promega) was used at 1:5000. Chemiluminescent detection was done with Pierce ECL Western Blotting substrate. Percentage of phosphorylated Rad53 was determined with ImageQuant software.

Immunofluorescence microscopy

Cells were grown to mid log phase, fixed in formaldehyde 3.7%, then spheroplasted. After being applied to slides, cells were fixed at -20˚C in methanol,

then in acetone. Slides were blocked 1hr in 1% BSA, and incubated overnight at 4˚C in anti-Lys20 antibody 1:50 (a generous gift of J. Aris). Secondary antibody 1:50 (Texas Red-conjugated AffiniPure Goat anti-mouse IgG, Jackson ImmunoResearch Laboratories) was applied at 37˚C for 2 hrs, then cells were DAPI stained 1 hr at 37˚C. Mounting medium was applied (Vectashield, Vector Laboratories, Burlingame,CA), and images were collected on an Axiovert 200M microscope (Carl Zeiss MicroImaging, Inc.) with a 100x 1.3 NA objective. Images were captured using a monochrome digital camera (Axiocam; Carl Zeiss MicroImaging, Inc.) and data analyzed with Axiovision software (Carl Zeiss MicroImaging, Inc.).

Acknowledgements

We appreciate the contributions of A. Clarke, E. Spedale, and V. Le to the early stages of the project. J. Aris, J. Babiarz, C. Chang, E. Dubois, R. Dutnall, P. Laybourn, J. Huh, S. Bulfer, R. Trievel, J. Rine, E. Dubois, R. Kamakaka, R. Gardner, R. Hampton and F. Robert provided reagents and advice. M. Niwa and A. Bicknell provided assistance with microscopy. M. Koch, R. Garza, S. Jacobsen, B. Emerson, B. Mendelsohn, F. Solomon and C. Chang read the manuscript and provided feedback. This work was initiated with support from NIH 5T32GM007240 and GM54649.

This material is currently under review as a manuscript at Genes and Development. It may appear there as Scott, EM and Pillus, L. Homocitrate Synthase

Connects Amino Acid Metabolism to Chromatin Functions through Esa1 and DNA Damage.

Table 2.1 Strains used in Chapter 2

Strain	Genotype	Source
LPY5	*MAT*a W303	(Thomas and Rothstein 1989)
LPY2888	*MAT*a S288C *esa1*Δ*::HIS3* + pLP 777	Lab collection
LPY3121	*MAT*a S288C *esa1*Δ*::HIS3* + pLP 852	Lab collection
LPY3291	*MAT*a S288C *esa1*Δ*::HIS3* + pLP 863	Lab collection
LPY3486	*MAT*a S288C	(Mortimer and Johnston 1986)
LPY6121	*MAT*a W303 *ESA1-13MYC*	Lab collection
LPY6282	*MAT*α W303 *trp1*Δ*0* rDNA::*ADE2CAN*1	Lab collection
LPY10182	*MAT*a W303 *gcn5*Δ*::kanMX*	Lab collection
LPY10697	*MAT*α W303 *trp1*Δ*0* rDNA::*ADE2CAN1 lys20*Δ*::kanMX lys21*Δ*::clonNAT esa1-414*	This study
LPY11402	*MAT*α W303 *esa1-414 lys20*Δ*::kanMX*	This study
LPY11411	*MAT*a W303 *trp1*Δ*0* rDNA*::ADE2CAN1 lys20*Δ*::kanMX lys21*Δ*::clonNAT*	This study
LPY11412	*MAT*α W303 *esa1-414 lys20*Δ*::kanMX lys21*Δ*::clonNAT*	This study
LPY11666	*MAT*α W303 *htz1*Δ*::kanMX esa1-414*	This study
LPY12169	*MAT*a W303 *GCN5-9MYC*	F. Robert
LPY12300	*MAT*α S288C *htz1*Δ*::kanMX*	This study
LPY12418	*MAT*α S288C *esa1*Δ*::HIS3 htz1*Δ*::kanMX* + pLP 863	This study
LPY12990	*MAT*a W303 *htz1*Δ*::kanMX lys20*Δ*::kanMX lys21*Δ*::clonNAT esa1-414*	This study
LPY12991	*MAT*a W303 *htz1*Δ*::kanMX lys20*Δ*::kanMX lys21*Δ*::clonNAT*	This study
LPY13022	*MAT*a W303 *ADE2 htz1*Δ*::kanMX lys20*Δ*::kanMX lys21*Δ*::clonNAT*	This study
LPY13024	*MAT*a W303 *htz1*Δ*::kanMX*	This study
LPY13836	LPY11411 + pLP1402	This study
LPY13837	LPY11411 + pLP1412	This study
LPY13949	*MAT*a W303 *htz1*Δ*::kanMX*	This study
LPY13951	*MAT*a W303 *htz1*Δ*::kanMX lys2*Δ	This study
LPY14368	LPY3486 + pLP1402	This study
LPY14369	LPY3486 + pLP1412	This study
LPY14370	LPY3291 + pLP1402	This study
LPY14371	LPY3291 + pLP1412	This study
LPY14681	LPY3291 + pLP796	This study
LPY14774	LPY6282 + pLP2365	This study
LPY14775	LPY6282 + pLP2366	This study
LPY14776	LPY11411 + pLP2365	This study
LPY14777	LPY11411 + pLP2366	This study
LPY14778	LPY3486 + pLP2365	This study

Table 2.1, continued

LPY14779	LPY3486 + pLP2366	This study
LPY14780	LPY3291 + pLP2365	This study
LPY14781	LPY3291 + pLP2366	This study
LPY14935	LPY6282 + pLP2295	This study
LPY14936	LPY6282 + pLP2296	This study
LPY14937	LPY11411 + pLP2295	This study
LPY14938	LPY11411 + pLP2296	This study
LPY14944	LPY6282 + pLP2384	This study
LPY14945	LPY11411 + pLP2384	This study
LPY14946	LPY3486 + pLP2384	This study
LPY14947	LPY3291 + pLP2384	This study
LPY15137	LPY6282 + pLP2391	This study
LPY15138	LPY11411 + pLP2391	This study
LPY15139	LPY3486 + pLP3291	This study
LPY15140	LPY3291 + pLP2391	This study
LPY15214	LPY6282 + pLP2402	This study
LPY15215	LPY11411 + pLP2402	This study
LPY15216	LPY3486 + pLP2402	This study
LPY15217	LPY3291 + pLP2402	This study
LPY15226	LPY6282 + pLP2404	This study
LPY15227	LPY11411 + pLP2404	This study
LPY15228	LPY3486 + pLP2404	This study
LPY15229	LPY3291 + pLP2404	This study

Table 2.2 Plasmids used in Chapter 2

Plasmids[a]		
Plasmid	Gene	Source
pLP61	pRS314	Lab collection
pLP362	pRS426	Lab collection
pLP777	*esa1- K256Q; Y325N* in pLP61	Lab collection
pLP796	*ESA1* in YEP352	Lab collection
pLP820	pRSETc	Lab collection
pLP831	*ESA1* in pRSETc	Lab collection
pLP852	*esa1-L327S* in pLP61	
pLP863	*esa1-414* in pLP61	Lab collection
pLP1402	pRS202	Lab collection
pLP1412	*LYS20* in pRS202	Lab collection
pLP1641	*GCN5* in pRS426	Lab collection
pLP1934	*LYS20* in pRSETc	This study
pLP2295	*lys20-S385F* (Fbr1)	This study
pLP2296	*lys20-R276K* (Fbr2)	This study
pLP2365	*lys20-E155A* in pRS202	This study
pLP2366	*lys20-R31A* in pRS202	This study
pLP2391	*lys20-ΔC10* in pRS202	This study
pLP2402	*lys20-ΔC10-NES* in pRS202	This study
pLP2404	*lys20-NES* in pRS202	This study

[a] pRS series of plasmids is described in (Sikorski and Hieter 1989)

Table 2.3 Oligos used for Chapter 2

Oligos[b]	
Oligo	Sequence
oLP944	GGGAATTCTCTCTTCGGTAGTGG
oLP1055	CGATGATGTTGACT**T**TATCATCAAGAAC
oLP1056	GTTCTTGATGATA**A**AGTCAACATCATCG
oLP1057	TTGCACAAGATCA**A**AGACATTGAAAACC
oLP1058	GGTTTTCAATGTCT**T**TGATCTTGTGCAA
oLP1303	TTCGACGCTG**GC**AGAAGGTGAA
oLP1304	TTCACCTTCT**GC**CAGCGTCGAA
oLP1305	ATTTTCCTCTG**C**AGATTCCTTCA
oLP1306	TGAAGGAATCT**G**CAGAGGAAAAT
oLP1363	GGGATCCTTTACATACCGATGGTGGCCAGTTCCGGTAC
oLP1364	GGGATCCCATACCGATGGTGGCCAGTTCCGGTAC
oLP1390	CAAGGATCCGAGCTAGCACTCAAGCTGGCTGGTCTGGAC ATCAACTAATCTAGAGG
oLP1391	CCTCTAGATTAGTTGATGTCCAGACCAGCCAGCTTGAGTG CTAGCTCGGATCCTTG
oLP1399	AAGGATCCTGAGGCGGATGGCTTAGTCCGC

[b]Nucleotides in **bold** in the above sequences are mutagenic, compared to the wild-type sequence.

Chapter 3 Expanded analysis strengthens connections of Esa1 to H2A

Introduction

Esa1 and H2A.Z

Esa1 acetylates H2A (Clarke et al. 1999; Smith et al. 1998) but the discovery that Esa1 also acetylates the H2A variant H2A.Z (Babiarz et al. 2006; Keogh et al. 2006; Millar et al. 2006) opened up a new field of study. Esa1 acetylates lysines 3, 8, 10 and 14 on the N-terminus of H2A.Z. Alleles of *HTZ1* (the gene that encodes H2A.Z) with these targets mutated have been generated to help characterize H2A.Z. Similarly, different conditional *esa1* alleles have been generated to characterize *esa1* mutant phenotypes (Clarke et al. 1999; Bird et al. 2002; Decker et al. 2008). Combining multiple alleles of both of these genes may elucidate details of the Esa1 H2A.Z interaction and refine understanding of regions in the proteins critical for this interaction.

Esa1 and H2A.Z share some other interactions. For example, four members (Act1 Arp4, Swc4 and Yaf9) of the SWR complex, the ATP dependent chromatin remodeling complex which inserts H2A.Z into chromatin (Krogan et al. 2003; Mizuguchi et al. 2004), are also members of the Esa1 containing HAT complex NuA4

(Fig 1.1). This suggests an interaction at a deeper level than targeted acetylation, an idea lent weight by the results in Chapter 2 that show the synthetic interaction of *ESA1* and *HTZ1*. Shared subunits of the NuA4 and SWR complexes may facilitate co-recruitment of the complexes to the same site, where H2A.Z could be inserted into chromatin and acetylated at once (reviewed in Lu et al. 2009). Esa1 is an essential enzyme, although the relevance of Esa1 catalytic activity for viability is a matter of debate (Decker et al. 2008) even the catalytic mechanism of Esa1 is still under discussion (Yan et al. 2000; Berndsen et al. 2007).

Expanding the List of Genetic Interactions with ESA1

Esa1 and the histone deacetlyase Sir2 have some opposing functions, yet it has been demonstrated that overexpression of *ESA1* can suppress the *sir2Δ* rDNA silencing defect (Clarke et al. 2006; Tamburini and Tyler 2005).

It is possible that other proteins known to interact with Esa1, Htz1 or both may affect their interaction. Large scale genetic screens (Lin et al. 2008) have found other genetic interactors for *ESA1*. Many of these have yet to be individually validated. When such interactions are explored in detail, the information that comes to light may provide clues to new roles for even a well-characterized protein. Several of the results presented in this chapter point to previously unsuspected roles for Esa1.

Esa1 and H2A Related Proteins

In this chapter, genetic interactions with *ESA1* are examined. These interactions are focused around H2A and H2B, the H2A variant H2A.Z and H2A-

associated chromatin proteins. One chromatin associated factor of significance is the well conserved H2A/H2B chaperone Nap1, first characterized in *Drosophila melanogaster* (Ito et al. 1996). Nap1 and Esa1 are also both connected to the cell cycle (Kellogg et al. 1995; Kellogg and Murray 1995; Clarke et al. 1999). Deletion of *NAP1* in yeast leads to few phenotypes. For example, mutants are defective in the M phase of the cell cycle (Kellogg et al. 1995). There is also a connection to both proteins through Lys20. Interactions between *ESA1* and *LYS20* were detailed in Chapter 2. Nap1 and Lys20 were reported to interact physically (Krogan et al. 2006). This seemed significant, as few proteins were reported to interact with Lys20 in this large scale interaction screen.

Nap1 is the chaperone for H2A (Ito et al. 1996). Chz1 (Chaperone for H2A.Z) was later identified as the protein that preferentially bound H2A.Z (Luk et al. 2007). Both Nap1 and Chz1 could bind H2A and H2A.Z in the absence of the other chaperone. More recent analysis presents data localizing Chz1 to the nucleus and speculates that Chz1 may function with the SWR complex in inserting H2A.Z into chromatin, whereas Nap1 plays a more major role in import, shuttling back and forth between nucleus and cytoplasm (Straube et al. 2010).

Esa1 and Set1

Some of the genetic interactions discussed in this chapter are between *ESA1* and chromatin associated factors as noted above. Other studies focus on interaction with the histone modifying enzyme, Set1, a histone methyltransferase. Set1 is responsible for methylating H3 at K4 (reviewed in Dehe and Geli 2006). Its human

homolog, MLL1 is implicated in leukemia (reviewed in Tenney and Shilatifard 2005). Any interactions between *SET1* and *ESA1* may thus be significant at several levels

Results

Esa1 and H2A.Z

To evaluate the interaction between *ESA1* and *HTZ1*, the *esa1 htz1Δ* double mutant was constructed. This double mutant was introduced briefly in Chapter 2, in the context of *LYS20* mediated dosage suppression. This *esa1 htz1Δ* double mutant (Fig 3.1) had growth defects when compared to either single mutant. It was also considerably more sensitive to multiple classes of DNA damage agents than either parent (Fig 3.1). Both hydroxyurea (HU) and camptothecin (CPT) cause DNA damage as described in Chapter 2. The *esa1 htz1Δ* mutants shown in Fig 3.1 were made with the *esa1-414* allele. To determine if other alleles of *esa1* had similar phenotypes with *htz1Δ* mutants, strains were constructed with other plasmid-borne alleles of *esa1*. In Fig 3.2, it is demonstrated that these alleles exhibit synthetic sickness with *htz1Δ*, the *esa1-414* allele has one of the strongest phenotypes. That multiple alleles exhibit synthetic sickness with *htz1Δ* validates the functional interaction.

In the first report of Htz1 as a substrate of Esa1, four lysines of Htz1 (K3, K8, K10, K14) were identified as targets of acetylation (Babiarz et al. 2006; Keogh et al. 2006; Millar et al. 2006). Because *esa1* is synthetic sick when *HTZ1* is also

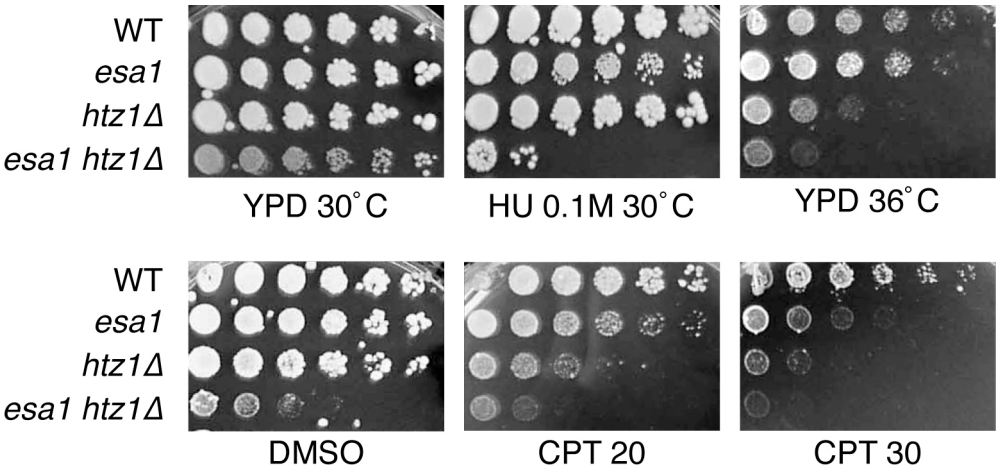

Figure 3.1 ***esa1 htz1*Δ double mutants are synthetically sensitive to high temperature, hydroxyurea and camptothecin.** YPD plates were grown 3 days. Cells were normalized before plating. Five-fold serial dilutions are shown. The *esa1-414* allele is used, unless otherwise indicated. YPD based plates are grown for 3 days at 30˚. DMSO plate is the growth control.

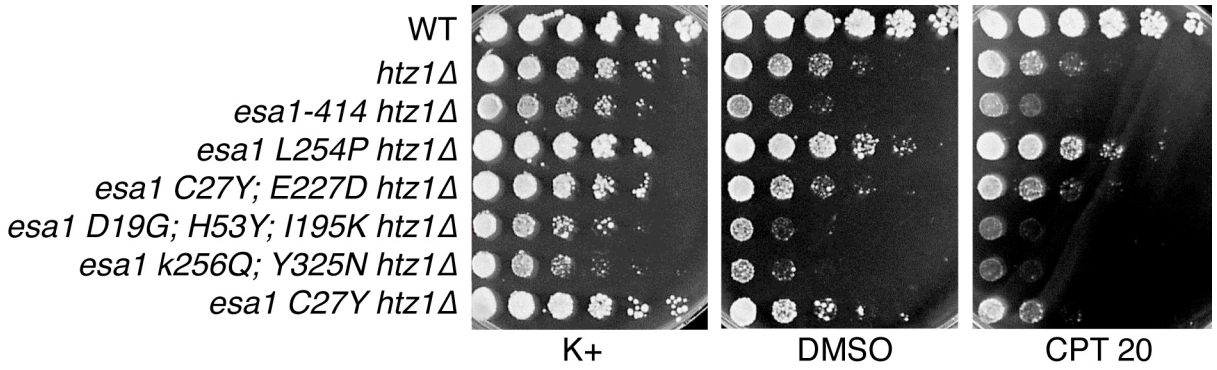

Figure 3.2 Alleles of *ESA1* have varying camptothecin sensitivity in combination with *htz1Δ*. Plasmid-borne alleles of *ESA1* were shuffled into *htz1*Δ mutants to generate these strains. Plates lack both uracil and leucine to facilitate plasmid selection. Plates incubated at 30˚. K+ (potassium buffer alone) plate and DMSO plate serve as growth controls.

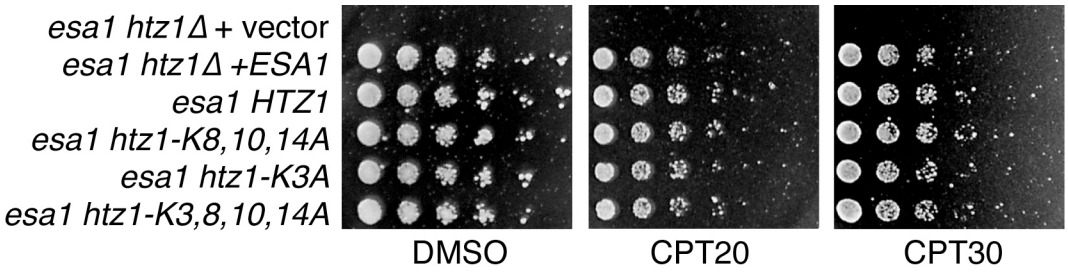

Figure 3.3 The *htz1* point mutants are not CPT^S (camptothecin sensitive) in combination with *esa1*.

unacetylated, it was possible that the sickness was due to the lack of the entire Htz1 protein or specifically due to the lack of the four lysines targeted for acetylation by Esa1. To address this possibility, the four target lysines were mutated to alanine. Strains were constructed with the *esa1-414* allele and different combinations of the mutated *htz1* (Fig 3.3).

When assayed on CPT plates, all *htz1* point mutants appeared as healthy as wild type. Surprisingly, mutation of these four residues did not confer the same DNA damage sensitivity as the null mutant. This result is consistent with a model whereby another region of the Htz1 protein is required for resistance to DNA damage and that this other region is what cooperates with Esa1 to promote resistance to damage. Mutation of the four lysine residues on H2A.Z does not cause DNA damage sensitivity by itself (Babiarz et al. 2006; Keogh et al. 2006). In Chapter 2, it was shown that overexpression of *LYS20* did not suppress the DNA damage sensitivity of *esa1 htz1*Δ (Fig 2.3). This may be due to deletion of the entire gene, so to determine whether *LYS20* could suppress the DNA damage sensitivity in the *htz1* point mutants, mutant strains were constructed and assayed. In Fig 3.4, *LYS20* is overexpressed in *esa1 htz1-K3A* strains. These data are difficult to interpret because the point mutant strains are not very sensitive to CPT, but *LYS20* overexpression does not appear to increase resistance to camptothecin. In parallel, *LYS20* is overexpressed in *esa1 htz1-K8,10,14A* strains (Fig 3.5) and in *esa1 htz1-K3,8,10,14* strains (Fig 3.6). Results for these two experiments are the same as for Fig 3.4. In all cases, significant alteration of the DNA damage sensitivity was not observed.

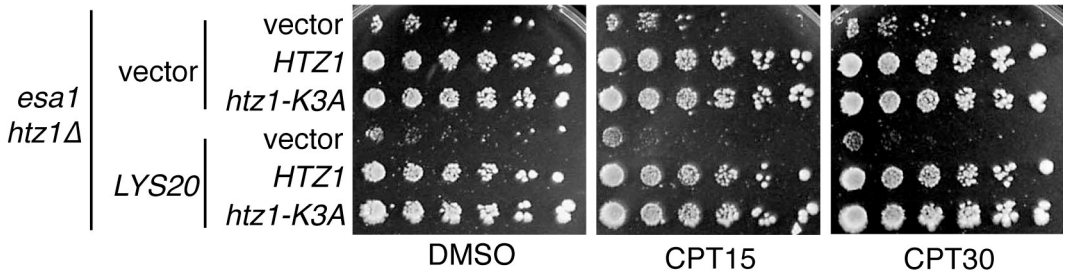

Figure 3.4 *htz1-K3A* point mutant in combination with *esa1* is not affected by overexpression of *LYS20*. Plates lack both uracil and leucine to maintain selection of plasmids. (*HTZ1* point mutants are on plasmids with a *URA3* marker; *LYS20* plasmids carry a *LEU2* marker).

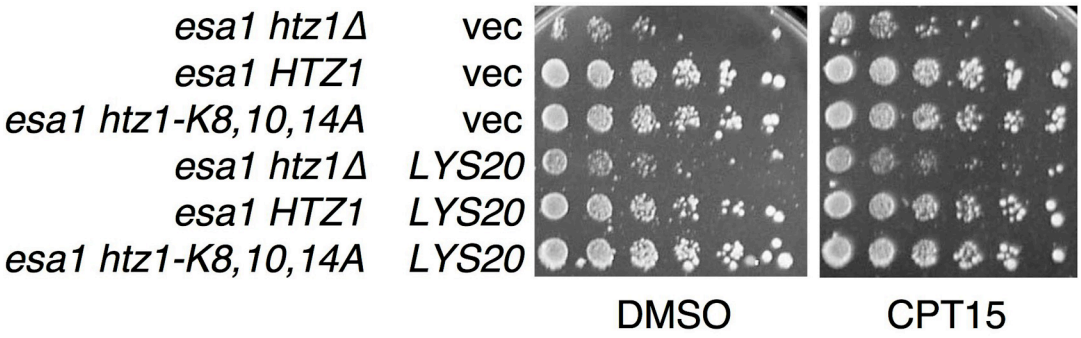

Figure 3.5 ***htz1-K8,10,14A*** **mutants in combination with** ***esa1*** **are not affected by overexpression of** ***LYS20.*** Plates lack both uracil and leucine to maintain plasmid selection (*HTZ1* point mutants are on plasmids carrying a *URA3* selectable marker; *LYS20* plasmids carry a *LEU2* selectable marker).

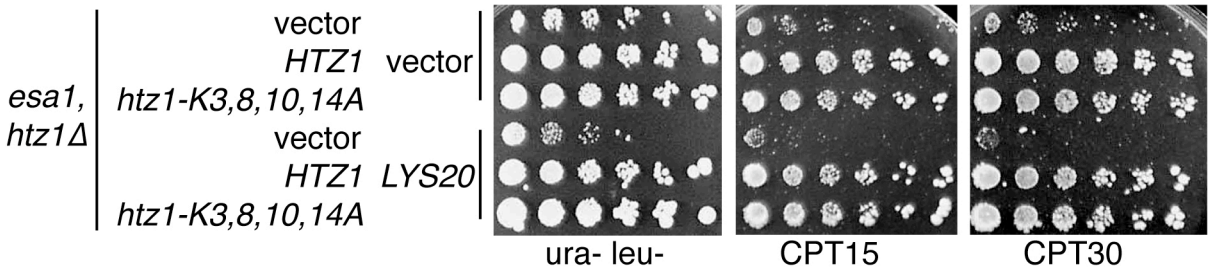

Figure 3.6 ***htz1-K3,8,10,14A*** **mutants in combination with** ***esa1*** **are not affected by overexpression of** ***LYS20.*** Plates lack both uracil and leucine to facilitate plasmid selection (*htz1* point mutants are on plasmids carrying a *URA3* marker; *LYS20* plasmids contain a *LEU2* marker).

Esa1, H2A.Z and Sir2

One other way to explain the above results is that another protein or protein complex may have a role in the interplay between *ESA1* and *HTZ1* making their function indirect. It was recently found that deletion of *SIR* genes suppressed the growth defect of *set1Δ htz1Δ* double mutants (Venkatasubrahmanyam et al. 2007). By analogy, *SIR2* deletion might rescue the *esa1 htz1Δ* synthetic growth defect as it did for the *set1Δ htz1Δ* mutant. Involvement of *SIR2* would provide a more direct link to chromatin. To assay the effect of *SIR2* deletion on the *ESA1 HTZ1* interaction, triple mutants were constructed. The *esa1- 414 htz1Δ sir2Δ* triple mutants were analyzed for temperature and DNA damage sensitivity and it was discovered that they are even more growth compromised than the *esa1 htz1Δ* double mutants. They have increased temperature sensitivity, showing reduced growth even at 34˚ (Fig 3.7) and are extremely sensitive to CPT (Fig 3.8). The growth on CPT is difficult to score, as the strain is also quite sensitive to DMSO, the vehicle used to dissolve CPT. The triple mutants have increased sensitivity to the same challenges as *esa1 htz1Δ* double mutants. Also in Fig 3.8, deletion of *SIR2* suppresses the CPT sensitivity of the *htz1Δ* mutant. One interesting aspect of this result is that *sir2Δ* mutants are not sensitive to DNA damage on their own, so there is no obvious explanation for why these mutations have the observed effects.

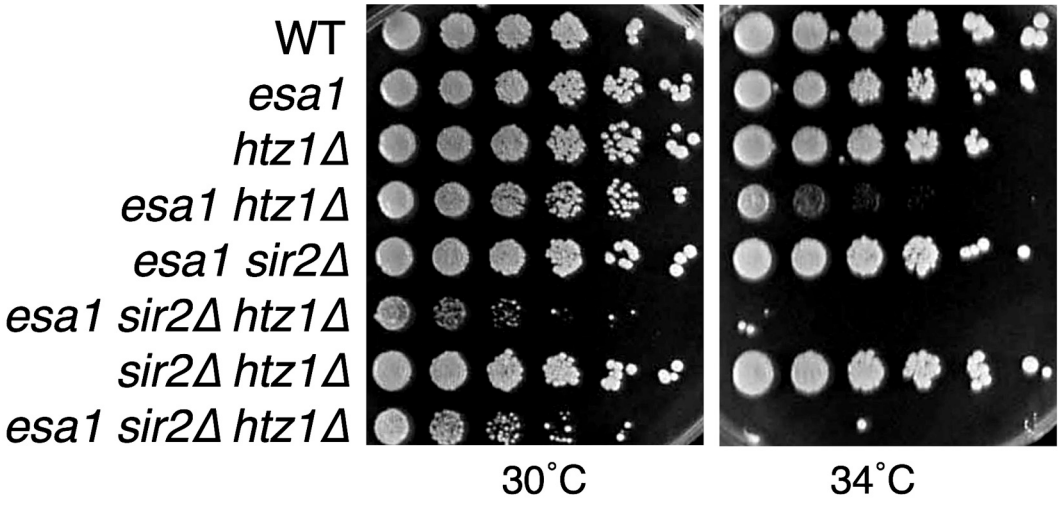

Figure 3.7 Triple *esa1 htz1Δ sir2Δ* mutants are more temperature sensitive than any double mutant. Plates are YPD, and are incubated at indicated temperatures. Modest temperature sensitivity of the triple mutant is visible even at 30˚.

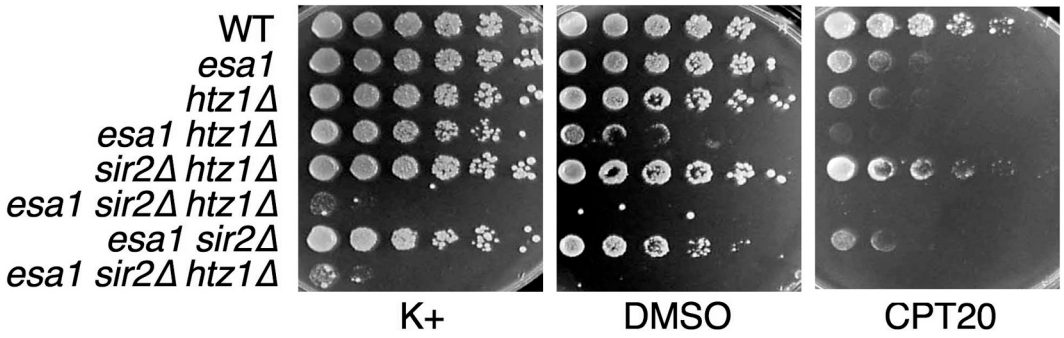

Figure 3.8 Triple *esa1 htz1*Δ *sir2*Δ mutants are more CPT sensitive than any double mutant and *sir2*Δ suppresses the CPT sensitivity of the *htz1*Δ mutant. DMSO plate and K+ (potassium phosphate buffered plate) are included as growth controls. Plates are YPD based.

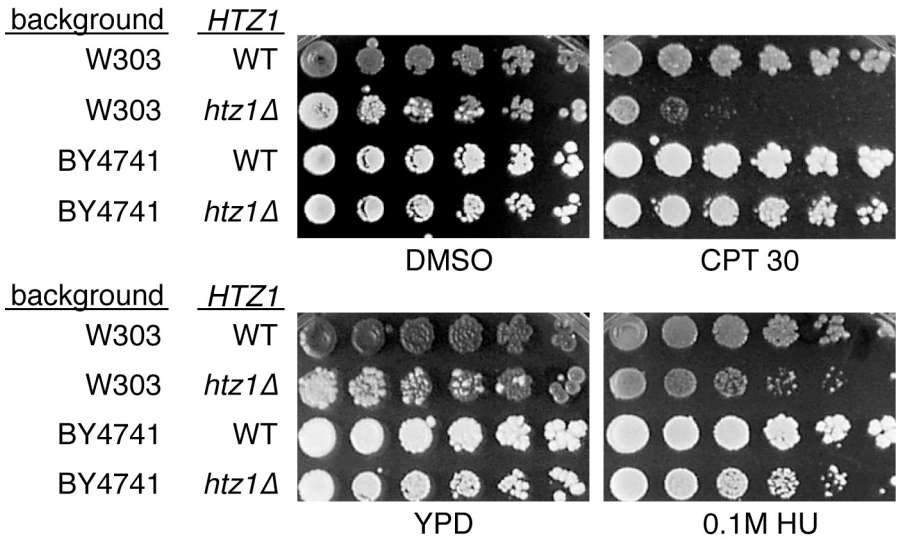

Figure 3.9 ***htz1*Δ mutants in the BY4741 background are not sensitive to DNA damage.** ***htz1*Δ mutants in the W303 genetic background are DNA damage sensitive.** HU (hydroxyurea) plates are YPD based and contain 100mM HU. CPT plates contain 30 μg/mL of CPT and all plates incubated at 30˚.

Effects of Genetic Background

The results presented above, detailing the mutant phenotypes of *HTZ1* in combination with *esa1* and *sir2Δ* extend previous analyses, showing that *htz1Δ* was sensitive to DNA damaging agents. The above analysis was conducted in either the W303 or S288C backgrounds. However, when the *htz1Δ* null mutant was dissected from the BY4741 collection, it did not seem as sensitive to genotoxins as strains in other backgrounds. To test this effect, *htz1Δ* mutants in BY4741 and in W303 were assayed on CPT and HU plates (Fig 3.9). As suspected, the BY4741 strains failed to show sensitivity. Given these results, consistent in two other backgrounds as well as the body of evidence published by other labs (reviewed in Dryhurst et al. 2004), we suspect that the *htz1Δ* strain in the BY4741 collection is flawed. However, this needs to be confirmed directly, otherwise effects of the robust BY4741 background cannot be ruled out.

NAP1 and ESA1 Genetically Interact

As seen in Chapter 2, deletion of *LYS20* and *LYS21* suppresses DNA damage phenotypes of *htz1Δ*. It has been reported that deletion of *NAP1* also suppresses some growth defects of *htz1* (Straube et al. 2010). By analogy to *HTZ1, NAP1* may also interact with *ESA1*. To evaluate this hypothesis, we generated *esa1 nap1Δ* double mutants and phenotyped them, paying specific attention to conditions where *esa1* was known to have a phenotype. The *esa1 nap1Δ* mutants showed synthetic temperature sensitivity at 35˚ (Fig 3.10) as well as increased DNA damage sensitivity (Fig 3.10)

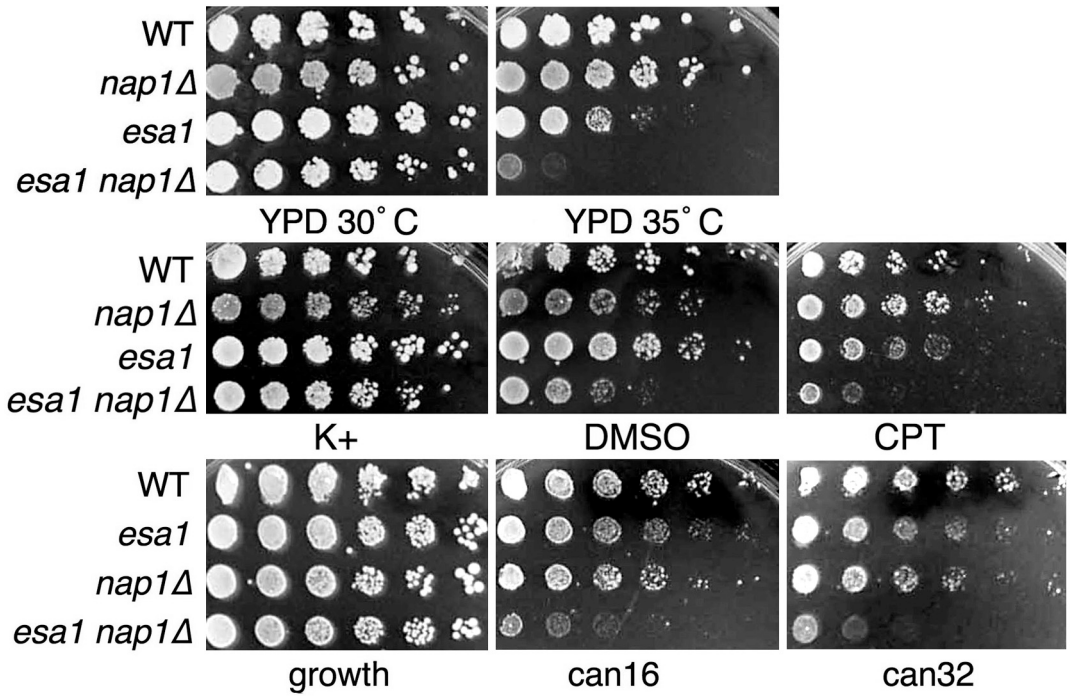

Figure 3.10 ***esa1 nap1*Δ mutants are synthetically sensitive to increased temperature, camptothecin (CPT) and display increased defects in rDNA silencing.** Plates were incubated for 2 days at 33˚, except for silencing plates which were incubated for 3 days at 30˚.

Figure 3.11 Overexpression of *LYS20* does not suppress the increased temperature or CPT sensitivity of *esa1 nap1*Δ mutants, but does further exacerbate the increased rDNA silencing defect of *esa1 nap1*Δ . Ura- plates are incubated at indicated temperatures For silencing assay, growth plate is Ade- Arg- Ura-, silencing plates contain an additional 16µg/mL or 32µg/mL of canavanine as specified. Plates were incubated at 30˚C unless otherwise indicated.

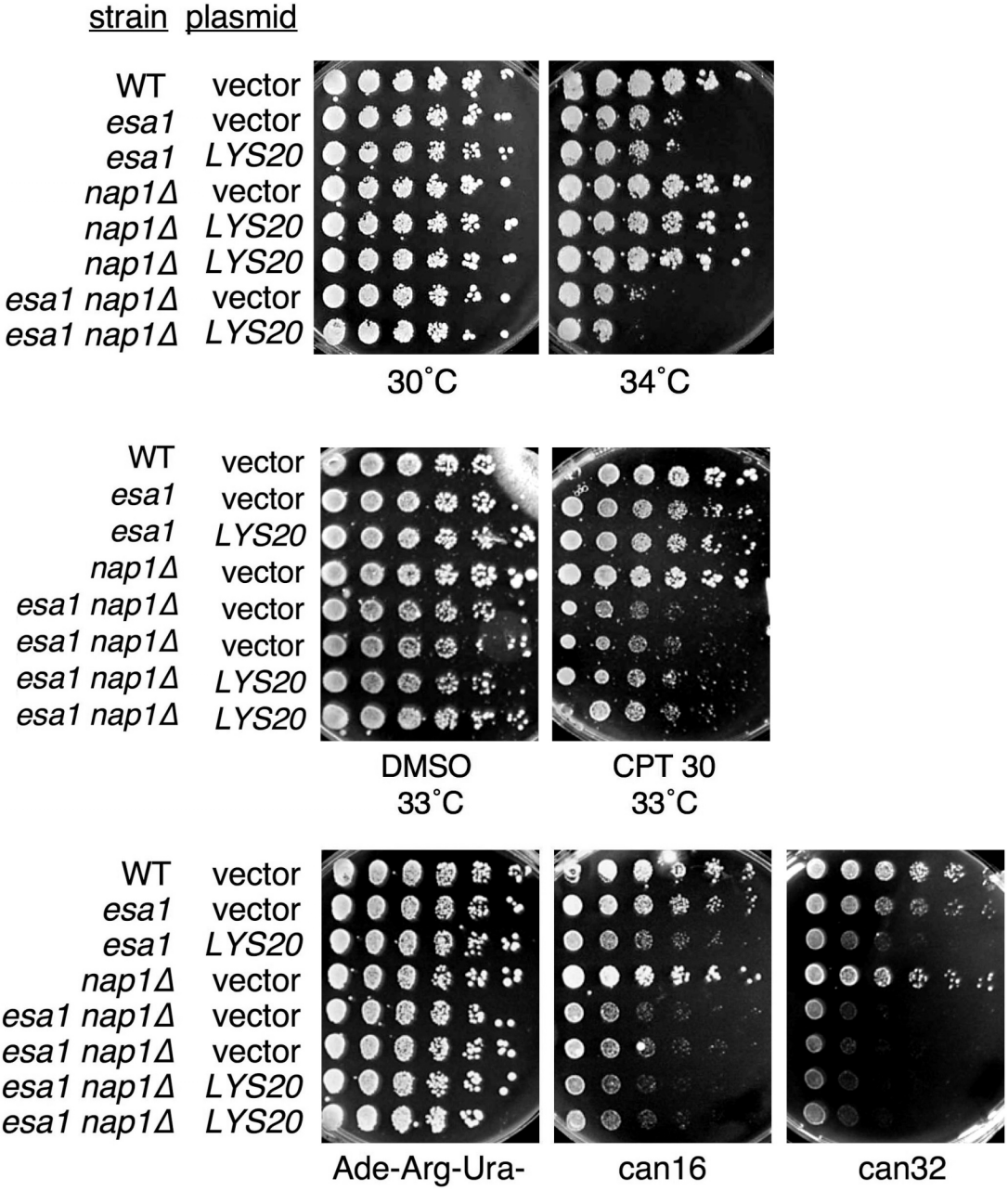
strain plasmid
WT vector
esa1 vector
esa1 LYS20
nap1Δ vector
nap1Δ LYS20
nap1Δ LYS20
esa1 nap1Δ vector
esa1 nap1Δ LYS20
30˚C
34˚C
WT vector
esa1 vector
esa1 LYS20
nap1Δ vector
esa1 nap1Δ vector
esa1 nap1Δ vector
esa1 nap1Δ LYS20
esa1 nap1Δ LYS20
DMSO 33˚C
CPT 30 33˚C
WT vector
esa1 vector
esa1 LYS20
nap1Δ vector
esa1 nap1Δ vector
esa1 nap1Δ vector
esa1 nap1Δ LYS20
esa1 nap1Δ LYS20
Ade-Arg-Ura-
can16
can32

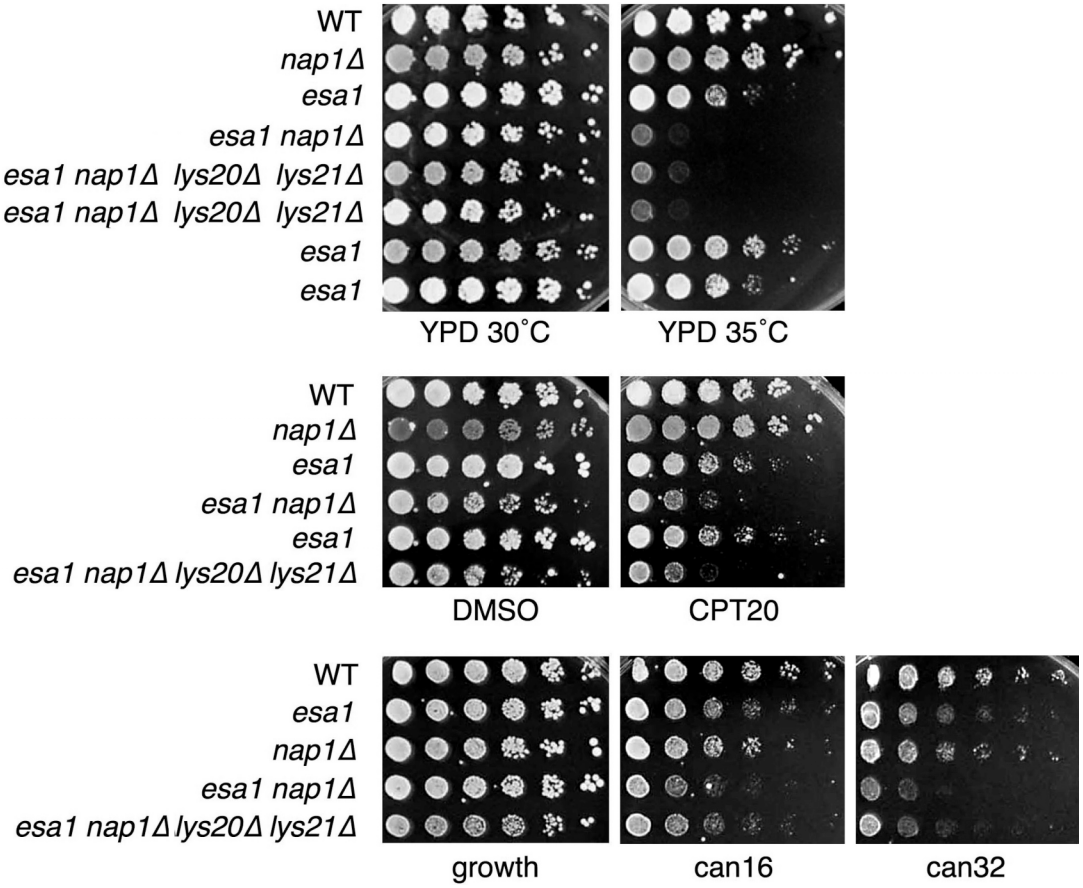

Figure 3.12 Deletion of *LYS20* and *LYS21* does not affect *esa1 nap1*Δ temperature sensitivity, CPT sensitivity or the *esa1 nap1*Δ rDNA silencing defect. The 30˚ plate serves as the growth control for 35˚ plate. For CPT assay, Growth plate contains DMSO; CPT plate contains 20µg/mL of CPT. Plates incubated at 33˚. For silencing assays, growth plate is Ade- Arg-, silencing plates contain an additional 16µg/mL or 32µg/mL of canavanine as specified. Plates were incubated at 30˚.

.

when assayed on CPT plates. They also displayed an exacerbated defect in rDNA silencing compared to either single mutant (Fig 3.10). Defects in growth at high temperature, rDNA silencing and DNA damage hypersensitivity are characteristic of *esa1* mutants. Single mutants in *NAP1* display none of these defects, yet *nap1Δ* exacerbates all defects in the *esa1* mutant. This may point to a mechanism for exacerbation dependent on Nap1's role in import of H2A/H2B. Overexpression of *LYS20* did not strongly suppress phenotypes of *esa1 htz1Δ* mutants (Chapter 2). If *LYS20* were overexpressed, would *esa1 nap1Δ* mutants behave like *esa1 htz1Δ* mutants, or more like *esa1* single mutants, wherein suppression would be observed? Figure 3.11 shows that *LYS20* overexpression does not affect the *esa1 nap1Δ* temperature sensitivity, CPT sensitivity (Fig 3.11) or the rDNA silencing defect (Fig 3.11). This indicates a phenotypic profile more similar to *esa1 htz1Δ*. The general conclusion to draw from this analysis is that combination of *esa1* with a mutation of some H2A related gene results in synthetic phenotypes that are not suppressed by overexpression of *LYS20*.

If *LYS20* overexpression does not suppress double mutant phenotypes, would deletion of *LYS20* and *LYS21* suppress DNA damage phenotypes, as it does in *htz1Δ*? To test this idea, *esa1 nap1Δ lys20Δ lys21Δ* mutants were constructed, and evaluated. These quadruple mutants appear similar to the *esa1 nap1Δ* double mutant with regards to temperature sensitivity (Fig 3.12), CPT sensitivity (Fig 3.12) and rDNA silencing (Fig 3.12). This implies that while there is a powerful synergy in the *esa1 nap1Δ* double mutant, *LYS20* and *LYS21* are not involved. The *nap1Δ lys20Δ lys21Δ* triple

mutant was also constructed and behaves like *nap1Δ* (data not shown), although as neither mutant has a strong sensitivity to DNA damage or high temperature, this is perhaps unsurprising.

ESA1 and EAF1 are Synthetically Lethal

Another candidate of interest for potential genetic interaction with *ESA1* is *EAF1* (Esa1- Associated Factor). Eaf1 had been biochemically defined as a component of NuA4 (Kobor et al. 2004), yet until the publication of two recent papers, (Auger et al. 2008; Mitchell et al. 2008) there was not evidence for its function in the complex. These studies established Eaf1 as a major structural component of NuA4. Upon deletion of Eaf1, the NuA4 complex was destabilized, leaving only a few small subcomplexes intact. Evaluation of an *esa1 eaf1Δ* double mutant would allow us to ask if NuA4 complex integrity was required for suppression of *esa1* mutant phenotypes. To this end, the *esa1 eaf1Δ* heterozygous diploid was constructed. Upon sporulation, no spores were recovered, thus and it appears that in the W303 background *esa1-414* is synthetically lethal with *eaf1Δ*. This synthetic lethality was also seen in a high throughput screen with a distinct genetic background and a different conditional allele of *ESA1* (Lin et al. 2008). This implies that NuA4 complex integrity is still vital for viability when Esa1 catalytic activity is compromised. Read another way, Esa1 catalytic activity is even more critical when NuA4 is not intact. Perhaps this indicates a breakdown of both piccolo and NuA4, without one of which the cell cannot survive.

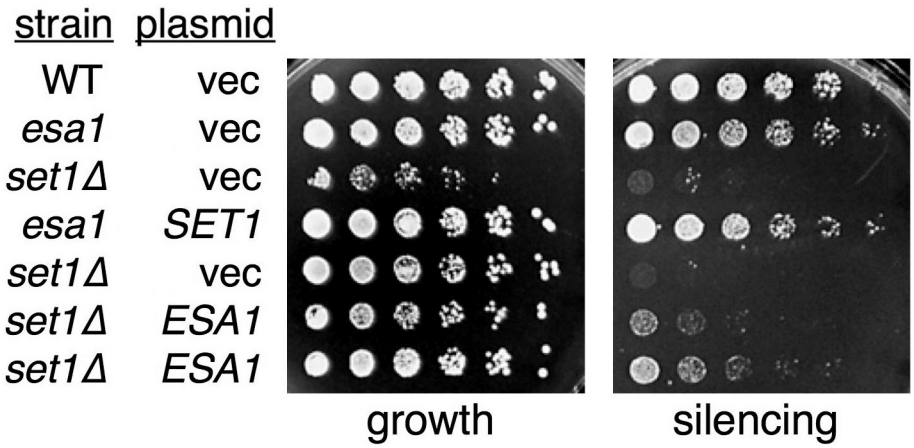

Figure 3.13 Overexpression of *ESA1* in a *set1*Δ strain partially rescues the *set1*Δ rDNA silencing defect. Growth plate is Ade-Arg-Ura-. Silencing plate is Ade-Arg-Ura- with 16µg/mL of canavanine.

Esa1 and Set1 at the rDNA

Esa1 has a well-established role in regulation of rDNA silencing. Deficiencies in rDNA silencing occur when *ESA1* is mutated. It has been shown that overexpression of *SIR2* can rescue *esa1*'s rDNA silencing defect (Clarke et al. 2006). While this result seemed counterintuitive, it did indicate that regulation of transcription at this locus was more complicated than previously expected. It was also possible that histone methylation could play some role in this regulation since histone methylases are also involved in rDNA transcription. For example, the histone methyltransferase Set1 has established roles in silencing (reviewed in Dehe and Geli 2006). Mutants in *SET1*, in addition to general growth defects, have severe defects in rDNA silencing as well. We therefore asked if overexpression of *ESA1* in a *set1Δ* mutant would affect the observed rDNA silencing defect. When assayed (Fig 3.13), the overexpression of *ESA1* did rescue *set1Δ* rDNA silencing defects, yet the converse was not true. The result has been repeated more than twice, with independent transformants each time.

This may indicate that without established histone methylation (*set1Δ*), histone acetylation alone is insufficient to support silencing. However, if methylation were downstream of acetylation, then supplying extra acetylation (in the form of *ESA1* overexpression) might leapfrog the missing step of methylation and restore silencing in the *set1Δ* mutant. Another explanation would be that it is not the acetylation provided by Esa1 that rescued *set1Δ* mutants, but some other contribution of Esa1 that does not rely on Esa1's HAT activity.

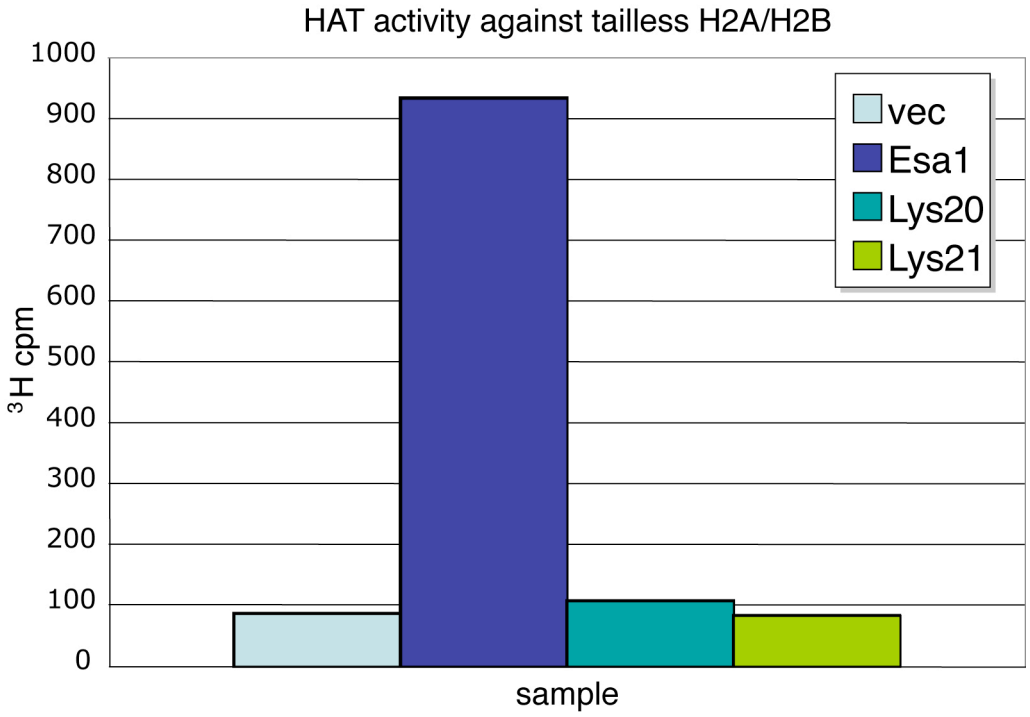

Figure 3.14 Esa1 acetylates tailless H2A/H2B. Graph represents scintillation counts of HAT assay reactions where extract containing recombinant Esa1 (rEsa1), rLys20, rLys21 or empty vector was incubated with tailless H2A/H2B as substrate and ^{3}H acetyl CoA. Reactions were spotted onto filters, washed and counted. Assay was performed once.

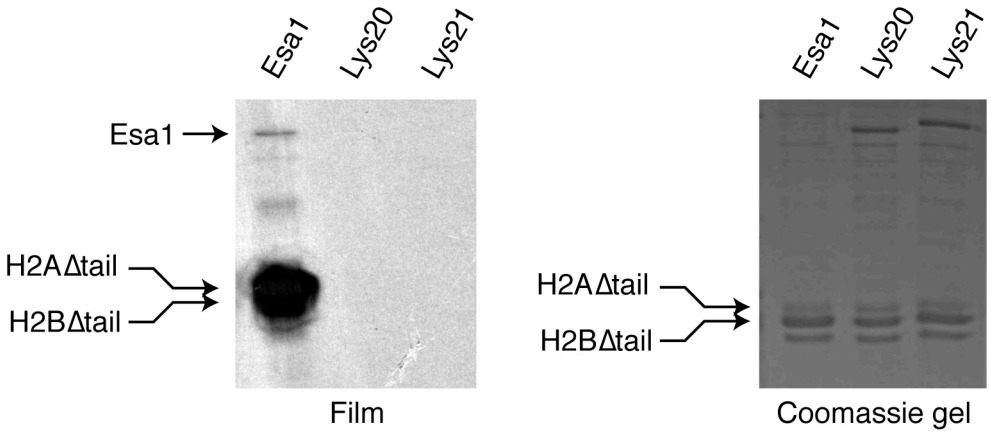

Figure 3.15 Esa1 robustly acetylates tailless H2A/H2B; Lys20 and Lys21 do not. Reactions described in Fig 3.14 were analyzed on an acrylamide gel and exposed to film. Activity against histone substrates is visible in the Esa1 lane of the film, as is Esa1 autoacetylation activity. At right is the Coomassie stained gel, showing staining of histone substrates. 40% of the reaction was run on the gel. For all lanes, the substrate was tailless H2A/H2B

Potential substrate residues for Esa1 in H2A/H2B

The specificity of Esa1 for residues on H3 and H4 is well characterized (Smith et al. 1998; Clarke et al. 1999; Suka et al. 2001). However, less is known about its specificity for residues on H2A where it acetylates K4 and K7 and H2B, where it has been shown only by ChIP to acetylate the histone, but the substrate residues have never been defined. To evaluate the H2A/H2B specificity, a HAT assay (described in Appendix A) was performed with recombinant Esa1, and recombinant H2A and H2B truncations as substrate (gift of Joon Huh and Bob Dutnall). H2A was missing residues 1-13, thus removing both known targets of acetylation, as well as the lysine residue at position 13. H2B was missing residues 1-30, removing the first 25% of the protein including 11 lysines and thus any potential targets in the N terminal tail. One might predict that Esa1 would not be active against these truncated recombinant substrate, however, when the assay was performed, robust activity was observed (Fig 3.14 and 3.15). Esa1 activity was assayed by scintillation counting of HAT reactions and by running reactions on acrylamide gels and exposing the gel to film. Robust activity was observed for Esa1.This strongly indicates that there are additional uncharacterized targets present on one or more of these histones. This result is similar to the prediction in this chapter of additional sites of Esa1 acetylation in Htz1 based on genetic data.

Discussion

Esa1 and Htz1

Mutational analysis conducted in this chapter reveals information about the synthetic interaction between Esa1 and Htz1. Most alleles of *ESA1* tested showed synthetic interaction with *htz1Δ* and many of these have compromised catalytic activity, implying that catalysis by Esa1 is playing a role. The converse is true for Htz1: point mutants in the only residues yet defined as Esa1 targets had no effect on DNA damage response. The synthetic interaction with *esa1* thus requires some other part of the protein besides the four N-terminal lysines. This other part could be in the form of other lysine targets for Esa1 acetylation that are buried deeper in the histone. Eleven lysine residues lie outside of this N- terminal region in Htz1. It could also be a larger domain that might play a role in assembly of Htz1-containing nucleosomes. Further study, in the form of extended mutational analysis of Htz1 will be necessary to determine which alternative is correct. A region of Htz1 required for nuclear localization has been identified in the first 24 residues of the protein; other fragments of the protein have been tested for function and localization (Straube et al. 2010). More regions of the protein will likely be identified that are required for various Htz1 functions. Large-scale mutational analysis such as that completed for the core histones (Matsubara et al. 2007; Nakanishi et al. 2008) will facilitate analysis.

Modification of Htz1

Htz1 is known to be SUMOylated at two sites (Kalocsay et al. 2009). Combining *esa1* with point mutants in these residues would test a role for SUMOylation in this genetic interaction. The finding that the four Esa1 target residues in the N-terminal tail of Htz1 are not required for resistance to DNA damage points to roles for globular domain or C-terminal residues as key. Roles for globular domain residues on other histones such as K56 on H3 (Celic et al. 2008) are known, and it is likely that there will be important residues in the globular domains of the histone variants as well.

The involvement of the Sir2 HDAC adds another layer of complexity to the *esa1 htz1* interaction. An obvious explanation for Sir2's involvement would be if Sir2 were the HDAC that deacetylated Htz1, in opposition to acetylation by Esa1 and Gcn5. To date, there is no evidence for this and in fact Hda1 has been identified as the deacetylase that is active on Htz1 (Lin et al. 2009). Sir2 may still play a distinct role in Htz1 deacetylation, perhaps at an unidentified residue. In this regard, deletion of *HDA1* in the *esa1 htz1Δ* mutant might be expected to suppress the *esa1 htz1Δ* mutant's synthetic phenotypes. The effect observed with *SIR2* deletion, however, is opposite: phenotypes get more severe in the triple mutants. More puzzling, the only *sir2Δ* containing double mutant with a synthetic phenotype was *sir2Δ htz1Δ* , where suppression was observed (Fig 3.7 and 3.8). The contribution of *SIR2* to DNA damage comes only in the absence of *HTZ1,* or *HTZ1*and *ESA1*. This provides one of the first links for *SIR2* to DNA damage, although the mechanisms are as yet unclear.

DNA damage

As discussed in Chapter 2, *htz1Δ* mutants are defective in Rad53 phosphorylation in response to DNA damage, therefore one way to elucidate the mechanism of Sir2 involvement would be to test Rad53 phosphorylation in response to DNA damage in this set of double and triple mutants. If there was no difference observed in Rad53 phosphorylation, it might point to more involvement of chromatin proteins and less involvement of the DNA repair machinery itself. FACS analysis might also shed light on the synthetic growth defect observed in the triple mutants if a cell cycle defect were uncovered. With regard to the DNA damage, the double and triple mutants have been assayed only on camptothecin, so further testing with other genotoxins such as HU, H_2O_2 and UV may help define specificity. Analysis of the *esa1 htz1Δ sir2Δ* triple mutants has been made with only the *esa1-414* allele; other alleles of *ESA1* could also be tested. Mutants in *ESA1* are also sensitive to MMS (Bird et al. 2002), providing a genotoxin with alkylating activity instead of double strand break-inducing properties.

Although the synthetic growth phenotype of the *esa1 htz1Δ sir2Δ* triple mutant is not informative by itself, it might be explained by what can rescue this phenotype. Known suppressors of the three genes, including *LYS20*, could be overexpressed in the triple mutant to see if suppression is still observed, or to determine if deletion of the other two factors removes something essential for the mechanism of suppression. Since *esa1* and *sir2Δ* mutants both have distinct silencing defects, silencing at the

rDNA, telomeres and cryptic mating-type loci should be assayed to ascertain the triple mutant phenotype. This would also assist in defining a silencing profile for *HTZ1*.

The rescue of *set1Δ* rDNA silencing defects by *ESA1* overexpression raises an intriguing connection. Methylation of H3K4 by Set1 requires prior ubiquitination of H2BK123 by Rad6 and Bre1 (reviewed in Osley 2004; Latham and Dent 2009). So far, this establishes a connection between Set1 and H2B. Esa1 may be involved as it targets H2B (Suka et al. 2001).

Furthermore, strains that are mutant in any component of the H2B ubiquitination pathway have cell cycle defects at G1/S and fail to hyperphosphorylate Rad53 after UV exposure (reviewed in Putnam et al. 2009). To determine whether the Rad53 pathway is at work in the interactions we have seen, Rad53 phosphorylation status after DNA damage could be probed as in Chapter 2. The *htz1Δ set1Δ* mutants whose growth defects were suppressed by *SIR3* deletion (Venkatasubrahmanyam et al. 2007) could also be tested for the status of Rad53 hyperphosphorylation upon induction of DNA damage. Recalling that *htz1Δ* mutants are defective in Rad53 hyperphosphorylation, it would be relevant to see if Rad53 is hyperphosphorylated in *sir2Δ htz1Δ* mutants and *esa1 sir2Δ htz1Δ* mutants. If changes were observed, it would be interesting to know if *SIR2* affects this. Either way, these data would help define a role for *SIR2* in regard to DNA damage, an area about which little is known. Also, it would be informative to know whether overexpression of *ESA1* in the *set1Δ* background alters the phosphorylation state of Rad53 in the *set1Δ* strain.

Another method of examining the DNA damage phenotypes would be to analyze which factors are present at the site of damage. Both Htz1 and Esa1 are recruited to sites of DNA damage, where H2A also has a role (Downs et al. 2000; Downs et al. 2004; Tamburini and Tyler 2005; Kalocsay et al. 2009).

Although recent research efforts have uncovered much about *HTZ1*, it is still a relatively understudied gene. New phenotypes are being reported for the *htz1Δ* mutant, such as its resistance to nickel (Osada et al. 2008). This is specific, not a general heavy metal effect. Exactly why *htz1Δ* mutants should be resistant to nickel remains a mystery, but an intriguing lead into the *in vivo* functions of Htz1. It remains to be determined if this phenotype is related to Htz1's function in chromatin, or whether it functions in some other process as well. If it is related to the chromatin function, then exposing the panel of mutants we have made such as *esa1 htz1Δ* and *esa1 htz1Δ sir2Δ* to nickel might shed some light on the interaction among these factors. It would also provide a way to tease out the contributions of *htz1Δ* in the multiple mutants, assuming none of the other single mutants are also nickel resistant.

Histone Chaperones

Two of the *HTZ1* genetic interactions have opposite effects: *esa1 htz1Δ* creates a synthetic sickness (Fig 3.1), whereas *nap1Δ htz1Δ* (Straube et al. 2010) is reported to be healthier than *htz1Δ*. DNA damage effects are yet to be assayed. This suggests that *NAP1* and *ESA1* have opposing functions in the context of *htz1Δ*, yet *esa1 nap1Δ* are themselves also synthetic sick. Triple mutant analysis, e.g. *esa1 nap1Δ htz1Δ* may help clarify these observations. Some of this analysis has been started by Jæ Chung,

and will be carried forward by him. He will also explore *in vivo* physical interactions among Esa1, Nap1, Chz1 and Htz1. Chz1, as discussed in the introduction, is the H2A.Z chaperone, analogous to Nap1 as an H2A/H2B chaperone. Contributions of *CHZ1* will also be analyzed in the combinatorial triple mutant analysis. Recent work (Straube et al. 2010) suggests that, based on localization, Chz1 functions are nuclear and coordinate with the SWR complex, whereas Nap1 may be dedicated to maintaining the cytoplasmic pool of histones. The panel of mutants proposed should be phenotyped for temperature sensitivity, DNA damage sensitivity, nickel effects, and Rad53 phosphorylation status upon DNA damage. Given the cell cycle phenotypes of both *nap1Δ* and *esa1*, it would be interesting to analyze mutants by FACS and see how deletion of other genes affects known phenotypes. This analysis will contribute to establishing how the four genes, *ESA1, HTZ1, NAP1* and *CHZ1* interact, and will describe a complex network.

Whereas many of the mutants under study are sensitive to DNA damage, it is worth recalling the example of the *lys20Δ lys21Δ* mutants presented in Chapter 2. These mutants were resistant to DNA damage, and the *htz1Δ* mutant DNA damage sensitivity was partially suppressed by deletion of *LYS20* and *LYS21*. Mutants in *NAP1* do not appear sensitive to DNA damage, but have not been assayed for DNA damage resistance. Furthermore, *nap1Δ lys20Δ lys21Δ* mutants should be tested to see if deletion of *NAP1* alters the DNA damage resistance observed in *lys20Δ lys21Δ*.

Physical interactions may also be significant as Nap1 may interact with Esa1. A precedent has been set by the report that Nap1 physically associates with the

mammalian HAT p300. Strikingly, Nap1 inhibited acetylation of core histones by p300, and had a role in promoting transcriptional activation (Asahara et al. 2002; Del Rosario and Pemberton 2008). Nap1 may do these things in concert with Esa1 in yeast.

Overexpression of *NAP1* has been shown to cause aberrant localization of Htz1-GFP (Straube et al. 2010). Localization analysis of Htz1-GFP could be carried out at different dosage levels of the histone chaperone genes, to see if Htz1 localization could be an explanation for some interactions. Obviously, this would not explain interactions observed in the *htz1Δ*.

This large body of new information about *ESA1* will help to structure further investigations. The genetic interactions with *NAP1* and *HTZ1*, together with the indication of additional sites of acetylation in H2A/H2B point to a connection between Esa1 and H2A/H2B/Htz1. This can be explored further by identifying the target residue(s) on H2A/H2B/Htz1. HAT assays on H2AK4,7A mutant histones are being done to show that Esa1 acetylates H2A/H2B histones in the absence of the two known targets. This is a modified repeat of the assay that used tailless H2A/H2B as substrate. Remaining H2A lysines will be successively mutated to find histones that Esa1 is no longer able to acetylate and thus identify the targets of Esa1 acetylation. Preliminary experiments have been done to purify FLAG-H2A/H2B from yeast and in the future, histones from point mutants in remaining lysine residues can also be purified and used as substrate in HAT assays, as shown in Fig 3.14 and 3.15. The critical residue or residues that are Esa1 targets will be mutated and the histones will no longer be

acetylated by Esa1 *in vitro*. The mutants in histone genes will also be phenotyped so that when the Esa1 targets are found, we will know if they have overlapping phenotypes with Esa1.

Taken together, results presented in this chapter further define the role of *ESA1* in multiple cellular processes. Genetic interactions are explored with the histone variant Htz1, the HDAC Sir2, the H2A/H2B chaperone Nap1 and the histone methyltransferase Set1. Novel targets of Esa1 acetylation are also uncovered on H2A and predicted on H2A.Z. The functional analyses reported here suggest expanded the roles of Esa1 in the cell through a series of interactions united by their intersections with H2A and its associated proteins.

Materials and methods

Strains and plasmids

HTZ1 point mutants were generated by site directed mutagenesis. The plasmid pLP2264 (*htz1*-K8,10,14A in pRS316) was made by direct mutagenesis of pLP2254 (wild type *HTZ1* in pRS316) with oLP982 and oLP983. Similarly, pLP2271 (*htz1*-K3A) was made by direct mutagenesis of pLP2254 with oLP980 and oLP981. Finally, pLP2275 (*htz1*-K3,8,10,14A) was made by direct mutagenesis of pLP2264 with oLP980 and oLP981.

rDNA silencing was assayed on plates lacking adenine and arginine (and other compounds as specified in the figure legends). Plates for silencing also contained 16,

32 or 48 μg/mL of canavanine as specified. Canavanine was first dissolved in water, filtered to sterilize and then added to cooled agar before plates were poured. Camptothecin plates and DMSO growth controls are buffered to pH 7.5 with potassium phosphate. DMSO is added to growth control plates to equal the concentration of DMSO in drug plates. Camptothecin is dissolved in DMSO at a stock concentration of 5mg/mL but is not sterilized. Working concentration is specified in figure legends. The working concentration of hydroxyurea is 100mM, diluted from an aqueous stock concentration of 3M. HU stock is filtered to sterilize.

HAT Assays

Detailed methods for the HAT assays are described in Appendix A. The recombinant tailless H2A/H2B was used at 10μg/reaction. 5μL bacterial extract and 0.5 μCi of tritiated Acetyl CoA were used per reaction. Film pictured in Fig 3.15 was dried and exposed directly to film with Kodak LE transcreen; in this case no transfer to nitrocellulose occurred.

Acknowledgements

Jae Chung has begun the analysis of *CHZ1* in combination with *ESA1*, *NAP1* and *HTZ1*. D.Kellogg (UCSC) provided the *nap1*Δ strain from which other mutants were derived. J. Wilhelm (UCSD) provided the Htz1-GFP strain that will be used in further analyses. M. Smith (UVA) and R. Kamakaka (UCSC) provided *htz1*Δ strains and plasmids. J. Huh and R. Dutnall provided the recombinant tailless H2A/H2B.

Table 3.1 Strains used in Chapter 3

Strains	
Strain	Genotype
LPY5	*MAT*a W303 WT
LPY4774	*MATa* W303 *esa1-414*
LPY4911	*MATα* W303 *esa1-414 rDNA::ADE2CAN1*
LPY6282	*MATα* W303WT rDNA::*ADE2CAN1 trp1Δ0*
LPY6491	*MATα* BY4741 WT *met15Δ0*
LPY6497	*MATa* BY4741 *lys2Δ0*
LPY6926	*MATα W*303 *set1Δ::HIS3 rDNA::ADE2CAN1*
LPY12805	*MATa* W303 *nap1Δ::kanMX*
LPY11160	*MAT?* W303 *esa1-414 sir2Δ::HIS3*
LPY11411	*MATa* W303 *lys20Δ::kanMX lys21Δ::clonNAT rDNA::ADE2CAN1*
LPY11564	*MATa* W303 *lys2Δ::HISG htz1Δ::kanMX*
LPY11648	*MATα* W303 *esa1-414 lys2Δ::HISG*
LPY11654	*MATa* W303 *htz1Δ::kanMX*
LPY11666	*MATα* W303 *esa1-414 htz1Δ::kanMX*
LPY12300	*MATα* S288C *htz1Δ::kanMX*
LPY12417	*MATα* S288C *esa1Δ::HIS3 htz1Δ::kanMX* + pLP863
LPY12418	*MATα* S288C *esa1Δ::HIS3 htz1Δ::kanMX* + pLP863
LPY12614	*MATα* S288C *esa1Δ::HIS3 htz1Δ::kanMX* + pLP780
LPY12615	*MATα* S288C *esa1Δ::HIS3 htz1Δ::kanMX* + pLP784
LPY12616	*MATα* S288C *esa1Δ::HIS3 htz1Δ::kanMX* + pLP776
LPY12617	*MATα* S288C *esa1Δ::HIS3 htz1Δ::kanMX* + pLP777
LPY12618	*MATα* S288C *esa1Δ::HIS3 htz1Δ::kanMX* + pLP783
LPY12808	*MATa* BY4741 *lys2Δ0 htz1Δ::kanMX*
LPY12811	*MATα* BY4741 *htz1Δ::kanMX met15Δ0*
LPY12824	*MATα* W303 *esa1-414 nap1Δ::kanMX rDNA::ADE2CAN1*
LPY12827	*MATa* W303 *nap1Δ::kanMX rDNA::ADE2CAN1*
LPY12828	*MATa* W303 *esa1-414 nap1Δ::kanMX rDNA::ADE2CAN1*
LPY13024	*MATa W303 htz1Δ::kanMX*
LPY13214	*MAT*α W303 *esa1-414 lys20Δ::kanMX lys21Δ::clonNAT nap1Δ::kanMX*
LPY13215	*MAT*α W303 *esa1-414 lys20Δ::kanMX lys21Δ::clonNAT nap1Δ::KanMX rDNA::ADE2CAN1*
LPY13216	*MAT*a W303 *esa1-414*
LPY13217	*MAT*a *W303 esa1-414 rDNA::ADE2CAN1*
LPY13254	*MATα W303 esa1-414 lys20Δ::kanMX lys21Δ::clonNAT nap1Δ::KanMX*
LPY13362	*MATα* W303 *esa1-414 htz1Δ::kanMX sir2Δ::HIS3*
LPY13364	*MATa* W303*htz1Δ::kanMX*
LPY13368	*MATa* W303 *esa1-414 htz1Δ::kanMX sir2Δ::HIS3*

Table 3.2 Plasmids used in Chapter 3

Plasmids	
Plasmid	Gene
pLP61	pRS314
pLP126	pRS316
pLP362	pRS426
pLP776	*esa1-D19G, H53Y, I195K* in pLP61
pLP777	*esa1-K256Q, Y325N* in pLP61
pLP780	*esa1-L254P* in pLP61
pLP783	*esa1-C27Y* in pLP61
pLP784	*esa1-C27Y,E227D* in pLP61
pLP796	*ESA1* in pRS426
pLP820	*pRSETc*
pLP831	*ESA1* in pRSETc
pLP863	*esa1-414* in pLP61
pLP1402	*pRS202*
pLP1412	*LYS20* in pRS202
pLP1623	pRS425
pLP1887	*SET1* in pRS426
pLP1934	*LYS20* in pRSETc
pLP1935	*LYS21* in pRSETc
pLP2254	*HTZ1* in pRS316
pLP2264	*htz1-K8,10,14A* in pRS316
pLP2271	*htz1-K3A* in pRS316
pLP2275	*htz1-K3,8,10,14A* in pRS316

Table 3.3 Oligos used in Chapter 3

Oligos	
Oligo	Sequence
oLP980	ATGTCAGGAGCAGCTCATGGAGG
oLP981	CCTCCATGAGCTGCTCCTGACAT
oLP982	CATGGAGGTGCAGGTGCATCCGGCGCTGCAGACAGTGG
oLP983	CCACTGTCTGCAGCGCCGGATGCACCTGCACCTCCATG

Chapter 4 Further analysis of Lys20 nuclear functions

Introduction

Nuclear roles for *LYS20* were established in Chapter 2. Since the discovery of nuclear roles for a metabolic enzyme was unexpected, an exploration of *LYS20*'s role in other nuclear processes was undertaken. In light of *LYS20*'s strong genetic interaction with *esa1*, we examined effects of *LYS20* on other phenotypes of *esa1* mutants. These studies help refine Lys20's role with regard to Esa1, as Lys20 is involved a subset of the same processes.

Much effort so far has focused *in vivo* genetic interactions and *in vitro* activities. Here, *in vivo* physical interactions are also explored, based both on these analyses and published results. This combined approach helps clarify Lys20's unique role and rules out processes that do not involve Lys20. In particular, this chapter will focus on histone acetylation, some physical characteristics of Lys20 and transcriptional silencing. Lys20's role in silencing of the rDNA locus will be the focus of some study. The rDNA locus encodes the structural and catalytic RNAs of ribosomes. This process relies on a group of histones, histone acetyltransferases (HATs) and histone deacetylases (HDACs) (reviewed in Conconi 2005; Koch and Pillus 2009). Mutations in any of these proteins may result in aberrant silencing at the

rDNA as is the case for the HATs Esa1 and Sas2 and the HDAC Sir2 (Suka et al. 2002; Clarke et al. 2006).

Results

LYS20 and histone acetylation

A possible mechanism for the suppression observed of *esa1* by overexpression of *LYS20* (Fig. 2.1) was that *LYS20* acted at the level of histone acetylation. To test this possibility, global levels of histone acetylation at Esa1 target residues were assayed using isoform specific antisera to detect acetylation at target residues in *esa1* mutants with and without overexpressed *LYS20.* It is established that *esa1* mutants have reduced acetylation at target residues (Clarke et al. 1999). These include H4K5, K8, K12, K16, H3K14 and H2AK7 (Clarke et al. 1999; Smith et al. 1998). If the hypothesis that *LYS20* suppresses *esa1* defects by acting at the level of histone acetylation is correct, overexpression of *LYS20* would restore histone acetylation in *esa1* mutants at some or all target residues. In Fig 4.1, it is shown that overexpression of *LYS20* does not strongly affect levels of acetylation at H4K5, K8 or K12. In Fig 4.2, H4K16 and H3K14 were also assayed. Also, an antiserum was used to detect acetylation across H4, known as pan-aceylated H4. No effect on acetylation was observed using any of these antisera. It was possible that a different target of Esa1 was affected by Lys20, so H2AK7ac antiserum was obtained (gift of M. Grunstein) that had previously been used for ChIP assays, and was used to evaluate Lys20-dependent changes in acetylation. Unfortunately, no H2A specific band could be detected

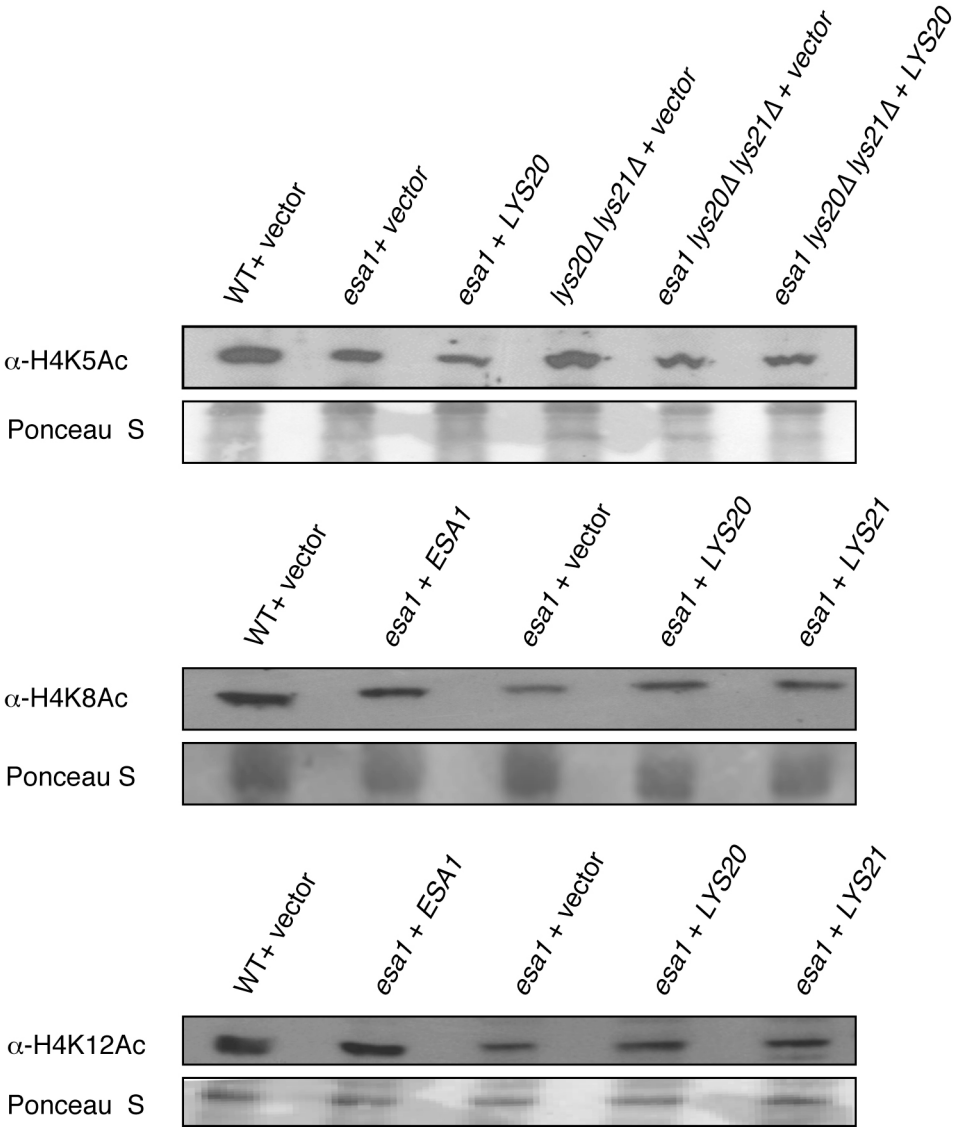

Figure 4.1 Overexpression of *LYS20* does not restore histone acetylation in *esa1* mutants at H4K5, H4K8 or H4K12. Ponceau S stains of membranes are included as loading controls.

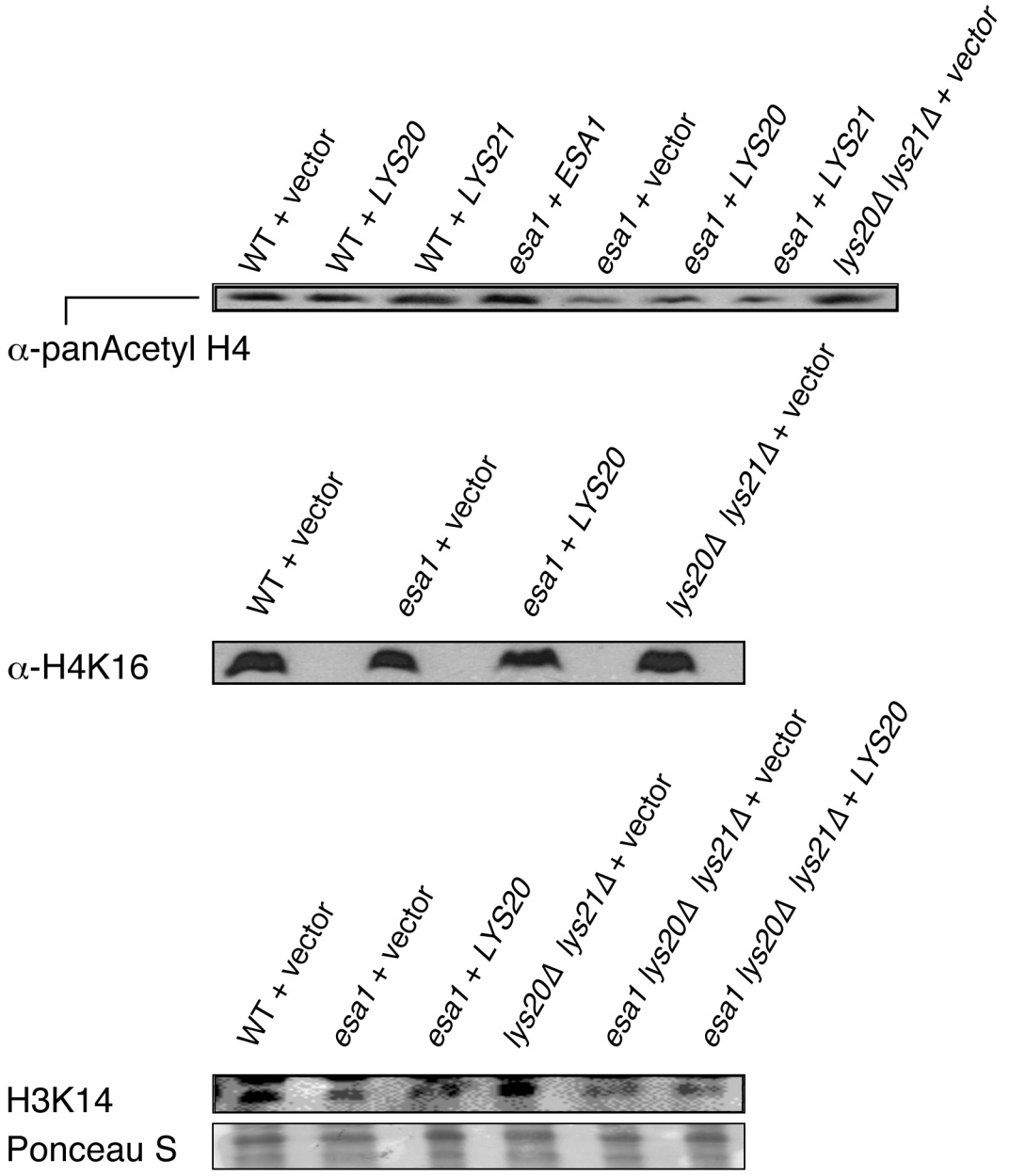

Figure 4.2 Overexpression of *LYS20* does not restore histone acetylation in *esa1* mutants at H4K16, across H4 or H3K14. Ponceau S stains of membranes are included as loading controls. The pan-acetyl H4 antibody detects acetylation across the N terminus of H4.

despite the inclusion of wild-type and H2AK7R samples as controls (data not shown).

Although restoration of bulk levels of histone acetylation was not observed, if suppression is mediated through histone acetylation, one might also expect decreases in acetylation, in *lys20Δ lys21Δ* mutants, especially in the presence of DNA damage. To test this possibility, levels of histone acetylation at three residues were assayed with acetyl specific antisera in the presence and absence of DNA damage. Changes were not observed at any residue (Fig 4.3). Acetylation levels of H4K12 appeared to change in response to camptothecin (CPT) induced DNA damage, but this effect was independent of the HCS status of the cell.

Thus, Lys20 does not affect global levels of acetylation at the residues tested. Acetylation levels at other residues may be affected by *LYS20* status. Targeted changes in histone acetylation might also be observed at specific loci, or sites of DNA damage, but the effects may be too small to observe when probing global levels.

LYS20 in transcriptional silencing

A phenotype of *esa1* that is perturbed by *LYS20* overexpression is transcriptional silencing. The involvement of *LYS20* is specific for silencing at the rDNA locus (using the *ADE2CAN1* marker at the 25S rDNA), with telomeric silencing unaffected by overexpression of *LYS20* (Chang, Clarke and Pillus, in prep.) *LYS20* overexpression also disrupts rDNA silencing in wild type cells (Chang, Clarke and Pillus, in prep). This effect is the opposite of what might be expected. Whereas *LYS20* overexpression suppresses the temperature sensitivity and camptothecin sensitivity of

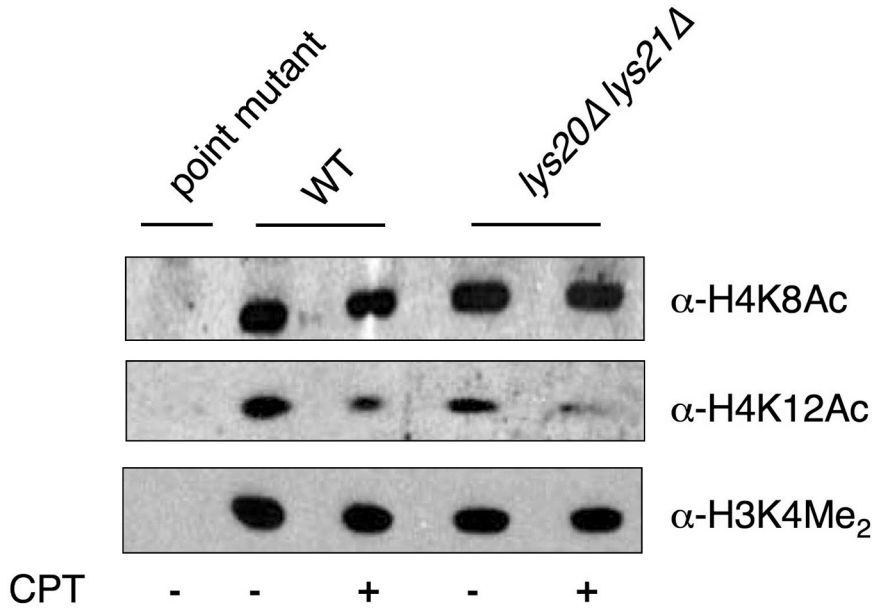

Figure 4.3 Global histone modification levels at three key residues are not affected by deletion of *LYS20* and *LYS21.* Levels of H4K12 acetylation decrease in the presence of CPT, but not in a *LYS20 LYS21* dependent manner. Histone point mutant extracts are included as negative controls for the antisera for H4K8 and H4K12. A *set1Δ* strain, in which all methylation at H3K4 is lost, is used as the control for the dimethyl H3K4 antibody.

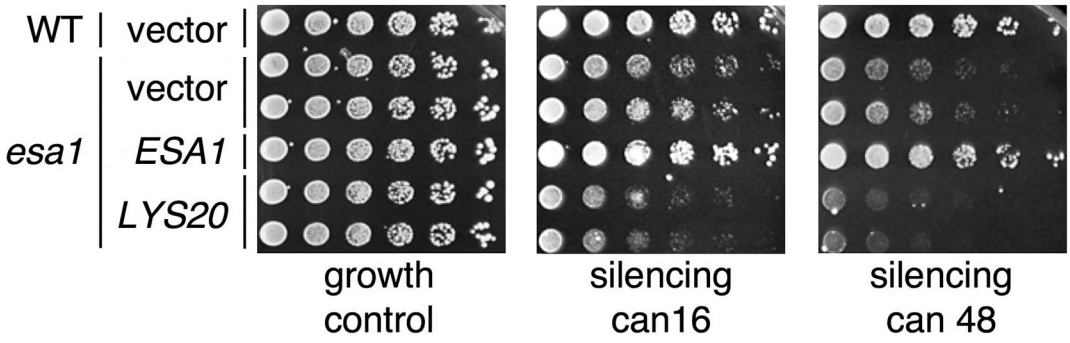

Figure 4.4 Overexpression of *LYS20* exacerbates the *esa1* rDNA silencing defect. All plates lack adenine, arginine and uracil, and silencing plates contain canavanine in indicated concentrations. Increased growth of a strain indicates more rDNA silencing.

esa1, it exacerbates *esa1*'s rDNA silencing defect (Fig 4.4). In an effort to understand this effect, *LYS20* was overexpressed in other chromatin related mutants. Next, overexpression in an HDAC-deleted strain with a known defect in rDNA silencing, *sir2Δ,* was tested. Overexpression of *LYS20* in *sir2Δ* mutants also enhanced the rDNA silencing defect (Fig 4.5). Disruption of silencing is also observed upon *LYS20* overexpression in wild type strains (Fig 4.5). *LYS20* was overexpressed in a strain with the gene encoding the histone acetyltransferase Hat1 deleted. Hat1 shares targets in H4 with Esa1, since they both acetylate H4K5 and H4K12 (reviewed in Parthun 2007).

Overexpression of *LYS20* in a *hat1Δ* mutant and in an *esa1 hat1Δ* double mutant also yielded the disruption in rDNA silencing (Fig 4.6), as it did in the *esa1* mutant. Thus, *LYS20* is able to create a silencing defect in addition to enhancing defects due to deletion of chromatin modifying enzymes. If it can create defects, what is the effect on the enhanced silencing found upon deletion of the gene encoding the HDAC Rpd3 (Sun and Hampsey 1999). Overexpression of *LYS20* powerfully disrupts even this increased silencing (Fig 4.7).

Next, *LYS20* overexpression was tested to determine its effect in a non-HAT or HDAC mutant. The histone methylase Set1 also plays a role in silencing at the rDNA (reviewed in Dehe and Geli 2006). Mutants in *set1Δ* are both extremely growth compromised and very defective in rDNA silencing. However, *LYS20* overexpression

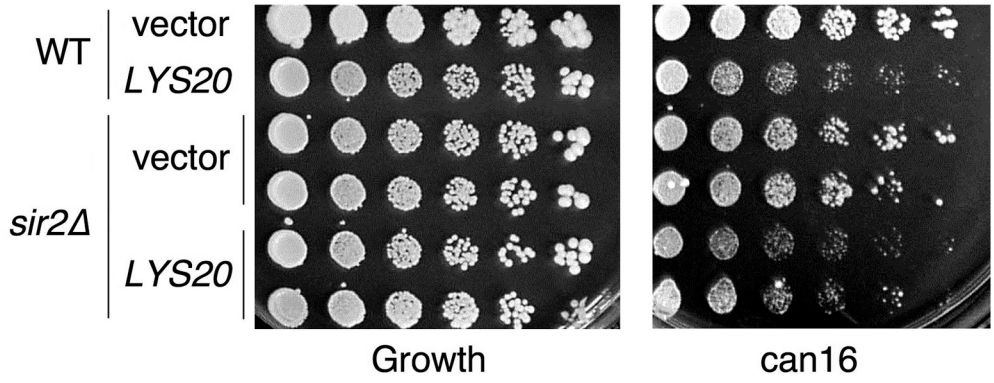

Figure 4.5 Overexpression of *LYS20* exacerbates the rDNA silencing defect of a *sir2Δ* mutant and creates a *de novo* silencing defect in wild type cells.

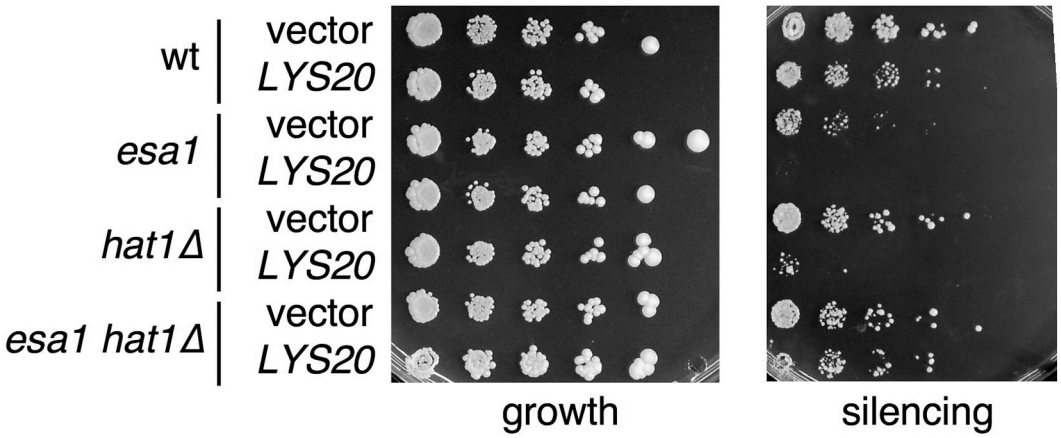

Figure 4.6 Overexpression of *LYS20* creates a silencing defect in *hat1Δ* and *esa1 hat1Δ* cells. Silencing plate contains 48 µg/mL of canavanine. Data generated by Kendra Lipinski.

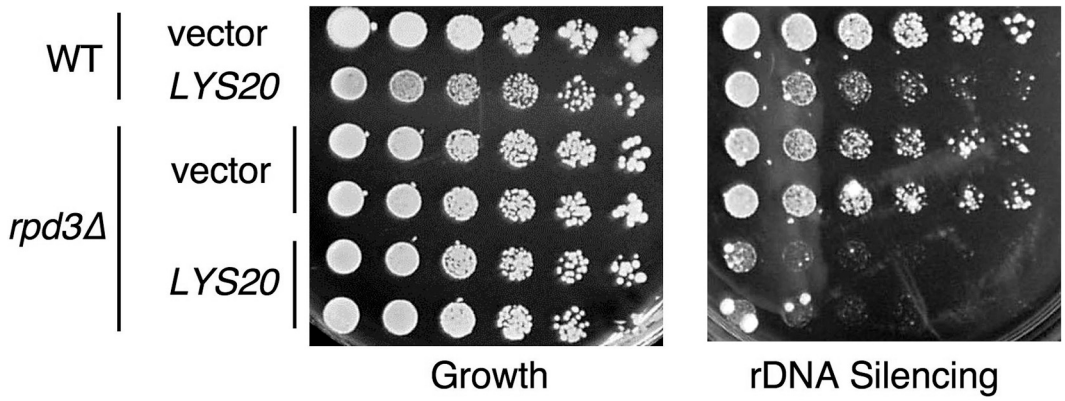

Figure 4.7 Overexpression of *LYS20* destroys the increased rDNA silencing of *rpd3Δ* cells. Silencing plate contains 32 µg/mL of canavanine.

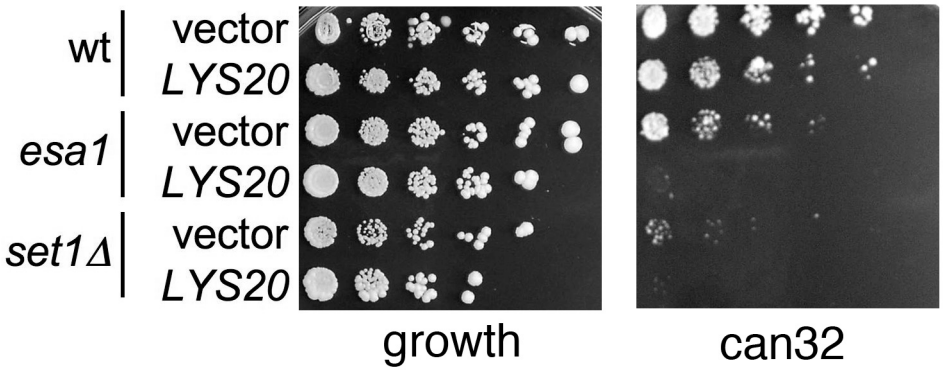

Figure 4.8 Overexpression of *LYS20* exacerbates the rDNA silencing defect of *set1Δ* mutants. Silencing plate contains 32 µg/mL of canavanine.

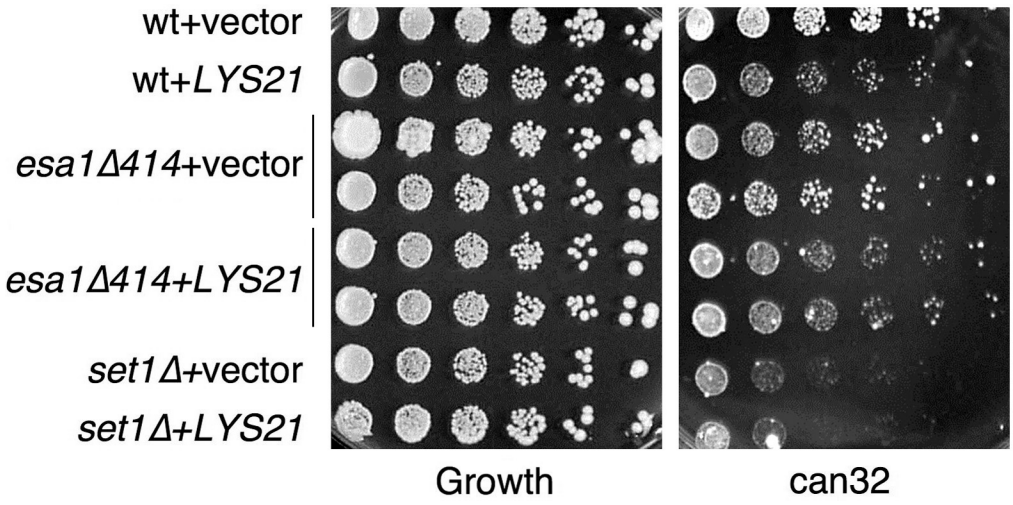

Figure 4.9 Overexpression of *LYS21*, like *LYS20* creates an rDNA silencing defect in wildtype strains and exacerbates the defect present in *esa1* and *set1Δ* mutants. Silencing plate contains 32µg/mL cananvanine.

makes even this severe silencing defect worse (Fig 4.8). Together, these results remain somewhat confounding and no single model has yet been developed to accomodate all of these data.

LYS21 also shares the property of dosage dependent rDNA silencing disruption. When overexpressed in *esa1* strains (Fig 4.9), it too worsens the rDNA silencing defect. Additionally, disruption of rDNA silencing was observed in wildtype strains (Fig 4.9). Similar to *LYS20*, *LYS21* exacerbated the defect of *sir2Δ* strains (Fig 4.9).

One possible explanation for the disruption of rDNA silencing observed upon overexpression of *LYS20* was that overexpressing *LYS20* raised intracellular levels of lysine or homocitrate in the cell and that the silencing phenotype was mediated via the metabolic function of HCS. To address this assays were performed by Kendra Lipinski on media with increased levels of lysine (Fig 4.10). Plates were poured which contained 20mM lysine in addition to canavanine. It seemed that addition of lysine to this concentration ameliorated the effects of *LYS20* overexpression. However, it also seemed to heal the rDNA defects of the *esa1* and *set1Δ* strains in a *LYS20* independent manner. This second observation requires reconsideration of the first observation. Both effects could simply be due to increased growth caused by addition of lysine to such high concentrations, although this is not obvious on the growth plates since we don't have that comparison. Additionally, as discussed in the introduction, the rDNA silencing assay depends upon canavanine, a chemical similar in structure to arginine.

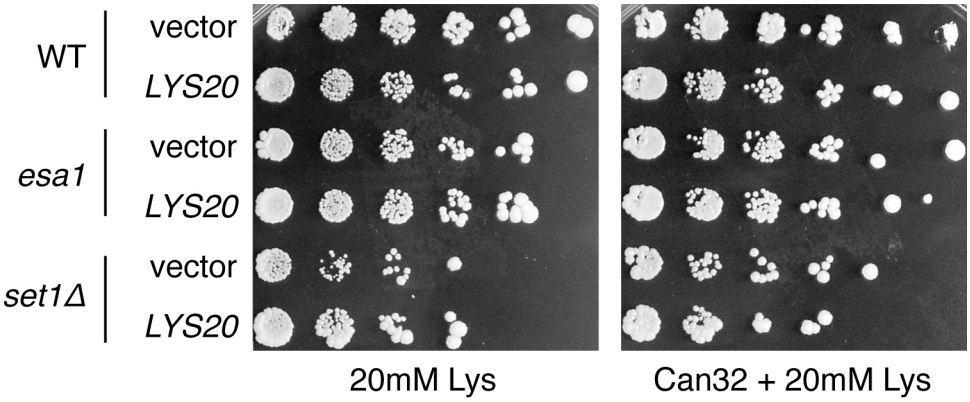

Figure 4.10 Addition of 20mM lysine to silencing plates restores rDNA silencing. Both the growth plate and the silencing plate contain 20mM lysine. Silencing plate contains 32µg/mL canavanine. Neither *esa1* nor *set1Δ* display a silencing defect on the silencing plates; even in the presence of *LYS20* overexpression, silencing appears normal as indicated by growth on silencing plates. Data generated by Kendra Lipinski**.**

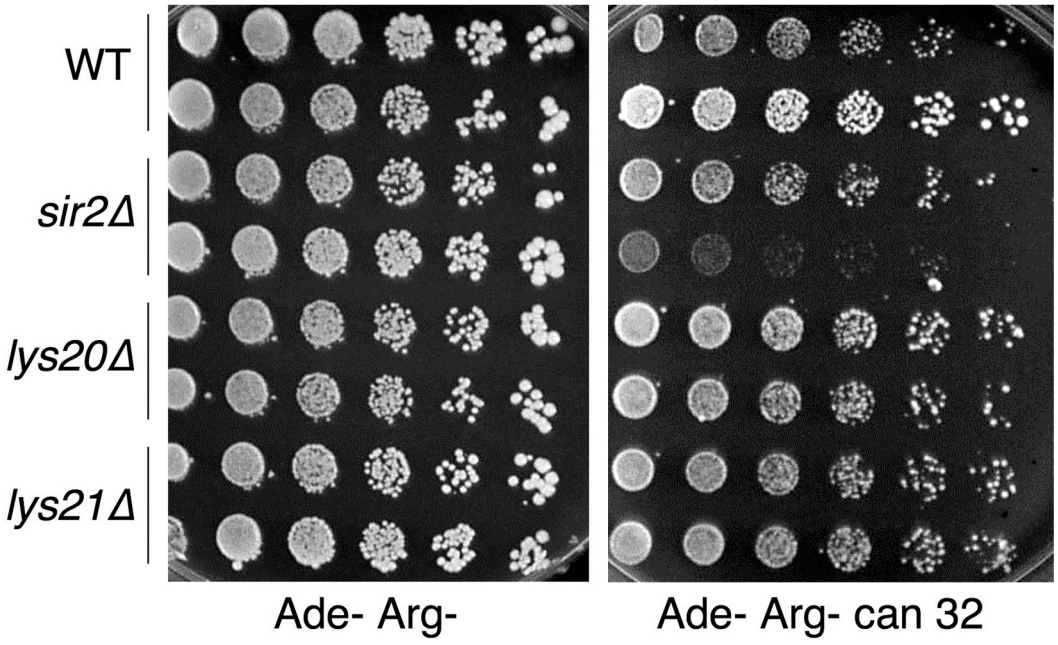

Figure 4.11 Deletion of either *LYS20* or *LYS21* does not cause defects in rDNA silencing. Silencing plate contains 32µg/mL of canavnine. The *sir2Δ* mutant is included as a positive control for a strain with an rDNA silencing defect.

Lysine may be similar enough in structure and charge to interfere with the transport or mechanism of action of canavanine.

If, as demonstrated, overexpression of *LYS20* and *LYS21* disrupts rDNA silencing, it would be logical that deletion of the HCSs would result in increased silencing at the rDNA locus. Double mutants in *LYS20, LYS21* were assayed for rDNA silencing (Fig 4.11). No defects were observed, but it was hard to discern if silencing might be modestly increased. To determine this, experiments should be repeated on higher concentrations of canavanine. Also, some variation in silencing was observed in the *sir2*Δ mutant used as a positive control, for reasons that are not clear. Either a different reporter could be used, or a different positive control less prone to variation. Based on the result that *LYS20* overexpression enhances rDNA silencing defects in *esa1*, it could be predicted that deletion of these enzymes would result in increased silencing at this locus, possibly suppressing the defect. Triple mutants (*esa1 lys20Δ lys21Δ)* were created and assayed for rDNA silencing (Fig 4.12). The triple mutants resemble *esa1* more than *lys20Δ lys21Δ.* Some suppression may be observed, but not strongly.

By parallel analysis, it was possible that *lys20Δ lys21Δ* would affect the increased silencing of the *rpd3Δ* mutant. To test this idea, *rpd3Δ lys20Δ lys21Δ* triple mutants were constructed and grown on canavanine plates (Fig 4.13). The results are variable and difficult to interpret. In some cases, it appears that if anything, the triple

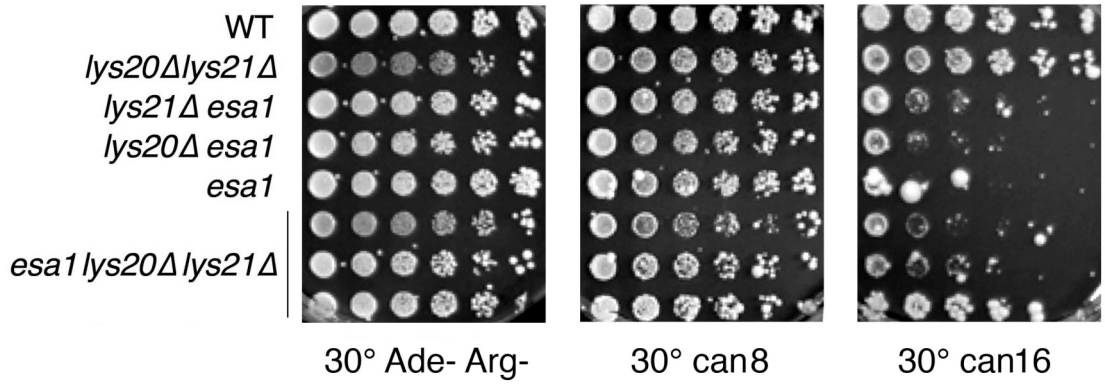

Figure 4.12 Deletion of *LYS20* and *LYS21* affects the *esa1* rDNA silencing defect. Silencing plate contains 8 or16µg/mL of canavanine. Plates were incubated at 30˚C. Triple mutants in *esa1 lys20Δ lys21Δ* have a phenotype intermediate between *esa1* and *lys20Δ lys21Δ*.

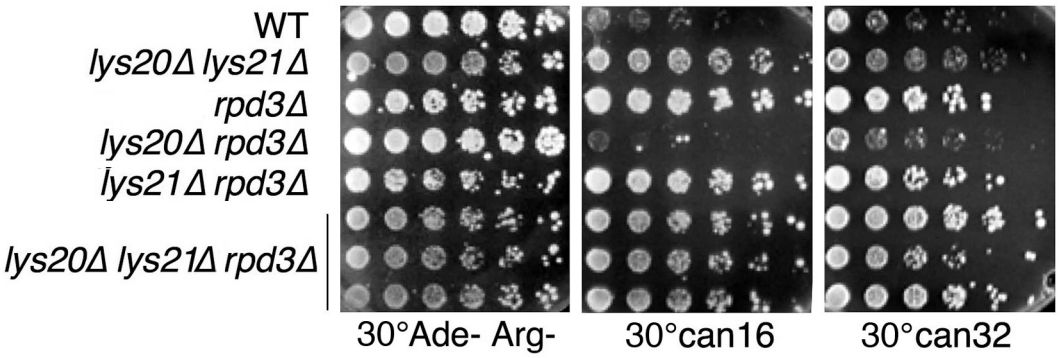

Figure 4.13 Deletion of *LYS20* and *LYS21* has variable effects on rDNA silencing in the *rpd3Δ* mutant. Triple mutants are three independent strains. Silencing plates contain either 16 or 32µg/mL of canavanine as specified.

mutants may have slightly increased silencing. This analysis could be repeated on media with higher canavanine concentrations to see whether the increased silencing can be observed more clearly with more cnanvanine present.

Since Lys20 is involved in silencing at the rDNA locus, it was possible that it might be involved in silencing at other loci. To address this, *LYS20* was overexpressed in wild type and *sas2Δ* mutant cells. Mutants in *SAS2* are defective in telomeric silencing (Reifsnyder et al. 1996), and it was possible that *LYS20* overexpression would suppress this defect. Alternatively, it might make the defect more severe as was the case for the rDNA silencing defect of *esa1* mutants. In Figure 4.14, telomeric silencing assays demonstrate that *LYS20* overexpression does not affect silencing at the telomeres, in the *sas2Δ* mutant, but may have a modestly disruptive effect in wild type cells.

Physical interactions and binding partners for Lys20

A directed search for Lys20 physical interactions *in vivo* relied on an immunoprecipitation (IP) approach. As reported in Chapter2, Lys20 associated *in vivo* with the HAT Gcn5. It seemed possible that Lys20 might also associate with Esa1. To this end, immunoprecipitations were performed in an Esa1-Myc strain. Antibodies directed against Lys20 and HCS were used to precipitate Lys20 and any associated proteins, and Esa1-Myc was probed for with anti-Myc antibody (Fig 4.15). Immunoprecipitations were performed on samples after HU treatment to induce DNA damage, although this did not affect the final results (Fig 4.15). The IP was also performed in cells that were overexpressing *LYS20*, and this too did not affect

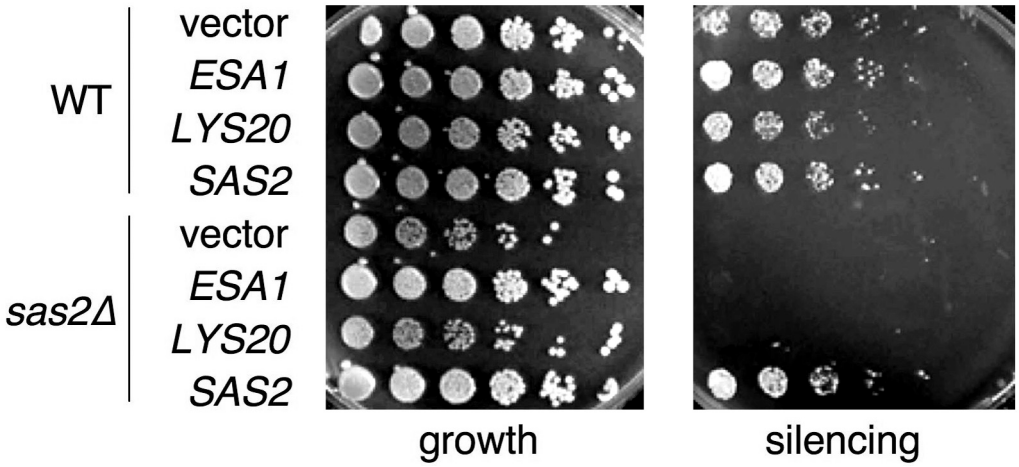

Figure 4.14 Overexpression of *LYS20* does not rescue the telomeric silencing defect of *sas2Δ* mutants. *LYS20* overexpression does not perturb telomeric silcncing in wildtype cells. Growth plates lack leucine; silencing plates lack leucine but contain 5-FOA.

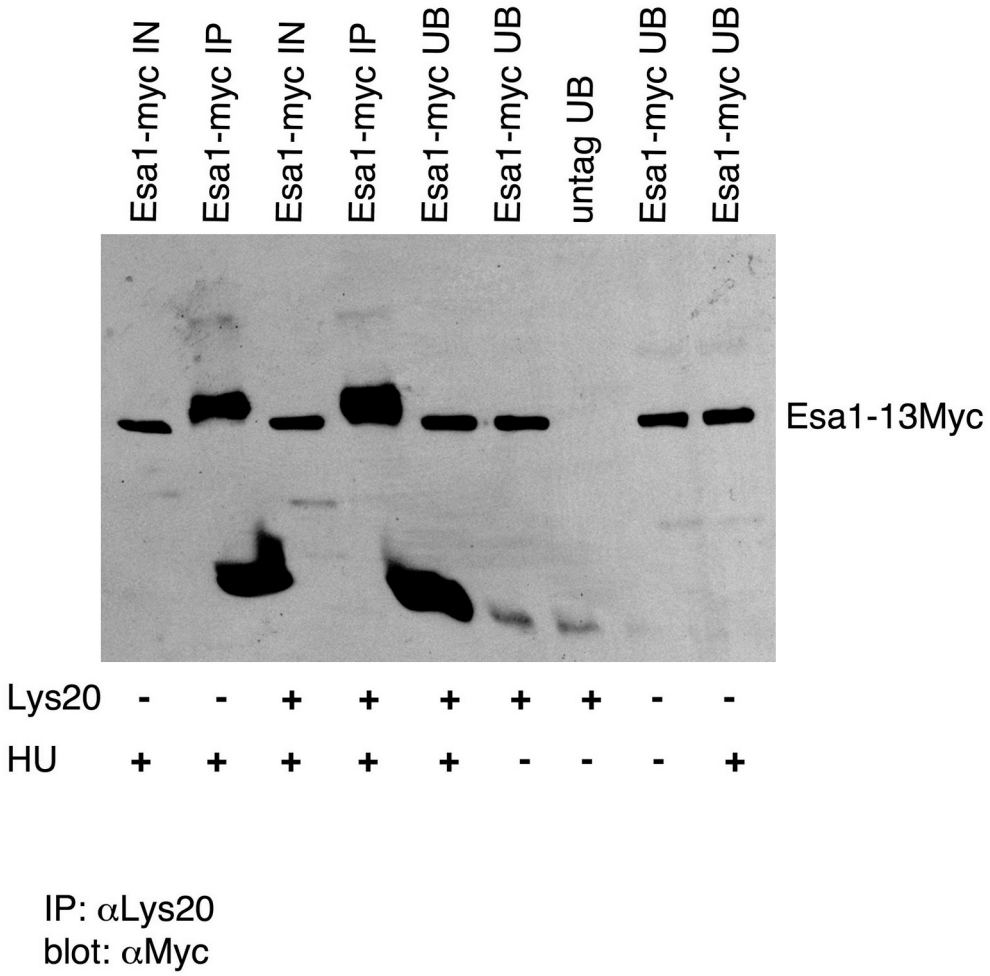

Figure 4.15 Esa1-Myc does not co-immunoprecipitate with Lys20.
IN indicates input, UB is unbound and IP is immunoprecipitated material. Experiment was done both under conditions of overexpressed Lys20 and at wildtype levels, indicted by + or -. Experiment was also done in cells with and without hydroxyurea (HU). Proteins were pulled down with anti-Lys20 antibody and Esa1-13Myc was detected with anti-Myc antibody. IN refers to input, UB is unbound and IP is immunoprecipitated material. Larger band in Esa1-Myc IP lanes is nonspecific.

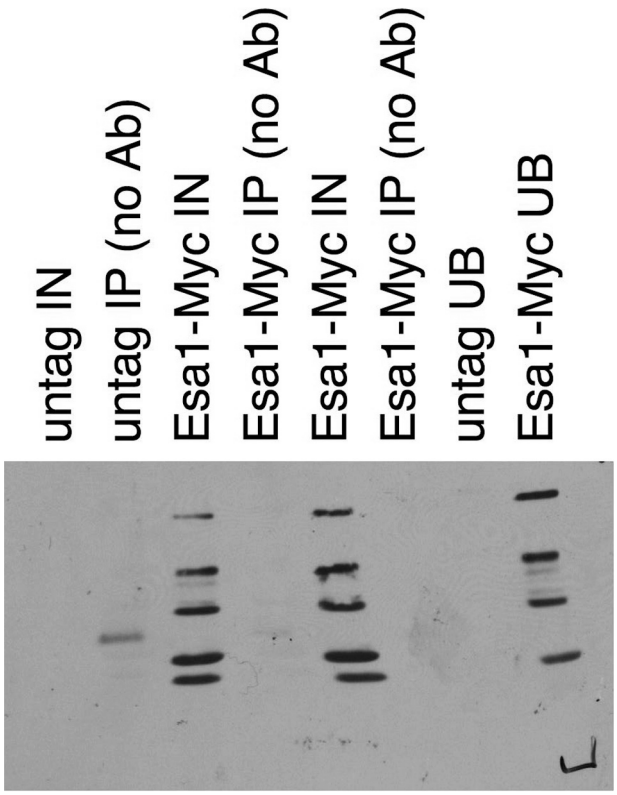

Figure 4.16 No antibody control immunoprecipitation shows very little nonspecific binding to antibody. In order to control for the presence of contaminating bands due to the antibody in the IP shown in Fig. 4.15, the same experiment was performed without Lys20 primary antibody. All bands disappear in the no Ab IP lanes, showing that contaminating bands are not due to presence of antibody. IN refers to input, UB is unbound and IP is immunoprecipitated material. No Ab means that no antibody was added to the reaction. Blot was probed with anti-Myc antibody.

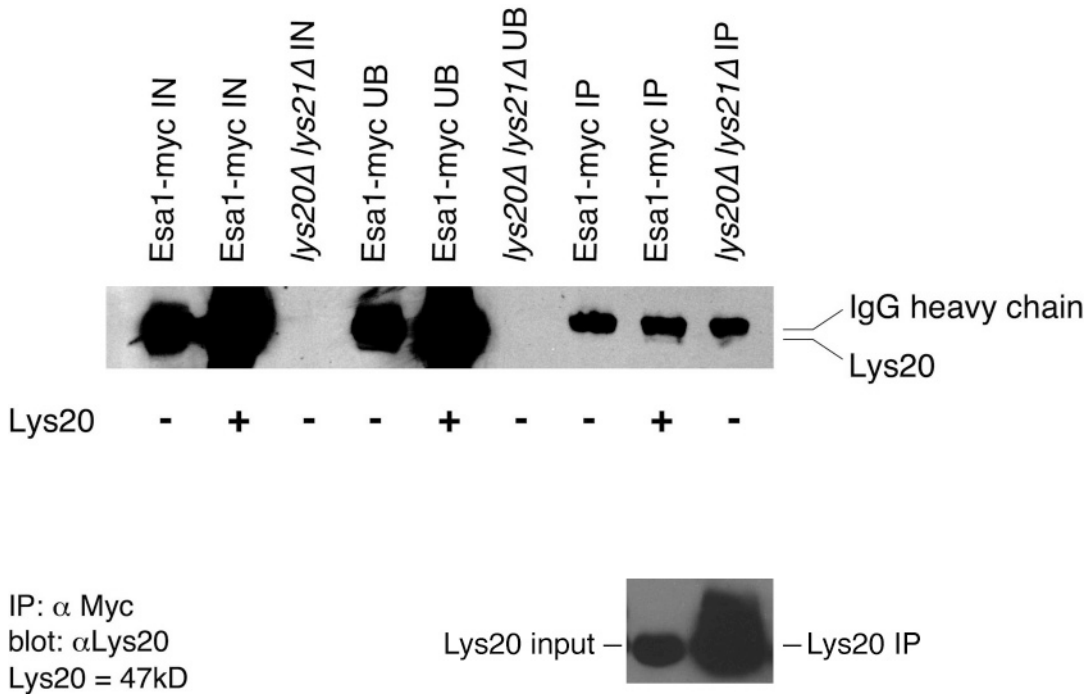

Figure 4.17 Lys20 does not coimmunoprecipitate with Esa1-Myc. IN indicates input, UB is unbound and IP is immunoprecipitated material. The *lys20Δ lys21Δ* strain is included as a negative control. Proteins were precipitated with anti-Myc antibody, to pull down Esa1-Myc and any associated material. Lys20 was detected with anti-Lys20 antibody. IN refers to input, UB is unbound and IP is immunoprecipitated material. Inset panel is antibody control showing that anti-Lys20 antibody efficiently precipitates Lys20 from cells.

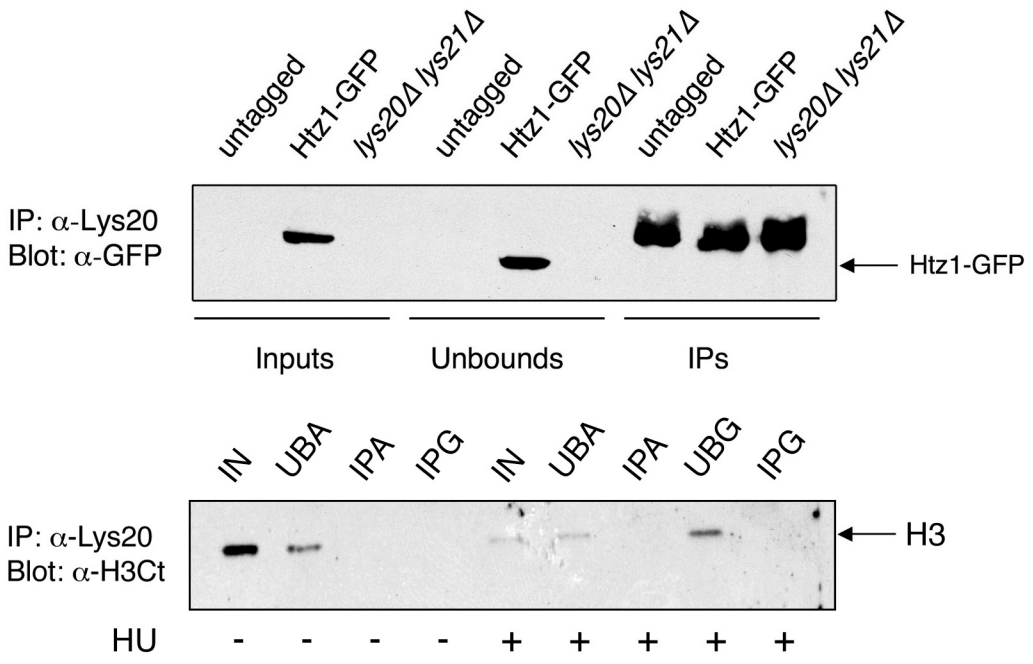

Figure 4.18 Lys20 does not co-immunoprecipitate with Htz1-GFP or histone H3. Untagged and *lys20Δ lys21Δ* strains are included as negative controls. Proteins were precipitated with anti-Lys20 antibody and Htz1-GFP was detected with anti-GFP antiserum. For H3 blot, IN refers to input, UB is unbound and IP is immunoprecipitated material. IPA refers to those immunopreciptations that used Protein A Sepharose, IPG lanes represent samples where Protein G Sepharose was used. Cells were treated with 0.1M hydroxyurea or not as indicated by + or – below blot. Proteins were precipitated with anti-Lys20 antibody and H3 was detected with antiserum against the C-terminus of H3 (H3Ct).

the results (Fig 4.15). Blots were difficult to interpret, with contaminating bands in places near to the position of Esa1-Myc, due to the IgG heavy chain from the antibody used in the IP. A negative control containing no antibody was performed for this IP, demonstrating that there were not high levels of nonspecific binding to the antibody (Fig 4.16). The reciprocal experiment was performed, by precipitating with anti-Myc antibody and detecting with anti-Lys20 (Fig 4.17). No interaction was observed. It was concluded that Esa1 and Lys20 do not physically interact under these conditions.

Similarly, it was possible that Lys20 interacted with histones *in vivo*. Given Lys20's interactions with Htz1 (Chapter 2), Htz1-GFP was tested to see if Lys20 and Htz1-GFP physically interacted. No interaction was observed (Fig 4.18). Histone H3 was also tested (Fig 4.18) and again no physical interaction was observed under the conditions tested.

Large scale studies have reported physical protein interactions for Lys20 and Lys21 (Krogan et al. 2006). One of the proteins physically interacting with Lys21 was the predicted DNA damage protein, Mag2. Other reported interactors include Lys20 discussed in Chapter 5, and several kinases as well as an RNA binding protein. Mag2 has never been characterized *in vivo* in *S. cerevisiae*; the paper that identified it was a computational analysis that predicted an involvement in DNA damage based on domain structure (Samanta and Liang 2003). However, given the DNA damage phenotypes of *LYS20* and *LYS21*, it seemed a promising interacting protein. Triple mutants were constructed in the BY4741 background so that the effect of *lys20Δ lys21Δ mag2Δ* could be analyzed. The mutants were assayed on DNA damaging

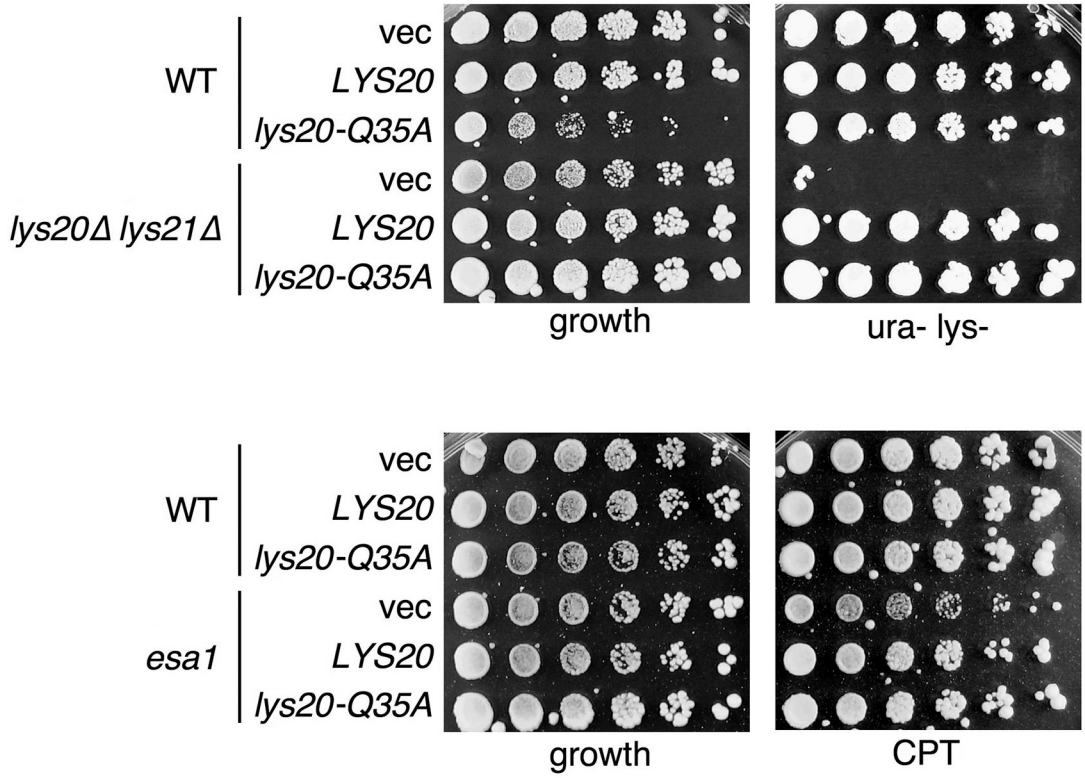

Figure 4.19 The *lys20-Q35A* point mutant does not affect lysine biosynthesis functions or DNA damage suppression. The mutant allele of *LYS20* causes no dominant effects when transformed into wild type cells.

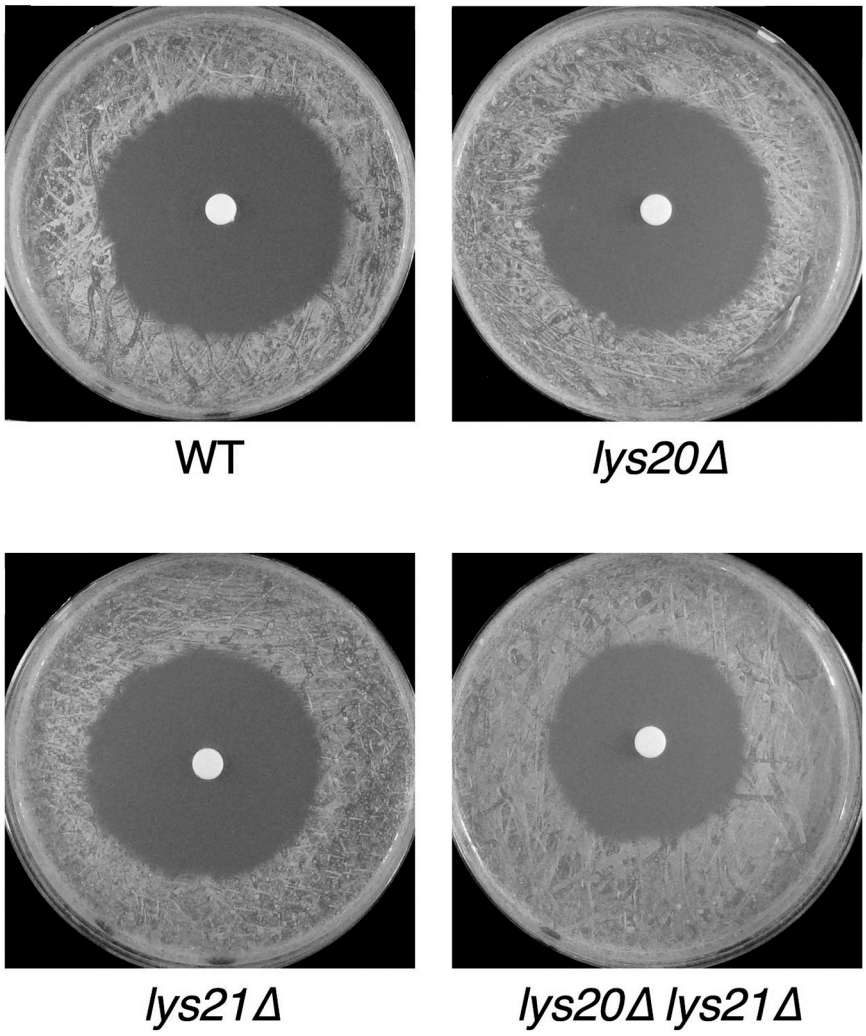

Figure 4.20 Halo assays reveal that *lys20Δ lys21Δ* mutants are resistant to hydrogen peroxide. Filters spotted with 20 µl 30% peroxide. SC plates were spread with .05 OD_{600} of cells and incubated with peroxide infused discs for 2 days at 30˚C. Plates were scanned and halos quantified with Imagequant. The size of the wild type (WT) halo was set at 100%, and relative to WT , the *lys20*Δ mutant halo was 123%, *lys21*Δ was 92% and the double mutant was 29%.

agents, but no phenotypes were observed for the single *mag2*Δ mutant or the *mag2*Δ *lys20*Δ *lys21*Δ triple mutants (data not shown). The simplest interpretation is that *MAG2* does not play a role in DNA damage.

Mutational analysis of Lys20

Metabolic roles for Lys20 must depend upon the ability to bind acetyl CoA and use it as an acetyl donor for the homocitrate synthase reaction. Putative HAT functions should also depend upon this ability. Mutation of a residue critical in the binding of acetyl CoA should abolish both functions. By comparison with the crystal structure of the *S. pombe* HCS (See Chapter 5), Q35 was selected as a potential residue in Lys20. It was mutated to alanine, and the mutant was tested for ability to promote lysine biosynthesis or suppress *esa1* phenotypes. The mutant could perform both functions (Fig. 4.19), implying that mutation of this residue is not sufficient to abolish acetyl CoA binding.

LYS20 and reactive oxygen species

Halo assays with hydrogen peroxide were performed to assess the sensitivity of the *lys20Δ, lys21Δ* and *lys20Δ lys21Δ* strains to reactive oxygen species, relative to wild type. Based on the size of the zone of cells killed by peroxide, relative resistance or sensitivity can be determined. In Fig 4.20, it appears that there is a smaller empty space or "halo" in the *lys20Δ lys21Δ* strains than in the wild type cells, suggesting that *lys20Δ lys21Δ* are resistant to peroxide. As noted in figure legend, plates were scanned and halos were quantified with ImageQuant software. The size of the wild type (WT)

halo was set at 100%, and relative to WT, the *lys20*Δ mutant halo was 123%, *lys21*Δ was 92% and the double mutant was 29%. The double mutant appeared resistant relative to the wild type.

Discussion

In search of the mechanism of LYS20 involvement in rDNA silencing

This chapter reports several approaches taken to evaluate the cellular role of the homocitrate synthases Lys20 and Lys21. Lys20 does not contribute to global acetylation at any of the histone H4 residues tested. Lys20 does have an undefined role in silencing at the rDNA locus, creating a general defect when overexpressed. The mechanism for this defect is not yet understood. Chromatin structure at the rDNA may be altered when Lys20 is overexpressed either indirectly or more directly by changes in acetylation or methylation.

A possible mechanism of the rDNA silencing defect observed upon overexpression of *LYS20* might be that Lys20 is present at the rDNA under normal conditions, but when overexpressed, accumulates to detrimental levels. To test this idea, ChIP analysis could be performed to evaluate Lys20 binding both under normal circumstances and during overexpression. If Lys20 is not detectable at the rDNA, then levels of other important silencing proteins such as Sir2 could be measured to determine if its occupancy is disrupted. Because *LYS20* overexpression also worsens the *sir2Δ* silencing defect, it is unlikely that the *LYS20* effect is mediated solely

through Sir2 or any other chromatin protein in the absence of which *LYS20* creates this defect. Additionally, *LYS20* could be overexpressed in other mutant strains to seek ones that may be insensitive to its effects. If found, this strain might provide a hint as to which silencing proteins mediate the *LYS20* effect.

In search of Lys20 interacting factors

A protein reported to interact physically with Lys21, and predicted to be involved in DNA damage, Mag2 does not interact genetically with *LYS20* or *LYS21,* nor is there evidence for its involvement in DNA damage.

Expanded analysis in this area could take the form of continuing investigation of reported physical interactors. For example, the ubiquitin protease Ubp14 is reported to interact with both Lys20 and Lys21 (Krogan et al. 2006). Histones are also known to be ubiquitinated (reviewed in Zhang 2003). Perhaps Lys20 and or Lys21 play a role in ubiquitination of nuclear substrates.

A more inclusive approach would be to use the monoclonal antibodies specific for HCS to ask broadly which, if any of the TAP-affinity interactors can be validated by IPs followed by mass spectrometry to confirm their identity.

Involvement of metabolic intermediates in Lys20 nuclear roles

The possible peroxide resistance of *lys20Δ lys21Δ* mutants provides another angle that can be used to understand the DNA damage phenotypes and their link to metabolism via a distinct mechanism. Possible links between peroxide resistance and metabolism are discussed in Chapter 6.

It remains a possibility that Lys20's effects on rDNA silencing are mediated through homocitrate or other metabolic intermediates. Further rDNA silencing assays can be done to address this with different concentrations of lysine in the media, including reduced lysine. The effects of homocitrate cannot be directly tested, as homocitrate is not readily available, but the products of reactions a few steps further down the pathway may be testable. For example, 2-aminoadipate and glutamate are both intermediates in the lysine biosynthesis pathway (Fig 1.1) and are commercially available. Other similar compounds could also be used, such as citrulline and ornithine. Arginine cannot be used, because cells will not take up canavanine in the presence of arginine. A different rDNA reporter could be used that does not depend upon canavanine. Additionally, the effects of concentration of lysine or other amino acids on the nuclear phenotypes of Lys20 can be investigated. Some experiments have been done to test the effect of lysine concentration on Lys20's nuclear functions. Silencing assays at the rDNA were performed by Viet Le in the presence of twice the standard concentration of lysine and half the standard concentration, but no clear conclusions could be drawn from these assays. Kendra Lipinski assayed localization of Lys20-GFP and Lys21-GFP by fluorescence microscopy in the absence of lysine. Depriving cells of lysine did not cause either Lys20-GFP or Lys21-GFP to localize to the cytoplasm even in the absence of the other isozyme. Changes in lysine or other amino acids could affect the ability of *LYS20* to suppress *esa1* camptothecin sensitivity, or the ability of *lys20Δ lys21Δ* to suppress the *htz1Δ* DNA damage sensitivity. Even if further analysis reveals that amino acid concentration does not

affect Lys20 nuclear roles, this would still be an important result and would aid in drawing a finer distinction between chromatin associated functions for Lys20 versus metabolic ones.

Structure and function mapping of Lys20

Finer mapping of Lys20 may also contribute to the goal of defining which regions of Lys20 are requires for metabolic versus nuclear roles. Mutational analyses presented in this chapter and in Chapter 2 identify several separation-of-function alleles of Lys20. The Q35A allele was constructed in an attempt to abrogate the acetyl CoA binding activity of the protein, an activity that should be essential for both HAT functions and HCS activity. However, mutation of Q35A did not result in a disruption of function. Perhaps mutation of other residues in combination with Q35A would be sufficient. Catalytic residues essential for HCS activity have been identified (Chapter 5), but as yet no residues are known that are required only to catalyze nuclear functions. The putative NLS is required for these functions, but it is most likely required for localization and not catalysis. It is possible that the nuclear functions are structural and not enzymatic. Further mapping of the Lys20 protein should help resolve this question and further disentangle the nuclear and metabolic roles from each other. If domains required for each function are identified, this might help define other bifunctional proteins by sequence or structural similarities. Mutants made in this analysis could also be tested to see if the physical interaction with Gcn5 (described in Chapter 2) remains intact. Also, mutant alleles should be tested to determine if they are resistant to DNA damage.

In defining functions for Lys20, and possible binding partners, the possibility of Lys20 higher order structure, such as homo- or heterodimers should be considered. The *S. pombe* HCS acts as a homodimer (Fig 5.3). *S. pombe* has only one HCS isozyme, but since there are two in *S. cerevisiae*, it is also worth considering that Lys20 and Lys21 act as a heterodimer *in vivo*. Published biochemical (Andi et al. 2004) and proteomic (Krogan et al. 2006) data suggest that Lys20 may be present in a number of higher order forms, including monomers and higher order complexes. The significance of this data is not yet known, but it will be an interesting area for future investigation.

Materials and Methods

Strains and plasmids

Strains and plasmids are listed in Table 4.1 and 4.2 respectively.

Histone immunoblots

Cells were grown to mid-log phase, normalized and harvested by centrifugation. They were resuspended in PBS with protease inhibitors and lysed by vortexing with glass beads at 4˚. Sample buffer was added to 1X and samples were boiled for 5 min. Lysate was cleared by spinning at 13000 rpm in an eppendorf microcentrifuge speed for 2 min. Samples were stored at -80˚C. 0.25 to 0.5 OD units of extract was run on an 18% acrylamide gel. Gels were transferred to 0.45µm nitrocellulose membrane, and blocked in 2% milk in phosphate buffered saline and Tween-20. Primary antibodies were used at a dilution of 1:2000-1:5000, diluted in 2%

milk and incubated overnight at 4˚C. Secondary antibodies anti-rabbit (Promega) were used at 1:5000 in 2% milk for at least 2 hrs. Blots were developed with Western Lightning developing reagents.

Immunoprecipitations

Cells were grown to mid log phase, normalized and harvested. They were resuspended in IP-Lysis buffer (50mM HEPES-KOH pH 7.5, 0.5M NaCl, 0.5% NP-40, 10% Glycerol, 1mM EDTA and protease inhibitors) and lysed by vortexing with glass beads. Lysates were cleared by centrifugation. Input samples were removed at this point and stored for future analysis. Antibody was added, and incubated at 4˚C for 4 hrs- overnight. 5µl anti Lys20 antibody was used per sample in combination with 5µl anti-HCS antibody. Both were gifts of J. Aris, (40C4 and 36C3, respectively). After incubation, aliquots of supernatant were removed and stored as unbound fraction for gel analysis. 75 µl of rehydrated Protein A sepharose was added to each sample and rocked at 4˚C for 1-2hr. Beads were spun down (2000 rpm for 10 sec at 4˚C) to harvest, washed, and residual buffer was aspirated from beads with a 30G needle. Beads were resuspended in 2.5X sample buffer and heated to 80˚C for 10 min. Esa1-IPs were run on 8% gels, Htz1 IPs were run on 12% gels. Gels were transferred for 2 hrs at 100V to nitrocellulose and blocked in 2% milk. Primary antibody concentrations varied: Anti-GFP antibody (gift of C. Zuker) was used at a concentration of 1:1000 and Anti-Myc antibody (9E10, gift of R. Hampton) was used at 1:7500. Secondary antibodies (anti-rabbit for GFP antibody, anti-mouse for Myc antibody) were used at a concentration of 1:5000. Membranes were detected with Pierce developing reagents.

Halo assays

Cells were grown in YPD to saturation at 30˚C. 0.05 OD_{600} of cells were plated on SC plates and dried. Sterile filter discs were placed in the middle of each plate with sterile forceps. 20µl of 30% hydrogen peroxide was spotted onto each sterile filter. Plates were dried and then incubated at 30˚C for 2 days. Halos were quantified with ImageQuant software.

Acknowledgements

Kendra Lipinski generated the data shown in Fig. 4.6 and 4.10. Viet Le performed similar experiments although results are not shown. Monoclonal anti-Lys20 antibody was a gift of John Aris. Anti-H2AK7Ac antiserum was a gift of Michael Grunstein. The anti-Myc 9E10 monoclonal antibody was a gift of Randy Hampton.

Table 4.1 Strains used in Chapter 4

Strains	
Strain	Genotype
LPY3291	*MAT*a S288C *esa1*Δ*::HIS3* + pLP 863
LPY3486	*MAT*a S288C
LPY4911	*MATα* W303 *esa1-414 rDNA::ADE2CAN1*
LPY4978	*MATα* W303 *sir2*Δ*::HIS3 rDNA::ADE2CAN1*
LPY5114	*MATa* W303 *rpd3*Δ*::LEU2 rDNA::ADE2CAN1*
LPY6121	*MAT*a W303 *ESA1-13MYC*
LPY6282	*MATα* W303 rDNA::*ADE2CAN1 trp1*Δ*0*
LPY6497	*MAT*a BY4741*lys2*Δ*0 MET15*
LPY6926	*MATα W303 set1*Δ*::HIS3 rDNA::ADE2CAN1*
LPY8835	*MAT*α W303 *set1*Δ*::HIS3 ADE2*
LPY9494	*MATα* W303 *lys20*Δ*::kanMX rDNA::ADE2CAN1 trp1*Δ*0*
LPY10284	*MATα* W303 *esa1-414 lys21*Δ*::kanMX rDNA::ADE2CAN1*
LPY10697	*MAT*a W303 *trp1*Δ*0* rDNA::*ADE2CAN1 lys20*Δ*::kanMX lys21*Δ*::clonNAT esa1-414*
LPY11021	*MAT?* W303 *sas2*Δ*::TRP1 TELVR::URA3*
LPY11024	*MAT?* W303 *TELVR::URA3*
LPY11056	*MAT*α *hta1-1 hta2-1 his3 ura3-52 rpd3*Δ + *H2A*
LPY11057	*MAT*α *hta1-1 hta2-1 his3 ura3-52 rpd3*Δ + H2AK7R
LPY11204	*MAT*α W303 *lys20*Δ*::KanMX rpd3*Δ*::LEU2 rDNA::ADE2CA*N1
LPY11205	*MATα* W303 *lys20*Δ*::KanMX lys21*Δ*::clonNAT rpd3*Δ*::LEU2 rDNA::ADE2CAN1*
LPY11207	*MATa* W303 *lys20*Δ*::KanMX lys21*Δ*::clonNAT rpd3*Δ*::LEU2 rDNA::ADE2CAN1*
LPY11208	*MATa* W303 *lys20*Δ*::KanMX lys21*Δ*::clonNAT rpd3*Δ*::LEU2 rDNA::ADE2CAN1 TELVR::URA3*
LPY11211	*MATα* W303 *lys20*Δ*::KanMX lys21*Δ*::clonNAT rpd3*Δ*::LEU2 rDNA::ADE2CAN1 HML::TRP1*
LPY11402	*MAT*a W303 *esa1-414 lys20*Δ*::kanMX*
LPY11411	*MATa* W303 *lys20*Δ*::kanMX lys21*Δ*::clonNAT rDNA::ADE2CAN1*
LPY11412	*MAT*a W303 *esa1-414 lys20*Δ*::kanMX lys21*Δ*::clonNAT*
LPY11419	*MATα* W303 *lys21*Δ*::clonNAT rDNA::ADE2CAN1 trp1*Δ*0*
LPY12169	*MAT*a W303 *GCN5-9MYC*
LPY12385	*MATα* W303 *hht1-hhf1*Δ*::kanMX hht2-hhf2*Δ*::kanMX hta2-htb2*Δ*::HPH rDNA::ADE2CAN1* + pLP218*1*
LPY12391	*MATα* W303 *hht1-hhf1*Δ*::kanMX hht2-hhf2*Δ*::kanMX hta2-htb2*Δ*::HPH rDNA::ADE2CAN1* + pLP218*1*

Table 4.1, continued

LPY12394	*MATα* W303 *hht1-hhf1Δ::kanMX hht2-hhf2Δ::kanMX hta2-htb2Δ::HPH rDNA::ADE2CAN1 + pLP*
LPY13390	*MATa* BY4741 *lys2Δ0 MET15 lys20Δ::kanMX lys21Δ::clonNAT*
LPY13452	*MATα* BY4741 *lys2Δ0 met15Δ0 mag2Δ::kanMX*
LPY13452	*MATα* BY4741 *lys2Δ0 met15Δ0 mag2Δ::kanMX*
LPY13730	*MATa* BY4741 *lys2Δ0 met15Δ0 lys20Δ::kanMX lys21Δ::clonNAT mag2Δ::kanMX*
LPY13730	*MATa* BY4741 *lys2Δ0 met15Δ0 lys20Δ::kanMX lys21Δ::clonNAT mag2Δ::kanMX*
LPY13731	*MATα* BY4741 *lys2Δ0 met15Δ0 lys20Δ::kanMX lys21Δ::clonNAT mag2Δ::kanMX*
LPY13731	*MATα* BY4741 *lys2Δ0 met15Δ0 lys20Δ::kanMX lys21Δ::clonNAT mag2Δ::kanMX*
LPY14068	*MAT*a W303 *hat1Δ::kanMX rDNA::ADE2CAN1*
LPY14070	*MATa* W303 *esa1-414 hat1Δ::kanMX rDNA::ADE2CAN1*
LPY14082	LPY6282 + pLP1402
LPY14083	LPY6282 + pLP1412
LPY14084	LPY14068 + pLP1402
LPY14085	LPY14068 + pLP1412
LPY14086	LPY6926 + pLP1402
LPY14087	LPY6926 + pLP1412
LPY14088	LPY4911 + pLP1402
LPY14089	LPY4911 + pLP1412
LPY14090	LPY14070 + pLP1402
LPY14091	LPY14070 + pLP1412
LPY14371	LPY3291 + pLP1412
LPY14681	LPY3291 + pLP796
LPY14751	*MATa* BY4741 *lys2Δ0 met15Δ0 GFP-HTZ1::HIS3* from JW lab
LPY14944	LPY6282 + pLP2384
LPY14945	LPY11411 + pLP2384
LPY14946	LPY3486 + pLP2384
LPY14947	LPY3291 + pLP2384

Table 4.2 Plasmids used in Chapter 4

Plasmids	
Plasmid	Genotype
pLP796	*ESA1* in YEP352
pLP1402	pRS202
pLP1412	*LYS20* in pRS202
pLP1920	*LYS21* in pRS426
pLP2145	*H4K8A*
pLP2146	*H4K12A*
pLP2181	*H4K5A*
pLP2384	*LYS20Q35A* in pRS202

Table 4.3 Oligos used in Chapter 4

Oligos	
Oligo	Sequence
oLP1312	GAAGGTGAA**GC**ATTTGCCAAC
oLP1313	GTTGGCAAAT**GC**TTCACCTTC

Nucleotides in bold are mutagenic relative to wild type sequence

Chapter 5 Structural and functional analysis of the *S. pombe* homocitrate synthase Lys4

Introduction

Homocitrate synthases (HCSs) are well conserved across fungal species (Fig 1.4), thus it was of interest to find if the functions observed for Lys20 were also true for one of its homologs. The structure of a homocitrate synthase (HCS) had not previously been published and so in collaboration with Stacie Bulfer and Ray Trievel at the University of Michigan at Ann Arbor, the *Schizosaccharomyces pombe* (*S. pombe)* homocitrate synthase Lys4 was selected for further analysis. In this chapter, Lys4 refers only to the *S. pombe* HCS, whereas all other genes are from *S. cerevisiae.* Lys4 proved a more tractable protein than *S. cerevisiae* Lys20 in purification and *in vitro* assays. The Trievel lab carried out purification, *in vitro* kinetic studies and crystallographic analysis of Lys4. This chapter will focus on the complementary *in vivo* mutational analysis of Lys4. These studies are detailed in the two following publications: (Bulfer et al. 2009; Bulfer et al. 2010).

Results

To test the *in vivo* function of the *S. pombe* HCS in *S. cerevisiae*, Lys4 was placed under the control of the *S. cerevisiae LYS2*0 promoter. The *LYS20* promoter would allow for protein expression and facilitate phenotyping in *S. cerevisiae.* PCR sewing was used to place the *LYS4* ORF under the control of the *LYS20* promoter as described in (Elion 1993) and diagrammed in Figure 5.1. Once the cloning was complete, the first task was to see if the *S. pombe* HCS could complement *S. cerevisiae* HCS function. The Lys4 construct was transformed into a *S. cerevisiae lys20*Δ *lys21*Δ strain that lacked HCS activity. The empty vector was also transformed as a negative control and wild type *LYS20* was included as a positive control. *S. pombe* Lys4 could complement an HCS null *S.cerevisiae* strain (*lys20*Δ *lys21*Δ) and restore lysine prototrophy (Fig 5.2).

Mutational analysis of LYS4

The structure of Lys4 was determined by the Trievel lab (Fig 5.3) (Bulfer et al. 2009). Briefly, Lys4 functions as a homodimer. It is a TIM barrel enzyme, and the active site is in the center of the barrel. It is similar to the structure of isopropylmalate synthase (IPMS), a leucine biosynthetic enzyme that is encoded by *LEU4* and *LEU9* in *S. cerevisae*. IPMSs also bind acetyl CoA and use it as an acetyl donor. Uniquely, Lys4 contains a lid domain that restricts access to the active site and acts as a potential regulatory motif. Structure of the active site was determined (Fig 5.4) and allowed catalytic residues lying in the active site to be identified. These were mutated to alanine and other residues in order to evaluate their critical catalytic roles *in vitro*

Figure 5.1 Schematic of PCR sewing strategy used to clone *LYS4* under the control of the *LYS20* promoter. First, the *LYS20* promoter region, beginning 283 base pairs upstream of the start codon (turquoise) is amplified by PCR with oLP944 (red) and oLP945 (blue). The *LYS4* ORF is amplified with oLP946 (purple) and oLP947 (black) (A). PCR products were combined, denatured and reannealed. Complementary regions in oLP945 and oLP946 anneal (B), and the hybrid product is amplified to generate the hybrid double stranded DNA molecule (C). This is then digested and ligated into pRS426 (D), as described in Materials and Methods.

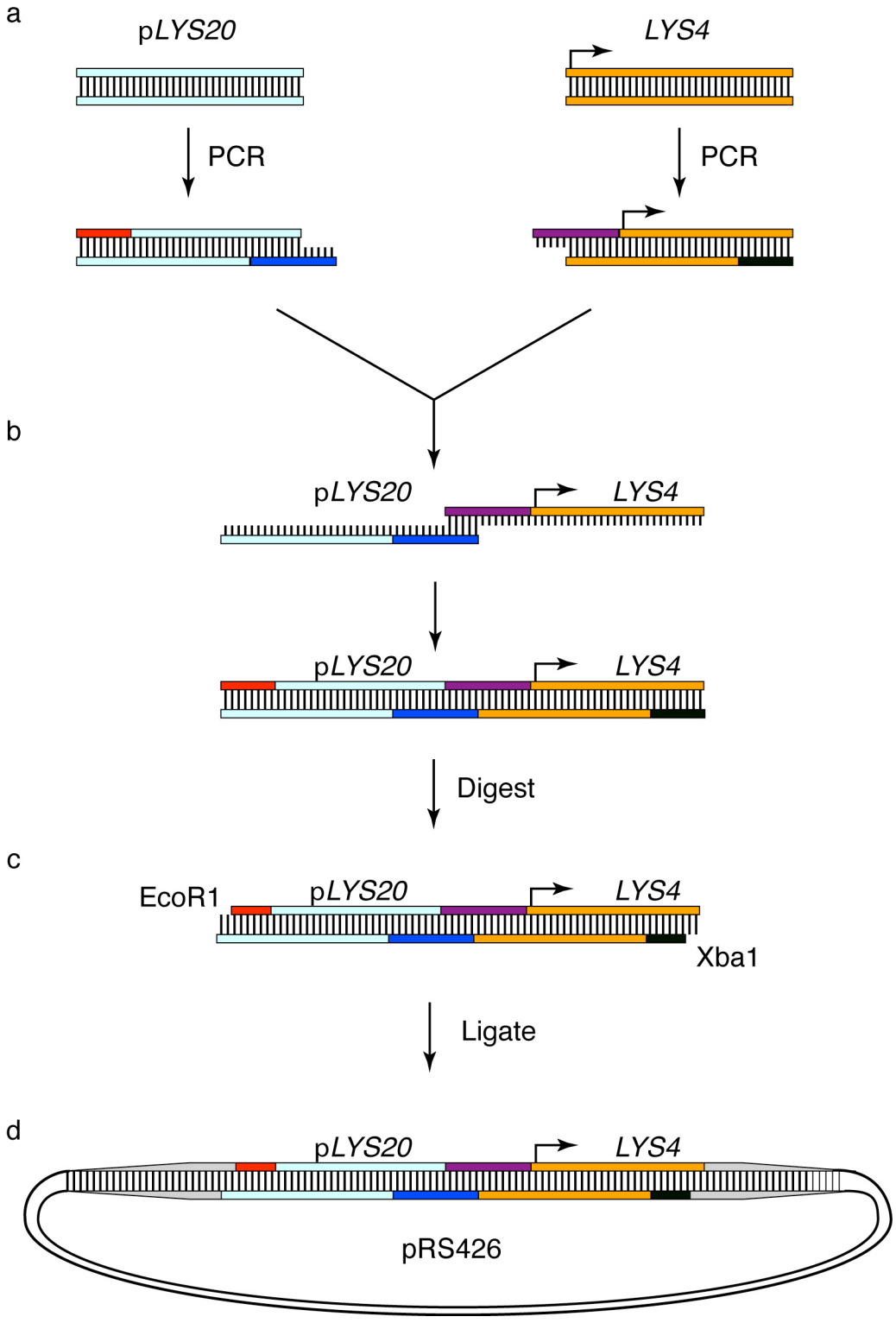
a
pLYS20
LYS4
PCR
PCR
b
pLYS20
LYS4
pLYS20
LYS4
Digest
c
EcoR1
pLYS20
LYS4
Xba1
Ligate
d
pLYS20
LYS4
pRS426

Figure 5.2 Wild type *LYS4* from *S. pombe* complements *S. cerevisiae* lysine auxotrophy. Most point mutants in active site residues are not able to complement. *LYS20,* vector*, LYS4* or *LYS4* point mutant constructs were transformed into HCS null *S. cerevisiae* to assay for ability to complement lysine auxotrophy. Cultures were normalized to OD_{600} 1 and five-fold serial dilutions were plated on ura- (growth control) or ura- lys- (to assay lysine biosynthesis) media. Plates were incubated at 30˚. All mutations are in *LYS4.*

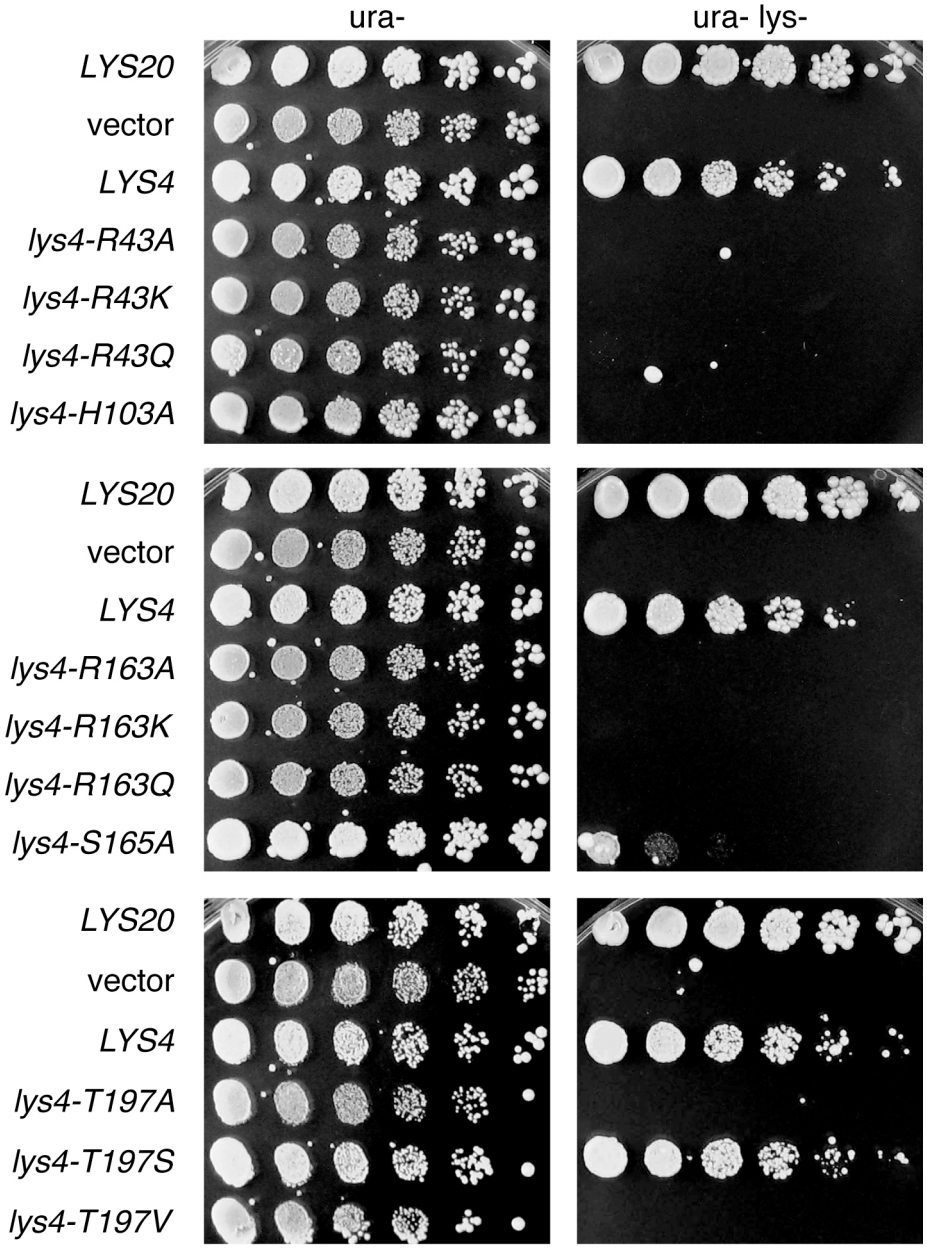
ura-
ura- lys-
LYS20
vector
LYS4
lys4-R43A
lys4-R43K
lys4-R43Q
lys4-H103A
LYS20
vector
LYS4
lys4-R163A
lys4-R163K
lys4-R163Q
lys4-S165A
LYS20
vector
LYS4
lys4-T197A
lys4-T197S
lys4-T197V

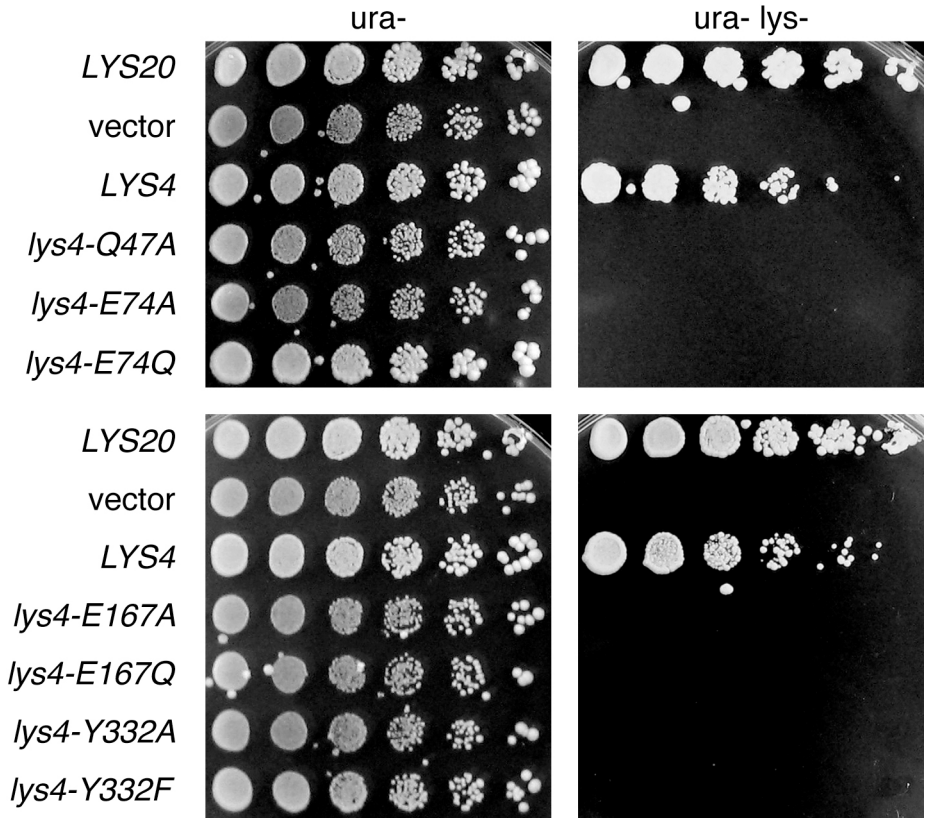

Figure 5.2, continued

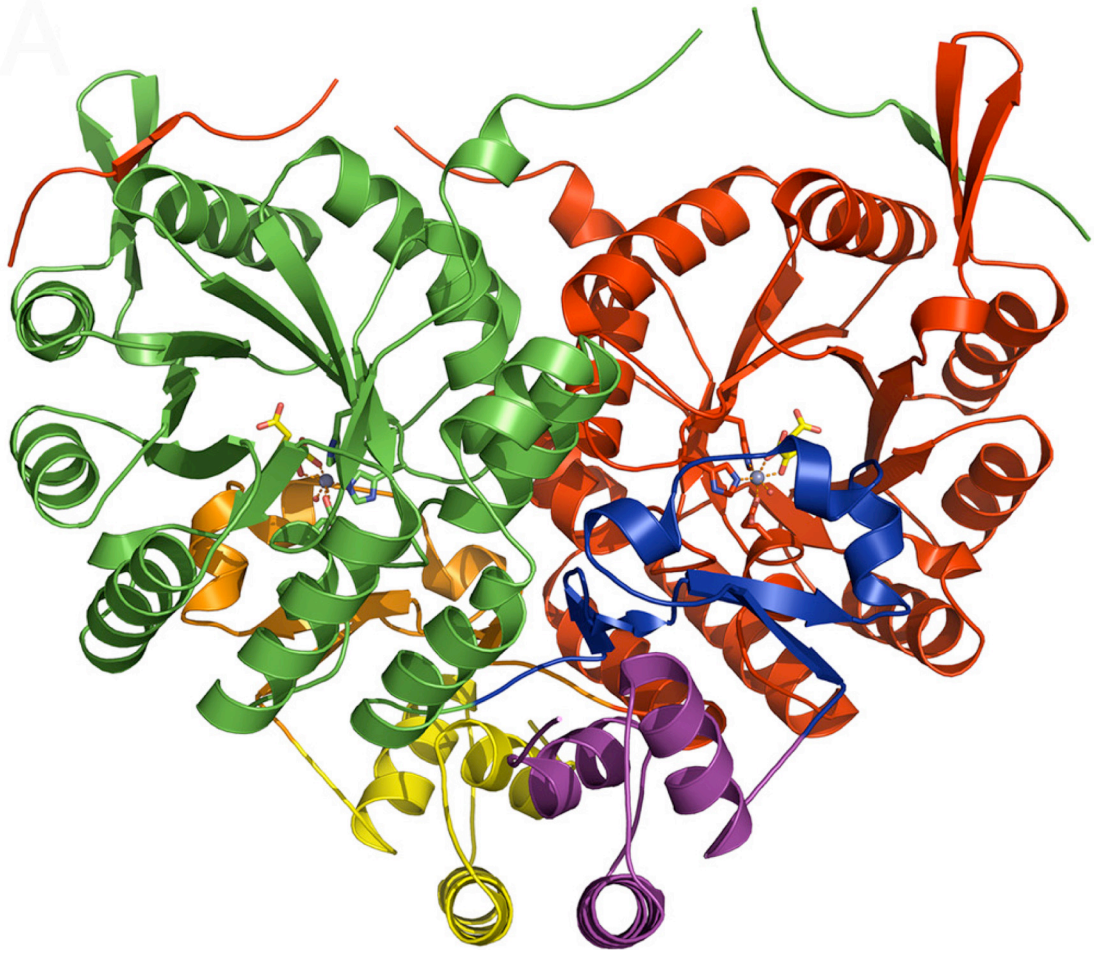

Figure 5.3 Lys4 is a homodimer. In the crystal structure of Lys4, two monomers are visible. Shown is a ribbon diagram of the SpHCS homodimer bound to 2-OG (closed lid motif) with the N-terminal domain, C-terminal subdomain I, and C-terminal subdomain II of monomer A depicted in red, orange, and yellow, respectively, and of monomer B depicted in green, blue, and violet, respectively. The Zn(II) atom is modeled as a dark gray sphere, and the bound 2-OG is rendered as sticks with yellow carbon atoms (Bulfer et al. 2009).

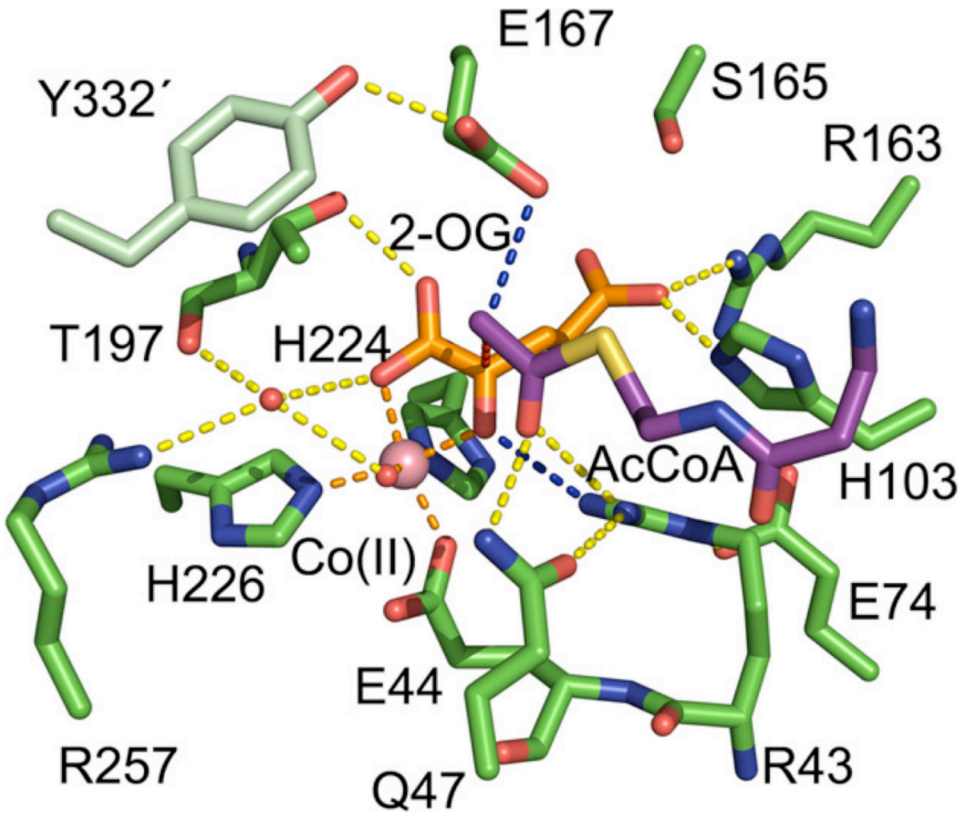

Figure 5.4 The active site of Lys4 with substrate (2-oxoglutarate; 2-OG) bound. Acetyl CoA (purple) is modeled into the active site. Catalytic residues in the active site of Lys4 are labeled. Dashed lines represent coordination of Zn (II) ion (orange), hydrogen bonding to 2-OG (yellow), hydrogen bonding to putative catalytic residues (blue).

Figure 5.5 *LYS4* and *LYS4* point mutants are recessive in *S. cerevisiae.* Dilution assay conducted as described in Figure 5.2. *LYS20*, vector, *LYS4* or *LYS4* point mutants were transformed into wild type *S. cerevisiae* to assay for dominant interference Ura- plate is a growth control; ura- lys- plate assays for lysine biosynthesis. Plates incubated at 30˚C.

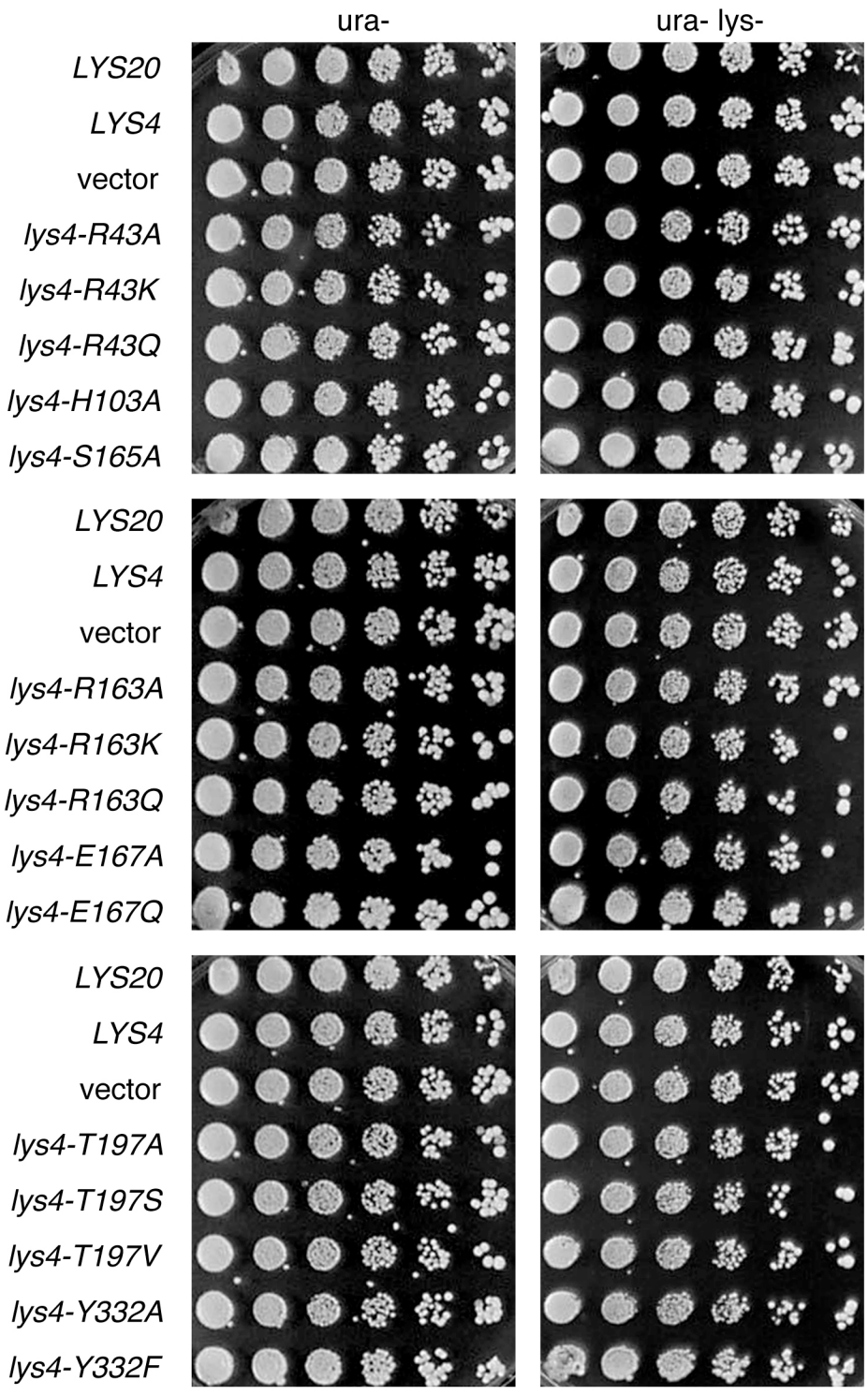
ura-
ura- lys-
LYS20
LYS4
vector
lys4-R43A
lys4-R43K
lys4-R43Q
lys4-H103A
lys4-S165A
LYS20
LYS4
vector
lys4-R163A
lys4-R163K
lys4-R163Q
lys4-E167A
lys4-E167Q
LYS20
LYS4
vector
lys4-T197A
lys4-T197S
lys4-T197V
lys4-Y332A
lys4-Y332F

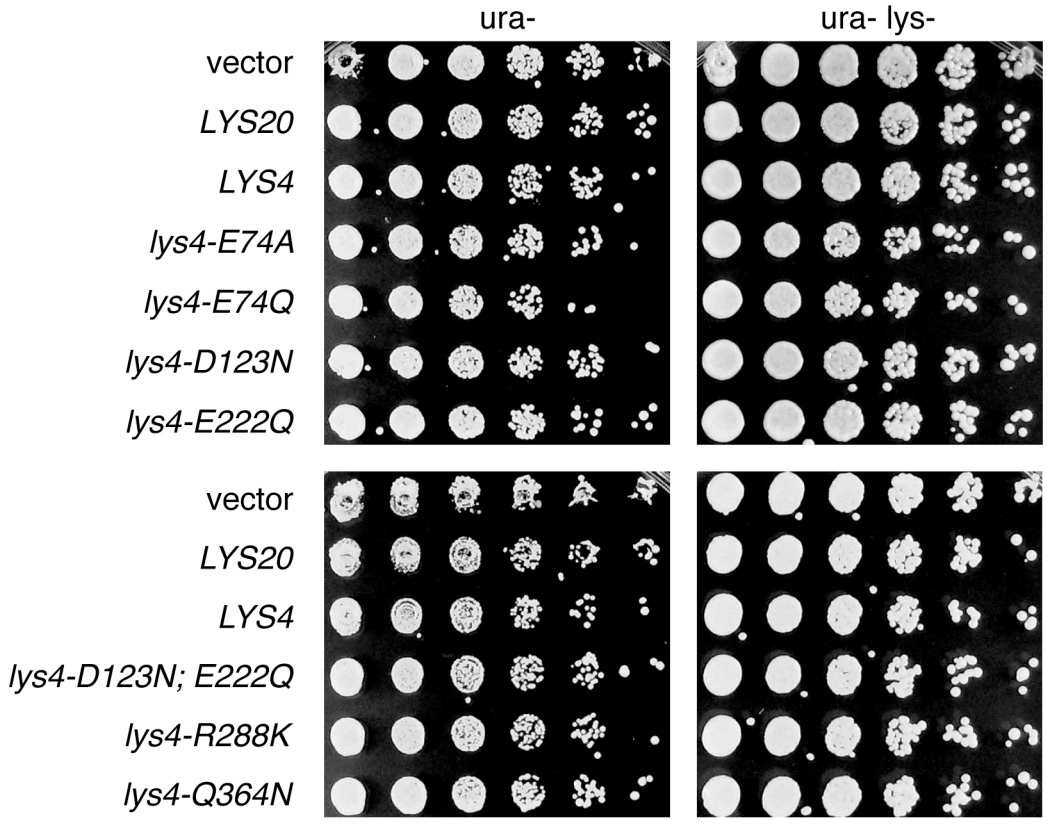

Figure 5.5, continued

and *in vivo*. Key residues were individually mutated by Stacie Bulfer. These mutants were tested to determine if they could rescue lysine auxotrophy of a *lys20*Δ *lys21*Δ *S.cerevisiae* strain (Fig 5.2). Locations of catalytic residues are mapped in the active site of the crystal structure (Fig 5.4).

With one exception, all mutants failed to rescue, indicating that each residue tested was indeed critical for catalytic activity. Strains harboring mutations in five of the active site residues, R43, H103, R163, E167 and Y332 showed no growth. The exception was the conservative substitution of T197 for serine. It is likely that this mutation allowed catalysis to take place albeit at a reduced rate (Bulfer et al. 2009). Strains with both the T197A and T197V mutant alleles failed to grow on lys- media, demonstrating that it is likely the hydroxyl functional group of T197 functioning in catalysis. Less growth was observed for S165A, suggesting that it is not as critical as the other residues tested.

The second class of mutants tested was located in the lid motif. These mutants (Q47A and E74A) also abolished catalysis as indicated by lack of growth on media lacking lysine (Fig 5.2). Lys4 and point mutants were also tested for dominance by transformation into a wild type strain and were found to be recessive (Fig 5.5) in that no dominant interference of the mutants in growth or lysine biosynthesis was observed.

A possible explanation for the results observed in Fig 5.2 was that the Lys4 point mutants could not restore lysine prototrophy because they were not expressed. However, all mutants were expressed in the cells, as shown by immunoblot (Fig 5.6).

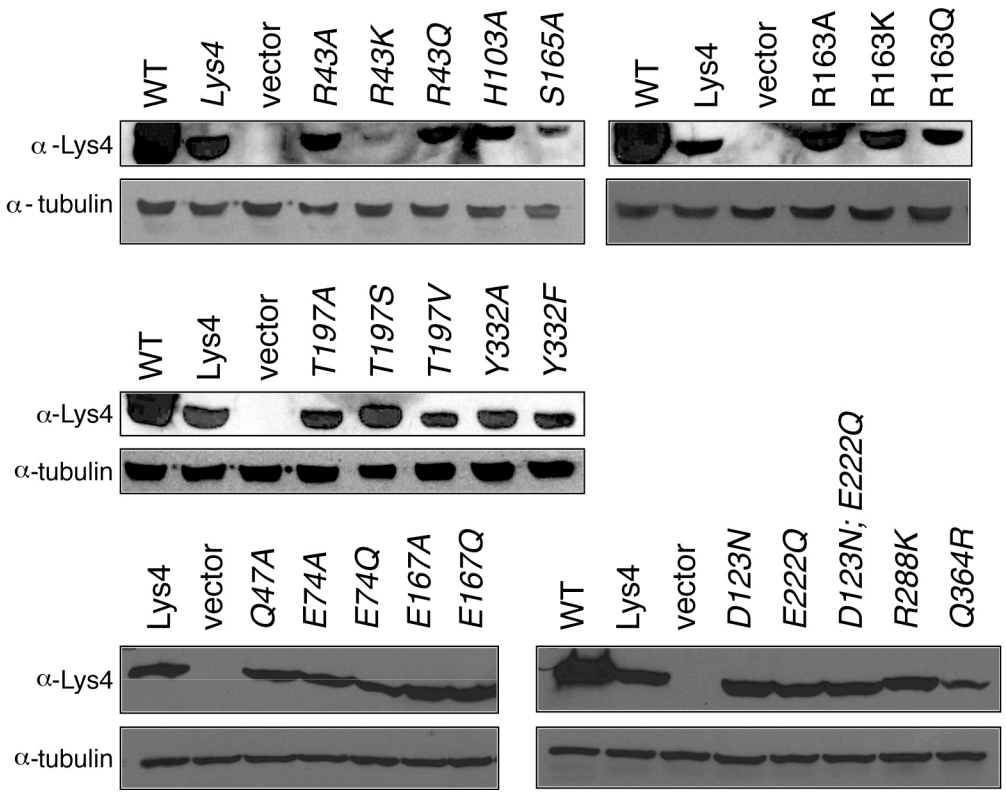

Figure 5.6 Point mutants in Lys4 are expressed in *S. cerevisiae.*
Expression of point mutants was assayed by immunoblotting with antibody that recognized homocitrate synthases, including Lys20, Lys21 and Lys4 (36C3, a gift of J. Aris). Anti-tubulin was used as a loading control.

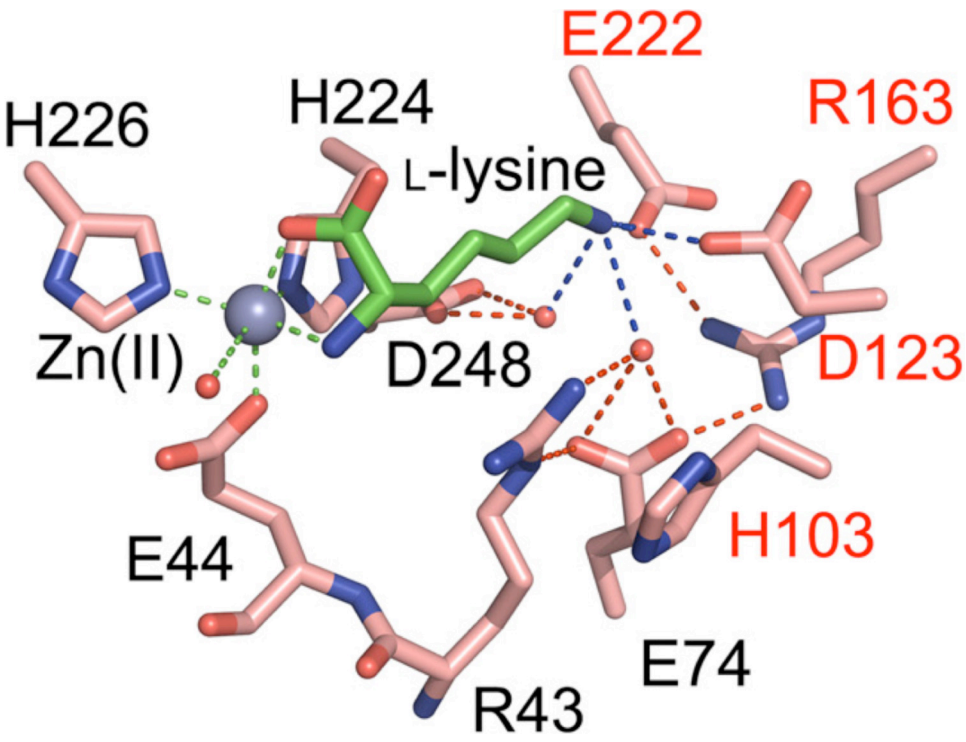

Figure 5.7 Crystal structure of Lys4 active site with lysine bound. (Lys4 is pink, lysine is green.) Coordination to Zn (II) ion (gray) is shown as green dashes, whereas potential hydrogen bonds to the inhibitor lysine are represented by blue dashes. Hydrogen bonds within the protein and to solvent molecules are displayed as red dashes. Residues composing the switch position are labeled in red (Bulfer et al. 2010).

Determining the mechanism of feedback inhibition by lysine

With catalytic residues established, regulation of Lys4 was investigated. It is known that HCS enzymes are feedback inhibited by lysine, parameters for Lys20 and Lys21 were reported (Feller et al. 1999). Feedback inhibition may proceed in one of two ways: either the inhibitor binds in the active site and directly competes with the substrate (direct inhibition) or the inhibitor binds elsewhere in the enzyme and inactivates it (allosteric inhibition), often by causing a conformational change. It was not known by which method HCS is regulated. If the direct inhibition model were correct, lysine would inhibit HCS activity by binding the active site and prevent access of the substrate, 2-oxoglutarate.

To resolve the question of regulatory mechanism, the crystal structure of Lys4 in the presence of high concentrations of lysine was determined by the Trievel lab. Lysine was observed to bind in the active site (Bulfer et al 2010.)(Fig 5.7). Residues D123 and E222 were found to be critical for the binding of the lysine.

Two residues of Lys20 that were insensitive to feedback inhibition were identified using a toxic lysine analog, aminoethylcysteine (AEC) mutations in (Feller et al. 1999). In *S. pombe* Lys4, these residues correspond to R288 and Q364, so these residues were mutated to test the effects on responsiveness to lysine inhibition. Mutations in residues critical for lysine binding would be expected to be resistant to feedback by lysine, and also be resistant to inhibition by toxic lysine analogs. These residues did not map to the active site of Lys4.

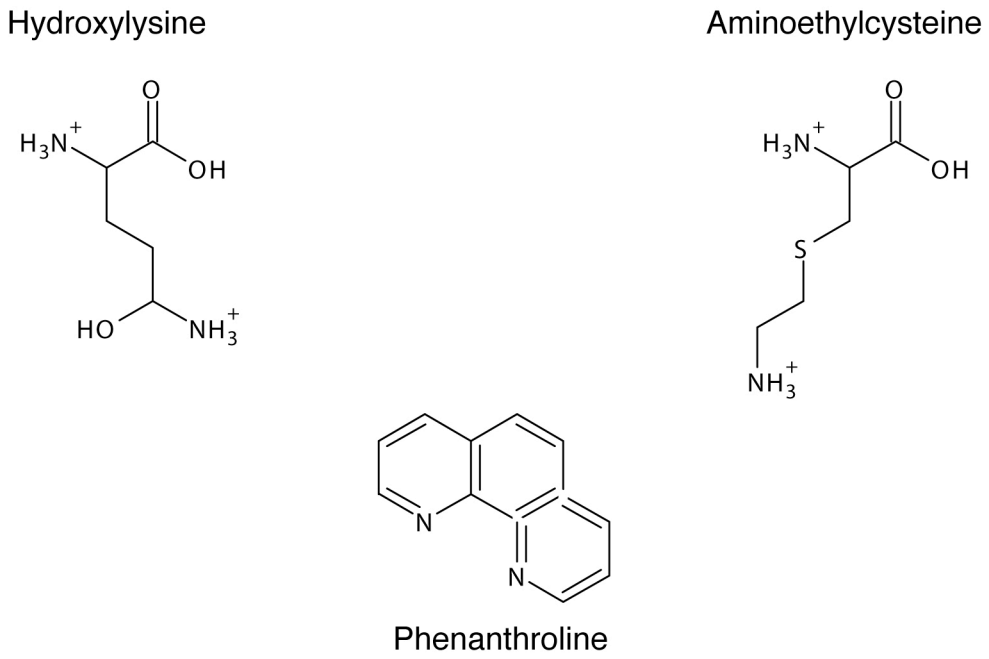

Figure 5.8 Chemical structures of hydroxylysine (Lys-OH) (upper left), aminoethylcysteine (AEC) (upper right), and phenanthroline (PNT) (bottom). Hydroxylysine and aminoethylcysteine are lysine analogues that were used to test Lys4 point mutants for insensitivity to feedback inhibition by lysine (Feller et al. 1999; Sinha et al. 1971). Phenanthroline is a compound that is reported to inhibit Lys20 homocitrate synthase activity *in vitro* (Gray et al. 1976)

Another compound, hydroxylysine, also a lysine derivative, was identified (Sinha et al. 1971) as an inhibitor of HCS activity. This drug works by a different mechanism than AEC. Structures of both compounds are shown in Figure 5.8. Potential lysine insensitive mutants were assayed for dominance (Fig 5.5), as previously done with the catalytic mutants and behaved recessively. Then, they were tested to see if they were able to carry out homocitrate synthesis (Fig 5.9), and most were competent for homocitrate synthase, if not as strongly as wild type Lys4. The E222Q mutant displayed the weakest growth, which implies that it may also be important for catalysis. The mutants were then assayed on AEC and hydroxylysine to test for lysine inhibition. D123N mutants were the most resistant, and R288K and Q364N mutants were also resistant, to a lesser extent. This provides strong *in vivo* evidence for the idea that feedback inhibition in HCSs proceeds by direct competition.

AEC and hydroxylysine are two molecules that have been demonstrated *in vivo* to intefere with HCS activity. Additional small molecules that appear to inhibit HCS activity *in vitro* have been reported (Gray and Bhattacharjee 1976b). One of these compounds is phenanthroline. Overexpression of Lys4 E74A and E74Q in a wild type strain may cause sensitivity to phenanthroline (Fig 5.10). This result, if repeatable, would indicate a dominant effect specific to phenanthroline, as the result was not seen when the two mutants were tested on phenanthroline (Fig 5.10) in the *lys20*Δ *lys21*Δ strain, nor did they have any dominant effect on wild type cells when assayed for lysine biosynthesis. However, in light of the nuclear functions demonstrated

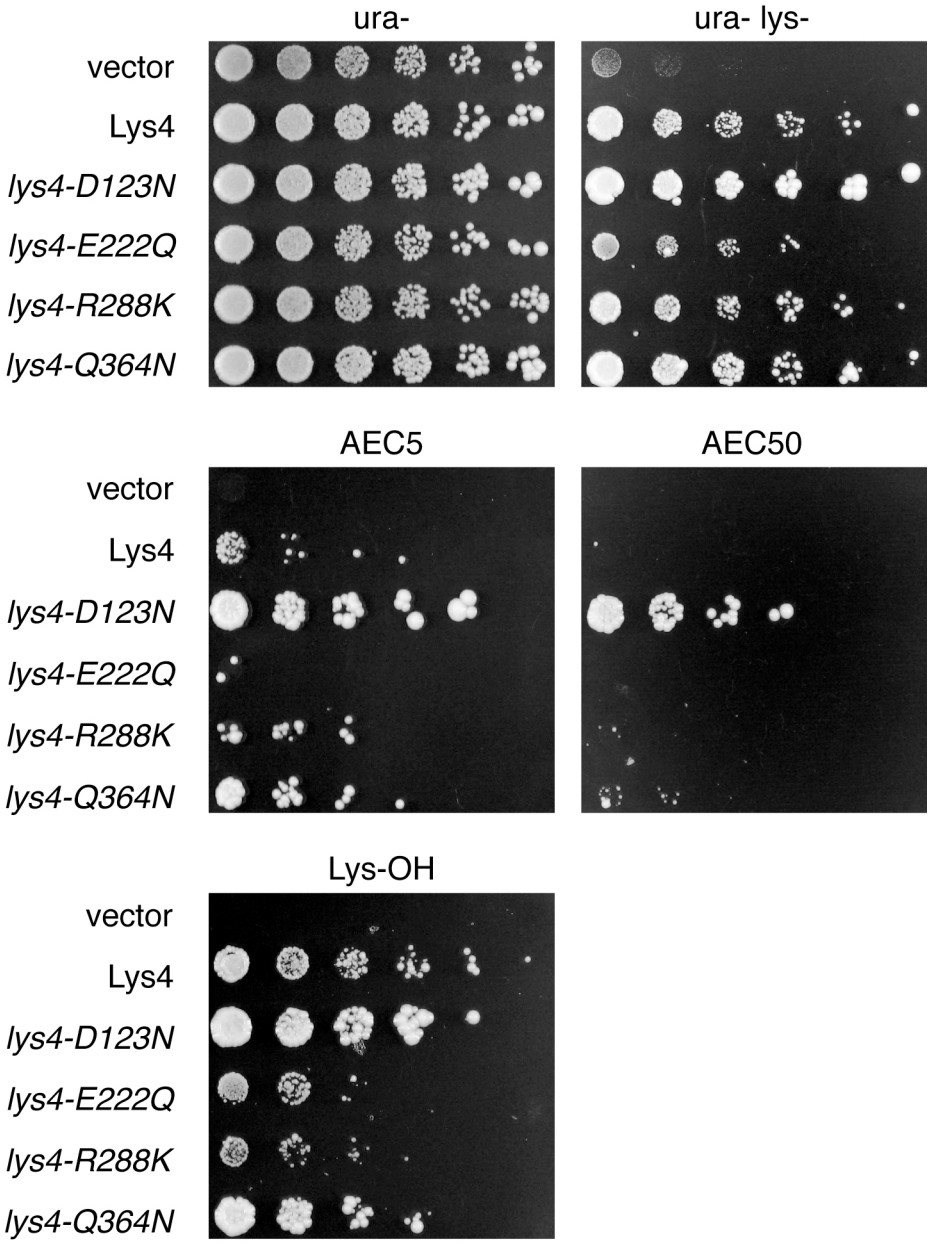

Figure 5.9 Point mutants in Lys4 involved in lysine feedback inhibition are competent for homocitrate synthesis. Point mutants are mostly resistant to AEC (aminoethylcysteine) at 5μg/mL and 50μg/mL and Lys-OH (hydroxylysine) at 1.2mM. Plates were incubated at 30˚C.

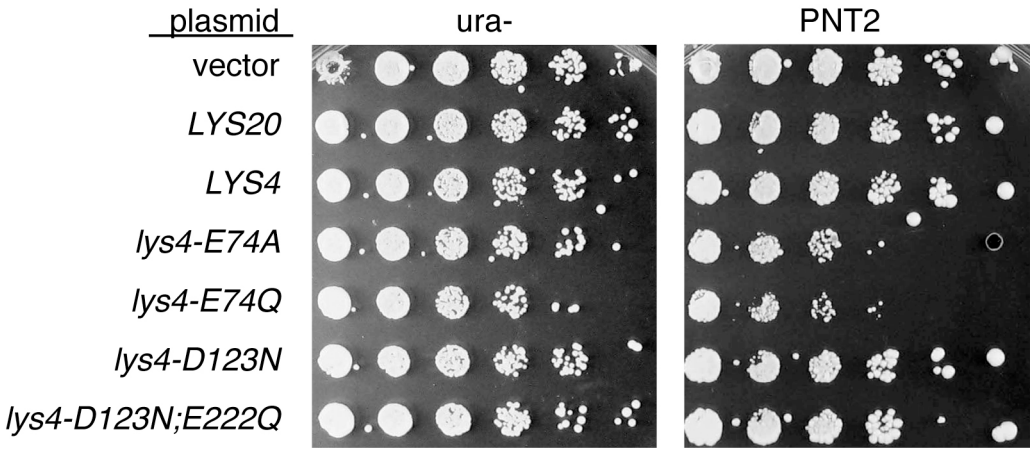

Figure 5.10 ***Lys4 E74A*** **and** ***E74Q*** **cause sensitivity to phenanthroline (PNT) when overexpressed in wildtype cells.** Growth plate is ura-, PNT plate is ura- with 2μg/mL PNT.

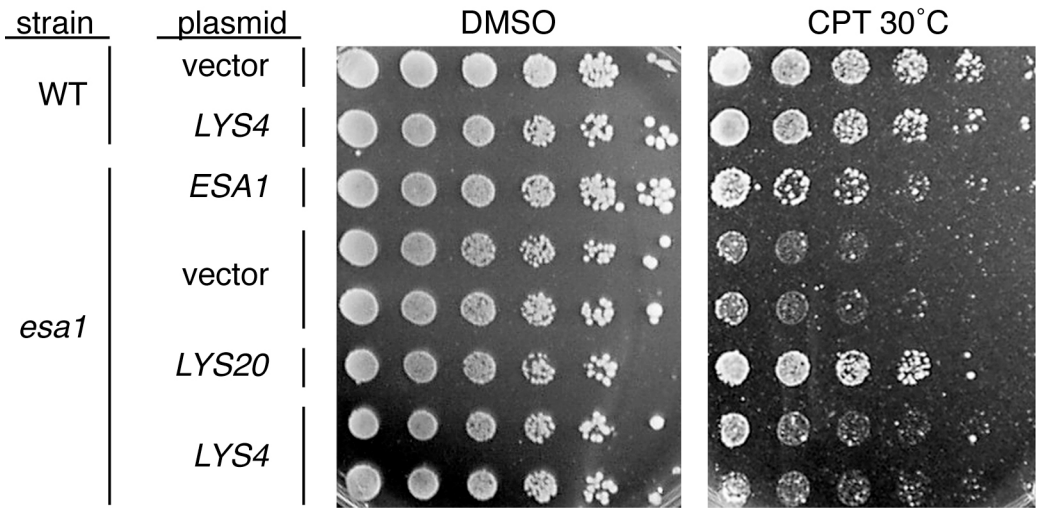

Figure 5.11 *LYS4* was transformed into indicated strains and assayed for ability to rescue *esa1* CPT^s. Unlike *LYS20*, it did not have a strong effect. Growth control plate contained DMSO in concentration equal to CPT plate. CPT plate contained CPT in DMSO at a concentration of 30μg/mL. Plates were incubated at 30˚C.

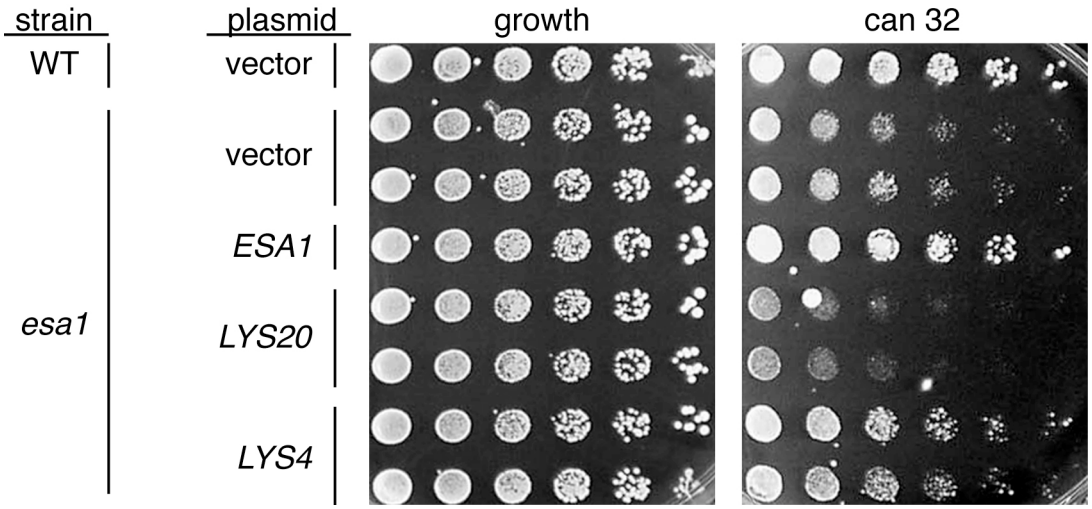

Figure 5.12 Unlike *LYS20*, *LYS4* overexpression does not exacerbate the *esa1* rDNA silencing defect. Silencing is indicated by growth on canavanine plate; a defect is indicated by lack of growth. The growth plate lacks uracil, adenine and arginine. The canavanine plate is contains 32μg/mL canavanine. Growth on can 32 plate indicates silencing.

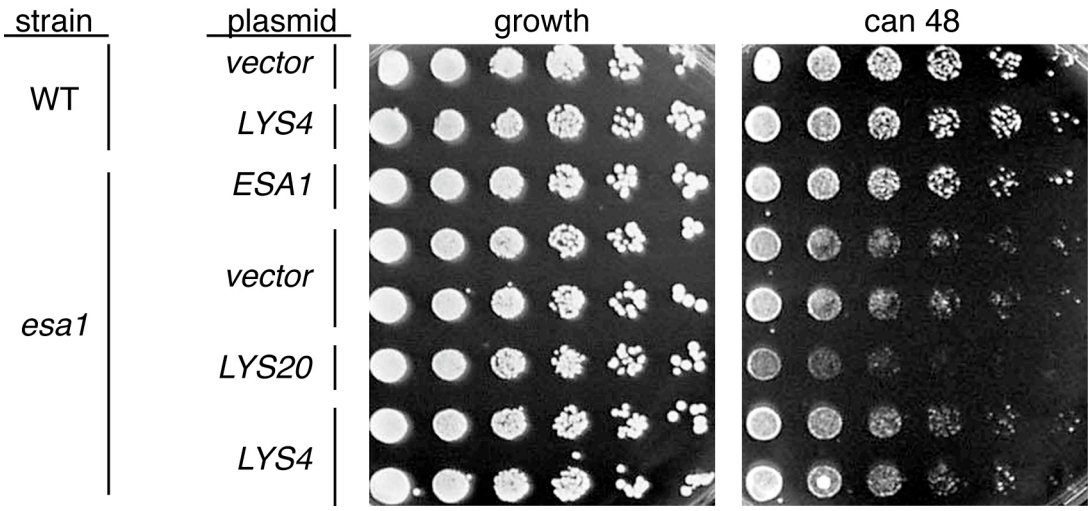

Figure 5.13 *LYS4* overexpression does not cause an rDNA silencing defect in wildtype cells, nor does it exacerbate the *esa1* rDNA silencing defect. The growth plate lacks uracil, adenine and arginine. The canavanine plate is the same and contains 48μg/mL canavanine. Plates incubated at 30˚C. Growth on silencing plate indicates silencing.

for Lys20 and this enzyme's conservation in pathogenic fungi, it would be useful to screen a collection of small molecules to identify further inhibitors of HCS activity.

Finally, *S. pombe LYS4* was assayed to see if it, like *S. cerevisiae LYS20*, was able to suppress *esa1* camptothecin sensitivity (CPT^s) (discussed in Chapter 2). As shown in Fig 5.11, it seems that if there is any suppression of *esa1* CPT^s, it is very weak. It can only be concluded that *LYS4* differs from *LYS20* in this regard. Similarly, *LYS4* was tested to see if it shared *LYS20*'s ability to create or exacerbate defects in rDNA silencing when overexpressed (discussed in Chapter 4, and Fig 5.12). *LYS4* did not exacerbate the rDNA silencing defects of *esa1* as overexpression of *LYS20* did, nor did it create rDNA silencing defects in wild type cells (Fig 5.13).

Discussion and future directions

Results presented in this chapter clearly establish that the *S.pombe LYS4*, which encodes the HCS enzyme, is able to cross complement in *S. cerevisiae* for homocitrate synthase activity. Crystallographic analysis establishes the first structure of an HCS enzyme and uncovers the novel lid domain, which helps regulate the enzyme by gating access to the active site. Residues critical for catalysis are identified and the requirement for these residues is confirmed *in vivo* (Bulfer et al. 2009). The mechanism for the observed feedback inhibition of the enzyme by lysine is established as one of direct competition between lysine and alpha- ketoglutarate (Bulfer et al. 2010).

Despite these advances in understanding of HCSs, much remains to be understood. It remains to be determined whether the nuclear functions of Lys20 discussed in Chapter 2 are shared by Lys4. Whereas it seems that *S. pombe* Lys4 does not share the DNA damage or rDNA silencing functions of Lys20 when expressed in *S. cerevisiae*, it is not known if it might do so in *S. pombe* cells. It is not known if Lys4 is nuclear in *S. pombe*, or if deletion of Lys4 might confer DNA damage resistance on *S. pombe* cells. It would be useful to define which HCS enzymes are bifunctional proteins like Lys20 and which, if any, are not.

Other fungal species, including pathogenic species, also contain HCS enzymes that are similar in sequence to Lys4 and Lys20, and these homologs should be studied to see if they have similar properties. In fact, the Lys4 structure is quite similar to the structure of the *Thermus thermophilus* HCS (Okada et al. 2010). This structure also identifies residues critical for catalysis and elucidates the mechanism of the enzyme. Additional residues are identified in this study that also contribute to catalysis. This study underscores the conservation of the HCS family in different organisms, as the *T. thermophilus* structure is similar to the *S. pombe* structure. Conservation of catalytic residues for *S. cerevisiae* Lys20 has been shown by mutational analysis (Chapter 2).

Elucidation of the mechanism of feedback inhibition provides an interesting starting point for future study of HCS enzymes. Since these enzymes are conserved in fungi and some archaea, but absent in other species, they make attractive targets for anti-fungal therapies (Zabriskie and Jackson 2000). It is not known if HCS enzymes in pathogenic fungal species also have DNA damage roles similar to Lys20, but as small

molecule inhibitors are developed, this remains an important consideration. In further characterizing both the *S. pombe* enzyme and the various mutants generated, it would be informative to further phenotype these mutants on phenanthroline containing media, and also media containing some of the Lys20- inhibiting compounds listed in (Gray and Bhattacharjee 1976b) and (Gray and Bhattacharjee 1976a). Certain of these compounds would likely be toxic to cells if supplied in the growth media, such as $HgCl_2$, but others, such as $CuSO_4$ or NaF may provide insight into the sensitivities of HCS *in vivo*. For example, could wild type cells grow on median that lacked lysine but contained $CuSO_4$, or would the copper sulfate inhibit homocitrate synthase activity *in vivo*? Inhibitory effects of other metabolites on HCS activity *in vitro* are reported (Gray et al. 1976). Both organic and inorganic classes of inhibitors could be tested to see if they affect Lys20's nuclear function, in an effort to distinguish the two functions biochemically as well as genetically. More HCSs from multiple species could also be tested in *S. cerevisiae* to see which homologs share Lys20's nuclear functions and which do not. In parallel with these efforts, a chemical genomics screening project is underway in collaboration with the Trievel lab. The screen searches for small molecule inhibitors of homocitrate synthase activity, in hope that they will be useful as antifungal therapies. Any information generated by these efforts will aid in development of a new class of antifungal agents.

Materials and Methods

Cloning of LYS4

Cosmid DNA containing *LYS4* (pLP2144) was obtained from John Woodward at the Sanger Institute. *LYS4* was amplified from this cosmid with oLP911 and oLP912. The oLP911 started 4 base pairs into the gene to remove the start codon, and oLP912 removed the last 2 base pairs of the gene and stop codon. The missing base pairs were reinserted during PCR sewing with the indicated oligos. The resulting PCR product was blunt end cloned into pBluescript (pLP74) with *Sma*I, to generate pLP2204. *LYS4* was placed under the control of the *LYS20* promoter by PCR sewing as described in (Elion 1993). The *LYS20* promoter, beginning 283 base pairs upstream of the start codon was amplified with oLP944 and oLP945 from pLP1412. *LYS4* was amplified from pLP2204 with oLP946 and oLP947. The two products were annealed and extended with oLP944 and oLP947. The resulting fragment was digested with *Eco*RI and *Xba*I and cloned into pRS426 (pLP362) to generate pLP2211. pRS 426 was digested with *Eco*RI and *Spe*I. *Xba*I and *Spe*I have compatible cohesive ends, however, when ligated together, the resulting sequence is neither an *Xba*I site not a *Spe*I site. (See Fig 5.1 for diagram.) Point mutants were generated by S. Bulfer using QuikChange mutagenesis kit (Stratagene) on pLP2211.

Growth media

Media were prepared as described in Chapter 2. Aminoethylcysteine was dissolved in water and used at a final concentration of 5 or 50μg/mL in ura- lys-

media. Hydroxylysine was dissolved in water and used at a final concentration of 1.2mM in ura- lys- media. Canavanine and camptothecin plates are as described in previous chapters.

Protein Immunoblotting

Expression levels of Lys4 and lys4 point mutants were determined by immunoblots. Strains were grown to mid log phase and TCA protein extracts were prepared (Foiani et al. 1994). Protein extracts (0.5 OD/ sample) were run on 8% gels and transferred to nitrocellulose for 1 hour at 100 volts. Membrane was blocked in 2% milk and blotted with anti-HCS antibody (1:5000) in 2% milk at 4˚C overnight. Monoclonal antibody 36C3 was used, which recognizes Lys20, Lys21 and Lys4 and was a gift of J. Aris. Secondary antibody was anti-mouse HRP (Promega), used at 1:5000 in 2% milk. Blots were developed with ECL reagent (Pierce). For loading controls, membranes were incubated in anti-tubulin antibody in 2% milk overnight at 4˚C. Secondary antibody was anti-rabbit HRP (1:5000) in 2% milk. Blots were developed as above.

Chemical structures were drawn with ACD/ChemSketch Freeware Release 12.00.

Acknowledgements

Stacie Bulfer and Ray Trievel performed all *in vitro* protein purification, analysis, kinetic studies and crystallography and also provided aminoethylcysteine.

Lorraine Pillus did platings for the AEC and hydroxylysine experiments. Hydroxylysine was a gift of Stuart Brody and Anti-HCS antibody was a gift of John Aris.

Note: Material in this chapter has been published as:

Crystal structure and functional analysis of homocitrate synthase, an essential enzyme in lysine biosynthesis. Bulfer SL, Scott EM, Couture JF, Pillus L, Trievel RC. *J Biol Chem.* 2009 Dec 18;**284**(51):35769-80.

Structural basis for L-lysine feedback inhibition of homocitrate synthase. Bulfer SL, Scott EM, Pillus L, Trievel RC. *J Biol Chem.* 2010 Apr 2;**285**(14):10446-53.

Table 5.1 Strains used in Chapter 5

Strains	
Strain	Genotype
LPY3291	MATa S288C esa1ΔHIS3 + pLP863
LPY3486	MATa S288C WT
LPY4908	MATa W303 WT rDNA::ADE2CAN1
LPY4911	MATα W303 rDNA::ADE2CAN1 esa1-414
LPY6282	MAT α W303 trp1Δ0 rDNA::ADE2CAN1
LPY9494	MATα W303 lys20Δ::kanMX6 rDNA::ADE2CAN1 trp1Δ0
LPY11411	MATa W303 lys20Δ::kanMX lys21Δ::clonNAT rDNA::ADE2CAN1
LPY11419	MATα W303 lys21Δ::clonNAT
LPY13821	LPY11411 + pLP2312
LPY13822	LPY11411 + pLP2313
LPY13823	LPY11411 + pLP2314
LPY13824	LPY11411 + pLP2315
LPY13825	LPY11411 + pLP2316
LPY13826	LPY11411 + pLP2317
LPY13827	LPY11411 + pLP2318
LPY13828	LPY11411 + pLP2319
LPY13829	LPY11411 + pLP2320
LPY13830	LPY11411 + pLP2321
LPY13831	LPY11411 + pLP2322
LPY13832	LPY11411 + pLP2323
LPY13833	LPY11411 + pLP2324
LPY13834	LPY11411 + pLP2325
LPY13835	LPY11411 + pLP2326
LPY13836	LPY11411 + pLP1402
LPY13837	LPY11411 + pLP1412
LPY13838	LPY11411 + pLP2211
LPY14039	LPY11411 + pLP2329
LPY14591	LPY11411 + pLP2355
LPY14592	LPY11411 + pLP2356
LPY14593	LPY11411 + pLP2357
LPY14594	LPY11411 + pLP2358
LPY14595	LPY11411 + pLP2359
LPY14596	LPY11411 + pLP2360
LPY14597	LPY11411 + pLP2361
LPY14623	LPY6282 + pLP1412
LPY14624	LPY6282 + pLP1402
LPY14625	LPY6282 + pLP2211
LPY14626	LPY6282 + pLP2355

Table 5.1, continued.

LPY14627	LPY6282 + pLP2356
LPY14628	LPY6282 + pLP2357
LPY14629	LPY6282 + pLP2358
LPY14630	LPY6282 + pLP2359
LPY14631	LPY6282 + pLP2360
LPY14632	LPY6282 + pLP2361
LPY14703	LPY6282 + pLP2312
LPY14704	LPY6282 + pLP2313
LPY14705	LPY6282 + pLP2314
LPY14706	LPY6282 + pLP2315
LPY14707	LPY6282 + pLP2316
LPY14708	LPY6282 + pLP2317
LPY14709	LPY6282 + pLP2318
LPY14710	LPY6282 + pLP2319
LPY14711	LPY6282 + pLP2320
LPY14712	LPY6282 + pLP2321
LPY14713	LPY6282 + pLP2322
LPY14714	LPY6282 + pLP2323
LPY14715	LPY6282 + pLP2324
LPY14716	LPY6282 + pLP2325
LPY14717	LPY6282 + pLP2326
LPY14370	LPY3291 + pLP1402
LPY14371	LPY3291 + pLP1412
LPY14681	LPY3291 + pLP796
LPY14368	LPY3486 + pLP1402

Table 5.2 Plasmids used in Chapter 5

Plasmids	
Plasmid	Gene
pLP74	pKS Bluescript
pLP362	pRS426
pLP796	*ESA1* in *pRS426?*
pLP863	*esa1-414* in pRS314
pLP1402	pRS202
pLP1412	*LYS20* in pRS202
pLP2144	*LYS4* cosmid; KanR
pLP2204	*Lys4* in pKS Bluescript
pLP2211	*LYS4* under control of *LYS20* promoter in pRS426
pLP2312	*LYS4 R43A*
pLP2313	*LYS4 R43K*
pLP2314	*LYS4 R43Q*
pLP2315	*LYS4 H103A*
pLP2316	*LYS4 S165A*
pLP2317	*LYS4 R163A*
pLP2318	*LYS4 R163K*
pLP2319	*LYS4 R163Q*
pLP2320	*LYS4 E167A*
pLP2321	*LYS4 E167Q*
pLP2322	*LYS4 T197A*
pLP2323	*LYS4 T197S*
pLP2324	*LYS4 T197V*
pLP2325	*LYS4 Y332A*
pLP2326	*LYS4 Y332F*
pLP2329	*LYS4 Q47A*
pLP2355	*LYS4 E74A*
pLP2356	*LYS4 E74Q*
pLP2357	*LYS4 D123N*
pLP2359	*LYS4 D123N; E222Q*
pLP2358	*LYS4 E222Q*
pLP2360	*LYS4 R288K*
pLP2361	*LYS4 Q364N*

Table 5.3 Oligos used in Chapter 5

Oligos	
Oligo	Sequence
oLP911	TGTGTCCGAAGCTAATGG
oLP912	AAGCAGACGCTTCTTTGG
oLP944	GGGAATTCTCTCTTCGGTAGTGG
oLP945	CCTGTATTGTTTTCCTAAAGATGTCTGTGTCCGAAGCTAATGG
oLP946	CCATTAGCTTCGGACACAGACATCTTTAGGAAAACAATACAGG
oLP947	ATCTAGATTAAGCAGACGCTTCTT

Chapter 6 Conclusions and future directions

Results presented in this thesis have demonstrated interactions among several genes. Major areas of focus included nuclear roles for Lys20 and connections of Esa1 with H2A at multiple levels. A recurring theme has been that even well characterized proteins, including histones, histone acetyltransferases and metabolic enzymes may have additional cellular roles.

Metabolic enzymes are increasingly returning to prominence as new roles are discovered. Instances of this phenomenon include the fumarase case discussed briefly in Chapter 2. According to a recent report, the Krebs cycle enzyme fumarase goes to the nucleus upon DNA damage and is a critical component of the DNA damage response pathway in yeast (Yogev et al. 2010). Many other moonlighting proteins are reviewed in (Jeffery 1999; Jeffery 2003). One trend is that metabolic enzymes in particular seem to have connections to DNA damage. For example, in mammalian cells, GAPDH (glyceraldehyde-3-phosphate dehydrogenase), an enzyme catalyzing a step in glycolysis has a dual function in DNA repair as a uracil DNA glycosylase (Meyer-Siegler et al. 1991). Aconitase is another bifunctional metabolic enzyme with roles in the Krebs cycle and in iron uptake regulation (Haile et al. 1992).

Fbp1 (Fructose bisphosphatase1) is an enzyme involved in gluconeogenesis but when *FBP1* is deleted, cells become resistant to DNA damage induced by reactive oxygen species and peroxides as discussed in Chapter 2 (Kitanovic and Wolfl 2006).

The mechanism of resistance is fundamentally metabolic: when Fbp1 is absent, metabolic flux is reduced, resulting in generation of a smaller quantity of reactive oxygen species. Mutants in *FBP1* thus accumulate less DNA damage due to ROS generated by metabolism and are relatively resistant to ROS mediated DNA damage. Fbp1 is similar to Lys20 in that both are metabolic enzymes whose absence renders cells resistant to DNA damage. Since *lys20*Δ *lys21*Δ mutants are resistant to multiple forms of DNA damage (Fig 2.4 and 2.7), the mechanism of resistance is likely to be more complex. Preliminary results suggest that *lys20*Δ *lys21*Δ mutants are also resistant to hydrogen peroxide. Halo assays (Fig 4.20) showed that *lys20*Δ *lys21*Δ mutants were less sensitive to peroxide than wild type cells. If confirmed, this implies that reactive oxygen species (ROSs) may explain part of *lys20*Δ *lys21*Δ DNA damage resistance.

Superoxide dismutase may link lysine and ROSs together (Slekar et al. 1996). Yeast have two superoxide dismutase enzymes (Sod1 and Sod2) that are responsible for detoxifying peroxide radicals (reviewed in Jamieson 1998). As expected, *sod1*Δ mutants are sensitive to peroxide but they are also auxotrophic for both lysine and methionine. The reason for these mutants' lysine auxotrophy remains undefined.

Lysine remains closely associated with ROS biology, however at another level. One of the most important cofactors for Sod1 is copper. Its copper chaperone is the Ccs1 protein that is essential for Sod1 function. Mutants in *CCS1* are also lysine auxotrophs. Indeed *CCS1* was first identified in a screen for genes involved in lysine biosynthesis and was originally named *LYS7* (reviewed in Bhattacharjee, 1985). It was

only when its copper chaperone function was discovered (Gamonet and Lauquin, 1998) that it was given a more functionally descriptive name, reflecting that it does not play a direct role in lysine biosynthesis.

Further Characterization of Lys20 activity

Lys20's nuclear localization was a mystery partially solved in this body of work. Yet, much about the enzyme's functions remains mysterious. HAT activity of Lys20 remains to be firmly established and characterized in detail. The material contained in Appendix A details many conditions under which optimization of activity was attempted. Two things seem to stimulate the weak activity that Lys20 does possess. These are using purified yeast histones as substrate and the addition of lysine or arginine to the reaction. Further HATs assays could be attempted with extra lysine and histones purified under non-denaturing conditions. Although the HCl extraction that yielded histones with activity is more gentle than the classic sulfuric acid extraction (Lo et al. 2004; Vaquero et al. 2006), it is still a harsh procedure which included TCA precipitation to concentrate. More gentle methods may preserve other acid-labile marks that would optimally stimulate Lys20 activity. Additionally, purified Lys20 and any associated protein might be more active than recombinant protein.

To elucidate further the mechanisms of DNA damage influenced by HCS, a more refined analysis of the DNA damage pathway will be necessary. As shown in Figure 2.10, deletion of *LYS20* and *LYS21* causes an increase in Rad53 hyperphosphorylation upon exposure to DNA damage. The point at which deletion affects the DNA damage repair pathway may therefore be upstream of Rad53

phosphorylation. Suppression of *esa1* DNA damage by *LYS20* overexpression does not appear to influence phosphorylation of Rad53. It therefore seems likely that processes downstream of Rad53 are implicated in this mechanism of suppression. Since NuA4 is recruited to DNA double strand breaks (Tamburini and Tyler 2005), it would be good to know if Lys20 participates in this process. The next step in deciphering Lys20's involvement in DNA damage repair is to find out the step in repair that Lys20 affects. It is possible that Lys20 and or Lys21 may be physically present at sites of DNA damage, interacting with other DNA repair proteins. A direct role, or one in recruiting repair enzymes, could be assayed by probing for Lys20's presence at sites of double strand breaks, such as the well-characterized inducible HO-cut model (Pellicioli et al. 2001). If it were not found there, then phosphorylation of the ATM/ATR kinases, a signal that the next major step in DNA damage repair is proceeding could be assayed in the *lys20*Δ *lys21*Δ mutants to look for defects.

A candidate gene approach to try to find the relevant DNA damage genes might simply be to mutate them in the *esa1* background and see upon which of them the suppression depends. This approach would be complicated as mutation of genes encoding DNA damage proteins might confer acute sensitivity on the strains, making *LYS20* mediated suppression difficult to observe.

Finding a signature of bifunctionality

Are there other metabolic enyzmes with functions in DNA damage repair? A simple way to address this question would be evaluate through the results of screens performed to identify DNA damage sensitivity. Any genes encoding metabolic

enzymes recovered in such screens may have been dismissed. They would be particularly significant in this analysis if they also contained acetyl CoA binding domains or NAD+ binding domains, (as many metabolic enzymes do). Either might suggest involvement with histone acetylation or NAD+ dependent histone deacetylases. Enzymes with atypical localization (as Lys 20's nuclear localization) might also suggest a hidden function. Some chromatin related proteins change localization, or substrate specificity in response to various circumstances. Two examples of this are the protein acetyltransferase Eco1 which acetylates certain lysine residues when the cell is in S-phase, but switches specificity upon DNA damage (Heidinger-Pauli et al. 2009). The HAT Hat1 changes subcellular localization, from both cytoplasmic and nuclear to nuclear only upon irradiation with heavy-ion particles or hydrogen peroxide (Lebel et al. 2010). Another way to look for bifunctionality is to consider that many enzymes are able to catalyze the reverse of their reactions, although usually with altered kinetics. Those that bind molecules such as homocitrate, which could conceivably act as acetyl donors, are also candidates for bifunctionality.

To answer the question of what Lys20 is doing at the rDNA, it would be informative to know if Lys20 is present at the rDNA or not. Lys20 has been reported to exist in a chromatin bound fraction (Chen et al. 1997). Understanding which genomic regions Lys20 binds and under which conditions may help further define it s nuclear roles.

New roles for Esa1

A distinct area of focus for future study comes from data revealing enhanced functional associations between Esa1 and H2A. *ESA1* interactions with both *HTZ1* and *NAP1* make connections to both H2A and DNA damage.

Histones are explicitly connected to DNA damage in multiple ways: in addition to histone mutations causing sensitivity to DNA damage (Downs et al. 2000), altered histone gene dosage also wreaks havoc on other cellular functions (Meeks-Wagner and Hartwell 1986). Rad53 contributes to degradation of excess histones in a manner that requires its kinase activity. When *RAD53* is mutated, excess histones accumulate, resulting in DNA damage sensitivity and other phenotypes (Gunjan and Verreault 2003). The connection between histone dosage and DNA damage suggests an expanded role for histone chaperones, as they modulate effective histone gene dosage.

In addition to the histone chaperones Nap1 and Chz1 (discussed in Chapter 3), a third chaperone, Asf1, is specific for H3 and H4 (reviewed in Mousson et al. 2007). Rad53 also binds to Asf1, and interferes with silencing by removing it from H3/H4 (reviewed in Mousson et al. 2007). Involvement of Asf1 has been demonstrated in DNA damage though it is not required for acetylation of H3K56 in response to HU induced DNA damage (Recht et al. 2006). This may provide a paradigm to assist in interpretation of the *ESA1* interaction with the histone chaperone gene *NAP1* (Fig 3.10), and define a role for the H2A.Z chaperone *CHZ1* in the network of interactions among *ESA1, HTZ1* and *NAP1*.

Together with interactions discussed in Chapter 3 among Esa1 and H2A, H2A.Z and histone chaperones, the evidence presented in Figs 3.14 and 3.15 suggests an expanded biochemical role for Esa1. Additional target residues for Esa1 on H2A and likely H2A.Z, when identified, may help clarify the mechanism of Esa1's other cellular roles, for example cell cycle functions. This work takes the first steps in describing nuclear roles for a metabolic enzyme previously thought to be dedicated to amino acid biosynthesis. The data presented here have also expanded understanding of several chromatin proteins, including HATs and histones. Further analyses will undoubtedly uncover more examples of bifunctionality at many levels, leading to a deeper appreciation of the true complexity of what may have originally been considered simple cogs in metabolism.

Appendix A Optimization of HAT assay conditions

Introduction

Weak Lys20 HAT activity is shown in Figure 2.12 . Despite many attempts at optimization, activity remained weak and erratic, though visible on many occasions. This Appendix details the various methods used in optimizing the HAT assays and those used in purifying substrate for the assays. In all experiments, recombinant Esa1 was used as a positive control and the empty vector served as the negative control. The optimization, while not successful in defining conditions that led to robust activity for Lys20, did uncover the fact that Esa1 HAT activity is stimulated by lysine and arginine.

Results

Preparation of proteins

To investigate the possible HAT activity for Lys20 and Lys21, both proteins were cloned into the pRSET expression vectors. The pRSET vectors encode N-terminal His_6 tags that can be used to purify the proteins. Empty vector and Esa1 in pRSET B were used as negative and positive controls, respectively. The plasmids were transformed into *E. coli* B834 DE3 cells with the pRARE plasmids for rare tRNAs. Lys20 and Lys21 were well expressed (Fig A.1).

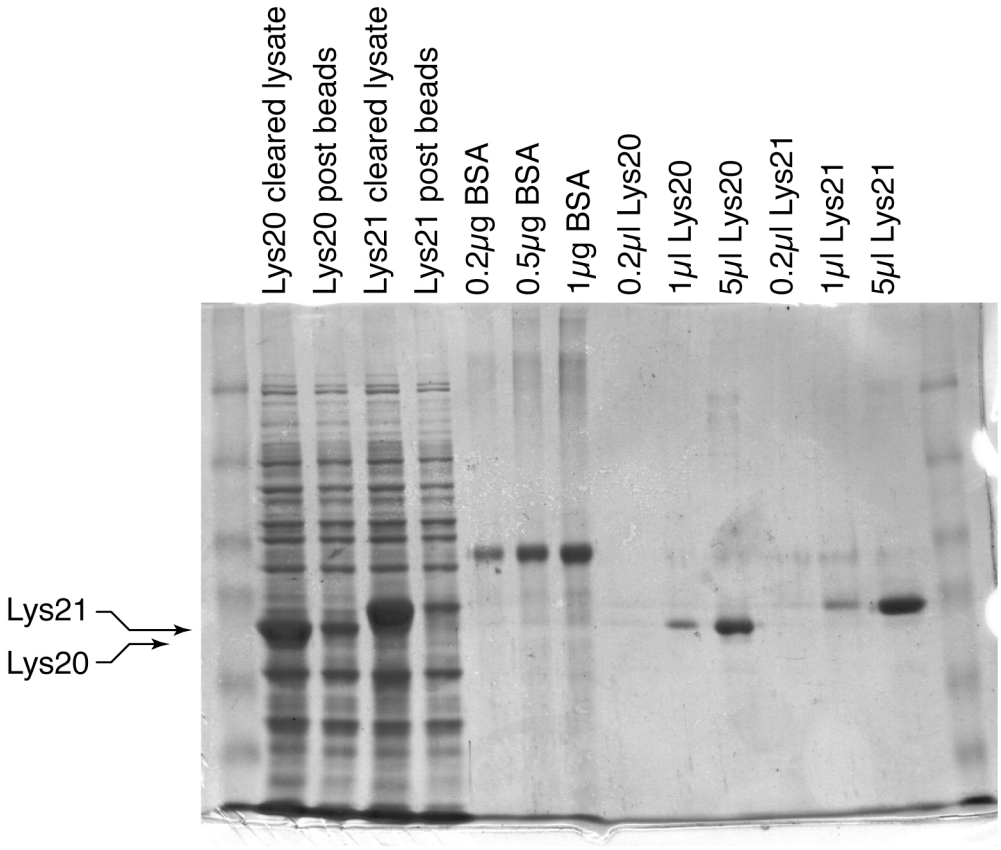

Figure A.1 Purification of recombinant Lys20 and Lys21 from *E. coli*. Cleared lysate from *E. coli* cells expressing recombinant, His-tagged Lys20 or Lys21 is shown before and after incubation with nickel-NTA beads, which should bind the His- tagged proteins. Depletion was efficient. Varying concentrations of BSA are loaded as controls to aid in quantitation. Three concentrations of purified Lys20 and Lys21 are loaded to show purity and allow for estimation of concentration. The total elution volume was 3 mL.

The yield of purified protein was roughly 1.5mg/protein per 50mL culture (Fig A.1).

The purified proteins were then tested for activity. To test for activity, an assay was used that depended on the HCS (homocitrate synthase) activity of Lys20 (Andi et al. 2004). Briefly, purified recombinant Lys20 and Lys21 were added to a reaction mix that included alpha ketoglutarate and Acetyl CoA, the two substrates of the HCS reaction. If HCS is active, the reaction products, homocitrate and CoA-SH will accumulate. At the end of the reaction, DTNB (dithio nitrobenzoate), Ellman's Reagent is added. In the presence of a reducing agent such as CoA-SH, Ellman's Reagent is reduced to a yellow compound (5'-thio-2-nitrobenzoate) that can be detected spectrophotometrically at 412 nm (Fig A.2). This assay was not entirely conclusive, but it seemed likely that there was some HCS activity in the purified proteins. Spectrophotometric HAT assays were also attempted with the purified protein, but failed to give clear results. As a result, the decision was made to attempt radioactive HAT assays with labeled Acetyl CoA in hopes of a clearer answer.

In preparing the HAT assays, it became clear that the purified Lys20 and Lys21 were not stable at 4˚ for extended periods. Stabilization was attempted according to previously published protocols (Andi et al. 2004), but this resulted in the protein precipitating in the tube.

Due to the high levels of expression of recombinant Lys20 and Lys21 (Fig A.1), it seemed possible that we could assay HAT activity directly from bacterial extract without protein purification. This approach had been used previously in

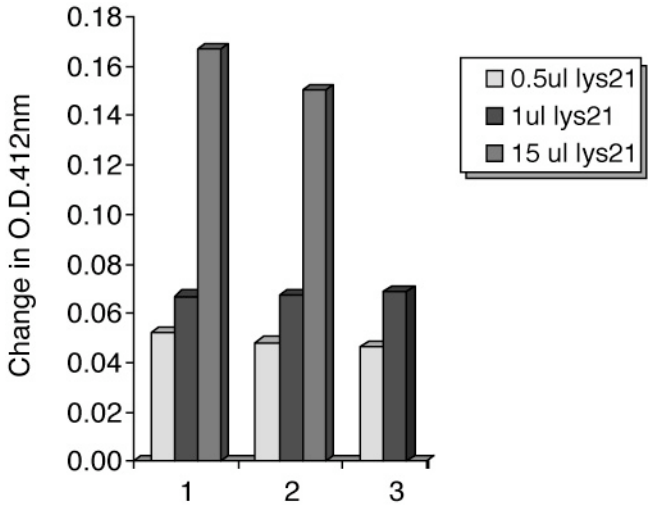

Figure A.2 Homocitrate synthase activity assay of that purified recombinant Lys21. 1, 2 and3 indicate replicate reactions, measured on same spectrophotometer. Y-axis units indicate change in OD_{412} from beginning to end of reaction for each sample. Similar results were observed for Lys20. Lys20 analysis was performed by Viet Le.

characterizing Esa1 HAT activity (Clarke et al. 1999). Bacterial extracts were found to have activity against calf thymus histones for Esa1. Low levels of activity were detected for Lys20 and Lys21. (Fig A.3). However, Esa1 activity was high in comparison as was background. Commercial calf thymus histones contain some contaminating acetyltransferase activity, and so it was decided to use recombinant histones to see if the elimination of background would allow for a clearer look at Lys20 and Lys21 HAT activity.

Recombinant yeast H2A/H2B (a gift of Joon Huh and Bob Dutnall) was used as substrate. Esa1 acetylated this substrate, however, Lys20 and Lys21 did not (Fig A.4). This was also true for recombinant Htz1, supplied by Josh Babiarz in Jasper Rine's lab. (Fig. A.4). Esa1 had activity towards rHtz1, but Lys20 did not. In either case, the recombinant H2A/H2B or Htz1 may not be the correct substrate for Lys20. One explanation for this observation is that yeast histones needed postranslational modifications in order to be acetylated by Lys20. This would explain the lack of activity against recombinant yeast histones.

To test this idea, yeast histones purified from growing cells were used as substrate. With yeast histones as substrate, background was reduced and Lys20 and Lys21 showed much stronger activity. This result, in combination with the observation that Lys20 and Lys21 had activity against the yeast histones purified by the Laybourn lab (Fig A.5) led to the idea that Lys20 and Lys21 had specificity towards yeast histones that had

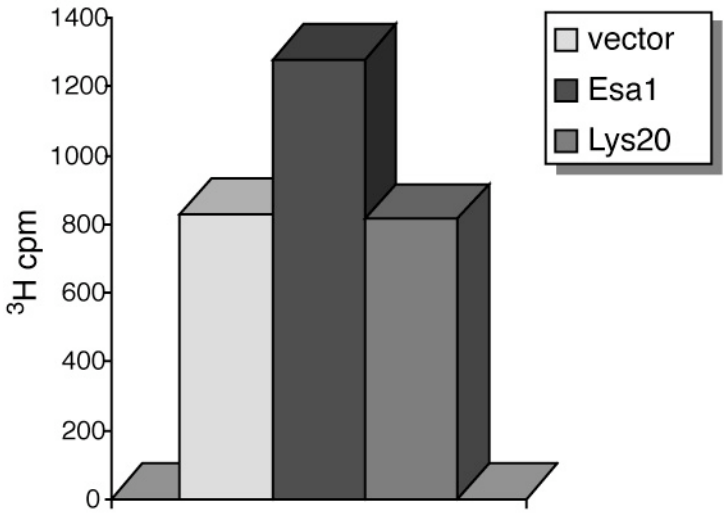

Figure A.3 Activity of Lys20 against Calf Thymus Histones is very close to background.

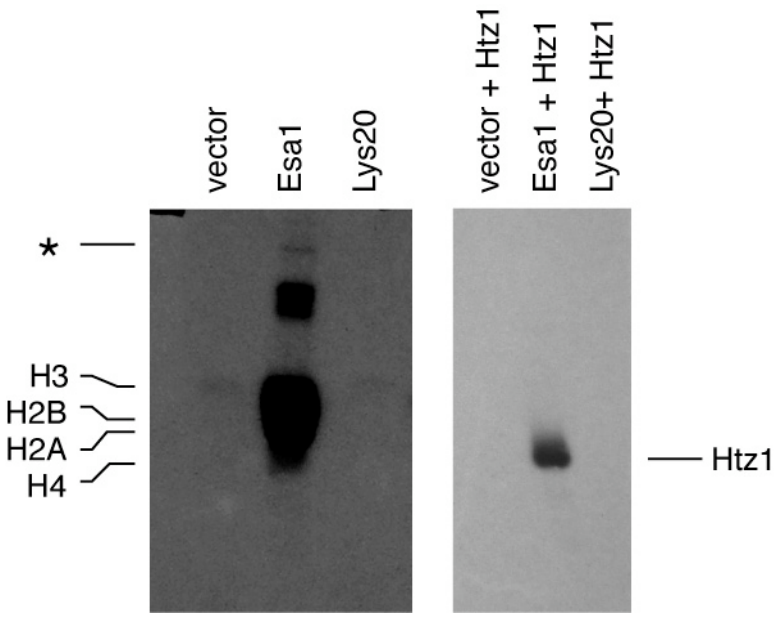

Figure A.4 Unlike Esa1, Lys20 has no activity against recombinant histones. In left panel, recombinant Esa1, Lys20 or empty vector extract were incubated with recombinant yeast H2A/H2B. Only Esa1 had activity against this substrate. In right panel, 5µg recombinant Htz1 was used as substrate and again, only Esa1 had activity towards this substrate. The * marks a band thought to represent autoacetylation of Esa1 (Yan, 2000).

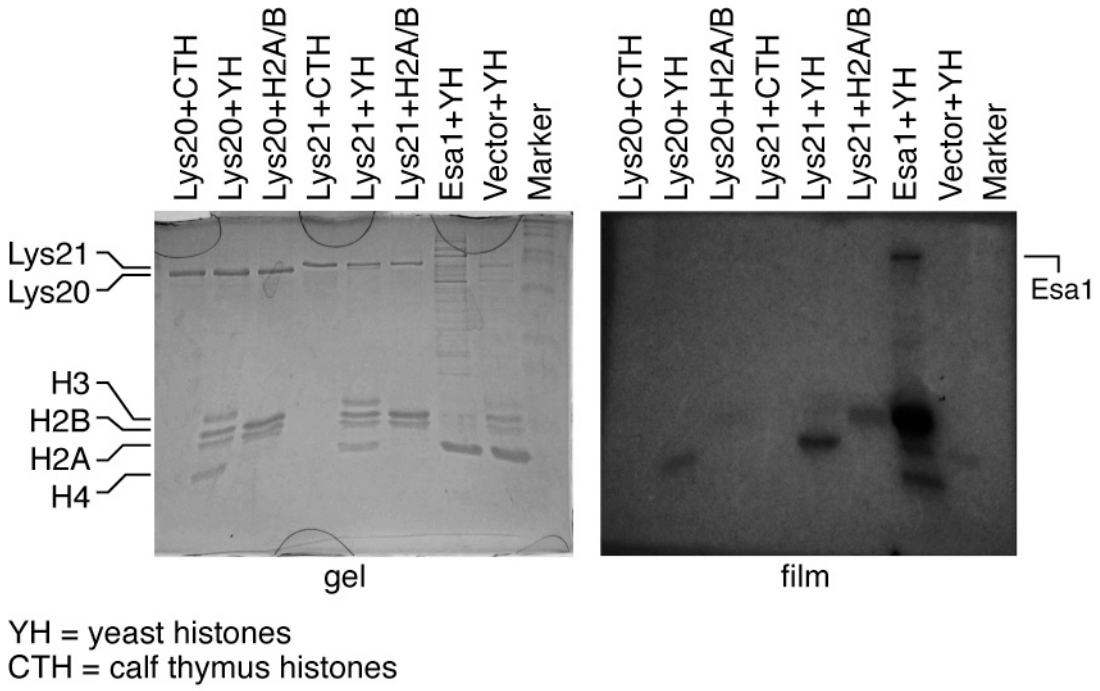

Figure A.5 Lys20 and Lys21 have activity towards histones purified from yeast. Histones purified from yeast by the Laybourn lab were used as substrate in this assay. Both Esa1 and Lys20 have activity, although Lys20's is much weaker. No background is apparent in the vector lane. YH indicates yeast histones, CTH indicates calf thymus histones. H2A/H2B indicates recombinant yeast H2A/H2B.

been made in yeast, possibly requiring some modifications to be present in order to acetylate them.

Histone substrates from yeast

To test the idea that pre-existing modifications were required for HCS activity acetylating histones, the histone proteins were purified from yeast using the acid extraction method (Lo et al. 2004). This method exploits the positive charge of histones, which makes them acid soluble when few other proteins are. Histones can be extracted in acid, and the other denatured proteins removed by centrifugation; the histones are themselves then precipitated from the acid in a fairly pure state. The protocol in (Lo et al. 2004) calls for sulfuric acid to be used, which is indeed the most efficient method. This protocol generated pure histones in reasonable abundance (Fig A.6). However, we had previously used these histones in immunoblots with antibodies specific to acetylated lysines on the histones. In doing so, we found that the sulfuric acid purified histones were not recognized by the antibodies and concluded that acid extraction destroyed the epitope. Similarly, when sulfuric acid purified histones were used as substrate for HAT assays, they were unacetylatable even by Esa1, usually a very robust HAT. Literature searches revealed that immunoblots on acid-extracted histones were possible, but that these histones had been extracted with hydrochloric acid instead of sulfuric acid (Vaquero et al. 2006). Histones were then purified from yeast with HCl (von Holt et al. 1989), and used as substrate in HAT assays. Esa1 did acetylate these histones (Fig 2.12) as did Lys20, when lysine was present, a factor that will be discussed later in this Appendix.

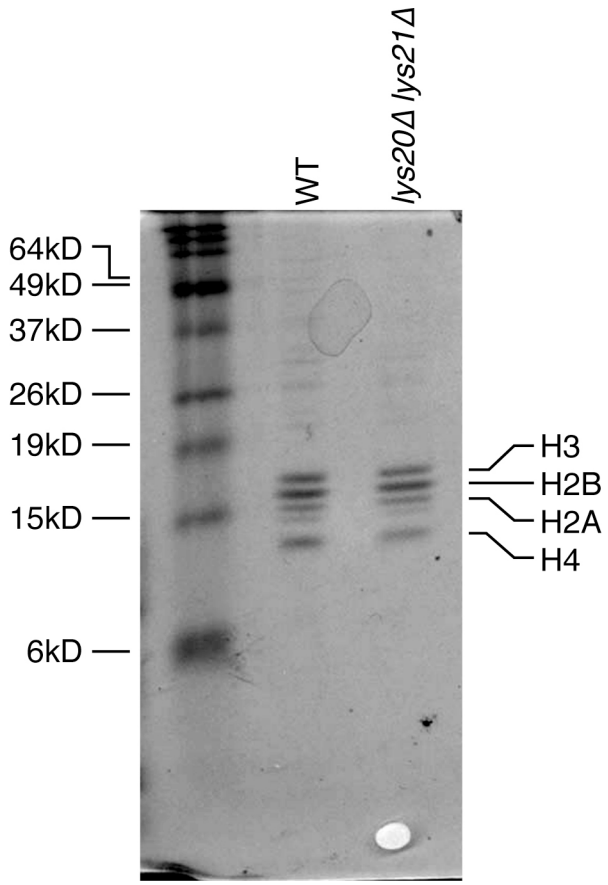

Figure A.6 Acid extracted histones purified from yeast are pure and present in reasonable abundance. Histones were extracted from both wild type yeast and *lys20*Δ *lys21*Δ strains using the sulfuric acid extraction method. Histones extracted with hydrochloric acid look very similar to those shown here.

Changing HAT assay conditions

Due to the continued weakness of the Lys20 signal in HAT assays, other factors were optimized. pH is one factor that plays a role in the efficiency of the HAT reaction. HAT assays were undertaken at a variety of pHs to see if this would provide optimal conditions for Lys20. pH 8, and 9 were tried (Fig A.7). Although signal was improved, background increased dramatically, as measured both by gel and by scintillation counting. This effect has been documented previously (von Holt et al. 1989) and is likely due to spontaneous hydrolysis of the radioactive acetyl CoA at higher pHs, which render the thioester bond more labile.

Another variable in the assays is the isotope in acetylCoA. Most of the assays have been done with tritiated acetyl CoA, however, tritium is a very low energy isotope. Acetyl CoA may also be labeled on the C2 carbon of the acetyl group, and ^{14}C is a higher energy isotope. In hope of increasing the weak signal of Lys20, we tried ^{14}C Acetyl CoA. This approach resulted in hugely increased background in all samples, including the negative control.(Fig A.8).

Using the HCl method for purifying histones from yeast, histones were also purified from mutant yeast strains, including *htz1*Δ and *nap1*Δ. When used as substrate in HAT assays, Lys20 did not seem to have specific activity towards these histones. More surprisingly, Esa1 activity towards these histones seemed to be altered. Altered mobility on a gel was also observed for these histones, indicating that something fundamental had changed in these mutants (Fig A.9). In principle, this biochemical

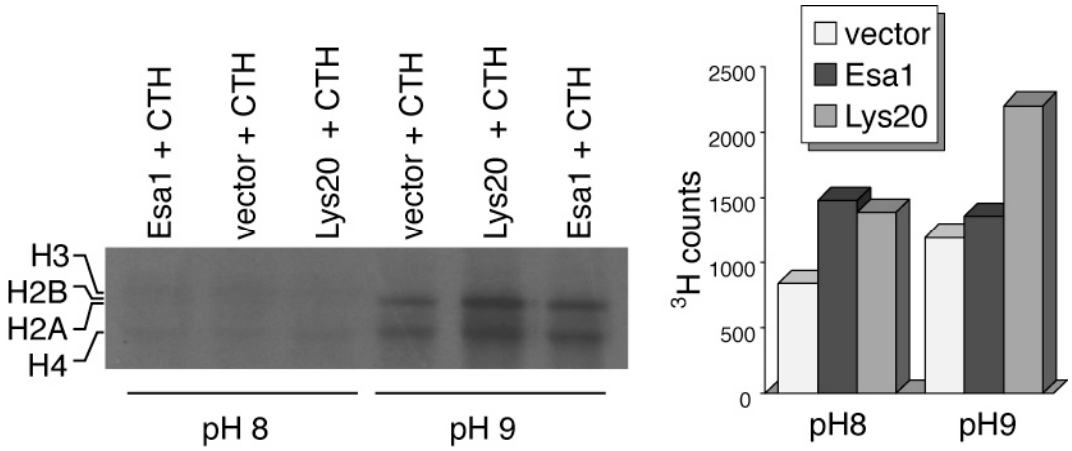

Figure A.7 Increased pH results in increased background activity in HAT assays. HAT reactions were performed once at pH8 (standard pH) and once at pH9. Increased activity was observed for all samples, including the empty vector negative control at the higher pH. CTH refers to calf thymus histones, used as substrate in all reactions. The reactions shown on the gel were also quantified by scintillation counting, which corroborated the result on the gel, that increased pH led to increased background. Y axis is in cpm of tritium.

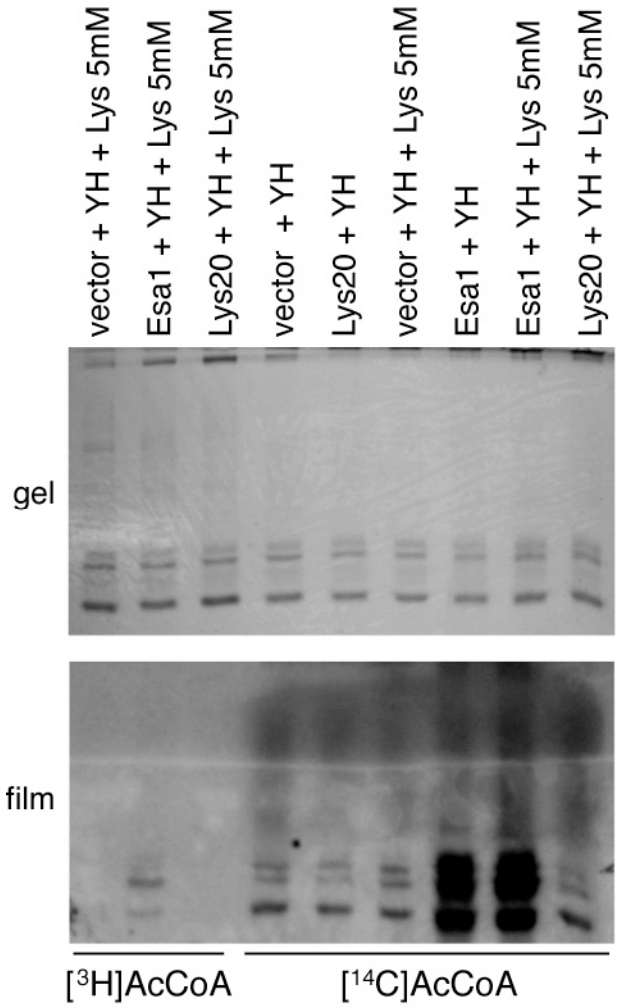

Figure A.8 Use of ^{14}C Acetyl CoA instead of ^{3}H acetyl CoA leads to increased background for all samples. 3H indicates the tritiated acetyl CoA was used as label, ^{14}C means that carbon-14 acetyl CoA was used. YH means that histones purified from yeast were used as substrate. Lysine was added to some samples at the indicated concentration.

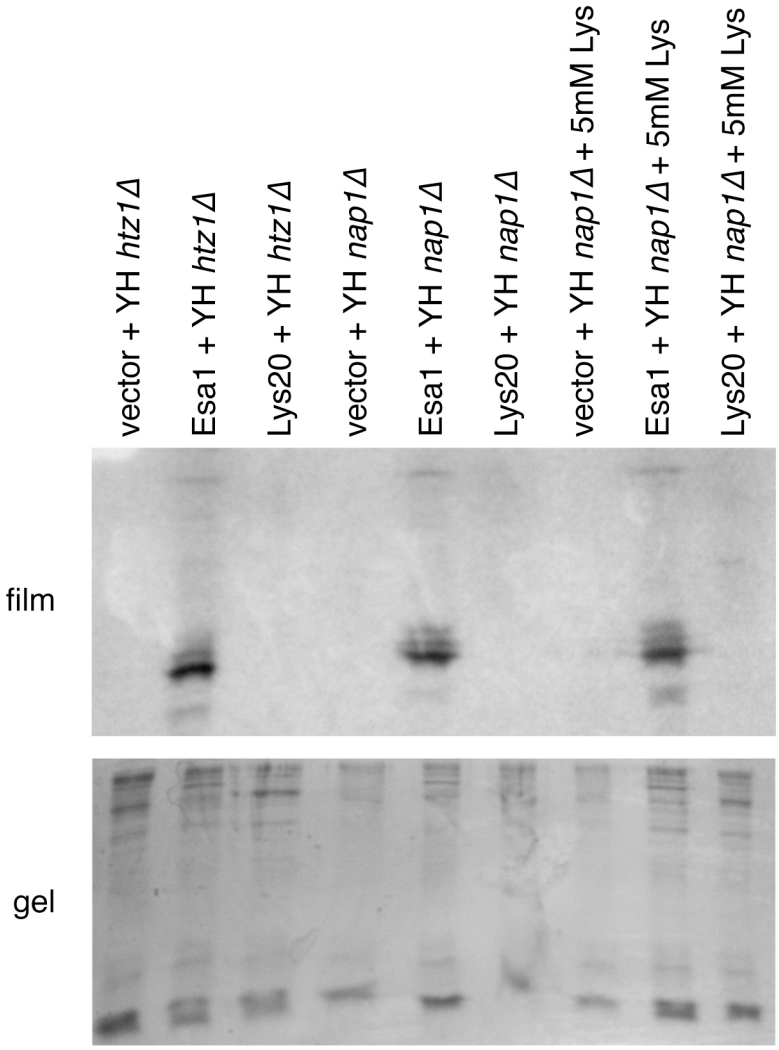

Figure A.9 Esa1 alone has activity against yeast histones purified from *htz1*Δ and *nap1*Δ strains. Some samples have lysine added, as indicated. Note that histones purified from these strains have an altered appearance compared to those in Fig A.6.

result strongly supports the genetic observation that *HTZ1* is required for suppression mediated by *LYS20*. However, the control of wild type YH is missing in this experiment. In future studies, it will be important to evaluate the mutant and wild type histones in parallel assays.

In attempts to optimize HAT activity of Lys20, the idea was tested that inhibiting the HCS activity of Lys20 might trigger the HAT activity. HCS activity is feedback inhibited by lysine, so lysine was added to the HAT reactions. Addition of lysine stimulated Lys20 HAT activity (Fig A.10). This was not due to increased pH of the HAT assay buffer (data not shown). Surprisingly, this stimulating effect was also observed on addition of lysine to Esa1. (Fig A.11) The reason for this observation is not yet understood. However, the amino acids and analogues were assayed to see if the effect would be specific to lysine or confined to a general class of small molecules. Arginine seemed to produce similar effects, as did N-ε-Acetyl-lysine (Fig A.12). Other compounds were tried, including ornithine, citrulline, hydroxylysine, Zinc and racemic lysine. Purified recombinant Nap1 (gift of Stacie Bulfer and Ray Trievel) was also added to assay. In these additional cases, either no effect was seen or the difference was less than that observed in Fig A.10.

In order to find a negative control substrate, polylysine was used as substrate in HAT reactions. Activity against polylysine was assayed by scintillation counting Neither Lys20 or Lys21 showed any activity, but vector showed some and Esa1 was strongly stimulated by polylysine addition (Fig A.13). There were no histones present in this reaction. Polylysine was the only addition. Either Esa1 is acetylating

Figure A.10 Lysine addition stimulates Lys20 HAT activity. Arginine and Lysine were added to 5mM. Arginine and lysine appear to affect Esa1 HAT activity.

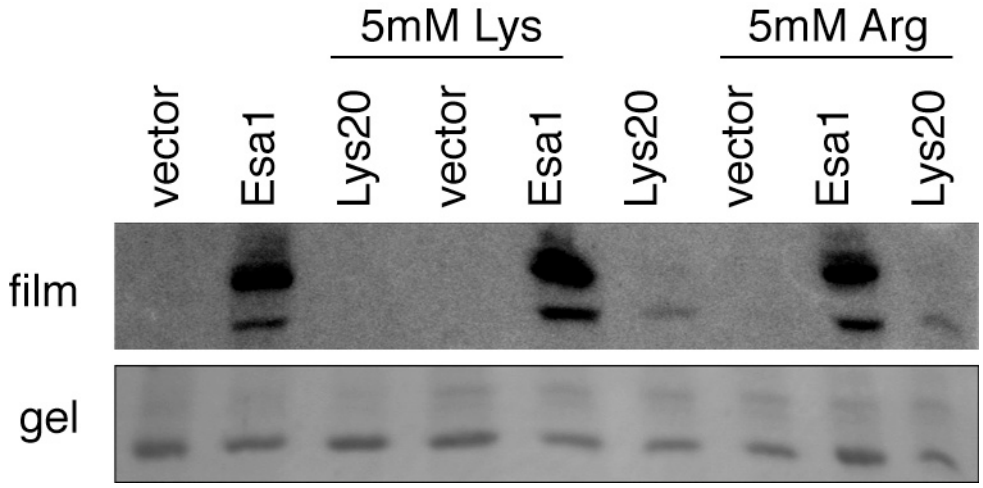
5mM Lys
5mM Arg
vector
Esa1
Lys20
vector
Esa1
Lys20
vector
Esa1
Lys20
film
gel

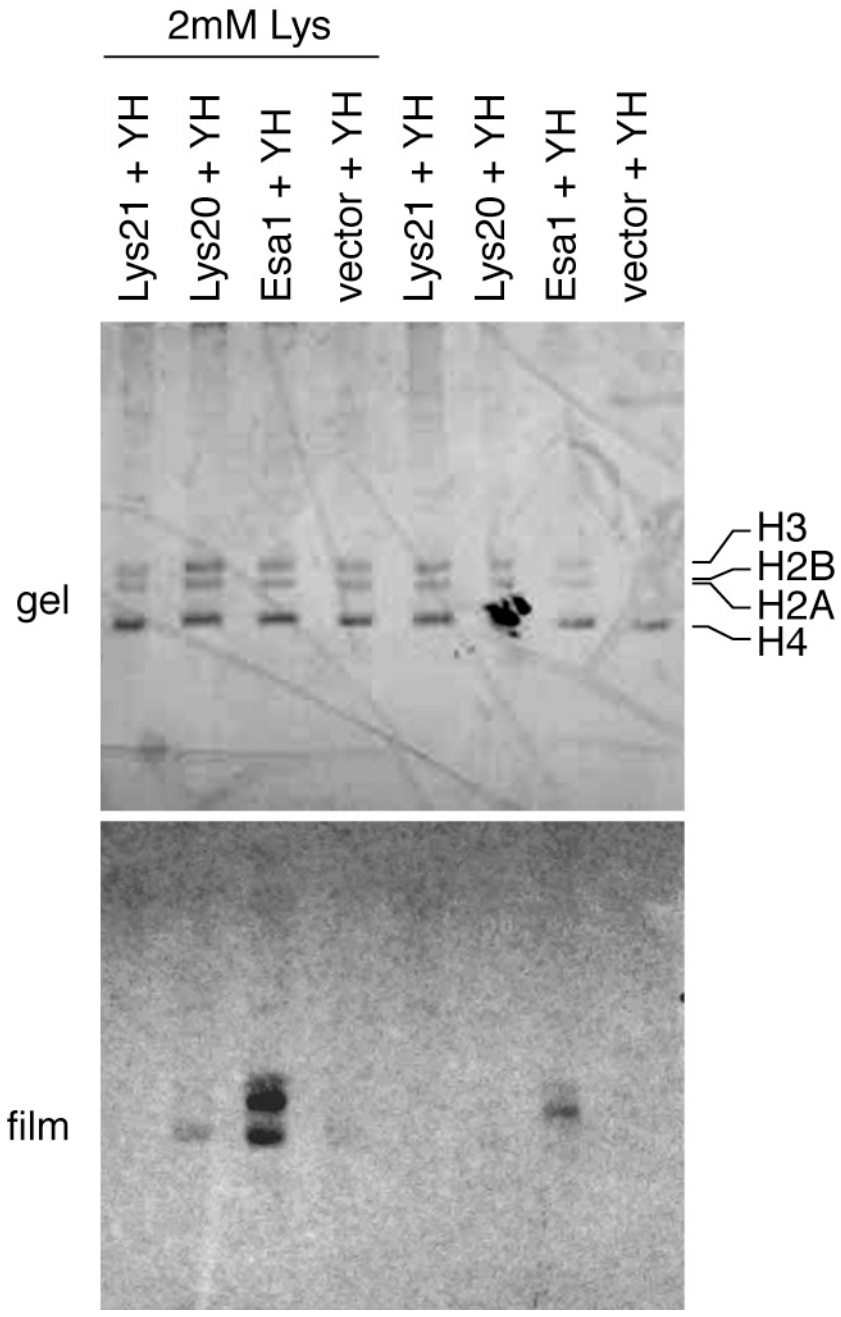

Figure A.10, continued

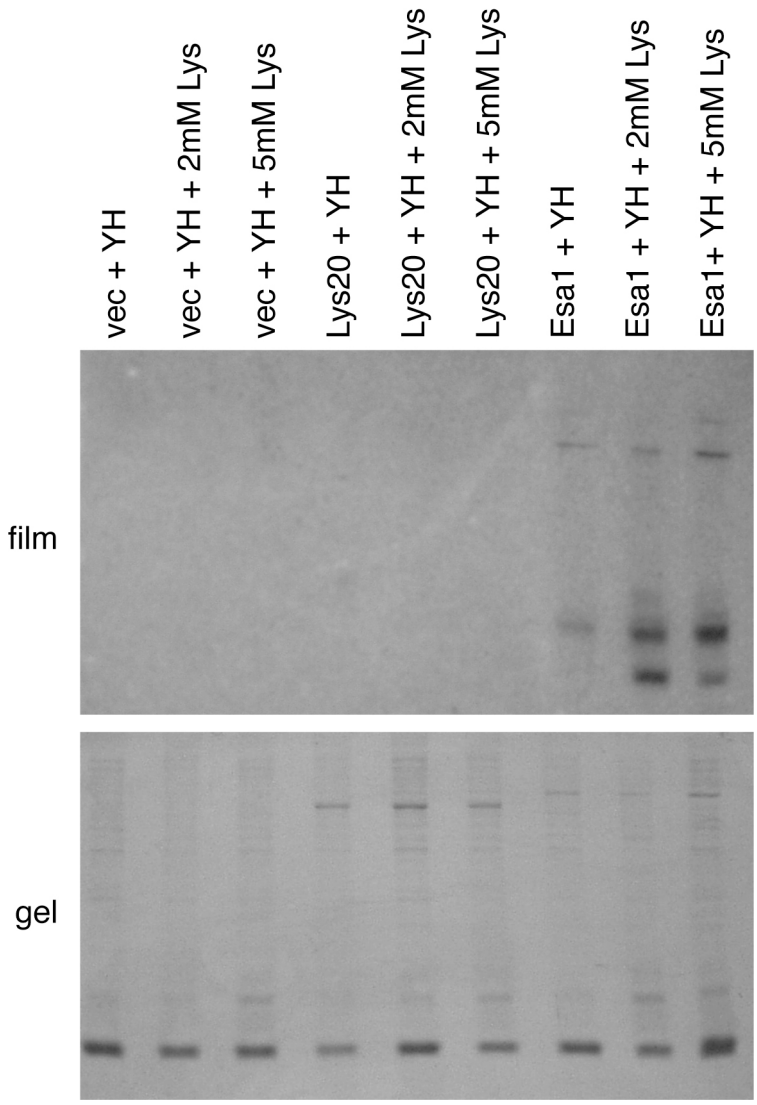

Figure A.11 Lysine stimulates Esa1 HAT activity.
Lysine was added at either 2mM or 5mM. Stimulation appears concentration dependent. Histones are acid extracted from yeast with HCl.

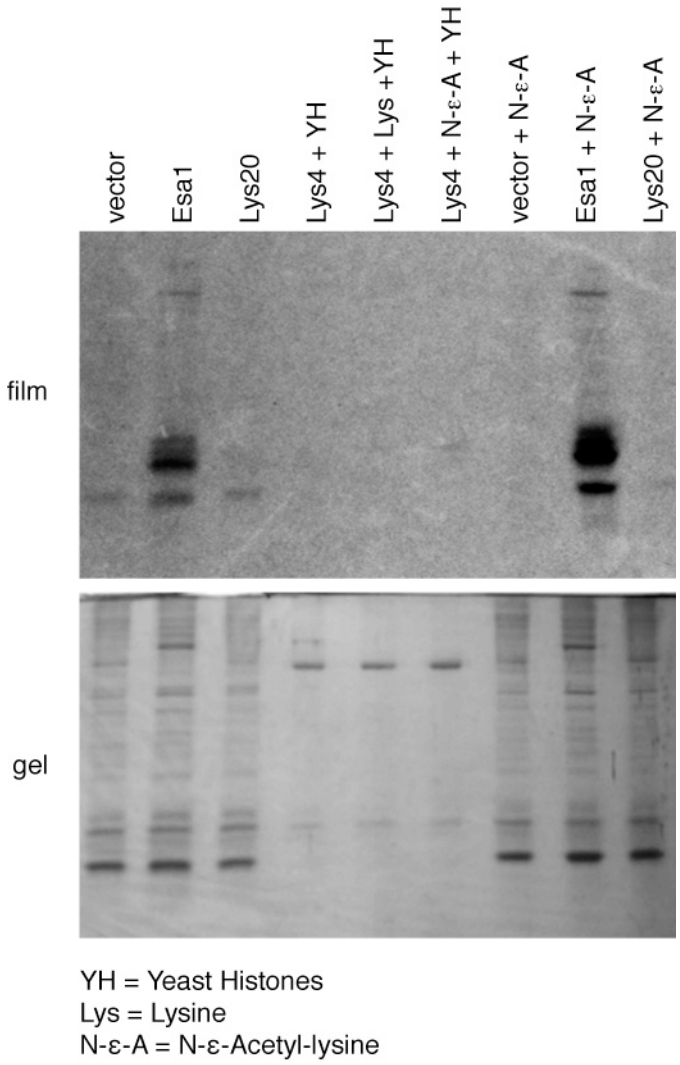

Figure A.12 Addition of N-ε-Acetyl-lysine stimulates Esa1 activity, but effects on Lys20 and Lys4 are inconclusive. Panel on bottom is coomassie stained gel after transfer. Top panel is film. HCl- extracted yeast histones were used as substrate.

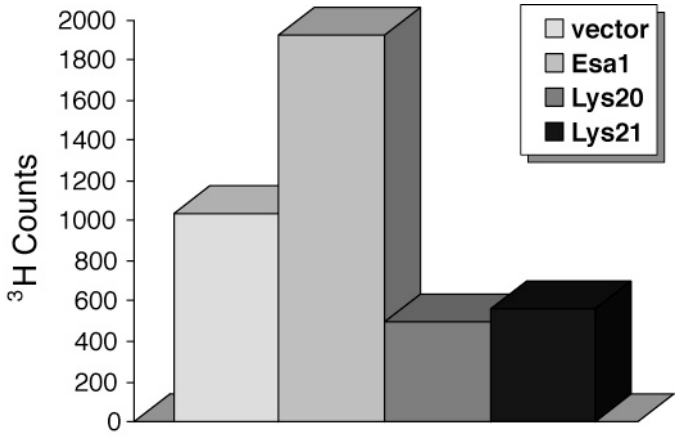

Figure A.13 Esa1 activity was high in the presence of polylysine. Y axis is in cpm of tritium. Polylysine was the only substrate added to these reactions. Esa1 activity is either directed towards the polylysine or polylysine is stimulating the autoacetylation activity. Background activity is present in the empty vector reaction as well.

polylysine, or polylysine is stimulating the autoacetylation activity of Esa1. Recalling the result in Figure A.11, that HAT activity is stimulated by additon of lysine, it seems that there is a role for lysine in Esa1 HAT activity. Evidence for additional target residues of Esa1 acetylation was presented in Chapter 3. In this appendix, we have advanced the biochemical understanding of Esa1 with the discovery of some small molecules that stimulate the HAT activity of Esa1 *in vitro*. Lysine and arginine in particular increase Esa1 activity when added to the reaction (Fig A.11). This could be due to the positively charged nature of these amino acids. Addition of the amino acids at concentrations up to 5mM does not change the pH of the reaction buffer. This was an important control to check, because increased pH in the HAT reaction increased nonspecific background activity (Fig A.7). Other amino acids were also assayed, but the effect was specific to lys and arg.

Discussion

The only success in attempts to optimize Lys20 HAT activity was the discovery that the HAT activity is stimulated by lysine addition. Other conditions tried did not result in increased Lys20 activity. Successful experiments may require Lys20 purified from yeast or histone or nucleosomal substrates purified in a gentler way than acid extraction and precipitation. It must also be considered that histones are not the preferred substrate for Lys20.

The mechanism to explain the observation that lysine stimulates the activity of Esa1 against histone substrates remains elusive. The catalytic mechanism of Esa11 remains a matter of debate, despite crystallographic analysis (Yan et al. 2000;

Berndsen et al. 2007). The activity against polylysine could simply be nonspecific activity, although the fact that activity is stimulated by free lysine does point to some physiological role for this observation. Increased lysine might simply act as a kinetic regulator to speed up the Kcat of Esa1. Structural analysis (Yan, 2000) shows no allosteric site for lysine binding so regulation by second site binding seems unlikely. Still, it seems more likely that if the lysine binds in the active site, it would behave more as a competitive inhibitor than as an activator. The polylysine is likely stimulating the autoacetylation of Esa1, which shows up as increased activity in Fig A.13.

Materials and methods

Cloning of LYS20 and LYS21

LYS20 and *LYS21* were first cloned into pLit28 (NEB). They were then subcloned into the expression vector pRSETc (Invitrogen, pLP 820), resulting in an N-terminal His_6 tag. Lys20 was inserted at the *Bam*HI/*Eco*RI sites, while Lys21 was inserted with the *Bam*HI site. ORFs were amplified by PCR. Integrity of the insert was verified by sequencing (UCSD Moores Cancer Center). Lys20 is pLP1934 and Lys21 is pLP1935.

Induction and expression of rLys20 and rLys21

For induction, pLP820 (empty vector) pLP 831 (Esa1), pLP1934 (Lys20) and pLP1935 (Lys21) were transformed into the *E. coli* expression strain B834 DE3 made

competent by the calcium chloride method. The strain contained the chloramphenicol marked pRARE plasmid (pLP 1936). 3 µl of miniprep DNA was used per transformation, and transformants were plated on LB-Amp- Cam media (contains both ampicillin and chloramphenicol). Plates were incubated at 37˚C, not longer than overnight.

In the evening, 10mL LB Amp Cam cultures were inoculated in triplicate with a single fresh transformant and incubated at 37˚C overnight. In the morning, the ODs of the cultures were measured and cultures were diluted to OD_{600} of 0.2-0.3 in 50ml of prewarmed LB Amp Cam media. Optical densities were measured after dilution. Cultures were returned to 37˚ to grow until cells had doubled once, and OD was approximately. 0.5-0.7. When target OD was reached, cells were shifted to 30˚ for induction and induced with 2mM IPTG. Induction proceeded at 30˚ for 3 hrs. it was determined that fresh transformants were required for optimal induction. Further, multiple cultures were inoculated because, for reasons not yet resolved, there was variability in the ability of transformants to grow in liquid culture.

Cell lysis

ODs were measured and cells were harvested in Oakridge tubes atmax speed in clinical centrifuge. Pellets were washed in 10 mL room temperature MQ water and cells were resuspended well in 5 mL cold lysis buffer (1/10 volume). Lysis Buffer contained 20mM Hepes (pH7.6), 0.3M KCl, RNAse 10µg/mL, Lysozyme 1mg/mL, Benzamidine 1mM, Pepstatin 2µg/mL, PMSF 1mM, Leupeptin 2µg/mL and TPCK 1µg/mL. Lysis was allowed to proceed in ice for 30 min. After this, lysate was

transferred to 15mL Falcon tubes for sonication. Samples were sonicated on ice with a Branson sonicator for 3-4 min, duty cycle 50% power 2 with microtip. Clearing of lysate was observed. Samples were transferred to Oakridge tubes and cleared by centrifugation in a Sorvall centrifuge in SS-34 rotor for 10 min, 10-12Krpm 4˚C. Alternatively, after sonication, lysate was sometimes aliquoted into eppendorf tubes and cleared in a microfuge for 10 min at 10krpm. Cleared lysate was transferred to an eppendorf tube and kept on ice for immediate use.

Purification of rLys20 and rLys21

Cleared lysate was transferred into fresh 15 mL Falcon tubes. 380µL Nickel-NTA beads (Qiagen) was addded. Beads were prewashed 3X with 1mL wash buffer . Wash Buffer contained 20mM Hepes pH 7.6, 300mM KCl, and 20mM imidazole. Beads were washed by resuspending 380µL beads in 1mL wash buffer. They were spun 1 min. 2800 rpm in eppendorf centrifuge and wash buffer was removed.

Samples were incubated 1hr 4˚ with rocking. Beads were spun down in Falcon tubes (clinical centrifuge power 6, 3-5 min.). Lysate was pipetted off checking for beads. Beads were transferred to eppendorf tubes, and washed 5 times with wash buffer. To elute, beads were resuspended three times in 1mL elution buffer. Elution Buffer contained 20mM Hepes pH7.6, 300mM KCl and 200mM imidazole. Beads were completely resuspended, incubated with rocking at least 1 min, spun down at 2800rpm, and eluate was collected. For dialysis, 3mL eluate was injected into 0.5-3mL capacity slide-a-lyzer cassettes. Cassettes, each with 3mL eluate were put into

1L dialysis buffer. Dialysis Buffer contained 20mM Hepes pH 7.6 and 300mM KCl. Dialysis proceeded overnight at 4˚ with stirring.

HAT Assay

2X HAT buffer was made and diluted to 1X. Buffer, histones, and 1-5ul lysate were added to eppendorf tube. Tubes were mixed and centrifuged briefly. Label (tritiated Acetyl CoA) was diluted with 1X HAT buffer so that 0.3μCi could be added per reaction in a volume of 10μl. Label was added to reaction mix, and spun to blend. Total volume was 50μL. Reaction proceeded at RT 30 min. 10μL of each reaction was spotted to p81 filter paper pinned to Styrofoam block. Filters dried for 20-30 min (In meantime, 10uL 5X sample buffer was added to remaining 40uL of reactions, heated to 80˚ for 5-10 min and frozen at –80˚.) Unpin filters and wash by swirling 3X 5min in pH9.2 $NaHCO_3$, 10mL per filter in a 1L beaker. Filters were repinned and let dry 30 min. Filters were then unpinned and placed in scintillation vials with scintillation fluid. Counting occurred in scintillation counter.

The 2X HAT Buffer consisted of 50mM Tris pH8.0, 20% glycerol, 2μg/mL each pepstatin, TPCK and leupeptin and 1mM each PMSF and benzamidine.

HAT Gel

18% acrylamide gels were run using 20μL frozen sample. When 6kD ladder band was near bottom of gel, gel was fixed 30 min. Gel was stained in Coomassie at least 2hr and destained at least 1hr. Gel was photographed on light box. Gel was fluorographed in Enhance or similar reagent, then dried at 80˚ 2-3hr or overnight

without heat. Dried gel was placed onto Kodak MS film, with transcreen, and exposed at –80˚ for 6 weeks.

Alternatively, gels were transferred to nitrocellulose for 1hr at 100 volts at 4˚C. Gel was coomassie stained after transfer and photographed. Membrane was dried in fume hood at least 20min or overnight. Then membrane was placed on Kodak MS film with LE transcreen, and exposed at –80˚ for 6-8 weeks.

Preparation of yeast histones as HAT assay substrate

Cells were grown overnight in appropriate media. In the morning, ODs were greater than 0.5. ODs may be at least as high as 3 with no adverse effects. Cell concentration was normalized among strains and cells were harvested at max speed, 5 min in clinical centrifuge, using Oakridge tubes. Cell pellets were washed with 10mL sterile water. Pellets were resuspended in 5mL Buffer A (50mMTris pH7,5, 30mM DTT). Tubes were incubated at 30˚ 15 min, shaking gently in 15 mL Falcons. Cells were pelleted and washed with 10mL buffer S (1.2M sorbitol, 20mM HEPES, pH 7.4). Pellets resuspended in 5mL buffer S with 0.4 mL 5mg/mL zymolyase. Tubes were incubated at 30˚ with gentle shaking 1-1.5 hr. Presence of spheroplasts, cells lacking cell wall due to zymolyase digestion, was ascertained with light microscope. 10mL ice-cold buffer B (1.2M sorbitol, 20mM PIPES, pH 6.8, 1mM $MgCl_2$) was added and samples were spun 5000 rpm in SS-34 rotor for 10 min.

Samples were kept on ice from here forward. Pellets were resuspended in 5mL Buffer NIB (250mM sucrose, 60mM KCl, 14mM NaCl, 5mMMgCl_2 1mM$CaCl_2$ 15mM MES pH 6.6, 0.8% Triton X-100 and 1mM each NaF and PMSF) and split

among 3 2mL tubes. Subsequent resuspension volumes are divided among all tubes for each sample. Tubes were incubated on ice 20 min, then spun 5 min at 3300 rcf at 4˚. This step was repeated twice. Pellets were resuspended in 5mL Wash buffer A (10mm Tris pH8.0, 30mM sodium butyrate, 75mM NaCl, 0.5% NP-40 and 1mM each NaF and PMSF) and incubated 20 min on ice. This step was repeated twice. Then pellets were resuspended in 5mLWash buffer B (10mm Tris pH8.0, 30mM sodium butyrate, 400mM NaCl, and 1mM each NaF and PMSF) and incubated on ice 10 min. this step was repeated once. Pellets were resuspended in 1mL acid (0.4 N sulfuric or 0.25N HCL) in incubated on ice 1hr, with intermittent vortexing. Tubes were spun at 4˚ 10krpm 10min, and supernatant was taken to a fresh tube. TCA (100%) was added to a final concentration of 20%. Proteins were precipitated overnight at 4˚. In the morning, tubes were spun 12000 rpm 30min 4˚. Pellets were washed with acetone 0.1% HCl, again with acetone, and dried on ice 30min, not longer. Histones were resuspended in 50mm Tris pH8, 10% glycerol.

Acknowledgements

Bob Dutnall and Joon Huh provided assistance with the cloning strategy for *LYS20* and *LYS21*. They also provided recombinant histone substrate and assisted with the homocitrate synthase activity assays. Chris Murawsky and Beverly Emerson provided discussion and recombinant histones, Deb Urwin and Jim Kadonaga provided discussion. Josh Babiarz and Jasper Rine provided recombinant Htz1. Ray Trievel and Stacie Bulfer provided recombinant Nap1 to be added to HAT assays.

Viet Le and Eric Spedale assisted in the cloning of *LYS20* and *LYS21* and assisted with preliminary purification and activity assays.

Table A.1 Strains used in Appendix A

Strains	
Strain	Genotype
LPY6282	*MAT*α W303*rDNA::ADE2CAN1*
LPY11411	*MAT*a W303 *lys20*Δ*::kanMX lys21::clonNAT rDNA::ADE2CAN1*
LPY11654	*MAT*a W303 *htz1*Δ*::kanMX*
LPY12827	*MATa* W303 *nap1*Δ*::kanMX rDNA::ADE2 CAN1*

Table A.2 Plasmids used in Appendix A

Plasmids	
Plasmid	Gene
pLP820	pRSETc
pLP831	*ESA1* in pRSETc
pLP1900	pLit28
pLP1921	*LYS20* in pLit28
pLP1934	*LYS20* in pLP820
pLP1935	*LYS21* in pLP820

Table A.3 Oligos used in Appendix A

Oligos	
Oligo	Sequence
oLP625	CGGGATCCGATATCCTACTATTTGGTGACCTTTGC
oLP678	CGGGAATCGATATCTTATTAGGCGGATGGC
oLP712	AACTGCAGGGATCCCGATGTCTGAAAATAACGAATTCC
oLP715	GCGAATTCTTATTAGGCGGATGGCTTAGTCCG

Appendix B Analysis of histone H4 point mutants in combination with *esa1*

Introduction

In expanding the list of genes that interact with *ESA1* (an analysis begun in Chapter 3), one obvious place to look is at the histones themselves. Many of the histone lysine residues that are targets of acetylation have phenotypes when mutated. Phenotypes of these mutants are similar to the set of phenotypes shared by Esa1 (Bird et al. 2002; Xu et al. 2005; Matsubara et al. 2007; Nakanishi et al. 2008) For example, silencing defects, sensitivity to genotoxins and slow growth are all common phenotypes among histone point mutants.

In order to test whether any of the histone residues that were specific targets of Esa1 had additional genetic interactions with *ESA1*, a series of double mutants was created in collaboration with a fellow graduate student, Christie Chang. This analysis was partially modeled on work in which the lysines on the H4 tail that were targets of Esa1 (K5,8,12 and 16) were mutated as a block to glutamine (Bird et al. 2002). When mutated en masse, the cells became sensitive to CPT and MMS, two drugs that damage DNA by different mechanisms. Based on these results, we then mutated each residue singly to determine its individual contribution and then combined each mutant with an *esa1* mutant. A previous study (Bird et al. 2002) mutated all of the lysines in

question to alanines, a mutation that is assumed to be neutral for the protein. To further analyze individual contributions of lysine residues, we made alanine mutations, and also mutated the lysines to glutamine (proposed to mimic a constituitively acetylated lysine residue, and to arginine, whose positive charge is proposed to mimic a constituitively unacetylated residue) (Megee et al. 1990).

Results

This analysis seeks to determine the phenotypes of H4K8, H4K12 and H4K16 mutants alone and in combination with *esa1*. Phenotyping was carried out on a variety of media. Temperature sensitivity as well as overall growth was scored on YPD and SC media (Fig B.1). Alone, H4K8, H4K12 and H4K16 mutants do not confer temperature sensitivity, but in combination with *esa1,* increased temperature sensitivity is observed. It was found that, in general, histone point mutants in combination with *esa1* mutants were more sensitive to increased temperature and grew more slowly than either single mutant.

Sensitivity to camptothecin (CPT) was assayed (Fig B.2). Camptothecin is a drug that causes DNA double strand breaks, as described in Chapter 2. Mutation of HK8 and H4K12 to both alanine and glutamine results in sensitivity to CPT. This same H4K8,12R mutation also exacerbates the *esa1* CPT sensitivity. An unexpected

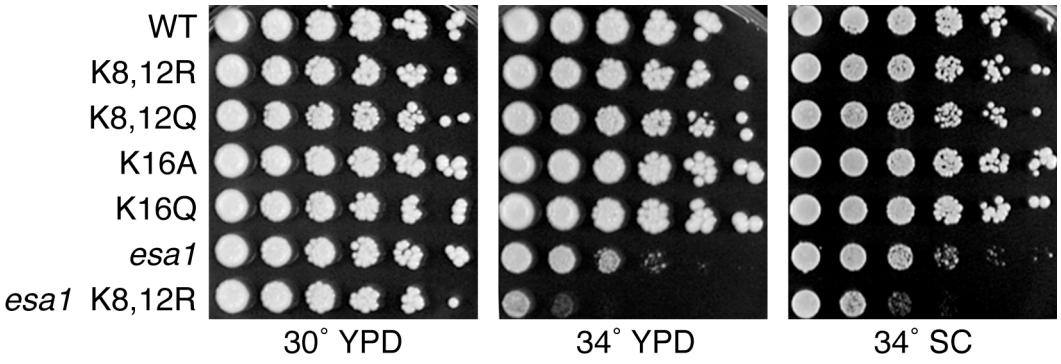

Figure B.1 Mutations of H4 K8, 12 in combination with *esa1* result in increased temperature sensitivity. Lysines 8 and 12 on Histone H4 were mutated to arginine (R), glutamine (Q), or alanine (A). Five- fold dilutions were plated on indicated media, where SC is synthetic complete.

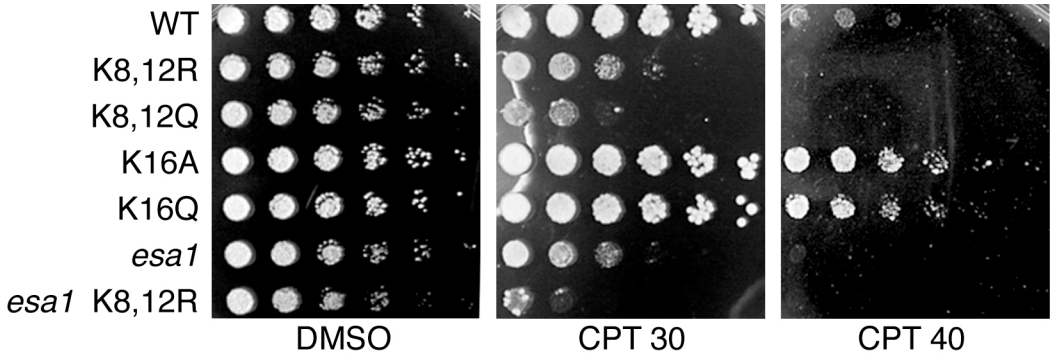

Figure B.2 Mutations in H4 K8, 12 result in increased camptothecin (CPT) sensitivity, especially in combination with *esa1;* H4K16 mutation results in resistance to CPT. Control plate contains DMSO, drug plates contain 30 µg/mL of CPT or 40 µg/mL as indicated. Plates incubated at 33˚C.

result came to light when the H4 K16 point mutants were plated on CPT: not only were they insensitive to the drug compared to the wild type, but it seemed that they were actually resistant. This was especially true for the H4 K16A and H4 K16Q mutants (Fig B.2).

Individually, H4K12A, H4K12R and H4K12Q mutants caused sensitivity, although not as much as they did in combination with H4K8 mutations (Fig B.3). The same trend was observed when the mutants were plated on hydroxyurea (HU) (Fig B.4). As this compound also induces DNA double strand breaks, although by a different mechanism, these data confirm that the results are observed with more than one type of DNA double strand damage.

With the knowledge that *esa1* mutants have rDNA silencing defects (Clarke et al. 2006), as do H4 mutants (Bird et al. 2002; Xu et al. 2005), rDNA silencing assays were performed to ascertain the contribution of each H4 residue to rDNA silencing. H4K12A and H4K12R mutants seemed to cause defects in the rDNA silencing (Fig. B.5). H4K12Q mutants, however, did not. H4K8,12 double mutants behaved more like H4K8 single mutants. In combination with *esa1,* mutation of both H4K8 and H4K12 increased the rDNA silencing defect only marginally (Fig B.6).

Finally, mutations in H4K16 were combined with *esa1*. This resulted in a marginal worsening of the rDNA silencing defect, only in the H4K16A mutant, not in the H4K16Q (Fig B.7). Finally the H4K5,8,12Q triple mutant was generated. In combination with *esa1,* this led to a profound defect in the rDNA silencing (Fig B.7).

An overall trend observed was that K to Q mutants were the healthiest mutants

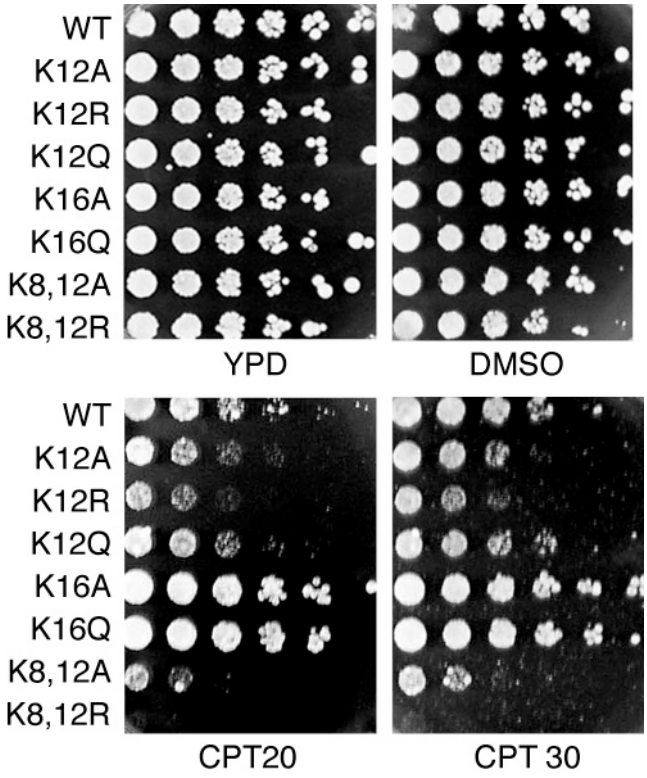

Figure B.3 Mutations in H4 K8, 12 result in increased camptothecin (CPT) sensitivity but H4K16 mutation results in resistance to CPT. Plates incubated at 30˚.

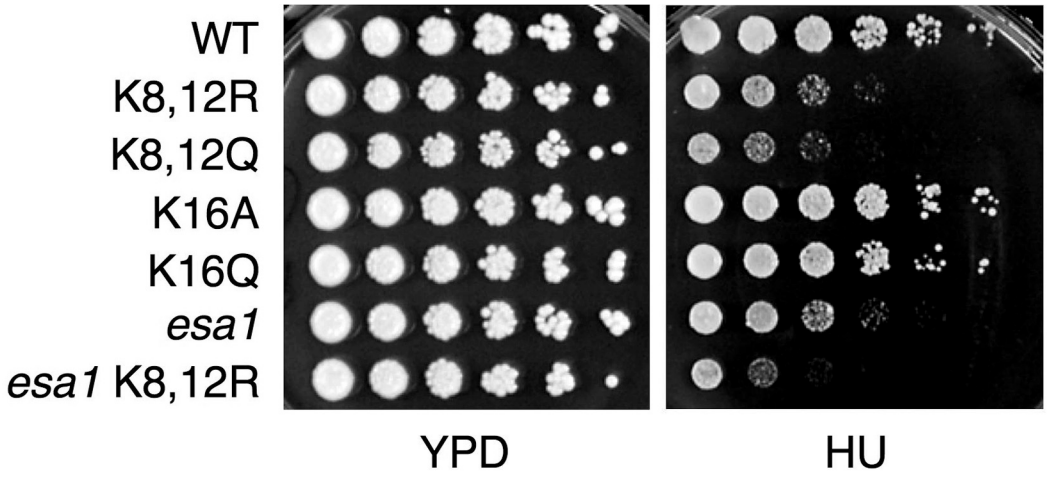

Figure B.4 Mutations in H4 K8, 12 result in increased hydroxyurea (HU) sensitivity, especially in combination with *esa1*. Growth control plate is YPD, drug plate contains 100mM of HU. Plates were incubated at 30˚.

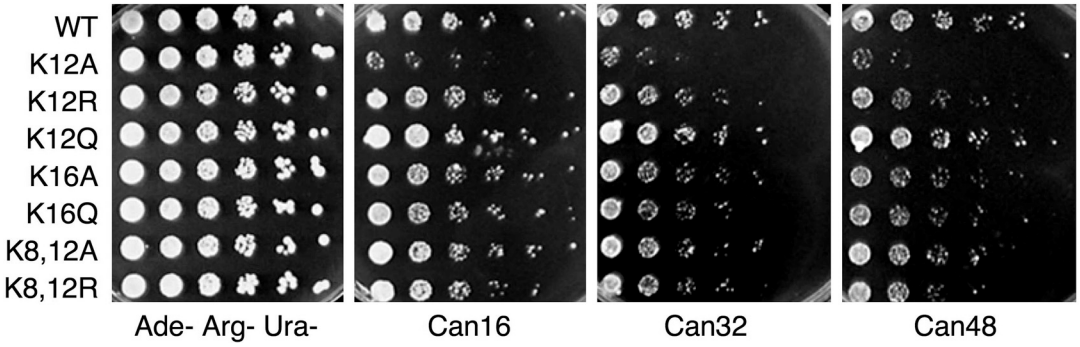

Figure B.5 Mutations in H4K12 alter rDNA silencing. Mutations were plated on various concentrations of canavanine to test the rDNA silencing of each strain. Growth control plate lacked adenine, arginine and uracil. Drug plates also lacked adenine, arginine and uracil but contained indicated concentrations of canavanine. Plates were incubated at 30˚C.

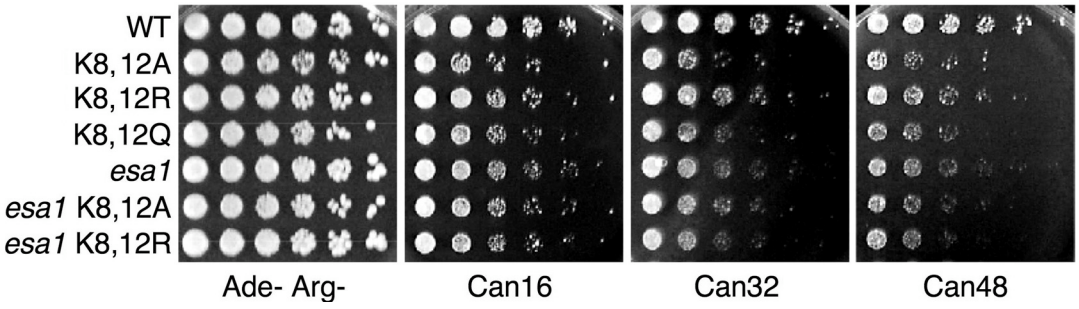

Figure B.6 Mutations in both H4K8 and H4K12 mildly alter rDNA silencing.

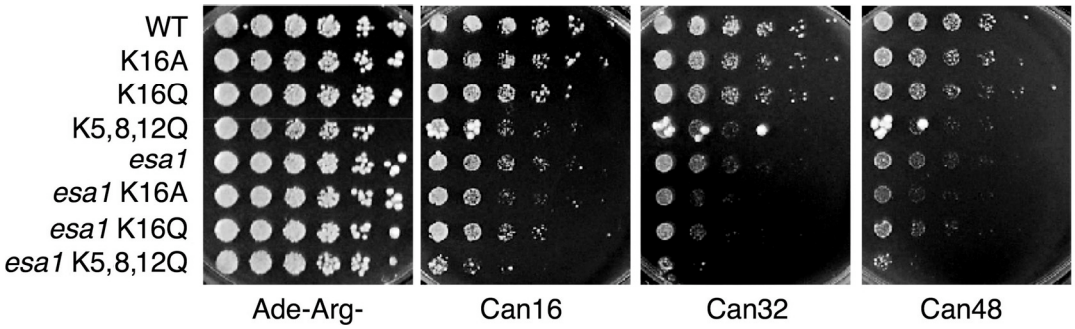

Figure B.7 rDNA silencing in H4 K16 and H4 K5,8,12 mutants is mildly altered, and more strongly affected in combination with *esa1*.

for any given residue, then K to A mutants, and finally K to R mutants. For K to R point mutants, there seemed to be a general decrease in cellular fitness, visible as weak growth under most conditions. Multiple mutants with H4 K16 were not made because it was previously shown (Bird et al. 2002) that H4K16 mutants on their own had only minimal contributions to DNA damage. This array of point mutants will be useful in evaluation of epistasis between the sensitive and resistant site.

Discussion

Any further mutant histone analysis should include such challenges as increased temperature, DNA damaging agents such as UV, HU and CPT, as well as silencing assays. Into the results of this analysis, it may be possible to incorporate the observation that H4K16A and H4K16Q mutants are resistant to CPT, especially if any of the new mutants also show this phenotype. If DNA damage phenotypes are discovered, it would be interesting to analyze them in combination with the H2A-S129A point mutants, a residue that is critical for response to DNA damage (Downs et al. 2000). Also, these mutans could be combine with the DNA damage resistant *lys20*Δ *lys21*Δ.

Materials and Methods

Strains and plasmids

All strains are derivatives of LPY8231. LPY11816 and LPY11817 contain pLP2212 (pJH33). In all other strains, this wild type plasmid has been shuffled out and replaced with indicated plasmid. Histone plasmids were made by site directed

mutagenesis of pLP1775 containing wild type H3 and H4. The plasmid pLP2208 was made by site directed mutagenesis of pLP2139 with oLP942 and 943. Other mutants made in this chapter were made by mutagenesis of pLP1775. oLP864 and 865 were used to generate pLP2125. oLP866 and 867 were used to generate pLP2126. oLP890 and 891 were used to generate pLP2139. oLP888 and 889 were used to generate pLP2142. oLP900 and 901 were used to generate pLP2146.

Acknowledgements

All experiments were performed in collaboration with Christie Chang. Additional experiments are published in Christie Chang's thesis (Chang, 2010). Myriam Ruault made the pLP1971, pLP1972 and pLP1990 constructs. Mitch Smith provided pLP2212.

Table B.1 Strains used in Appendix B

Strains	
Strain	Genotype
LPY11816	*MATα* W303 *hht1-hhf1Δ::kanMX hht2-hhf2Δ::kanMX hta2-htb2Δ::HPH rDNA::ADE2CAN1*
LPY11817	*MATα W303 esa1-414 hht1-hhf1Δ::kanMX hht2-hhf2Δ::kanMX hta2-htb2Δ::HPH rDNA::ADE2CAN1*
LPY11850	LPY11817 + pLP2125
LPY11851	LPY11817 + pLP2126
LPY11993	LPY11816 + pLP2139
LPY12026	LPY11817 + pLP2142
LPY12071	LPY11817 + pLP2146
LPY12383	LPY11816 + pLP1775
LPY12384	LPY11817 + pLP1775
LPY12394	LPY11816 + pLP2146
LPY12395	LPY11816 + pLP2142
LPY12396	LPy11816 + pLP2125
LPY12397	LPY11816 + pLP2139
LPY12398	LPY11816 + pLP2126
LPY12399	LPY11816 + pLP1990
LPY12400	LPY11816 + pLP1972
LPY12409	LPY11816 + pLP1971
LPY12410	LPY11817 + pLP1971
LPY12411	LPy11817 + pLP1990
LPY12412	LPY11817 + pLP1972
LPY12413	LPY11816 + pLP2208
LPY12414	LPY11817 + pLP2208

Table B.2 Plasmids used in Appendix B

Plasmids		
Plasmid	Gene	Source
pLP1775	H3-H4 in pRS314	
pLP1971	H3-H4K5,8,12Q	M. Ruault
pLP1972	H3-H4K16Q	M. Ruault
pLP1990	H3-H4K16A	M. Ruault
pLP2125	H3-H4K12Q	
pLP2126	H3-H4K8,12Q	
pLP2139	H3-H4K8,12R	
pLP2142	H3-H4K12R	
pLP2146	H3-H4K12A	
pLP2208	H3-H4K8,12A	
pLP2212	H2A-H2B, H3-H4	M. Smith

Table B.3 Oligos used in Appendix B

Oligos	
Oligo	Sequence
oLP864	AAGGTCTAGGA**C**AAGGTGGTGCCAAGC
oLP865	GCTTGGCACCACCTT**G**TCCTAGACCTT
oLP866	GTAAAGGTGGT**C**AAGGTCTAGGA**C**AAGGTGGTGCC
oLP867	GGCACCACCTT**G**TCCTAGACCTT**G**ACCACCTTTAC
oLP888	AAGGTCTAGGACGA**GG**TGGTGCCAAGC
oLP889	GCTTGGCACCA**CC**TCGTCCTAGACCTT
oLP890	GTAAAGGTGGT**CG**AGGTCTAGGA**CG**AGGTGGTGCC
oLP891	GGCACCACCT**CG**TCCTAGACCT**CG**ACCACCTTTAC
oLP900	AAGGTCTAGGA**GC**AGGTGGTGCCAAGC
oLP901	GTCTGGCACCACCT**GC**TCCTAGACCTT
oLP942	TCCGGTAGAGGTAAAGGTGGT**GC**AGGTCTAGGA**GC**AGGT GGTGCC
oLP943	GGCACCACCT**GC**TCCTAGACCT**GC**ACCACCTTTACCTCTA CCGGA

Nucleotides in bold are mutagenic relative to wild type sequence.

References

Allard S, Utley RT, Savard J, Clarke A, Grant P, Brandl CJ, Pillus L, Workman JL, Côté J. 1999. NuA4, an essential transcription adaptor/histone H4 acetyltransferase complex containing Esa1p and the ATM-related cofactor Tra1p. *EMBO J* **18**: 5108-5119.

Allen RM, Chatterjee R, Madden MS, Ludden PW, Shah VK. 1994. Biosynthesis of the iron-molybdenum cofactor of nitrogenase. *Crit Rev Biotechnol* **14**: 225-249.

Andi B, West AH, Cook PF. 2004. Stabilization and characterization of histidine-tagged homocitrate synthase from *Saccharomyces cerevisiae. Arch Biochem Biophys* **421**: 243-254.

Andi B, West AH, Cook PF. 2005. Regulatory mechanism of histidine-tagged homocitrate synthase from *Saccharomyces cerevisiae.* I. Kinetic studies. *J Biol Chem* **280**: 31624-31632.

Asahara H, Tartare-Deckert S, Nakagawa T, Ikehara T, Hirose F, Hunter T, Ito T, Montminy M. 2002. Dual roles of p300 in chromatin assembly and transcriptional activation in cooperation with nucleosome assembly protein 1 in vitro. *Mol Cell Biol* **22**: 2974-2983.

Auger A, Galarneau L, Altaf M, Nourani A, Doyon Y, Utley RT, Cronier D, Allard S, Cote J. 2008. Eaf1 is the platform for NuA4 molecular assembly that evolutionarily links chromatin acetylation to ATP-dependent exchange of histone H2A variants. *Mol Cell Biol* **28**: 2257-2270.

Babiarz JE, Halley JE, Rine J. 2006. Telomeric heterochromatin boundaries require NuA4-dependent acetylation of histone variant H2A.Z in *Saccharomyces cerevisiae. Genes Dev* **20**: 700-710.

Berger SL. 2002. Histone modifications in transcriptional regulation. *Curr Opin Genet Dev* **12**: 142-148.

Berndsen CE, Albaugh BN, Tan S, Denu JM. 2007. Catalytic mechanism of a MYST family histone acetyltransferase. *Biochemistry* **46**: 623-629.

Bhattacharjee JK. 1985. alpha-Aminoadipate pathway for the biosynthesis of lysine in lower eukaryotes. *Crit Rev Microbiol* **12**: 131-151.

Bird AW, Yu DY, Pray-Grant MG, Qiu Q, Harmon KE, Megee PC, Grant PA, Smith MM, Christman MF. 2002. Acetylation of histone H4 by Esa1 is required for DNA double-strand break repair. *Nature* **419**: 411-415.

Bordoli L, Husser S, Luthi U, Netsch M, Osmani H, Eckner R. 2001. Functional analysis of the p300 acetyltransferase domain: the PHD finger of p300 but not of CBP is dispensable for enzymatic activity. *Nucleic Acids Res* **29**: 4462-4471.

Boudreault AA, Cronier D, Selleck W, Lacoste N, Utley RT, Allard S, Savard J, Lane WS, Tan S, Côté J. 2003. Yeast enhancer of polycomb defines global Esa1-dependent acetylation of chromatin. *Genes Dev* **17**: 1415-1428.

Boulikas T. 1990. Poly(ADP-ribosylated) histones in chromatin replication. *J Biol Chem* **265**: 14638-14647.

Brownell JE, Allis CD. 1995. An activity gel assay detects a single, catalytically active histone acetyltransferase subunit in Tetrahymena macronuclei. *Proc Natl Acad Sci U S A* **92**: 6364-6368.

Bryk M, Banerjee M, Murphy M, Knudsen KE, Garfinkel DJ, Curcio MJ. 1997. Transcriptional silencing of Ty1 elements in the *RDN1* locus of yeast. *Genes Dev* **11**: 255-269.

Bulfer SL, Scott EM, Couture JF, Pillus L, Trievel RC. 2009. Crystal structure and functional analysis of homocitrate synthase, an essential enzyme in lysine biosynthesis. *J Biol Chem* **284**: 35769-35780.

Bulfer SL, Scott EM, Pillus L, Trievel RC. 2010. Structural basis for L-lysine feedback inhibition of homocitrate synthase. *J Biol Chem* **285**:10446-53.

Carrozza MJ, Utley RT, Workman JL, Cote J. 2003. The diverse functions of histone acetyltransferase complexes. *Trends Genet* **19**: 321-329.

Celic I, Masumoto H, Griffith WP, Meluh P, Cotter RJ, Boeke JD, Verreault A. 2006. The sirtuins Hst3 and Hst4p preserve genome integrity by controlling histone H3 lysine 56 deacetylation. *Curr Biol* **16**: 1280-1289.

Celic I, Verreault A, Boeke JD. 2008. Histone H3 K56 hyperacetylation perturbs replisomes and causes DNA damage. *Genetics* **179**: 1769-1784.

Chang CS, Pillus L. 2009. Collaboration between the essential Esa1 acetyltransferase and the Rpd3 deacetylase is mediated by H4K12 histone acetylation in *Saccharomyces cerevisiae. Genetics* **183**: 149-160.

Chen S, Brockenbrough JS, Dove JE, Aris JP. 1997. Homocitrate synthase is located in the nucleus in the yeast *Saccharomyces cerevisiae. J Biol Chem* **272**: 10839-10846.

Choy JS, Kron SJ. 2002. NuA4 subunit Yng2 function in intra-S-phase DNA damage response. *Mol Cell Biol* **22**: 8215-8225.

Clarke A. 2001. Genetic and biochemical charactrization of *ESA1:* an essential histone acetyltransferase involved in cell cycle progression and transcriptional silencing. in *Biology*. University of Colorado at Boulder, Boulder.

Clarke AS, Lowell JE, Jacobson SJ, Pillus L. 1999. Esa1p is an essential histone acetyltransferase required for cell cycle progression. *Mol Cell Biol* **19**: 2515-2526.

Clarke AS, Samal E, Pillus L. 2006. Distinct roles for the essential MYST family HAT Esa1p in transcriptional silencing. *Mol Biol Cell* **17**: 1744-1757.

Collins SR, Miller KM, Maas NL, Roguev A, Fillingham J, Chu CS, Schuldiner M, Gebbia M, Recht J, Shales M et al. 2007. Functional dissection of protein complexes involved in yeast chromosome biology using a genetic interaction map. *Nature* **446**: 806-810.

Conconi A. 2005. The yeast rDNA locus: a model system to study DNA repair in chromatin. *DNA Repair (Amst)* **4**: 897-908.

Decker PV, Yu DY, Iizuka M, Qiu Q, Smith MM. 2008. Catalytic-site mutations in the MYST family histone Acetyltransferase Esa1. *Genetics* **178**: 1209-1220.

Dehe PM, Geli V. 2006. The multiple faces of Set1. *Biochem Cell Biol* **84**: 536-548.

Del Rosario BC, Pemberton LF. 2008. Nap1 links transcription elongation, chromatin assembly, and messenger RNP complex biogenesis. *Mol Cell Biol* **28**: 2113-2124.

Downs JA, Allard S, Jobin-Robitaille O, Javaheri A, Auger A, Bouchard N, Kron SJ, Jackson SP, Cote J. 2004. Binding of chromatin-modifying activities to phosphorylated histone H2A at DNA damage sites. *Mol Cell* **16**: 979-990.

Downs JA, Lowndes NF, Jackson SP. 2000. A role for *Saccharomyces cerevisiae* histone H2A in DNA repair. *Nature* **408**: 1001-1004.

Doyon Y, Côté J. 2004. The highly conserved and multifunctional NuA4 HAT complex. *Curr Opin Genet Dev* **14**: 147-154.

Driscoll R, Hudson A, Jackson SP. 2007. Yeast Rtt109 promotes genome stability by acetylating histone H3 on lysine 56. *Science* **315**: 649-652.

Dryhurst D, Thambirajah AA, Ausio J. 2004. New twists on H2A.Z: a histone variant with a controversial structural and functional past. *Biochem Cell Biol* **82**: 490-497.

Duncan EM, Muratore-Schroeder TL, Cook RG, Garcia BA, Shabanowitz J, Hunt DF, Allis CD. 2008. Cathepsin L proteolytically processes histone H3 during mouse embryonic stem cell differentiation. *Cell* **135**: 284-294.

Durant M, Pugh BF. 2006. Genome-wide relationships between TAF1 and histone acetyltransferases in *Saccharomyces cerevisiae. Mol Cell Biol* **26**: 2791-2802.

Elion EA. 1993. Constructing Recombinant DNA Molecules by the Polymerase Chain Reaction. in *Current Protocols in Molecular Biology* (eds. AF M, B Roger, KR E, MD D, SJ G., JA Smith, S Kevin). Wiley Interscience.

Feller A, Ramos F, Pierard A, Dubois E. 1999. In *Saccharomyces cerevisae,* feedback inhibition of homocitrate synthase isoenzymes by lysine modulates the activation of *LYS* gene expression by Lys14p. *Eur J Biochem* **261**: 163-170.

Foiani M, Marini F, Gamba D, Lucchini G, Plevani P. 1994. The B subunit of the DNA polymerase alpha-primase complex in *Saccharomyces cerevisiae* executes an essential function at the initial stage of DNA replication. *Mol Cell Biol* **14**: 923-933.

Friis RM, Wu BP, Reinke SN, Hockman DJ, Sykes BD, Schultz MC. 2009. A glycolytic burst drives glucose induction of global histone acetylation by picNuA4 and SAGA. *Nucleic Acids Res.* **12**:3969-80.

Gadal O, Strauss D, Kessl J, Trumpower B, Tollervey D, Hurt E. 2001. Nuclear export of 60s ribosomal subunits depends on Xpo1p and requires a nuclear export sequence-containing factor, Nmd3p, that associates with the large subunit protein Rpl10p. *Mol Cell Biol* **21**: 3405-3415.

Gamonet F, Lauquin GJ. 1998. The *Saccharomyces cerevisiae LYS7* gene is involved in oxidative stress protection. *European journal of biochemistry / FEBS* **251**: 716-723.

Georgakopoulos T, Thireos G. 1992. Two distinct yeast transcriptional activators require the function of the Gcn5 protein to promote normal levels of transcription. *EMBO J* **11**: 4145-4152.

Gray GS, Bhattacharjee JK. 1976a. Biosynthesis of lysine in *Saccharomyces cerevisiae*: regulation of homocitrate synthase in analogue-resistant mutants. *J Gen Microbiol* **97**: 117-120.

Gray GS, Bhattacharjee JK. 1976b. Biosynthesis of lysine in *Saccharomyces cervisiae*: properties and spectrophotometric determination of homocitrate synthase activity. *Can J Microbiol* **22**: 1664-1667.

Gunjan A, Verreault A. 2003. A Rad53 kinase-dependent surveillance mechanism that regulates histone protein levels in *S. cerevisiae. Cell* **115**: 537-549.

Haile DJ, Rouault TA, Harford JB, Kennedy MC, Blondin GA, Beinert H, Klausner RD. 1992. Cellular regulation of the iron-responsive element binding protein: disassembly of the cubane iron-sulfur cluster results in high-affinity RNA binding. *Proc Natl Acad Sci U S A* **89**: 11735-11739.

Hakoyama T, Niimi K, Watanabe H, Tabata R, Matsubara J, Sato S, Nakamura Y, Tabata S, Jichun L, Matsumoto T et al. 2009. Host plant genome overcomes the lack of a bacterial gene for symbiotic nitrogen fixation. *Nature* **462**: 514-517.

Han J, Zhou H, Horazdovsky B, Zhang K, Xu RM, Zhang Z. 2007. Rtt109 acetylates histone H3 lysine 56 and functions in DNA replication. *Science* **315**: 653-655.

Heidinger-Pauli JM, Unal E, Koshland D. 2009. Distinct targets of the Eco1 acetyltransferase modulate cohesion in S phase and in response to DNA damage. *Mol Cell* **34**: 311-321.

Hicks GR, Raikhel NV. 1995. Protein import into the nucleus: an integrated view. *Annu Rev Cell Dev Biol* **11**: 155-188.

Horton P, Nakai K. 1997. Better prediction of protein cellular localization sites with the k nearest neighbors classifier. *Proc Int Conf Intell Syst Mol Biol* **5**: 147-152.

Hsiang YH, Hertzberg R, Hecht S, Liu LF. 1985. Camptothecin induces protein-linked DNA breaks via mammalian DNA topoisomerase I. *J Biol Chem* **260**: 14873-14878.

Huertas P. 2010. DNA resection in eukaryotes: deciding how to fix the break. *Nat Struct Mol Biol* **17**: 11-16.

Huh WK, Falvo JV, Gerke LC, Carroll AS, Howson RW, Weissman JS, O'Shea EK. 2003. Global analysis of protein localization in budding yeast. *Nature* **425**: 686-691.

Humpal SE, Robinson DA, Krebs JE. 2009. Marks to stop the clock: histone modifications and checkpoint regulation in the DNA damage response. *Biochem Cell Biol* **87**: 243-253.

Hyland EM, Cosgrove MS, Molina H, Wang D, Pandey A, Cottee RJ, Boeke JD. 2005. Insights into the role of histone H3 and histone H4 core modifiable residues in *Saccharomyces cerevisiae. Mol Cell Biol* **25**: 10060-10070.

Imai S, Armstrong CM, Kaeberlein M, Guarente L. 2000. Transcriptional silencing and longevity protein Sir2 is an NAD-dependent histone deacetylase. *Nature* **403**: 795-800.

Ito T, Bulger M, Kobayashi R, Kadonaga JT. 1996. Drosophila NAP-1 is a core histone chaperone that functions in ATP-facilitated assembly of regularly spaced nucleosomal arrays. *Mol Cell Biol* **16**: 3112-3124.

Jamieson DJ. 1998. Oxidative stress responses of the yeast *Saccharomyces cerevisiae*. *Yeast* **14**: 1511-1527.

Jeffery CJ. 1999. Moonlighting proteins. *Trends Biochem Sci* **24**: 8-11.

Jeffery CJ. 2003. Moonlighting proteins: old proteins learning new tricks. *Trends Genet* **19**: 415-417.

John S, Howe L, Tafrov ST, Grant PA, Sternglanz R, Workman JL. 2000. The something about silencing protein, Sas3, is the catalytic subunit of NuA3, a yTAF(II)30-containing HAT complex that interacts with the Spt16 subunit of the yeast CP (Cdc68/Pob3)-FACT complex. *Genes Dev* **14**: 1196-1208.

Jones E, Fink G. 1982. Regulation of Amino Acid and Nucleotide Biosynthesis in Yeast. in *The Molecular Biology of the Yeast Saccharomyces cerevisiae: Metabolism and Gene Expression* (eds. J Strathhern, E Jones, J Broach), pp. 181-299. Cold Spring Harbor Laboratory.

Kalocsay M, Hiller NJ, Jentsch S. 2009. Chromosome-wide Rad51 spreading and SUMO-H2A.Z-dependent chromosome fixation in response to a persistent DNA double-strand break. *Mol Cell* **33**: 335-343.

Kellogg DR, Kikuchi A, Fujii-Nakata T, Turck CW, Murray AW. 1995. Members of the NAP/SET family of proteins interact specifically with B-type cyclins. *J Cell Biol* **130**: 661-673.

Kellogg DR, Murray AW. 1995. *NAP1* acts with Clb1 to perform mitotic functions and to suppress polar bud growth in budding yeast. *J Cell Biol* **130**: 675-685.

Keogh MC, Mennella TA, Sawa C, Berthelet S, Krogan NJ, Wolek A, Podolny V, Carpenter LR, Greenblatt JF, Baetz K et al. 2006. The *Saccharomyces cerevisiae* histone H2A variant Htz1 is acetylated by NuA4. *Genes Dev* **20**: 660-665.

Kitanovic A, Wolfl S. 2006. Fructose-1,6-bisphosphatase mediates cellular responses to DNA damage and aging in *Saccharomyces cerevisiae. Mutat Res* **594**: 135-147.

Kobor MS, Venkatasubrahmanyam S, Meneghini MD, Gin JW, Jennings JL, Link AJ, Madhani HD, Rine J. 2004. A protein complex containing the conserved Swi2/Snf2-related ATPase Swr1p deposits histone variant H2A.Z into euchromatin. *PLoS Biol* **2**: E131.

Koch M, Pillus L. 2009. Silent chromatin formation and regulation in the yeast *Saccharomyces cerevisiae*. in *Handbook of Cell Signaling* (eds. R Bradshaw, E Dennis), pp. 2427-2436. Academic Press, Oxford.

Kosuge T, Hoshino T. 1998. Lysine is synthesized through the alpha-aminoadipate pathway in *Thermus thermophilus*. *FEMS Microbiol Lett* **169**: 361-367.

Krogan NJ, Baetz K, Keogh MC, Datta N, Sawa C, Kwok TC, Thompson NJ, Davey MG, Pootoolal J, Hughes TR et al. 2004. Regulation of chromosome stability by the histone H2A variant Htz1, the Swr1 chromatin remodeling complex, and the histone acetyltransferase NuA4. *Proc Natl Acad Sci U S A* **101**: 13513-13518.

Krogan NJ, Cagney G, Yu H, Zhong G, Guo X, Ignatchenko A, Li J, Pu S, Datta N, Tikuisis AP et al. 2006. Global landscape of protein complexes in the yeast *Saccharomyces cerevisiae. Nature* **440**: 637-643.

Krogan NJ, Keogh MC, Datta N, Sawa C, Ryan OW, Ding H, Haw RA, Pootoolal J, Tong A, Canadien V et al. 2003. A Snf2 family ATPase complex required for recruitment of the histone H2A variant Htz1. *Mol Cell* **12**: 1565-1576.

Kuo MH, Brownell JE, Sobel RE, Ranalli TA, Cook RG, Edmondson DG, Roth SY, Allis CD. 1996. Transcription-linked acetylation by Gcn5p of histones H3 and H4 at specific lysines. *Nature* **383**: 269-272.

Lafon A, Chang CS, Scott EM, Jacobson SJ, Pillus L. 2007. MYST opportunities for growth control: yeast genes illuminate human cancer gene functions. *Oncogene* **26**: 5373-5384.

Latham JA, Dent SY. 2009. The H2BK123Rgument. *J Cell Biol* **186**: 313-315.

Lebel EA, Boukamp P, Tafrov ST. 2010. Irradiation with heavy-ion particles changes the cellular distribution of human histone acetyltransferase HAT1. *Mol Cell Biochem*.**1-2** :271-84.

Lee DY, Huang CM, Nakatsuji T, Thiboutot D, Kang SA, Monestier M, Gallo RL. 2009. Histone H4 is a major component of the antimicrobial action of human sebocytes. *J Invest Dermatol* **129**: 2489-2496.

Lin YY, Lu JY, Zhang J, Walter W, Dang W, Wan J, Tao SC, Qian J, Zhao Y, Boeke JD et al. 2009. Protein acetylation microarray reveals that NuA4 controls key metabolic target regulating gluconeogenesis. *Cell* **136**: 1073-1084.

Lin YY, Qi Y, Lu JY, Pan X, Yuan DS, Zhao Y, Bader JS, Boeke JD. 2008. A comprehensive synthetic genetic interaction network governing yeast histone acetylation and deacetylation. *Genes Dev* **22**: 2062-2074.

Lisby M, Rothstein R. 2009. Choreography of recombination proteins during the DNA damage response. *DNA Repair (Amst)* **8**: 1068-1076.

Lo WS, Henry KW, Schwartz MF, Berger SL. 2004. Histone modification patterns during gene activation. *Methods Enzymol* **377**: 130-153.

Lu PY, Levesque N, Kobor MS. 2009. NuA4 and SWR1-C: two chromatin-modifying complexes with overlapping functions and components. *Biochem Cell Biol* **87**: 799-815.

Lucchini G, Hinnebusch AG, Chen C, Fink GR. 1984. Positive regulatory interactions of the *HIS4* gene of *Saccharomyces cerevisiae*. *Mol Cell Biol* **4**: 1326-1333.

Luger K, Mader AW, Richmond RK, Sargent DF, Richmond TJ. 1997. Crystal structure of the nucleosome core particle at 2.8 A resolution. *Nature* **389**: 251-260.

Luk E, Vu ND, Patteson K, Mizuguchi G, Wu WH, Ranjan A, Backus J, Sen S, Lewis M, Bai Y et al. 2007. Chz1, a nuclear chaperone for histone H2AZ. *Mol Cell* **25**: 357-368.

Makalowska I, Ferlanti ES, Baxevanis AD, Landsman D. 1999. Histone Sequence Database: sequences, structures, post-translational modifications and genetic loci. *Nucleic Acids Res* **27**: 323-324.

Masumoto H, Hawke D, Kobayashi R, Verreault A. 2005. A role for cell-cycle-regulated histone H3 lysine 56 acetylation in the DNA damage response. *Nature* **436**: 294-298.

Matsubara K, Sano N, Umehara T, Horikoshi M. 2007. Global analysis of functional surfaces of core histones with comprehensive point mutants. *Genes Cells* **12**: 13-33.

Meeks-Wagner D, Hartwell LH. 1986. Normal stoichiometry of histone dimer sets is necessary for high fidelity of mitotic chromosome transmission. *Cell* **44**: 43-52.

Megee PC, Morgan BA, Mittman BA, Smith MM. 1990. Genetic analysis of histone H4: essential role of lysines subject to reversible acetylation. *Science* **247**: 841-845.

Meneghini MD, Wu M, Madhani HD. 2003. Conserved histone variant H2A.Z protects euchromatin from the ectopic spread of silent heterochromatin. *Cell* **112**: 725-736.

Mersfelder EL, Parthun MR. 2006. The tale beyond the tail: histone core domain modifications and the regulation of chromatin structure. *Nucleic Acids Res* **34**: 2653-2662.

Meyer-Siegler K, Mauro DJ, Seal G, Wurzer J, deRiel JK, Sirover MA. 1991. A human nuclear uracil DNA glycosylase is the 37-kDa subunit of glyceraldehyde-3-phosphate dehydrogenase. *Proc Natl Acad Sci U S A* **88**: 8460-8464.

Millar CB, Xu F, Zhang K, Grunstein M. 2006. Acetylation of H2AZ Lys 14 is associated with genome-wide gene activity in yeast. *Genes Dev* **20**: 711-722.

Mitchell L, Lambert JP, Gerdes M, Al-Madhoun AS, Skerjanc IS, Figeys D, Baetz K. 2008. Functional dissection of the NuA4 histone acetyltransferase reveals its role as a genetic hub and that Eaf1 is essential for complex integrity. *Mol Cell Biol* **28**: 2244-2256.

Mizuguchi G, Shen X, Landry J, Wu WH, Sen S, Wu C. 2004. ATP-driven exchange of histone H2AZ variant catalyzed by SWR1 chromatin remodeling complex. *Science* **303**: 343-348.

Mizzen CA, Yang XJ, Kokubo T, Brownell JE, Bannister AJ, Owen-Hughes T, Workman J, Wang L, Berger SL, Kouzarides T et al. 1996. The TAF(II)250 subunit of TFIID has histone acetyltransferase activity. *Cell* **87**: 1261-1270.

Moore JD, Yazgan O, Ataian Y, Krebs JE. 2007. Diverse roles for histone H2A modifications in DNA damage response pathways in yeast. *Genetics* **176**: 15-25.

Moroianu J. 1999. Nuclear import and export pathways. *J Cell Biochem* **Suppl 32-33**: 76-83.

Mortimer RK, Johnston JR. 1986. Genealogy of principal strains of the yeast genetic stock center. *Genetics* **113**: 35-43.

Mousson F, Ochsenbein F, Mann C. 2007. The histone chaperone Asf1 at the crossroads of chromatin and DNA checkpoint pathways. *Chromosoma* **116**: 79-93.

Nakanishi S, Sanderson BW, Delventhal KM, Bradford WD, Staehling-Hampton K, Shilatifard A. 2008. A comprehensive library of histone mutants identifies nucleosomal residues required for H3K4 methylation. *Nat Struct Mol Biol* **15**: 881-888.

Nathan D, Ingvarsdottir K, Sterner DE, Bylebyl GR, Dokmanovic M, Dorsey JA, Whelan KA, Krsmanovic M, Lane WS, Meluh PB et al. 2006. Histone sumoylation is a negative regulator in *Saccharomyces cerevisiae* and shows dynamic interplay with positive-acting histone modifications. *Genes Dev* **20**: 966-976.

Neuwald AF, Landsman D. 1997. GCN5-related histone N-acetyltransferases belong to a diverse superfamily that includes the yeast Spt10 protein. *Trends Biochem Sci* **22**: 154-155.

Nishida H, Nishiyama M, Kobashi N, Kosuge T, Hoshino T, Yamane H. 1999. A prokaryotic gene cluster involved in synthesis of lysine through the amino adipate pathway: a key to the evolution of amino acid biosynthesis. *Genome Res* **9**: 1175-1183.

Nitiss J, Wang JC. 1988. DNA topoisomerase-targeting antitumor drugs can be studied in yeast. *Proc Natl Acad Sci U S A* **85**: 7501-7505.

Okada T, Tomita T, Wulandari AP, Kuzuyama T, Nishiyama M. 2010. Mechanism of substrate recognition and insight into feedback inhibition of homocitrate synthase from *Thermus thermophilus*. *J Biol Chem* **285**: 4195-4205.

Osada S, Gomita U, Imagawa M. 2008. Toxicity of nickel compounds mediated by *HTZ1*, histone variant H2A.Z, in *Saccharomyces cerevisiae. Biol Pharm Bull* **31**: 2007-2011.

Osley MA. 2004. H2B ubiquitylation: the end is in sight. *Biochim Biophys Acta* **1677**: 74-78.

Parthun MR. 2007. Hat1: the emerging cellular roles of a type B histone acetyltransferase. *Oncogene* **26**: 5319-5328.

Pinto I, Winston F. 2000. Histone H2A is required for normal centromere function in *Saccharomyces cerevisiae. EMBO J* **19**: 1598-1612.

Pray-Grant MG, Schieltz D, McMahon SJ, Wood JM, Kennedy EL, Cook RG, Workman JL, Yates JR, 3rd, Grant PA. 2002. The novel SLIK histone acetyltransferase complex functions in the yeast retrograde response pathway. *Mol Cell Biol* **22**: 8774-8786.

Putnam CD, Jaehnig EJ, Kolodner RD. 2009. Perspectives on the DNA damage and replication checkpoint responses in *Saccharomyces cerevisiae*. *DNA Repair (Amst)* **8**: 974-982.

Quezada H, Aranda C, DeLuna A, Hernandez H, Calcagno ML, Marin-Hernandez A, Gonzalez A. 2008. Specialization of the paralogue *LYS21* determines lysine biosynthesis under respiratory metabolism in *Saccharomyces cerevisiae. Microbiology* **154**: 1656-1667.

Raisner RM, Madhani HD. 2008. Genomewide screen for negative regulators of sirtuin activity in *Saccharomyces cerevisia*e reveals 40 loci and links to metabolism. *Genetics* **179**: 1933-1944.

Recht J, Tsubota T, Tanny JC, Diaz RL, Berger JM, Zhang X, Garcia BA, Shabanowitz J, Burlingame AL, Hunt DF et al. 2006. Histone chaperone Asf1 is required for histone H3 lysine 56 acetylation, a modification associated with S phase in mitosis and meiosis. *Proc Natl Acad Sci U S A* **103**: 6988-6993.

Reifsnyder C, Lowell J, Clarke A, Pillus L. 1996. Yeast SAS silencing genes and human genes associated with AML and HIV-1 Tat interactions are homologous with acetyltransferases. *Nat Genet* **14**: 42-49.

Robert F, Pokholok DK, Hannett NM, Rinaldi NJ, Chandy M, Rolfe A, Workman JL, Gifford DK, Young RA. 2004. Global position and recruitment of HATs and HDACs in the yeast genome. *Mol Cell* **16**: 199-209.

Rusche LN, Kirchmaier AL, Rine J. 2003. The establishment, inheritance, and function of silenced chromatin in *Saccharomyces cerevisiae. Annu Rev Biochem* **72**: 481-516.

Saban N, Bujak M. 2009. Hydroxyurea and hydroxamic acid derivatives as antitumor drugs. *Cancer Chemother Pharmacol* **64**: 213-221.

Samanta MP, Liang S. 2003. Predicting protein functions from redundancies in large-scale protein interaction networks. *Proc Natl Acad Sci U S A* **100**: 12579-12583.

Sanchez Y, Desany BA, Jones WJ, Liu Q, Wang B, Elledge SJ. 1996. Regulation of RAD53 by the ATM-like kinases MEC1 and TEL1 in yeast cell cycle checkpoint pathways. *Science (New York, NY* **271**: 357-360.

Sapountzi V, Logan IR, Robson CN. 2006. Cellular functions of TIP60. *Int J Biochem Cell Biol* **38**: 1496-1509.

Segurado M, Tercero JA. 2009. The S-phase checkpoint: targeting the replication fork. *Biol Cell* **101**: 617-627.

Selth L, Svejstrup JQ. 2007. Vps75, a new yeast member of the NAP histone chaperone family. *The Journal of biological chemistry* **282**: 12358-12362.

Shahbazian MD, Grunstein M. 2007. Functions of site-specific histone acetylation and deacetylation. *Annu Rev Biochem* **76**: 75-100.

Shia WJ, Li B, Workman JL. 2006. SAS-mediated acetylation of histone H4 Lys 16 is required for H2A.Z incorporation at subtelomeric regions in *Saccharomyces cerevisiae. Genes Dev* **20**: 2507-2512.

Sikorski RS, Hieter P. 1989. A system of shuttle vectors and yeast host strains designed for efficient manipulation of DNA in *Saccharomyces cerevisiae. Genetics* **122**: 19-27.

Sinha AK, Kurtz M, Bhattacharjee JK. 1971. Effect of hydroxylysine on the biosynthesis of lysine in *saccharomyces*. *J Bacteriol* **108**: 715-719.

Slekar KH, Kosman DJ, Culotta VC. 1996. The yeast copper/zinc superoxide dismutase and the pentose phosphate pathway play overlapping roles in oxidative stress protection. *J Biol Chem* **271**: 28831-28836.

Smith ER, Eisen A, Gu W, Sattah M, Pannuti A, Zhou J, Cook RG, Lucchesi JC, Allis CD. 1998. *ESA1* is a histone acetyltransferase that is essential for growth in yeast. *Proc Natl Acad Sci U S A* **95**: 3561-3565.

Smith JS, Caputo E, Boeke JD. 1999. A genetic screen for ribosomal DNA silencing defects identifies multiple DNA replication and chromatin-modulating factors. *Mol Cell Biol* **19**: 3184-3197.

Song OK, Wang X, Waterborg JH, Sternglanz R. 2003. An N-alpha-acetyltransferase responsible for acetylation of the N-terminal residues of histones H4 and H2A. *J Biol Chem* **278**: 38109-38112.

Squatrito M, Gorrini C, Amati B. 2006. Tip60 in DNA damage response and growth control: many tricks in one HAT. *Trends Cell Biol* **16**: 433-442.

Starai VJ, Celic I, Cole RN, Boeke JD, Escalante-Semerena JC. 2002. Sir2-dependent activation of acetyl-CoA synthetase by deacetylation of active lysine. *Science* **298**: 2390-2392.

Sterner DE, Belotserkovskaya R, Berger SL. 2002. SALSA, a variant of yeast SAGA, contains truncated Spt7, which correlates with activated transcription. *Proc Natl Acad Sci U S A* **99**: 11622-11627.

Sterner DE, Berger SL. 2000. Acetylation of histones and transcription-related factors. *Microbiol Mol Biol Rev* **64**: 435-459.

Straube K, Blackwell JS, Jr., Pemberton LF. 2010. Nap1 and Chz1 have separate Htz1 nuclear import and assembly functions. *Traffic* **11**: 185-197.

Struhl K. 1998. Histone acetylation and transcriptional regulatory mechanisms. *Genes Dev* **12**: 599-606.

Suka N, Luo K, Grunstein M. 2002. Sir2p and Sas2p opposingly regulate acetylation of yeast histone H4 lysine16 and spreading of heterochromatin. *Nat Genet* **32**: 378-383.

Suka N, Suka Y, Carmen AA, Wu J, Grunstein M. 2001. Highly specific antibodies determine histone acetylation site usage in yeast heterochromatin and euchromatin. *Mol Cell* **8**: 473-479.

Sun Z, Fay DS, Marini F, Foiani M, Stern DF. 1996. Spk1/Rad53 is regulated by Mec1-dependent protein phosphorylation in DNA replication and damage checkpoint pathways. *Genes Dev* **10**: 395-406.

Sun ZW, Hampsey M. 1999. A general requirement for the Sin3-Rpd3 histone deacetylase complex in regulating silencing in *Saccharomyces cerevisiae. Genetics* **152**: 921-932.

Suto RK, Clarkson MJ, Tremethick DJ, Luger K. 2000. Crystal structure of a nucleosome core particle containing the variant histone H2A.Z. *Nat Struct Biol* **7**: 1121-1124.

Takahashi H, McCaffery JM, Irizarry RA, Boeke JD. 2006. Nucleocytosolic acetyl-coenzyme a synthetase is required for histone acetylation and global transcription. *Mol Cell* **23**: 207-217.

Talbert PB, Henikoff S. 2010. Histone variants--ancient wrap artists of the epigenome. *Nat Rev Mol Cell Biol* **11**: 264-275.

Tamburini BA, Tyler JK. 2005. Localized histone acetylation and deacetylation triggered by the homologous recombination pathway of double-strand DNA repair. *Mol Cell Biol* **25**: 4903-4913.

Tenney K, Shilatifard A. 2005. A COMPASS in the voyage of defining the role of trithorax/MLL-containing complexes: linking leukemogensis to covalent modifications of chromatin. *J Cell Biochem* **95**: 429-436.

Terry LJ, Shows EB, Wente SR. 2007. Crossing the nuclear envelope: hierarchical regulation of nucleocytoplasmic transport. *Science* **318**: 1412-1416.

Thambirajah AA, Li A, Ishibashi T, Ausio J. 2009. New developments in post-translational modifications and functions of histone H2A variants. *Biochem Cell Biol* **87**: 7-17.

Thomas BJ, Rothstein R. 1989. Elevated recombination rates in transcriptionally active DNA. *Cell* **56**: 619-630.

Toleman C, Paterson AJ, Whisenhunt TR, Kudlow JE. 2004. Characterization of the histone acetyltransferase (HAT) domain of a bifunctional protein with activable O-GlcNAcase and HAT activities. *The Journal of biological chemistry* **279**: 53665-53673.

Tucci AF, Ceci LN. 1972. Homocitrate synthase from yeast. *Arch Biochem Biophys* **153**: 742-750.

Vaquero A, Scher MB, Lee DH, Sutton A, Cheng HL, Alt FW, Serrano L, Sternglanz R, Reinberg D. 2006. SirT2 is a histone deacetylase with preference for histone H4 Lys 16 during mitosis. *Genes Dev* **20**: 1256-1261.

Venkatasubrahmanyam S, Hwang WW, Meneghini MD, Tong AH, Madhani HD. 2007. Genome-wide, as opposed to local, antisilencing is mediated redundantly by the euchromatic factors Set1 and H2A.Z. *Proc Natl Acad Sci U S A* **104**: 16609-16614.

von Holt C, Brandt WF, Greyling HJ, Lindsey GG, Retief JD, Rodrigues JD, Schwager S, Sewell BT. 1989. Isolation and characterization of histones. *Methods Enzymol* **170**: 431-523.

Wellen KE, Hatzivassiliou G, Sachdeva UM, Bui TV, Cross JR, Thompson CB. 2009. ATP-citrate lyase links cellular metabolism to histone acetylation. *Science* **324**: 1076-1080.

Willis N, Rhind N. 2009. Regulation of DNA replication by the S-phase DNA damage checkpoint. *Cell Div* **4**: 13.

Wu PY, Winston F. 2002. Analysis of Spt7 function in the *Saccharomyces cerevisiae* SAGA coactivator complex. *Mol Cell Biol* **22**: 5367-5379.

Xu EY, Bi X, Holland MJ, Gottschling DE, Broach JR. 2005. Mutations in the nucleosome core enhance transcriptional silencing. *Mol Cell Biol* **25**: 1846-1859.

Xu F, Zhang K, Grunstein M. 2005. Acetylation in histone H3 globular domain regulates gene expression in yeast. *Cell* **121**: 375-385.

Xu H, Andi B, Qian J, West AH, Cook PF. 2006. The alpha-aminoadipate pathway for lysine biosynthesis in fungi. *Cell Biochem Biophys* **46**: 43-64.

Xu J, Zhang X, Pelayo R, Monestier M, Ammollo CT, Semeraro F, Taylor FB, Esmon NL, Lupu F, Esmon CT. 2009. Extracellular histones are major mediators of death in sepsis. *Nat Med* **15**: 1318-1321.

Yan Y, Barlev NA, Haley RH, Berger SL, Marmorstein R. 2000. Crystal structure of yeast Esa1 suggests a unified mechanism for catalysis and substrate binding by histone acetyltransferases. *Mol Cell* **6**: 1195-1205.

Yan Y, Harper S, Speicher DW, Marmorstein R. 2002. The catalytic mechanism of the Esa1 histone acetyltransferase involves a self-acetylated intermediate. *Nat Struct Biol* **9**: 862-869.

Yogev O, Singer E, Shaulian E, Goldberg M, Fox TD, Pines O. 2010. Fumarase: a mitochondrial metabolic enzyme and a cytosolic/nuclear component of the DNA damage response. *PLoS Biol* **8**: e1000328.

Zabriskie TM, Jackson MD. 2000. Lysine biosynthesis and metabolism in fungi. *Nat Prod Rep* **17**: 85-97.

Zhang K, Chen Y, Zhang Z, Zhao Y. 2009. Identification and verification of lysine propionylation and butyrylation in yeast core histones using PTMap software. *J Proteome Res* **8**: 900-906.

Zhang Y, Xiong Y. 2001. A p53 amino-terminal nuclear export signal inhibited by DNA damage-induced phosphorylation. *Science* **292**: 1910-1915.

Zhang Y. 2003. Transcriptional regulation by histone ubiquitination and deubiquitination. *Genes Dev* **17**: 2733-2740.

Zhou Z, Elledge SJ. 1992. Isolation of *crt* mutants constitutive for transcription of the DNA damage inducible gene *RNR3* in *Saccharomyces cerevisiae. Genetics* **131**: 851-866.